



University
of Glasgow

<https://theses.gla.ac.uk/>

Theses Digitisation:

<https://www.gla.ac.uk/myglasgow/research/enlighten/theses/digitisation/>

This is a digitised version of the original print thesis.

Copyright and moral rights for this work are retained by the author

A copy can be downloaded for personal non-commercial research or study, without prior permission or charge

This work cannot be reproduced or quoted extensively from without first obtaining permission in writing from the author

The content must not be changed in any way or sold commercially in any format or medium without the formal permission of the author

When referring to this work, full bibliographic details including the author, title, awarding institution and date of the thesis must be given

Enlighten: Theses

<https://theses.gla.ac.uk/>
research-enlighten@glasgow.ac.uk

wo 7
1

A THEORETICAL AND EXPERIMENTAL INVESTIGATION INTO
THE COMPONENT LOSSES IN THE WORKING PASSAGES OF
TURBO MACHINERY.

SUMMARY

JOHN H. NEILSON B.Sc., A.M.I.Mech.E.

ProQuest Number: 10662288

All rights reserved

INFORMATION TO ALL USERS

The quality of this reproduction is dependent upon the quality of the copy submitted.

In the unlikely event that the author did not send a complete manuscript and there are missing pages, these will be noted. Also, if material had to be removed, a note will indicate the deletion.



ProQuest 10662288

Published by ProQuest LLC (2017). Copyright of the Dissertation is held by the Author.

All rights reserved.

This work is protected against unauthorized copying under Title 17, United States Code
Microform Edition © ProQuest LLC.

ProQuest LLC.
789 East Eisenhower Parkway
P.O. Box 1346
Ann Arbor, MI 48106 – 1346

Introduction.

It is the function of the elements in a turbine or compressor stage to effect the transformation of energy from one form to another with the minimum loss. In the past losses and efficiencies in the elements and stages of turbo-machinery have been defined and measured in a variety of different ways each associated with the designer or research worker in a particular field. The steam turbine designer has in the main been concerned with high speed flow in impulse or fifty degree reaction stages. In the gas turbine plant the degree of reaction varies not only from stage to stage but with blade height within a particular stage and in axial flow compressors the designer has been concerned with low speed flow, where for many applications the working fluid could be regarded as incompressible.

Present day trends are towards steam turbine stages with varying amounts of reaction in the moving blade and to compressor stages with rising operating Mach numbers, the working fluid can no longer be regarded as incompressible.

Summary.

The enthalpy loss in a blade element, which is the net loss of high grade energy caused by friction forces, is shown to consist of a basic friction loss plus an auxiliary loss which accounts for the "heating" effect of the friction work. The auxiliary loss is positive for compressions and negative for expansions. Relations are derived between the enthalpy loss and other methods commonly used to express the irreversibilities in the blade elements. The equations involved are applicable to static or moving elements in axial flow

turbines or compressors with high or low speed flow.

Factors affecting turbine or compressor stage efficiencies are accounted for by (a) defining an efficiency for the flow process in the stage and by (b) using the concept of blading (diagram) efficiency. It is shown that, while the "total to static" stage efficiency is directly proportional to the blading efficiency, the "total to total" stage efficiency is almost independent of blading efficiency if the process efficiency and blading efficiency are high.

Expressions are developed for the blading efficiency and load factor in a stage for any given reaction effect in the rotor blade. It was found that the conditions for maximum blading efficiency could best be obtained in terms of a criterion which is called here the "reaction coefficient". This analysis will fill the gap between existing theories applying to the impulse blade and the fifty degree reaction blade.

In most of the previous work in this field of blading research, use is made of "atmospheric" air in a wind tunnel. It was appreciated that a steam circuit could readily be adapted as a variable density tunnel. Hence, using superheated steam as the working fluid, it was decided to explore the flow and loss characteristics for a small rectangular nozzle and impulse blade pair over a range of Reynolds number and Mach number. An impact tube and traversing gear were designed to operate in a relatively high pressure and temperature stream and were so arranged that the entire exit area of either the nozzle or blade could be completely traversed.

A considerable amount of calculation is however involved in

relating the local impact tube readings to local values of efficiency and in converting these local values into mean effective values. Hence a procedure is given here which will ease this transformation and will take account of compressibility effects, of variable density flow and of supersonic flow with the possibility of a shock wave formation upstream of the impact tube.

The nozzle loss is confined to a thin wall boundary layer with isentropic flow elsewhere in the nozzle. The larger blade loss, which is very sensitive to quite small amounts of reaction or compression in the blade passage, is greatest on the convex side of the blade. For this small nozzle, the stream attains a constant efflux angle in only a small central core of the flow with large variation in angle as the nozzle boundaries are approached. This efflux angle pattern remains unchanged with varying Reynolds number and subsonic Mach number. When the Mach number increases beyond unity however, the pattern changes so that the stream conforms more to the geometric outlet angle.

The observed variation in blade loss coefficient at high Reynolds number is compared with other similar work and confirms that a critical Reynolds number exists at 2×10^5 below which value there is a substantial increase in blade loss.

2
THE UNIVERSITY OF GLASGOW

A THEORETICAL AND EXPERIMENTAL INVESTIGATION INTO

THE COMPONENT LOSSES IN THE WORKING PASSAGES OF

TURBO MACHINERY

THESIS SUBMITTED FOR THE DEGREE OF DOCTOR OF

PHILOSOPHY

BY

JOHN H. NEILSON B.Sc., A.M.I.Mech.E.

1961.

GLASGOW
UNIVERSITY
LIBRARY

Contents.

	Page.
Summary.	iv.
Index of Figures and Plates.	xii.
Nomenclature.	xiii.
Introduction.	xvii.
Review.	xxii.

Part 1 (a).	Methods of obtaining the high grade energy exchanged between the working fluid and its surroundings in flow and non flow processes with particular reference to the effect of friction in the steady flow process.	1.
Section 1.	Processes without friction.	2.
Summary.	-----	9.
Section 2.	The steady flow process with friction in the elements of turbo-machinery.	10.
Summary.	-----	19.
Part 1 (b).	Losses and loss coefficients in axial flow turbo-machinery elements - a review of the methods used to express losses in blade elements and their interrelationships.	21.
Section 1.	The axial flow turbine blade element.	22.
Section 2.	The axial flow compressor blade element.	25.
Summary.	-----	28.
Part 1 (c).	Efficiencies in axial flow turbine and compressor stages. - A method of expressing the efficiency of the flow process in the stage and the interrelationships between the process efficiency, the stage efficiency and the blading efficiency.	31.

		Page.
Section 1.	Efficiencies in the turbine stage.	32.
Summary.	-----	44.
Section 2.	The axial flow compressor stage.	47.
Summary.	-----	54.
Part 1 (d).	Conditions for maximum blading efficiency in axial flow turbines and compressors - factors affecting the choice of design parameters for the stage.	56.
Summary.	-----	66.
Part 2 (a).	The determination in a static test rig of local total head efficiency of expansion and of stream condition by means of an impact tube.	71.
Summary.	-----	86.
Part 2 (b).	The conversion of local values of efficiency and of efflux angle into mean effective values.	87.
Summary.	-----	94.
Part 3.	An experimental investigation into the flow of superheated steam through a small nozzle and impulse blade pair yielding results on flow pattern and efficiency with varying Reynolds number and Mach number.	96.
	Object of the experimental work.	97.
	Description of the apparatus.	98.
	Limitations set by the experimental rig on the applicability of the experimental results.	117.
	Test programme, calculations and results.	118.
Series 1.	Test conditions.	124.
	Specimen calculations, and tables for tests 1 and 1A.	125.

	Page.
Series 1.	Final results. 144.
Series 2.	----- 151.
	Test conditions. 153.
	Final results. 155.
Series 3.	----- 164.
	Test conditions groups 1, 2 and 3. 166 - 168.
	Specimen calculations (group 3). 169.
	Final results. 170.
	Effect of supersonic Mach number on efflux angle. 174.
<hr/>	
Discussion of results.	176.
Conclusions.	188.
Bibliography.	191.
Appendix 1.	194.
	Specimen tables of observed and derived results series 2 tests 1 and 1A. 196.
	Specimen tables of observed and derived results series 3 (group 3). 211.
Appendix 2.	see separate book.
<u>Contents of Appendix 2.</u>	
Series 1.	Tables of observed and derived results for tests 2 - 4 and 2A - 4A. 2 - 32.
Series 2.	Tables of observed and derived results for tests 2 - 6 and 2A - 6A. 33 - 83.
Series 3.	Tables of observed and derived results for groups 1 and 2. 84 - 103.
Appendix 3.	An examination of the variation of loss coefficients with Mach number and Reynolds number with a particular reference to the existence of critical values of these parameters. 218.
Summary.	----- 234.
Acknowledgments.	----- 236.

Summary.

Introduction.

In the thermodynamic design of turbines and compressors it is essential firstly to decide on the basic features of the machine. In turbines, for example, one must determine whether high specific mechanical energy output is the aim or whether one may sacrifice some of this high specific output for an increase in gross stage efficiency. It is then necessary to decide on such factors as blade speeds, stream velocities and degree of reaction or compression. Formerly in steam turbine practice the blading was either of pure impulse design or a 50° reaction design, and for these cases the principles on which the rotor speeds and steam velocities were determined were widely known and practiced. With the advent of the gas turbine plant however, more use is being made of blading where the degree of reaction is other than 50° or zero, both in the turbine and compressor, and this trend is finding its way into present day steam turbine practice. Once the above mentioned design features have been established, it is necessary to have available data on friction coefficients, efflux angles etc. and these are normally obtained from experiments on the proposed blading. With the development of the gas turbine plant and especially with the axial flow compressor, this work has usually been done in atmospheric wind tunnels, where air, passing into the atmosphere through the proposed blading, is examined with impact or pitot tubes and yawmeters.

Purpose of the Present Work.

In the turbine or compressor stage the stage loss is a loss of mechanical work energy which is affected by the loss of high grade energy in the elements of the stage. These element losses are due to the effect of friction forces and it is necessary to understand fully the nature of a friction loss and to be able to correlate the various ways in which the irreversibilities in the elements may be expressed. Part of the loss of mechanical work in the stage can however be dissociated from the friction losses in the elements and depends on the form of the stage velocity triangles. In turn the form of the velocity triangles is dependant on the initial choice of such design parameters as the degree of reaction and the loading factor for the stage.

When dealing with efficiencies in the turbine stage it is desirable to separate friction effects from effects associated with the form of the velocity triangles. It is the object of the present work to redefine the efficiencies associated with the stage so as to separate these effects and to do so in such a manner that the concepts may be applied to either the compressor or the turbine stage.

Due to the increasing interest in stages which are not either of an impulse or a fifty degree reaction design it is proposed to analyse the influence on the stage efficiency of degree of reaction, blade speed to jet speed ratio and loading factor. The analysis should be comprehensive enough to embrace turbine stages designed for any positive or negative degree of reaction and the theory evolved should be applicable to the compressor stage.

In most of the previous work in this field of blading research use has been made of "atmospheric" air in a wind tunnel. It was appreciated that a steam circuit could readily be adapted as a variable density tunnel. Hence it was decided to explore the flow and loss characteristics for a small rectangular nozzle and blade pair using superheated steam as the working fluid. This entailed more attention to the design of the instrumentation compared with the "atmospheric" tunnel but the scheme allowed for testing over a wider range of conditions.

Part 1.

Using the concept of high and low grade energy the net useful high grade energy released by unit mass of working fluid in any steady flow process is shown to be $-\int VdP - \int f v_r$, where V is the specific volume of the working fluid, dP the elemental change in pressure, f the friction force per unit mass and v_r the relative velocity of the working fluid, the term $\int f v_r$ being the friction work done in the process. Comparing an adiabatic steady flow process with a similar isentropic process the net loss of useful high grade energy, which is often referred to as the enthalpy loss is shown to be $\int f v_r + \int dP (V - V_s)$ where V_s is the isentropic specific volume. Thus the enthalpy loss is divided into a basic friction work loss term plus an auxiliary loss term which accounts for the heating effect of the friction work. The auxiliary term is positive for compressions and negative for expansions.

The enthalpy loss is related to other methods used to express the irreversibilities in blade elements. Relationships are derived between the enthalpy loss, the total head pressure loss, the increase in entropy, the enthalpy loss coefficient, the total head pressure loss coefficient, the blade velocity coefficient, the blade drag coefficient and the efficiency of the expansion or compression process in the blade. The equations involved are applicable to static or moving elements in axial flow turbines and compressors with high and low speed flow.

Two stage efficiency definitions are used in turbine work, the total to static stage efficiency is the criterion of performance where the exhaust kinetic energy is degenerated by friction and the

total to total stage efficiency is used where the exhaust kinetic energy is not degenerated. These stage efficiencies are derived as functions of (a) a blading or diagram efficiency and (b) an efficiency for the steady flow process in the stage. The diagram efficiency depends on the form of the stage velocity triangles which in turn depends on the choice of design parameters for the stage. These design parameters are the blade speed to jet speed ratio, the degree of reaction based on the inlet total head condition of the working fluid and the loading factor. The efficiency of the expansion process in the stage depends on the friction losses in the elements and is derived in terms of the loss coefficients in the static and moving blade rows.

It is shown that the total to static stage efficiency is directly proportional to the blading efficiency while the total to total efficiency is sensibly independent of blading efficiency provided that both the blading efficiency and process efficiency are high.

The axial flow compressor stage efficiency is also derived in terms of a blading efficiency and in terms of an efficiency for the compression process in the stage.

Having shown that the turbine stage efficiencies are dependant on the blading efficiency, an analysis is given of the way in which the blading efficiency varies with speed ratio and degree of reaction. It was found that the blading efficiency and loading factor could best be expressed in terms of (a) the blade speed to tangential jet speed ratio and (b) a reaction coefficient for the stage, defined as the ratio of the reaction effect in the moving blade to the

kinetic energy available at inlet to the moving blade. The relationships between this reaction coefficient, the total head degree of reaction and other ways in which degree of reaction is sometimes defined are derived and the relative merits of the different definitions discussed. The variation of loading factor and blading efficiency is presented in graphical form. The optimum speed ratio for any given reaction coefficient is obtained along with the value of the maximum blading efficiency. The analysis is developed for stages where the degree of reaction is positive, zero, or negative and it is shown that when a stage is designed for maximum blading efficiency the value of the blading efficiency increases and the loading factor decreases as the degree of reaction is increased.

The way in which the blading efficiency of a compressor stage depends on the design parameters of the stage can be seen by looking upon the compressor stage as a similar turbine stage in which all of the stage velocities are reversed in direction.

Part 2.

The Determination in a static test rig of Local Total Head Efficiency of Expansion and of Stream Condition by means of an Impact Tube and the Conversion of Local Values into Mean Effective Values.

The material herein is associated with the experimental methods of obtaining efficiency and efflux angle. Even when dealing with the "incompressible" flow of air through blading there is a considerable amount of calculation involved in relating the local

impact tube or pitot tube readings to local values of efficiency and further in converting these local values into mean effective values. The calculations become even more complex when account must be taken of compressibility effects, of variable density flow and of supersonic flow with the possibility of a shock wave formation upstream of the impact tube. Hence in this section a procedure is given which will ease the transformation of the local impact tube readings into local efficiency and local stream condition and finally will allow these local values to be correctly converted into mean effective values.

Part 3.

An Experimental Investigation into the Flow of Superheated Steam through a Small Nozzle and Impulse (zero pressure drop) Blade yielding results on Flow Pattern and Efficiency with Varying Reynolds Number and Mach Number.

In this section experiments are described in which the flow and loss characteristics of a small nozzle and impulse blade pair were investigated using superheated steam as the working fluid. The nozzle is of rectangular cross-section and was made to suit a standard set of impulse blading. An impact tube and traversing gear were designed so that the entire exit area of either the nozzle or blade could be completely traversed. By this means local values of total head pressure and efflux angle were obtained at nozzle and blade outlet for a range of Reynold's number covering subsonic and supersonic Mach numbers. The results were converted to mean effective values of efficiency and efflux angle by the methods

described in Part 2, and serve partly as an example of the application of these methods to blading research. It was found that the greater part of the total loss across the nozzle and blade pair occurs in the "parallel" passage of the blade and that this loss is very sensitive to quite small amounts of reaction or compression in the blade passage. The nozzle loss is confined to a thin wall boundary layer with isentropic flow elsewhere in the nozzle. The boundary layer in the blade passage is more pronounced than in the nozzle and is thickest on the convex side of the blade. The efficiency of both the nozzle and of the nozzle and blade pair rise with increasing Mach number as the value of unity is approached. At low Mach numbers there is a rise in nozzle efficiency as the Mach number decreases but the efficiency of the nozzle and blade pair, where the losses are greater, does not show this characteristic. For this small nozzle, the stream attains a constant efflux angle in only a small central core of the flow, with large variations in angle as the nozzle boundaries are approached. This efflux angle pattern remains unchanged with varying Reynolds number and subsonic Mach number. The efflux angles in the central core however rise slightly with increasing Mach number up to unity. As the Mach number progressively increases beyond unity the efflux angle pattern changes so that there is less variation in angle across the nozzle and the stream conforms more and more to the geometric outlet angle.

The tests on the impulse blade indicate a sharp rise in blade loss as the chord Reynolds number is reduced to 2×10^5 . In

appendix 3 the variation of loss coefficient at high Reynolds number is compared with similar work by Armstrong⁴⁰ and helps to confirm his conclusion that a critical Reynolds number exists at 2×10^5 , below which value there is a substantial increase in blade loss.

Index of Figures and Plates.

Fig.	Page.	Fig.	Page.	Fig.	Page.
1.	f 2.	38.	99.	67.	203.
2.	" 10.	39.	105.	68.	204.
3.	" 15.	40.	106.	69.	215.
4.	" 17.	41.	107.	70.	219.
5.	" 22.	42.	108.	71.	220.
6.	" 25.	43.	109.	72.	221.
7.	" 32.	44.	113.	73.	222.
8.	" 36.	45.	119.	74.	228.
9.	" 40.	46.	120.	75.	231.
10.	" 45.	47.	122.		
11.	" 47.	48.	134.	Plate.	Page.
12.	" 48.	49.	135.	1.	100.
13.	" 51.	50.	146.	2.	101.
14.	" 57.	51.	147.	3.	102.
15, & 16.	" 58.	52.	148.	4.	103.
17, 18 & 19.	" 59.	53.	149.	5.	110.
20 & 21.	" 60.	54.	150.	6.	112.
22, 23 & 24.	" 61.	55.	157.		
25 & 26.	" 62.	56.	158.		
27.	" 64.	57.	159.		
28 & 29.	73.	58.	160.		
30.	74.	59.	161.		
31.	77.	60.	162.		
32.	78.	61.	163.		
33.	79.	62.	171.		
34.	80.	63.	172.		
35.	81.	64.	173.		
36.	84.	65.	175.		
37.	88.	66.	195.		

f ---"facing page"

Nomenclature.

b	-----	Breadth.
C_D	-----	Drag coefficient.
C_L	-----	Lift coefficient.
c_p	-----	Specific heat at constant pressure.
D	-----	Mean diameter.
da	-----	Elemental area.
DH	-----	Heat drop.
e	-----	Specific internal energy.
f	-----	Force of friction.
fda	-----	Fraction of the elemental area da.
fV	-----	Ratio of actual to isentropic specific volume.
F	-----	Force normal to vane.
G	-----	Reaction coefficient.
G_c	-----	Compression coefficient.
g	-----	Acceleration due to gravity.
H	-----	Specific enthalpy.
H.M.D.	----	Hydraulic mean diameter.
h	-----	Blade height.
i	-----	Incidence.
J	-----	Mechanical equivalent of heat.
K	-----	Blade velocity coefficient.
M	-----	Mass or Mach number.
m	-----	Mass flow rate.
P/c	-----	Pitch to chord ratio.
P	-----	Pressure.
P_1	-----	Inlet total head pressure static tests.
P_2	-----	Exit static pressure ----- " "
P_3	-----	Exit total head pressure -- " "
P_4	-----	Static pressure after a normal shock jump at exit ---- static tests.
P_5	-----	Total head pressure after a normal shock jump at exit ---- static tests.
Q	-----	Heat quantity.
R	-----	Degree of reaction or gas constant.

R_o	-----	Total head degree of reaction.
R_c	-----	Degree of compression.
R_{oc}	-----	Total head degree of compression.
R_n	-----	Reynolds number.
r	-----	Radius.
s	-----	Blade velocity.
t/c	-----	Maximum thickness to chord ratio.
T	-----	Temperature.
t	-----	time.
u	-----	Radial velocity of the working fluid.
V	-----	Specific volume.
v	-----	Absolute velocity of the working fluid.
v_a	-----	Axial velocity or acoustic velocity.
v_r	-----	Relative velocity of the working fluid.
v_w	-----	Absolute whirl or tangential velocity of the working fluid.
W_I	-----	Specific work input.
W_D	-----	Specific work output.
Y	-----	Total head pressure loss coefficient.
Z	-----	Work done or loading factor.
ϵ	-----	Enthalpy loss coefficient.
ϕ or s	----	Entropy.
γ	-----	Isentropic index.
ω_v	-----	Angular velocity of blade or vane.
ω	-----	Absolute angular velocity of the working fluid.
α	-----	Angle between the absolute velocity vector leaving the nozzle blade and the plane of rotation, in a turbine stage and angle between the absolute velocity vector entering the stator blade and the plane of rotation, in a compressor stage. Referred to as the nozzle outlet angle and stator blade inlet angle respectively. --- also local efflux angle in static tests.
β	-----	Angles between the relative velocity vectors associated with the moving blade and the plane of rotation. Referred to as the "blade" angles.

ϕ -----	Angle between tangent to vane and the radius.
θ -----	Gas deflection.
μ -----	Coefficient of viscosity.
γ -----	Isentropic index.
ρ -----	Blade speed to jet speed ratio or density.
σ -----	Blade speed to tangential jet speed ratio.
ρ' -----	Blade speed to jet speed corresponding to the stage total head heat drop.
σ' -----	Blade speed to tangential jetspeed corresponding to the stage total head heat drop.
h -----	An imperial coefficient.
η -----	Efficiency.
η_{ts} -----	Total to static stage efficiency.
η_{tt} -----	Total to total stage efficiency.
η_B -----	Blading or diagram efficiency.
η_b -----	Total head efficiency of expansion in nozzle and blade pair. -- static tests.
η_n -----	Total head efficiency of expansion in nozzle -- static tests.
Σ -----	Prefix designating summation.
\bar{x} -----	Denotes a mean value of x.

Subscripts.

() _{SY}	-----	denotes "system".
() _{SU}	-----	denotes "surroundings".
() _f	-----	denotes "with friction".
() _c	-----	denotes compression.
() _o	-----	denotes total head condition.
() _r	-----	denotes velocity or condition relative to the moving blade.
() _s	-----	denotes condition after an isentropic process in general.
() _{ss}	-----	denotes condition after an isentropic process in the stage.
() _N	-----	denotes "for the nozzle blade" in a turbine stage.
() _D	-----	denotes "for the diffuser or stator blade" in a compressor stage.
() _R	-----	denotes "for the rotor blade" in turbine or compressor stages.
() _s	-----	denotes "for the stage" in turbines or compressors.
() _p or ϕ	----	denotes "profile or centre line" coefficient.
() _t	-----	denotes "total or three dimensional" coefficient.
() _n	-----	denotes nozzle outlet -- static tests.
() _b	-----	denotes blade outlet -- static tests.

Introduction.

Since the impetus given to blading research by the advent of the gas turbine plant, and especially by the compressor unit there has been an increasing interest in turbines and compressors of widely differing types. These types include the radial and axial flow turbine or compressor and the use of the shock wave in supersonic compressors. Against this varied background it is necessary to be clear as to the nature and effect of losses in the working passages in turbo machinery and as to how the losses may best be determined experimentally.

The principal parts in turbines and compressors are the static elements which act as nozzles or diffusers and the moving elements which as well as being nozzles or diffusers are agents for the transfer of mechanical energy. The function of the static elements is the interchange of enthalpy and kinetic energy while that of the moving elements is the interchange of enthalpy on the one hand with kinetic and mechanical energy on the other. The principal factors affecting the efficiency of these energy interchanges, may be grouped under two headings.

These are:--

- (1) Those which cause the degeneration of high grade kinetic energy into low grade energy.
- (2) Those involved in the design and operation of the turbine or compressor and which influence the conversion of high grade energy to mechanical work energy.

The degeneration of high grade energy affects both the moving and static elements and the losses to which the elements are

liable under this heading are:-

(a) The boundary layer or skin friction loss:-

This loss is characterized by a velocity gradient in the flow in the vicinity of the solid boundaries.

(b) Turbulent flow loss:-

This type of loss can effect the region within the boundary layer as well as the main stream and is due to random velocity variations with time, which are superimposed on the main velocity of flow. These random velocities cause an interchange of mass between adjacent streamlines with the result that shear stresses are set up within the body of the fluid.

(c) Eddy Motion or vorticity losses:-

This is caused by small variations in static pressure normal to the principal direction of the flow resulting in secondary circulatory motions being imposed on the main flow. The kinetic energy for these secondary motions reduces the energy of the main stream.

(d) Losses due to the separation of the boundary layer:-

Under certain circumstances especially in decelerating flow the low energy boundary layer separates from the wall and is energised by the main flow. This results in momentum mixing with consequent loss.

(e) Shock losses at the entrance to the elements:-

These losses are due to misalignment of the fluid stream and blade inlets causing eddy formations.

(f) Discontinuity losses:-

These losses are inherent in shock discontinuities or sudden changes in pressure, specific volume, temperature and velocity and occur only in supersonic flow. These losses (a) to (f) are known as reheat losses due to the fact that as the kinetic energy disappears, the stream is "heated" by an energy quantity equal to that of the lost kinetic energy.

Losses under the second heading are:-

(g) Deviation losses:-

This loss is due to the variation in the direction of the fluid flow from the direction dictated by the solid boundaries of the machine elements and affects the transfer of mechanical energy only.

and

(h) Leaving losses:-

These are losses in the amount of mechanical energy transferred because of the retention in the fluid stream of kinetic energy.

Other parasitic losses are those due to disc friction, windage and leakage of the working fluid past the machine elements.

The parameters which influence losses may be classified as:-

(1) Those due to the geometry of the machine elements.

For example, the shape of the cross sections normal to the flow, the curvature of the axis of the elements, and the surface finish of the boundaries.

(2) Those due to the properties of the working fluid.

For example:- pressure, temperature, density, velocity, and viscosity.

The object of the investigation is to analyse the effect of these losses on the efficiency of energy transformation, to determine the conditions for maximum mechanical energy transfer from or to a working fluid, to establish a technique for measuring losses in machine elements with variable density flow and to apply the technique to determine losses in a nozzle and blade pair.

With regard to the effect of friction, an attempt has been made to show the basic nature of a frictional process, and to distinguish the friction work from the net loss of useful energy which is usually loosely called the loss or friction loss. An analysis is made for the general case of the flow of the working fluid through a radial flow machine and the equations developed, with suitable modification, may then readily be applied to any type of stationary or moving element. Particular reference is made to the effect of friction on the energy transfer terms in turbo machinery and to the different effects of friction in expansion and compression processes.

A section of theory is devoted to the efficient transfer of mechanical energy. In it a criterion is given which determines the best operating speed of the rotor blade for any given amount of reaction or compression in the blade passage. In the theory it is found to be convenient to define a term called "Reaction"

Coefficient" and the criterion mentioned above is given as a function of this Reaction Coefficient. The conflicting factors of high specific mechanical energy output and blading efficiency are discussed for turbine blades with reaction or compression in the blade passage and for compressor blading.

In testing for the effect of friction in turbine or compressor elements, if the total head condition of the working fluid entering the machine element is known, a traverse of the outlet area with an impact tube will allow local values of the loss in total head pressure to be obtained. In the experimental work here the machine elements used are a small rectangular nozzle and blade pair with superheated steam as the working fluid and the arrangement is such that the density of the steam in the test section may be readily controlled and varied. The object is to test the nozzle and blade pair for friction losses and efflux angles under various operating conditions and, taking a broader view, to establish a method of translating the results of the traverse readings into mean values of efficiency and efflux angle which would be applicable to any type of machine element. To this end a section is devoted to the determination of local efficiency and local state point of the fluid from the observed impact tube readings. These local values over the cross-section of the flow are then reduced to mean effective values. The method used applies generally in that the effect of large density change within the element and the effect of supersonic speeds may be accounted for.

Review.

The problems presented by the flow of the working fluid through the elements of turbo machinery have been tackled from many viewpoints and with increasing intensity since the turn of the century. On the theoretical side the classical theories of potential flow, based on Euler's equations of motion for a non viscous fluid, represented a major step forward in an attempt to describe by mathematics the nature of fluid flow past and around solid boundaries. These equations were used, for example, to calculate the pressure distribution around cylinders, spheres, and aerofoils and gave results which were found to be in substantial agreement with observations. Various anomalies were however apparent and these were suspected to be due to the neglect of fluid friction. The Navier Stokes equations of motion, which account for fluid friction, were found to be capable of solution in only a few simple cases.

Prandtl was the first to give a practical approach to the problem of fluid friction and to its effect on fluid flow. He divided the flow around bodies into regions where friction could be neglected and where the classical theories of potential flow could be applied and into regions where friction had to be accounted for, these he referred to as boundary layers. Even at this stage Prandtl's theories were the results of mathematical treatment confirmed by observation.

The initial experimental work was of course associated with steam turbines. In 1910 Brilling¹ investigated loss characteristics

for plate type impulse turbine blades. Using a static test rig he determined the effect of different blade inlet forms and of steam deflection on the blade velocity coefficient. The coefficient was shown to decrease with increasing steam deflection for a given inlet form.

The most systematic approach to finding experimental coefficients in the early days was due to the work of the Steam Nozzle Research Committee of the Institution of Mechanical Engineers. This Committee was formed in 1914 with the initial aim of providing much needed information on the efficiency of typical steam turbine nozzle forms. The bulk of the experimental work took place between 1921 and 1930 and is summarized in the sixth and final report². In the Committee's apparatus the impulse principle was used to obtain a nozzle velocity coefficient. The momentum of the steam jet issuing from the nozzle was measured by the force exerted by it on a flat plate which was placed at right angles to the direction of the jet. Great care was taken to ensure that all of the jet momentum was absorbed at the plate and, since the plate had to be at right angles to the mean direction of the jet, preliminary experiments to determine the efflux angle of the jet were necessary. This efflux angle was initially measured by a metal vane placed in the jet. Tests were made on "cast in" impulse nozzles, "built up" impulse nozzles, Parsons blade type nozzles and on elementary nozzles with a straight axis. In the bulk of the experiments the efflux angle was always less than the nominal outlet angle of the nozzle. In addition it was found that as the pressure ratio across the

nozzle was decreased the efflux angle increased and so approached a value nearer the geometric outlet angle. The difference between the efflux angle and the geometric angle was found to depend on the nozzle plate thickness and it was thought that the proximity of the flat surface, inclined at a small angle to the stream at outlet, caused a suction effect on the jet. Thus with the curved type of outlet in the Parsons nozzles or with a chamfered outlet the deviation of the jet from the geometric angle was not so great. In general the nozzle velocity coefficient was found to decrease with increasing steam velocity from low velocities up to approximately 800 ft/sec, to remain fairly constant to about 1600 ft/sec and to increase there after. The minimum values of the coefficient were found to be sensitive to the length of the parallel portion, a large parallel portion being detrimental. It was also found that a roughness on the nozzle profile, produced by machining a screw thread on the nozzle had an adverse effect on the coefficient. In an interesting series of experiments on straight elementary nozzles with different inlet forms, it was found that at high velocity (about 2,000 ft/sec) a nozzle with sharp inlet had a velocity coefficient almost as high as a similar nozzle with a rounded inlet.

The impulse plate method of the Committee's apparatus was used in an improved form by Giffen and Orang³ in work preceeding 1939 but not published until 1946. The object of this was to investigate the rising characteristic of nozzle velocity coefficient with decreasing steam velocity at low speeds as

obtained by the Nozzle Research Committee and the results were in apparent disagreement with those obtained by the Committee.

In a Parsons Memorial Lecture in 1939 Guy⁴ describes experiments with which he was associated wherein the vane method of measuring efflux angle was dispensed with and a yawmeter used to find local values of efflux angle at the exit of typical steam nozzles. He again found that the mean efflux angle increased with increasing steam speed and found that at higher velocities the mean efflux angle is given very closely by \sin^{-1} opening/pitch.

In 1940 Dollin⁵ used the reaction principle to obtain steam nozzle efficiency. He supported the nozzles in a static testing machine in such a way that they had limited freedom of torsional and axial movement and by means of balances measured the forces necessary to restore the nozzles to their original position. This was claimed to be superior to the impulse plate method because, in addition to giving efficiency, it also gave mean efflux angle. The results of tests on a group of reaction nozzles showed that, as the pressure ratio was decreased, the nozzle efficiency continuously increased up to the critical pressure ratio. Also the mean efflux angle was always greater than that given by \sin^{-1} opening/pitch and indeed decreased slightly with decreasing pressure ratio.

Stodola⁶ also gives the results of efflux angle tests but in this case on single convergent parallel nozzles with overcritical expansion. The nozzles were mounted in a nozzle holder with the axis of the nozzle pointing vertically upwards

and the outlet face of the nozzle machined off obliquely to the axis. The efflux angle distribution was apparently obtained by photographing the steam jet and making measurements from the photographs. The results show that for small pressure ratios, in the region of 0.2, the nozzle angle increased by as much as 44 degrees at the inner or shorter boundary with a small positive or negative deviation at the outer boundary.

A considerable impetus to blading research came however with the advent of the gas turbine plant. The need for a compressor which would be efficient at wide operating conditions led to a great deal of work on compressor blading. The principal contribution is that of Howell⁷ in his paper "Fluid Dynamics of Axial Compressors" in which he pays particular attention to the variation of blade loss with incidence of the gas stream. Air was used as the working fluid in wind tunnels with cascades of wooden blades, and detailed traverses were made of the outlet flow areas of the cascade with pitot or impact tubes and yawmeters. Thus for a given compressor cascade average values, usually the arithmetic mean values, of total head loss and of stream deflection were obtained for various tunnel settings or incidence angles of the inlet stream. This in turn gave the permissible range of efficient operation of the cascade, since points of positive or negative stall were obtained by the above methods. In addition the total loss at a given incidence was divided into a profile loss or skin friction loss which could be measured at the mid height of the cascade, a secondary loss due to trailing

vortices formed by unequal static pressure distribution within the blade passage and an annulus loss due to skin friction at the annulus walls. Fluid speed effects on the loss characteristics in compressor cascades were allowed for by making use of criteria known as critical and maximum Mach number. Critical Mach number is reached at inlet to the blading when, at a given incidence, there is a distinct increase in loss as the inlet speed is raised. Maximum Mach number is obtained when the cascade chokes and the losses are so great that there is no pressure rise in the blading. Maximum Mach number was found to increase continuously from large negative incidence to large positive incidence. Critical Mach number on the other hand increases from large negative incidence to approximately zero incidence and decreases thereafter. The progressive increase in loss between critical and maximum Mach number is expressed in a simple graphical form in terms of the actual inlet Mach number and the efficiency at critical Mach number. Proceeding from the results of his research Howell evolved rules of procedure which are the present day basis of subsonic compressor design. Details of these are given in papers by Howell⁸ and by Howell and Bonham⁹.

Todd¹⁰ in his paper "Practical Aspects of Cascade Wind Tunnel Research" gives details of low speed and high speed (up to Mach No. of one) wind tunnels and of the methods and instruments used in observing flow pattern and loss. The methods given in this paper are substantially the same as those used by other investigators including Howell. The success of the cascade work

on compressor blading led to an appreciation of the need for more information on turbine blading. Ainley¹¹ in his paper "The Performance of Axial Flow Turbines" gives results of similar cascade wind tunnel testing on turbine blade sections. The work on turbine blading is however not as comprehensive as that on compressor blading and is often limited to cascade testing and subsequent modification of a proposed blade section until a suitable profile is obtained. Attempts have been made, notably by Weske¹² and Carter¹³ to correlate the results of cascade testing with the classical theories, mentioned previously, of potential flow in order to obtain a logical procedure of calculation which would relate the known basic laws to the performance of a turbine or compressor stage. These methods have still to obtain widespread recognition and experimental work is still the basis of the design.

A feature of all cascade wind tunnel work is the use of the pitot tube or impact tube to measure local total energy leaving the blade. The tube itself has been the subject of much investigation notably by Todd^{10 & 14} and Hodkinson¹⁵. With suitable precautions it gives an accurate method of obtaining local values of blade loss. In a supersonic stream, however, modification must be made to the observed impact tube pressure to obtain the stream total head pressure, due to the formation of a detached shock wave in front of the impact tube hole. Details of these modifications are given by Bairstow¹⁶ and Durand¹⁷.

The volume of present day knowledge on the behaviour of turbine and compressor elements is considerable. The future needs of industry will nevertheless demand an increasing research programme on blading elements. The effects of high and low deflection and of varying degrees of reaction in turbine blades, the effects of blade form and pitch especially in supersonic compressors, the effects of compressibility, Reynolds number, secondary flows and of radial equilibrium are some of the subjects requiring further investigation. One disadvantage of cascade wind tunnels is that the test sections normally operate at one pressure and usually the exhaust from the cascade is to the atmosphere. This atmospheric exhaust has many obvious advantages, but it does preclude testing to find the effects of large density change. In addition the design of a variable density wind tunnel with its associated compressor is relatively difficult and is expensive. The apparatus used here, while not giving the flexibility of variable change inherent in the atmospheric cascade tunnel, does give a simple way of obtaining a variable density test section using a steam boiler plant in place of a compressor circuit.

PART 1 (a).

Methods of obtaining the high grade energy exchanged between the working fluid and its surroundings in flow and non flow processes with particular reference to the effect of friction in the steady flow process.

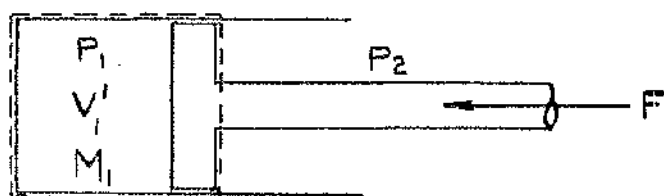


FIGURE 1a.

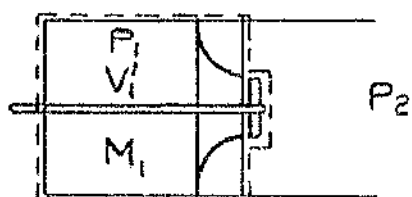
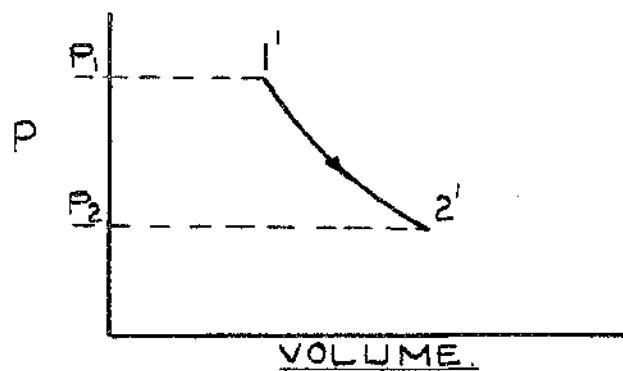


FIGURE 1b.

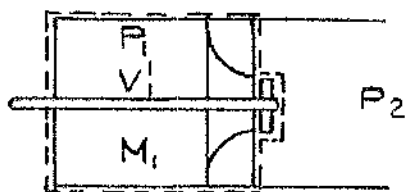
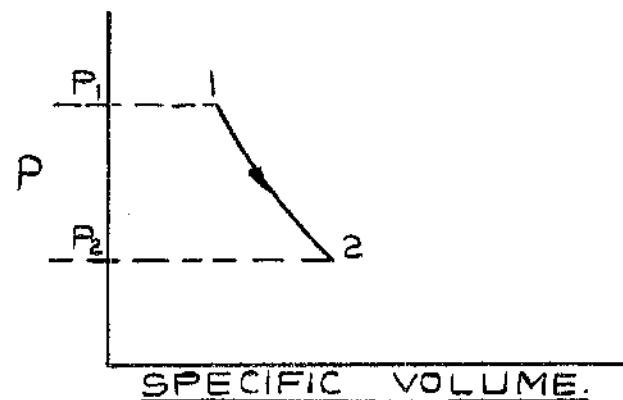


FIGURE 1c.

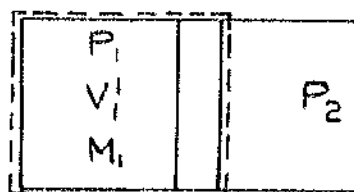
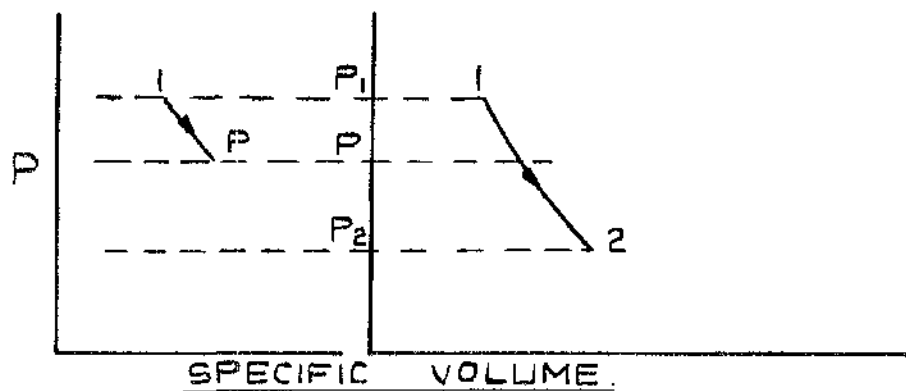


FIGURE 1d.

FIG. 1.

Part 1 (a).

Methods of Obtaining the high grade energy exchanged between the Working Fluid and its surroundings in Flow and Non-flow processes with particular reference to the effect of friction in a Steady Flow Process.

In turbines and compressors we are concerned in the main with the steady flow process and in particular with the transfer of mechanical work energy from or to the working fluid. Since the relationships between kinetic energy changes, mechanical work transfer terms and the changes in the properties of state of the working fluids in steady flow processes, are but one particular (though extremely important) application of more general laws, it is fruitful to consider the methods available for obtaining energy transfer in different processes.

Section 1 - Processes without friction.

Consider a cylinder fitted with a "weightless" piston where the space between the piston and the cylinder head is filled with M_1 lbs of a perfect gas at pressure P_1 and specific volume V_1 . (Figs 1a, b, c, and d). The volume of gas involved is then $V_1' = M_1 V_1$. The original boundary of the system is shown by the dotted lines and the pressure of the fluid in the surroundings of the system is P_2 ($P_2 < P_1$). In considering the subsequent behaviour of the gas in the system we shall presume that no heat crosses the system boundary and that effects of friction may be neglected.

In case (a) (fig. 1a) suppose that the gas expands slowly to P_2 so that at all times equilibrium is established between the gas and its surroundings. This means that a variable restraining force (F) must be maintained at the piston rod, of such a magnitude that this force, together with the force exerted on the piston by the fluid surroundings, is only slightly less than the gas force on the piston. The total

work done by the gas which appears entirely as displacement work at the piston (the fluid boundary) is given by

$$\frac{P_1 V_1' - P_2 V_2'}{\gamma - 1} = M_1 \left(\frac{P_1 V_1 - P_2 V_2}{\gamma - 1} \right) \quad (1).$$

This total work may be divided into useful external work done on the force, F , and into work which is absorbed by the surrounding fluid at the fluid boundary. The useful external work is then

$$M_1 \left[\left(\frac{P_1 V_1 - P_2 V_2}{\gamma - 1} \right) - P_2 (V_2 - V_1) \right] \quad (2).$$

and this equation may be rearranged to give

$$M_1 \left(\frac{P_1 V_1 - P_2 V_2}{\gamma - 1} \right) = M_1 \left(1 - \left(\frac{P_2}{P_1} \right)^{\frac{1}{\gamma}} \right) P_2 V_2 \quad (3).$$

In case b and c (fig 1b and c) a stop is fitted to the piston and the gas in the system is initially contained in a rigid closed vessel. We shall presume that the piston is fitted with a suitably shaped nozzle, which may be opened or closed instantaneously, and that at the nozzle exit an ideal impulse rotor is fitted, which is capable of absorbing all of the kinetic energy supplied to it. Suppose that the nozzle is opened allowing the pressure inside the vessel to fall.

In practice, if the vessel is large compared with the throat area of the nozzle, and if the nozzle is suitably designed we may assume isentropic expansion in the vessel and in the nozzle.

Let M , P and V be the instantaneous mass, pressure and specific volume of the gas remaining in the vessel sometime after the nozzle is first opened.

$$\text{Then } \frac{M}{M_1} = \left(\frac{P}{P_1} \right)^{\frac{1}{\gamma}} \text{ and } \frac{dM}{dP} = \frac{1}{\gamma} \frac{M_1}{\left(\frac{P_1}{P} \right)^{\frac{1}{\gamma}}} P^{\frac{1-\gamma}{\gamma}} \quad (4).$$

By applying the steady flow energy equation to the instantaneous ejection of mass δM through the nozzle, the elemental kinetic energy generated at the nozzle exit, when the pressure inside

the vessel is P , is given by

$$\Delta M \frac{\gamma}{\gamma-1} (P V - P_2 V_2) \quad (5).$$

Hence the total kinetic energy generated at nozzle exit, as the pressure inside the vessel falls from P_1 to P , is given by

$$\int_{P_1}^P \frac{1}{\gamma-1} \frac{M_1}{(P_1)^{\frac{1}{\gamma}}} (P)^{\frac{1-\gamma}{\gamma}} (P V_1 (\frac{P_1}{P})^{\frac{1}{\gamma}} - P_2 V_2) dP \quad (6).$$

this gives

$$\frac{M_1 V_1}{\gamma-1} (P_1 - P) - M_1 \frac{\gamma}{\gamma-1} (1 - (\frac{P}{P_1})^{\frac{1}{\gamma}}) P_2 V_2 \quad (7).$$

and is identical with the work obtained at the turbine.

Case b. If the pressure inside the vessel is allowed to fall to P_2 , then from equation 7 it can be shown that the total kinetic energy is given by

$$M_1 (\frac{P_1 V_1 - P_2 V_2}{\gamma-1}) - M_1 (1 - (\frac{P_2}{P_1})^{\frac{1}{\gamma}}) P_2 V_2 \quad (8).$$

which is identical with equation 3.

In this event all of the original M_1 lbs of gas whether finally inside or outside the vessel, has expanded from 1 - 2.

$M_1 (1 - (\frac{P_2}{P_1})^{\frac{1}{\gamma}})$ is the mass which has discharged from the

vessel and has been exhausted against the back pressure P_2 .

Rogers and Mayhew¹⁸ approach the problem of case (b) by applying the unsteady flow energy equation and they show that the kinetic energy (or turbine work) is equal to the decrease of internal energy of the gas in the vessel minus the enthalpy of the fluid which has left the vessel. It can of course be shown that this gives the same result as that derived in equation 8.

Case c. If the process is stopped by closing the nozzle when the pressure inside the vessel reaches P , then the total kinetic energy generated can be shown from equation 7

to be

$$M_1 \left(\frac{P}{P_1} \right)^{\frac{1}{\gamma}} \left(\frac{P_1 V_1 - PV}{\gamma - 1} \right) + M_1 \left(1 - \left(\frac{P}{P_1} \right)^{\frac{1}{\gamma}} \right) \left(\frac{P_1 V_1 - P_2 V_2}{\gamma - 1} \right) - M_1 \left(1 - \left(\frac{P}{P_1} \right)^{\frac{1}{\gamma}} \right) P_2 V_2 \quad (9).$$

Here $M_1 \left(\frac{P}{P_1} \right)^{\frac{1}{\gamma}}$ is the mass which remains inside the vessel and has expanded from 1 - P (fig 1c). $M_1 \left(1 - \left(\frac{P}{P_1} \right)^{\frac{1}{\gamma}} \right)$ is the mass which has expanded from 1 - 2 and has been discharged against the back pressure P_2 .

In cases a and b all of the original mass of gas expands from the initial state (1) to the final pressure P_2 . The total high grade energy released appears entirely as displacement work in (a) and as a combination of displacement work and kinetic energy in (b). For either case the total high grade energy released is given by $\int_{SY} PdV$, where P is the

pressure of the gas in the system (SY) and dV is the elemental change in total volume. In (a) and (b) the displacement work done, by the gas in the system, on the fluid surrounding the system is $M_1 \left(1 - \left(\frac{P_2}{P_1} \right)^{\frac{1}{\gamma}} \right) P_2 V_2$.

Here $M_1 \left(1 - \left(\frac{P_2}{P_1} \right)^{\frac{1}{\gamma}} \right) V_2$ is the total volume of surrounding fluid which is displaced and P_2 is the constant pressure of the fluid in the surroundings. This displacement work at the fluid boundary can be written as $\int_{SU} PdV$, where P is the pressure of the surrounding fluid and dV the total elemental change in volume at the surroundings. This boundary displacement work, which is absorbed by the surrounding fluid, is not in general useful work and the useful high grade energy released, (equations 3 or 8), may be written as

$$\int_{SY} PdV - \int_{SU} PdV \quad (10).$$

In case (c) where the process ceases when the pressure in the vessel is P , the system may be divided into two parts. The first part being that which contains the mass, $M_1 \left(\frac{P}{P_1}\right)^{\frac{1}{\gamma}}$, which is finally left in the vessel, and has expanded from $1 - P$. The second is that containing the mass, $M_1 \left(1 - \left(\frac{P}{P_1}\right)^{\frac{1}{\gamma}}\right)$ which is finally outside the vessel having expanded from $1 - 2$. Although no single pair of properties can be used to describe the final state of the gas in the system, the total high grade energy released is obtained by finding $\int PdV$ for each of the parts of the system (equation 9). Thus for case (c) the useful high grade energy released is given by

$$\begin{array}{lll} \int PdV & + & \int PdV & - & \int_{SU} PdV \\ \text{Mass remaining} & & \text{mass finally} & & \\ \text{in the vessel.} & & \text{outside the} & & \\ & & \text{vessel.} & & \end{array}$$

In the general case a system may be divided into a number of parts and in addition the system may be in contact with surrounding fluid at a number of points, at each of which the fluid pressure may be different, and indeed at each point the fluid pressure may vary during the process. For this general case the useful high grade energy released will be given by

$$\sum_{SY} \left[\int PdV \right] - \sum_{SU} \left[\int PdV \right] \quad \text{--- (11).}$$

In case (d), (fig 1d) the weightless piston is initially fitted with a stop. If the stop is suddenly removed the gas in the system is subjected to a free unrestrained expansion and directional kinetic energy will be released in various amounts throughout the system. Referring again to cases (b) and (c), the rate at which the process proceeds depends on the size of the nozzle in relationship to the vessel, and in thermodynamics the energy relationships are independent of the time taken for a process to be completed. Thus in case

(d) removal of the stop at the weightless piston is equivalent to replacing the piston with a nozzle of the same area. The process proceeds at a rapid rate and approach velocity will be generated in the vessel as well as at the nozzle exit. In practice the directional kinetic energy will be reabsorbed as random molecular energy but, if one postulates that viscous drag forces will be absent, then case (d) is the same thermodynamic problem as cases a, b, or c. The system in case (d) cannot be conveniently divided into two parts as in case (c), and to obtain the high grade energy released, at any given time, (by using equation 11) the pressure-volume history of all the elements of the system would have to be accounted for.

In a steady flow process a mass of gas, contained within a system boundary, already possesses kinetic energy as the system moves towards a control volume. During this approach to the control volume the properties of state of the gas remain constant and there is no deformation of the system boundary. Within the control volume all of the elements of mass in the system suffer the same series of pressure volume changes. Again in the exhaust the properties of state remain constant. The total high grade energy released is given by

$$\int_{SY} P dV.$$

To obtain the useful high grade energy released, one must consider the displacement work done on the system by the fluid boundary at inlet, where the pressure is constant at P_1 , as well as the work done by the system on the fluid boundary at exhaust, where the pressure is constant at P_2 .

Thus from equation 11 the net displacement work absorbed by the fluid surroundings is

$$\sum_{SU} [P dV] = - P_1 \int dV_1 + P_2 \int dV_2 = - P_1 V_1 + P_2 V_2$$

and the useful high grade energy released is

$$\int_{SY} PdV + P_1 V_1 - P_2 V_2 = - \int_{SY} VdP \quad \text{_____ (12).}$$

Section 1 - Summary.

There are a number of ways for obtaining work done and kinetic energy changes in closed systems and in open systems with steady and unsteady flow. These include the non-flow energy equation, the steady and unsteady flow energy equations. These relationships have been applied here, to processes where friction may be neglected, to illustrate the meaning that may be attached to areas on the pressure volume diagram in all of these systems.

It is shown that, when any of the elements of mass, which together comprise the total mass within a system, suffer a pressure-volume change the summation of $\int PdV$ for all such elements gives the total high grade energy released in the process. This high grade energy may appear as a combination of mechanical shaft work, displacement mechanical work, displacement work done at the fluid boundary on the surrounding fluid, and in increase of directional kinetic energy, which is retained by some or all of the elements of mass.

A distinction is made between the total high grade energy released in the process and the useful high grade energy released. The useful high grade energy released being the total high grade energy less the displacement work done on the fluid surrounding the system. This useful high grade energy for any flow or non-flow process is given by equation 11 and for the particular case of a steady flow process equation 11 reduces to $-\int_{SY} VdP$.

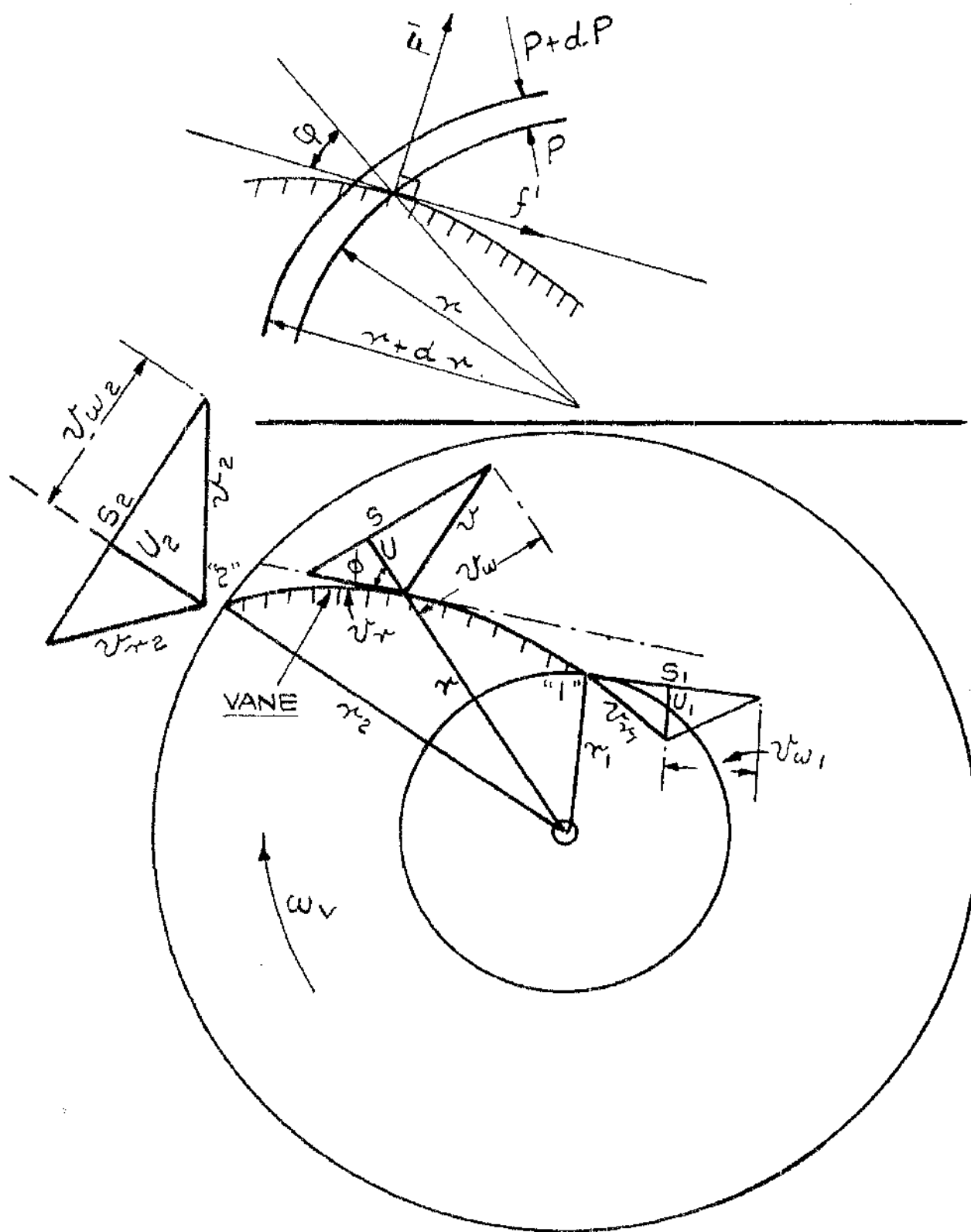


FIG. 2.

Section 2. - The steady flow process with friction in the elements of Turbo Machinery.

In all actual turbo-machinery elements there is some degeneration of high grade energy to low grade molecular energy by friction forces. In the previous section we have seen how the high grade energy involved in a process may be obtained. In this section the influence of friction on the relationships derived in section 1a will be considered by studying a steady flow process through the rotor blades of a centrifugal machine (Fig. 2.).

In the flow of any real fluid through the blades of turbines or compressor elements the properties and velocity of the fluid are not constant over any given cross-section in the flow. As the fluid molecules pass through the blade passage, those molecules in immediate contact with the blade surface are at rest relative to the blade. Thus there is relative motion between layers of molecules resulting in momentum transfer from one layer to another. This involves resistance to the flow and results in a drag force on the blade. Hence in any real flow, friction results in an uneven distribution of properties and velocity normal to the mean direction of the flow. In addition, it is the difference in static pressure at a given cross-section between the concave and convex sides of the blades, that results in blade lift.

In an account of blading performance for axial flow turbines and compressors by Shepherd¹⁹, the lift and drag forces on the blade are related to the change of whirl velocity between inlet and outlet, to give the work energy transferred. Since friction is involved it follows that the whirl components of velocity are not uniform over the inlet or outlet cross-section and the use of average values of these velocity components is implied in Shepherd's analysis. Thus Shepherd combines the effects of a non uniform distribution of fluid properties with the essentials of a one dimensional

flow treatment.

As a general example of a steady flow process with friction consider the motion of a working fluid through the rotor blades of a centrifugal compressor. The arrangement is shown in fig 2. The fluid enters at radius r_1 at the rate of m lb/sec and leaves at radius r_2 . The rotor vane is defined by the path 1 - 2, lying between the inner and outer radii and ω_v is the angular velocity of the vane. At radius r let

u = the radial velocity of the fluid.

s = the tangential velocity of the vane.

ω = the absolute angular velocity of the fluid.

v_w = the absolute tangential velocity of the fluid.

v_r = the velocity of the fluid relative to the vane.

v = the absolute velocity of the fluid.

V = the specific volume of the fluid.

ϕ = the angle between the tangent to the vane and the radius r .

and b = the breadth of the passage.

We shall presume that the properties and velocities are constant with angular position at a given radius, a state which is approached as the number of blade passages is increased. In such a one dimensional treatment it is then necessary to presume that the force of friction is concentrated at the boundary (see Rogers and Mayhew²⁰).

Thus at radius r

let f^1 = the total friction force tangential to the vane.

and F^1 = the total force normal to the vane.

As each element of mass arrives at radius r its acceleration along and perpendicular to the radius may be shown to be

$$\frac{du}{dt} - \omega^2 r \text{ and } r \frac{d\omega}{dt} + 2u\omega \text{ respectively.}$$

Thus for a continuum of particles passing through radius r the radial and tangential external forces on the fluid are

$$m (du - \omega^2 r dt) = F^1 \sin \phi - f^1 \cos \phi - dP \frac{2\pi r b}{\omega}$$

and $m (r\dot{\omega} + 2u\dot{\omega}dt) = F^1 \cos \varphi + f^1 \sin \varphi$ respectively.

This gives the radial force per unit mass flow as

$$du - \omega^2 r dt = F \sin \varphi - f \cos \varphi - \frac{dP^2}{m} \frac{r}{b} \quad (13).$$

and the tangential force per unit mass flow as

$$r\dot{\omega} + 2u\dot{\omega}dt = F \cos \varphi + f \sin \varphi \quad (14).$$

Where F and f are forces per unit mass flow.

The elemental work input at radius r per unit mass is obtained from equation 14 as

$$dWI = (r\dot{\omega} + 2u\dot{\omega}dt) r \omega_V \quad (15).$$

$$\text{now } v_W = \omega r, \quad dv_W = \omega dr + r\dot{\omega} \text{ and } udt = dr \quad (16).$$

$$\therefore dWI = (rdv_W + v_W dr) \omega_V \quad (17).$$

This well known relationship is given by Hunsaker and Rightmire²¹. In their generalized approach to the problem the external forces are obtained by considering the momentum of particles entering and leaving a control volume and the rate of change of momentum is referred to two arbitrary directions mutually at right angles. In the analysis shown here some simplification is obtained by choosing at the outset reference directions along and at right angles to the radius. Since however this involves a moving coordinate system, account must be taken in equations 13, and 14 of centrifugal and coriolis accelerations. (Shapiro²²). For turbines and compressors the control volume is the space within an annulus concentric with the axis of rotation. In Hunsaker's analysis it is assumed that the momentum within the control volume does not vary with time and that the velocity and direction of the fluid are uniform entering and leaving the control surfaces, that is at the inner and outer radii of the annulus. These assumptions are in accord with the provisions stated earlier when dealing with a one dimensional flow with friction. From the geometry of the velocity triangle at r , $u^2 + (s - v_W)^2 = v_r^2$ or in differential form

$$\therefore s dv_W + v_W ds = \omega_V (rdv_W + v_W dr) = u du + s ds + v_W dv_W - v_r dv_r \quad (18).$$

Hence from 17

$$dWI = \omega_V (r dv_W + v_W dr) = v dv + s ds - v_r dv_r \quad (19).$$

Equation 17 is an exact differential

$$\therefore WI = (s_2 v_{W_2} - s_1 v_{W_1}) = \frac{v_2^2 - v_1^2}{2} + \frac{s_2^2 - s_1^2}{2} + \frac{v_{r_1}^2 - v_{r_2}^2}{2} \quad (20).$$

From 16, and using the mass flow equation, 13 and 14 may be expressed as

$$du - \frac{v_W^2}{u} \frac{dr}{r} = F \sin \phi - f \cos \phi - \frac{dPV}{u} \quad (21).$$

and

$$dv_W + v_W \frac{dr}{r} = F \cos \phi + f \sin \phi \quad (22).$$

Eliminating F from 21 and 22 gives

$$udu - v_W^2 \frac{dr}{r} = u \tan \phi dv_W + uv_W \tan \phi \frac{dr}{r} - dPV - \frac{fu}{\cos \phi} \quad (23).$$

now $u \tan \phi = s - v_W$, $u = v_r \cos \phi$ and $\frac{dr}{r} = \frac{ds}{s}$.

Hence from 23

$$udu + v_W dv_W = s dv_W + v_W ds - dPV - f v_r \quad (24).$$

Hence from 19

$$dPV + f v_r = dWI - v dv \quad (25).$$

and

$$dPV + f v_r = s ds - v_r dv_r \quad (26).$$

Equations 25 and 26 apply to any steady flow process with friction. There is no restriction in the proof to adiabatic flow and the equations may be used where there is a combination of friction and heating from a reservoir external to the system. The steady flow energy equation gives

$$dH - dQ = dWI - v dv \quad (27).$$

$$\text{or } de + PdV + VdP - dQ = dWI - v dv \quad (28).$$

where dH and de are the changes in enthalpy and internal energy in the process and dQ is the heat supplied from an external reservoir.

Interpretation of equation 25 for steady flow compression and expansion processes.

For a compression process from 1 - 2, equation 25 gives

$$\int_1^2 dPV + \int_1^2 fv_r = WI + \frac{v_1^2 - v_2^2}{2} \quad \text{_____ (29).}$$

$WI + \frac{v_1^2 - v_2^2}{2}$ is the total high grade energy absorbed in the

compression and $\int_1^2 fv_r$ is the friction work. Thus of the total high grade energy utilized in the process a proportion of it, the friction work, is degenerated and $\int_1^2 dPV$ gives that part of the high grade energy used, which is usefully employed in creating the pressure rise. For an expansion process equation 25 is best written as

$$- dPV = dWD + vdv + fv_r \quad \text{_____ (30).}$$

or for an expansion from 1 - 2

$$\int_2^1 dPV = WD + \frac{v_2^2 - v_1^2}{2} + \int_1^2 fv_r \quad \text{_____ (31).}$$

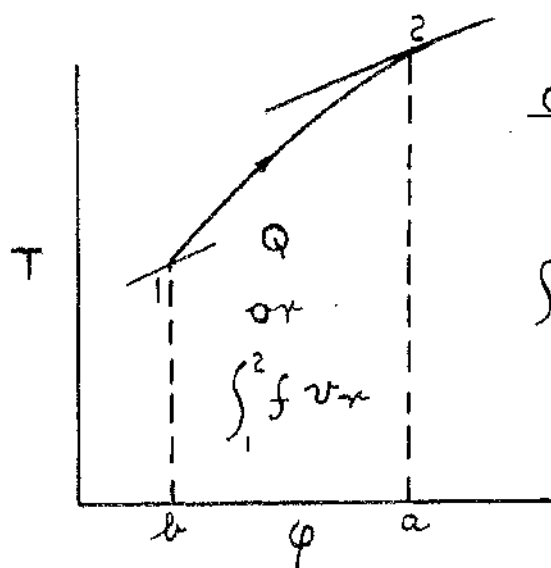
where $\int_2^1 dPV$ is a positive area on the P- V diagram.

In section 1A it was shown that for an isentropic steady flow process - $\int dPV$, (equation 12), gave the useful high grade energy released. The total high grade energy released being the sum of the useful high grade energy and the work absorbed by the fluid surroundings. In considering equations 30 or 31 a further distinction must be made. The term $\int_2^1 dPV$ may again be regarded as the total useful high grade energy which is ever released during the expansion process.

However during the process a part of this energy is degenerated by friction to low grade energy so that the net useful high

grade energy released is $\int_2^1 dPV - \int_1^2 fv_r$ or $WD + \frac{v_2^2 - v_1^2}{2}$

Comparison of an adiabatic steady flow process with friction and a similar diabatic process without friction.



$Q =$ HEAT SUPPLIED IN
DIABATIC PROCESS.

$\int_1^2 f v r =$ FRICTION WORK IN
ADIABATIC PROCESS.

FIG. 3.

Suppose that in the diabatic process the heat supplied from an external reservoir is such that the path traced out by the state point of the working fluid is the same as that in the adiabatic process.

Hence from 25

for the adiabatic, $\int_1^2 dPV + \int_1^2 fv_r = \int_1^2 (dWI - vdv)_f$ _____(32).

and for the diabatic $\int_1^2 dPV = \int_1^2 (dWI - vdv)_{f=0}$ _____(33).

For a compression process since $\int dPV$ is common 32-33, or $\int_1^2 fv_r$, gives the extra high grade energy required to effect the pressure rise.

For an expansion $\int_1^2 fv_r$ is the loss of useful high grade energy released.

From 27 for the adiabatic

$$dH = (dWI - vdv)_f \text{ _____(34).}$$

and for the diabatic

$$dH - dQ = (dWI - vdv)_f = 0 \text{ _____(35).}$$

Since dH is common 34 - 35 = 32 - 33 gives

$$\int_1^2 dQ = \int_1^2 fv_r \text{ _____(36).}$$

i.e. the friction work in the adiabatic process is equal to the low grade heat energy supplied in the diabatic process. Hence referring to figure 3, the area a 2 1 b on the T/ϕ diagram represents the heat supplied in the diabatic process or the friction work in the adiabatic process.

Interpretation of the "non-flow" energy equation applied to a system which is subjected to an adiabatic one dimensional steady flow process with friction.

For an adiabatic steady flow process with friction equations 28 and 25 give

$$0 = de + PdV - fv_r \text{ _____(37).}$$

In the non-flow adiabatic process in a closed system this equation is usually written, $o = de + dWD$. dWD is then the net total high grade energy released. Equation 37 is in accord with the conclusions₂ reached for isentropic processes in section 1a. The $\int_1^2 PdV$ again gives the total high grade energy released and includes the work absorbed by the surrounding fluid. The net useful total high grade energy released is obtained by subtracting the friction work from $\int_1^2 PdV$, and this quantity of high grade energy is obtained by depleting the store of internal energy of the system. Equation 37 may be written as

$$o + fv_r = de + PdV \quad \text{_____} (38).$$

In the form of equation 38 the friction term appears along with the external heat term suggesting that in its effect friction is of the same nature as heat. In equation 37 on the other hand friction appears as a work term. In fact friction is the mechanism whereby high grade work energy is degenerated to low grade energy and as is shown in the comparison of the diabatic and adiabatic process the effect on the working fluid, of the low grade energy created, is the same as that of supplying the same amount of heat from an external reservoir. (see equation 36).

In present day concepts heat is considered as energy in transfer across the boundary of a system. With this definition there should be no need to refer to "external" heat since all of the heat entering the system must come from an external source. In a one dimensional treatment of fluid friction the friction force occurs at the boundary and the low grade energy created could be considered as crossing into the system at the boundary. Since in the actual process however, friction occurs within the body of the fluid there would appear to be room for the terms internal heating or reheating.

The adiabatic steady flow process in axial flow turbo-machinery elements.

Equation 27 gives

$$dH + v dv = dWI \quad \text{_____ (39).}$$

$$\text{or} \quad H_{o2} - H_{o1} = WI \quad \text{_____ (40).}$$

i.e. the change in total head enthalpy is equal to the work input.

For axial flow elements where there is no appreciable radial shift equations 25, 26, and 27, which are alternative expressions for the net useful high grade energy, give

$$dH + v_r dv_r = 0 \quad \text{_____ (41).}$$

$$\text{or} \quad H_{o2r} - H_{o1r} = 0 \quad \text{_____ (42).}$$

i.e. the relative stagnation enthalpy remains constant across the moving blade row, the relative stagnation enthalpy being that obtained by complete diffusion of the relative velocity.

From 25, 26 and 27 the total high grade energy involved may be expressed as :-

For compression:-

$$\text{the total high grade energy absorbed is}$$

$$WI + \frac{v_1^2 - v_2^2}{2} = \int_1^2 dPV + \int_1^2 f v_r = \frac{v_{r1}^2 - v_{r2}^2}{2} = H_2 - H_1 \quad \text{_____ (43)}$$

and for an expansion :-

$$\text{the net useful high grade energy released is}$$

$$WD + \frac{v_2^2 - v_1^2}{2} = \int_2^1 dPV - \int_1^2 f v_r = \frac{v_{r2}^2 - v_{r1}^2}{2} = H_1 - H_2 \quad \text{_____ (44)}$$

Comparison of an adiabatic flow process and a similar isentropic process for axial flow elements.

Consider an adiabatic steady flow process (1 - 2) and an isentropic process from the same inlet state point to the same final pressure. (see figures 4A and 4B).

For the isentropic compression process the high grade energy absorbed is

$$WI_s + \frac{v_1^2 - v_2^2}{2} = \int_1^{2s} dPV_s = \frac{v_{r1}^2 - v_{r2s}^2}{2} = H_{2s} - H_1 \quad (45).$$

and for the isentropic expansion the useful high grade energy released is

$$WD_s + \frac{v_{2s}^2 - v_1^2}{2} = \int_{2s}^1 dPV_s = \frac{v_{r2s}^2 - v_{r1}^2}{2} = H_1 - H_{2s} \quad (46).$$

From 43 and 45 the extra high grade energy required in adiabatic compression compared with the isentropic compression is

$$43 - 45 = \int_1^2 f v_r + \int_1^2 dP(V - V_s) = \frac{v_{r2s}^2 - v_{r2}^2}{2} = H_2 - H_{2s} \quad (47).$$

and this is a loss of initial high grade energy.

For the expansions the loss of useful high grade energy released is

$$46 - 44 = \int_1^2 f v_r - \int_2^1 dP(V - V_s) = \frac{v_{r2s}^2 - v_{r2}^2}{2} = H_2 - H_{2s} \quad (48).$$

The loss of useful high grade energy in 47 and 48 is known as the enthalpy loss.

Referring to figures 4a and 4b the enthalpy loss may be divided into the basic friction work loss in the process,

($\int_1^2 f v_r$ = area a2lb on the T/ϕ diagram), plus an auxiliary

loss term, ($\int_1^2 dP(V - V_s)$ = area 122_s on the P/V or T/ϕ

diagrams), which is the result of the "heating" effect of the friction work. Kearton²³ refers briefly to this division of the enthalpy loss for compressions. For the expansion process, fig 4b, the auxiliary term is negative showing that the increase in specific volume causes some of the basic friction work loss to be returned as useful high grade energy. In similar expansion and compression processes therefore, where the basic friction work is the same, the loss of high grade energy will be greatest in the compression process.

Section 2 - Summary.

In a steady flow process in the elements of turbo-machinery the friction work is given by $\int f v_r$ where f is the friction force per unit mass and v_r the velocity of the working fluid relative to the moving blade. Friction is the mechanism by which high grade energy is degenerated to low grade energy. The low grade energy produced is equal in magnitude to the friction work and causes an increase in the internal energy and in the specific volume of the working fluid. This "heating" effect of friction is the same as that which would occur in a diabatic process without friction where the heat supplied from an external reservoir is equal in magnitude to the friction work. In a steady flow compression process, where one is interested in the efficient utilization of available high grade energy to create a pressure rise, the friction work is that proportion of the total high grade energy used, which is degenerated and does not produce pressure rise. The high grade energy which is usefully absorbed is given by $\int dPV$.

For the steady flow expansion process the term $-\int dPV$ gives the total useful high grade energy ever produced during the process. During the process however, part of this energy, the friction work, is degenerated and the difference $(-\int VdP - \int f v_r)$ is the net useful high grade energy released. Comparing a steady adiabatic flow process with a similar isentropic process, the loss of useful high grade energy is given by

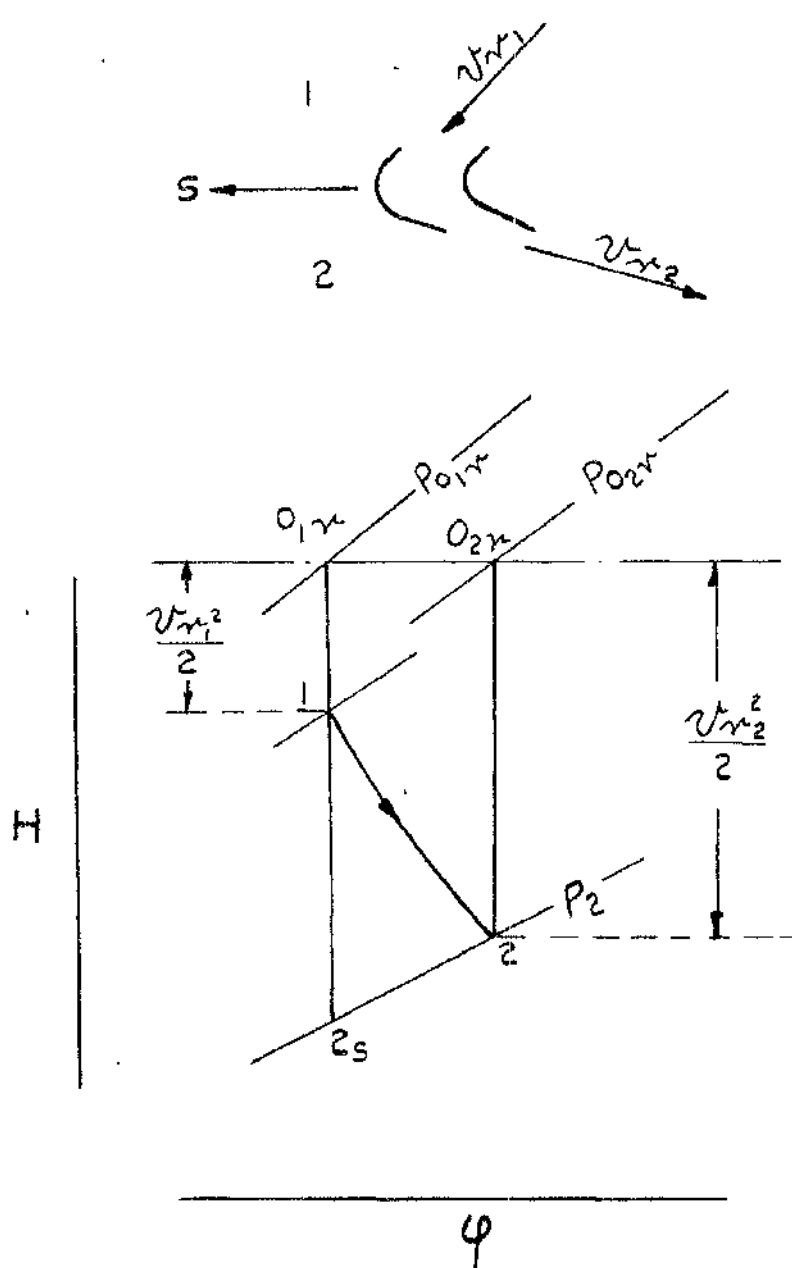
$$\int f v_r + \int dP(V - V_s).$$

The "heating" effects of the basic friction work loss causes an increase in the specific volume of the working fluid so that the actual specific volume (V) is greater than the isentropic specific volume (V_s). Hence the loss of high grade energy may be divided into a friction work term plus

an auxiliary loss term reflecting this heating effect of the friction work. In compressions the auxiliary loss term is positive so that friction results in more high grade energy being required. In expansions the auxiliary loss term is negative and there is a return of some of the friction work as useful high grade energy.

PART 1 (b).

Losses and loss coefficients in axial flow turbo-machinery elements - a review of the methods used to express losses in blade elements and their interrelationships.



ADIABATIC EXPANSION (1-2) IN THE ROTOR BLADE OF A TURBINE STAGE.

FIG. 5.

Part 1 (b).

Losses and Loss Coefficients in Axial Flow Turbo-Machinery Elements. - A review of the methods used to express losses in blade elements and their interrelationships.

Section 1.-The axial flow turbine blade element.

Consider a steady adiabatic expansion in the rotor blade of an axial flow turbine stage from inlet state point 1 to the state point 2. (fig 5).

The loss of useful high grade energy known as the enthalpy loss is given by equation 48 as

$$\int_1^2 f v_r - \int_2^1 dP(V - V_s) = \frac{v_{r2s}^2}{2} - \frac{v_{r2}^2}{2} = H_2 - H_{2s}$$

dividing by $\frac{v_{r2}^2}{2}$ this gives

$$\frac{H_2 - H_{2s}}{\frac{v_{r2}^2}{2}} = \frac{\frac{1}{2}}{\frac{v_{r2}^2}{v_{r2s}^2}} - 1 \quad \text{--- (49).}$$

The ratio $\frac{H_2 - H_{2s}}{\frac{v_{r2}^2}{2}} = \xi$ is known as the enthalpy loss

coefficient. The ratio $\frac{v_{r2}}{v_{r2s}} = K$, is the blade velocity

coefficient and the ratio $\frac{v_{r2}^2}{v_{r2s}^2} = \zeta$ or is the relative

total head efficiency of expansion in the moving blade.

Equation 49 gives the relationship between these methods of expressing the loss as

$$\xi = \frac{H_2 - H_{2s}}{\frac{v_{r2}^2}{2}} = \frac{1}{K^2} - 1 = \frac{1}{\zeta} - 1 \quad \text{--- (50).}$$

ζ or

The irreversibility in the expansion may also be expressed

as the increase in entropy during expansion i.e. as

$\phi_2 - \phi_{2s}$ or $\phi_2 - \phi_1$. For this adiabatic process the change in entropy is entirely due to internal friction effects and is sometimes called the internal entropy change. It can be shown that, where such an irreversible increase in entropy occurs in a cycle, the loss of cycle work is given by the product of the change in entropy and the lowest temperature at which heat is rejected in the cycle.

From figure 5 assuming the relationships for a perfect gas the entropy increase is given by

$$\phi_2 - \phi_{2s} = c_p \log_e \frac{T_2}{T_{2s}} \quad (51).$$

Equation 42 gives $H_{o2r} = H_{o1r}$ or $T_{o2r} = T_{o1r}$ and, while

there is no change in relative total head temperature across the moving blade row, the drop in relative total head pressure affords another way of expressing the loss.

From 51

$$\begin{aligned} \phi_2 - \phi_{2s} &= c_p \log_e \frac{T_2}{T_{o2r}} \times \frac{T_{o1r}}{T_{2s}} = c_p \log_e \left(\frac{p_{o1r}}{p_{o2r}} \right)^{\frac{\gamma-1}{\gamma}} \\ \therefore \phi_2 - \phi_{2s} &= -c_p \log_e \left(1 - \frac{H_2 - H_{2s}}{H_2} \right) \\ &= c_p \log_e \left(1 + \frac{p_{o1r} - p_{o2r}}{p_{o2r}} \right)^{\frac{\gamma-1}{\gamma}} \quad (52). \end{aligned}$$

This relates the entropy increase with the enthalpy loss and with the loss in relative total head pressure. This loss in relative total head pressure furnishes a useful method of determining losses in practice and is usually expressed as a total head pressure loss coefficient defined as

$$y = \frac{p_{o1r} - p_{o2r}}{\frac{1}{2} \rho_2 v_{r2}^2} \quad (53).$$

Substituting in 52 for the enthalpy loss and total head pressure loss from 50 and 53 respectively gives

$$\begin{aligned}\phi_2 - \phi_{2s} &= -c_p \log_e \left(1 - \frac{\epsilon v_{r2}^2}{c_p T_2} \right) \\ &= c_p \log_e \left(1 + \frac{\gamma \frac{1}{2} \rho_2 v_{r2}^2}{p_{02r}} \right)^{\frac{\gamma-1}{\gamma}} \quad (54).\end{aligned}$$

This gives

$$\begin{aligned}\phi_2 - \phi_{2s} &= -c_p \log_e \left(1 - \epsilon \frac{\gamma-1}{2} M_{2r}^2 \right) \\ &= c_p \log_e \left(1 + \frac{\gamma \frac{\gamma}{2} M_{2r}^2}{\left(1 + \frac{\gamma-1}{2} M_{2r}^2 \right)^{\gamma/(\gamma-1)}} \right)^{\frac{\gamma-1}{\gamma}} \quad (55).\end{aligned}$$

Where M_{2r} is the relative outlet Mach number.

Equation 52 relates the losses while equation 55 relates the corresponding loss coefficients. Useful approximate relationships may be obtained from these equations using the series expression for $\log(1+x)$ where x is small.

Hence approximately from 52 and 55

$$\begin{aligned}\therefore \phi_2 - \phi_{2s} &= \frac{H_2 - H_{2s}}{T_2} = R \left(\frac{p_{01r} - p_{02r}}{p_{02r}} \right) = \epsilon R \frac{\gamma}{2} M_{2r}^2 \\ &= \frac{\gamma R \frac{\gamma}{2} M_{2r}^2}{\left(1 + \frac{\gamma-1}{2} M_{2r}^2 \right)^{\gamma/(\gamma-1)}} \quad (56).\end{aligned}$$

Hence approximately

$$\gamma = \epsilon \left(1 + \frac{\gamma-1}{2} M_{2r}^2 \right)^{\frac{\gamma}{\gamma-1}} \quad (57).$$

and when $M_{2r} < 1$

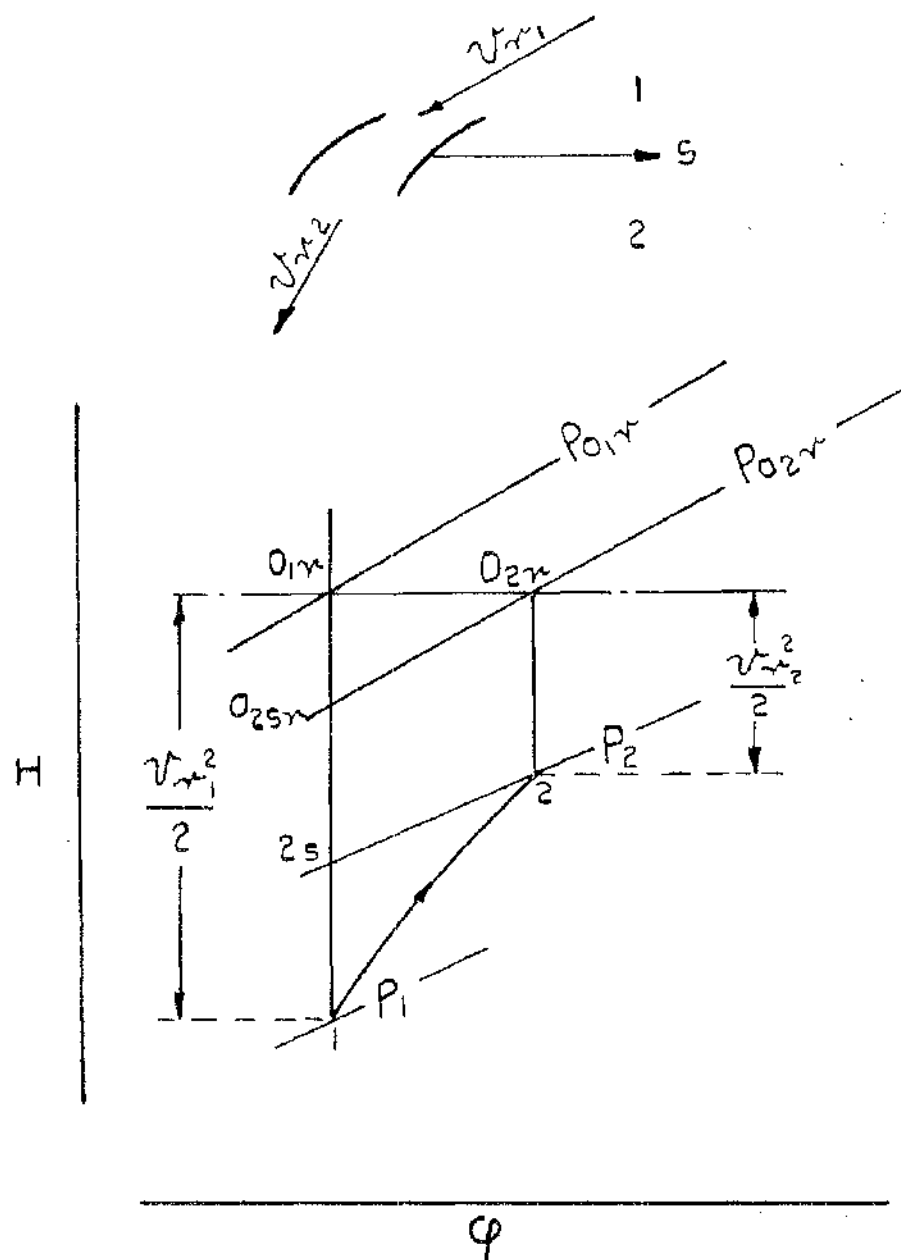
$$\gamma = \epsilon \left(1 + \frac{\gamma}{2} M_{2r}^2 \right) \quad (58).$$

and for incompressible flow

$$\gamma = \epsilon \quad (59).$$

A further method of expressing the irreversibility in the blade is the use of a blade drag coefficient (C_D). This is given in terms of the pressure loss coefficient (γ) as

$$C_{D\text{①}} = \gamma p/c \frac{\cos^3 \alpha_m}{\cos^2 \alpha_2} \quad (60).$$



ADIABATIC COMPRESSION (1-2) IN THE
ROTOR BLADE OF A COMPRESSOR STAGE.

FIG. 6.

where p/c is the pitch to chord ratio for the blade, α_m the mean direction of the fluid as it passes through the blade and α_2 the fluid efflux angle, the angles being measured from the axial direction.

The enthalpy and total head pressure loss coefficients are sometimes defined as

$$\zeta_s = \frac{H_2 - H_{2s}}{\frac{1}{2} v_{r2s}^2} \quad \text{--- (61).}$$

$$\text{and } Y_s = \frac{p_{01r} - p_{02r}}{\frac{1}{2} \rho_{2s} v_{r2s}^2} \quad \text{--- (62).}$$

If these definitions are used relationships similar to those above are obtained but in terms of the relative isentropic outlet Mach number M_{2sr} .

Section 2 - The axial flow compressor element.

Consider an adiabatic steady flow compression process in the rotor blades of an axial flow compressor stage from the inlet state point 1 to state point 2 (fig 6).

In the compression 1 - 2 the loss of high grade energy compared with an isentropic compression from state point 1 to the same outlet static pressure is given by equation 47 as

$$\text{Enthalpy loss} = H_2 - H_{2s} \quad \text{--- (63).}$$

In compressions however one is often concerned with the energy absorbed in the actual adiabatic process in reaching the final outlet total head pressure. Compared with an isentropic compression from state point 1 to the outlet total head pressure the loss is given by

$$\text{"total head" enthalpy loss} = H_{02r} - H_{02sr} \quad \text{--- (64).}$$

The general expression for enthalpy loss is given in equation 47 as

$$\int f v_r + \int dP (V - V_s)$$

In equations 63 and 65 the friction work term is common (as is the entropy increase) but because the specific volume V_2 is greater than the specific volume V_{2s} the auxiliary loss term is greater in 64. Hence $H_{o2r} - H_{o2sr} > H_2 - H_{2s}$

In compressions either of these definitions of enthalpy loss may be used and they are related approximately by the expression

$$H_{o2r} - H_{o2sr} = \frac{T_{or}}{T_2} (H_2 - H_{2s}) \quad \text{_____ (65).}$$

For the compression the enthalpy loss coefficient is defined

as
$$\xi_c = \frac{H_{o2r} - H_{o2sr}}{\frac{1}{2} v_{r1}^2}$$

$$\text{Thus } \xi_c = \frac{H_{o2r} - H_{o2sr}}{\frac{1}{2} v_{r1}^2} = 1 - \frac{H_{o2sr} - H_1}{H_{o1r} - H_1} = 1 - \zeta_{orc} \quad \text{_____ (50d)}$$

where ζ_{orc} is the relative total head efficiency of compression for the moving blade.

The total head pressure loss coefficient for a compression is defined as

$$\gamma_o = \frac{p_{o1r} - p_{o2r}}{\frac{1}{2} \rho_1 v_{r1}^2} \quad \text{_____ (53c).}$$

By methods similar to that for an expansion process it may be shown that the entropy increase is related to the enthalpy and total head pressure losses by the relationship

$$\begin{aligned} \phi_2 - \phi_{2s} &= -c_p \log_e \left(1 - \frac{H_{o1r} - H_{o2sr}}{H_{o1r}} \right) \\ &= -c_p \log_e \left(1 - \frac{p_{o1r} - p_{o2r}}{p_{o1r}} \right)^{\frac{\gamma-1}{\gamma}} \quad \text{_____ (52c).} \end{aligned}$$

and substituting in 52c for the enthalpy and pressure losses from 50c and 53c gives

Part 1(b) - Summary.

The loss of useful high grade energy in a rotating turbine blade passage is variously expressed as an increase in entropy, a blade velocity coefficient, an enthalpy loss coefficient or as a total head pressure loss coefficient. The relationships between these various methods for expressing the loss are given in equations 50 and 55. They may be applied to a static nozzle or blade row in which case the relative velocities, Mach numbers etc become absolute values. Approximate relationships between the coefficients which suffice in many applications are given in equations 56 to 59.

The method by which the loss in the blade row is expressed has historical associations with the techniques of loss measurement available at the time to the research worker. The earliest method was that used by the steam turbine designer in which he "worked back" from overall test figures to determine the efficiencies of the elements. Later the impulse plate method was used to determine the total force of the jet issuing from a nozzle or blade. Here the loss was expressed as a nozzle or blade velocity coefficient. With the advent of the gas turbine, with its associated pitot tube technique for loss determination, the losses are given as a total head pressure loss coefficient. When comparing data from these sources it should be borne in mind that the steam turbine data may be obtained from high speed tests whereas the gas turbine cascade tests are usually for Mach numbers less than 0.5. Before making a comparison therefore, Mach number effects should be accounted for by applying equation 57. In addition, results from tests using the impulse plate method give three dimensional loss in the blade. Horlock²⁴, who has previously summarized for the turbine nozzle or moving blade the relationships given in this section, points out that the results apply to an imaginary two dimensional flow having the same flow rate and overall losses as the actual stream. In a three dimensional

flow there is a small discrepancy between the square of the velocity coefficient and the total head efficiency. This discrepancy increases with decrease in nozzle efficiency. Values for this discrepancy are given by Kearton²⁵.

With regard to the total head efficiency of the nozzle or blade row Kearton²⁶ uses a different method to express the loss. He splits the total loss into two parts. The first part is the loss of kinetic energy between the outlet of the previous row and the immediate inlet to the row under consideration. This loss is accounted for by using a carry over coefficient. The remainder of the total loss is then attributed to effects within the blade passage.

Horlock points out that this division of the total loss is artificial since the boundary layer behaviour within the blade is dependant on the entry flow. In addition it has been shown here that the bulk of the blade passage loss is given by $\int f v_r$ and the average value of v_r within the passage is affected by the entry velocity.

Loss coefficients and efficiencies for axial flow compressor blading are defined in this section and their inter-relationship is given in equations 50c and 55c, the corresponding approximate forms are given in equations 56c and 59c. Most of the present data on compressor blade loss is for low speed flow (Mach number < 0.5) where the loss is expressed as a total head pressure loss coefficient. However there is a tendency at present for the operating Mach numbers to greatly exceed 0.5. This in turn necessitates high speed cascade testing where it may be convenient to express the loss as an enthalpy loss coefficient.

In turbine and compressor rotor blade elements (figs 5 and 6) the high grade energy released (or absorbed) in the process is given by the enthalpy difference $H_1 - H_2$ (or $H_2 - H_1$) and for each case the loss of high grade energy is given by

$H_2 - H_{2s}$. On the other hand the quantities $H_{o1r} - H_2$
 (and $H_{o1r} - H_1$) which appear in the definitions of relative
 total head efficiency cannot be expressed in terms of high
 grade energy associated with the moving blade. The loss
 in the rotor blade however depends largely on the term
 $\int f v_r$ which suggest that the blade be examined in a static
 test rig, where the pressure and temperature at inlet are the
 same as those for the moving blade, but where the inlet
 velocity is made equal to the actual inlet relative velocity.
 In this case the quantities $H_{o1r} - H_2$ and $H_{o1r} - H_1$ are the
 high grade energy released or absorbed respectively in the
 static test rig, in expansion or compression from or to the
 total head pressure. Again in the compressor element (figure
 6) two definitions for enthalpy loss are given. These are
 the enthalpy loss $H_2 - H_{2s}$ and the "total head" enthalpy loss
 $H_{o2r} - H_{o2rs}$. The relationship between them is given in
 equation 65. The total head loss has a meaning in terms of
 high grade energy only for a simulated static test on the
 element. These points are referred to again in the
 definitions of efficiency given in the next section.

PART 1 (o).

Efficiencies in axial flow turbine and compressor stages. ----

A method of expressing the efficiency of the flow process in the stage and the interrelationships between the process efficiency, the stage efficiency and the blading efficiency.

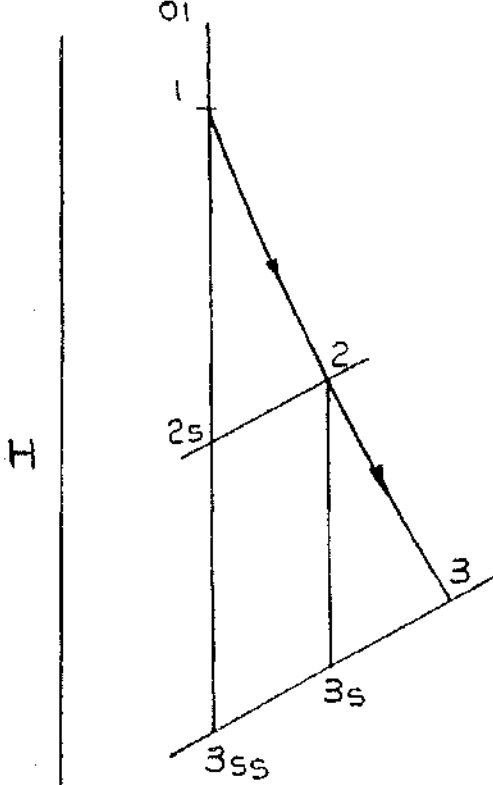


FIGURE 7A
(THE STAGE).

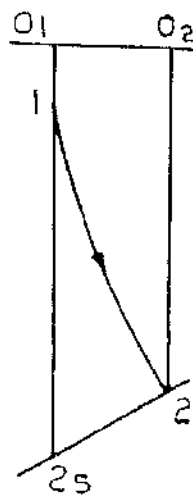


FIGURE 7B
(THE NOZZLE
BLADE)

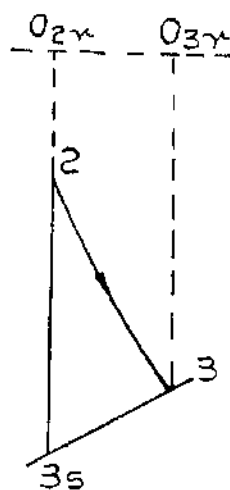


FIGURE 7C
(THE ROTOR BLADE
-RELATIVE
ENTHALPIES.)

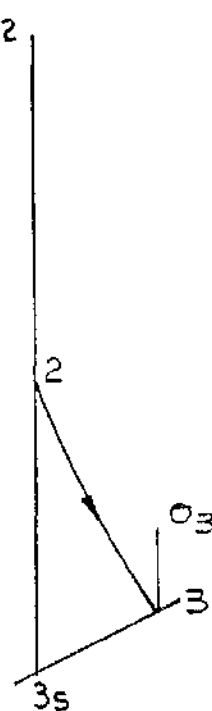


FIGURE 7D
(THE ROTOR
BLADE)

ϕ

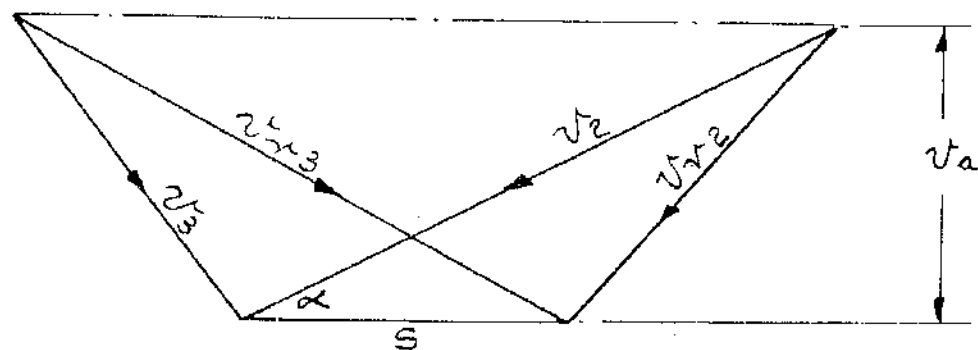
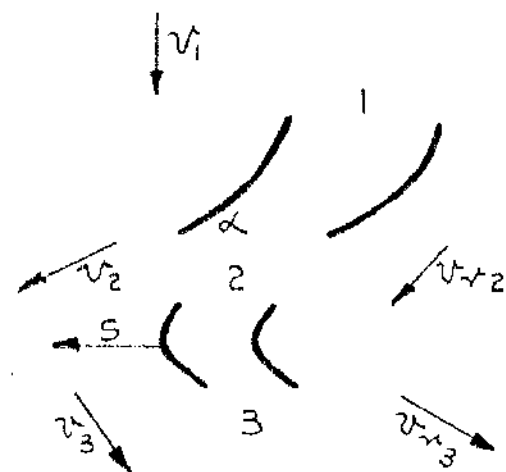


FIGURE 7E

THE AXIAL FLOW TURBINE STAGE.

FIG. 7.

Section 1. - Efficiencies in the Turbine Stage.

The function of the following section is to correlate the various ways in which the efficiency of a turbine stage may be defined and to relate these efficiencies to the losses in the individual elements which comprise the stage. Definitions of the efficiency of a turbine stage depend on the application for which the stage is intended. The function of most turbine stages, one possible exception being the turbine of a turbo-jet engine, is the efficient production of mechanical work energy and stage efficiency definitions reflect this fact. In all turbine stages however one is concerned with a steady flow process in the stage and in the elements which comprise the stage. At the outset here an efficiency definition for the steady flow process is given which is applicable either to the nozzle row, the moving blade row or to the stage, and which is independent of the use made of the stage.

Consider the turbine stage shown in figure 7. The working fluid enters the turbine nozzle at condition 1, total head condition 01, and expands adiabatically to the state point 3 at outlet from the moving row.

(1) The efficiency of expansion.

The efficiency of the expansion process in the nozzle (N), or in the rotor blade (R) or in the stage (s) may be defined as

$$\eta = \frac{\text{Net useful high grade energy released in adiabatic expansion from the inlet condition to the exhaust pressure.}}{\text{Useful high grade energy released in isentropic expansion from the inlet condition to the exhaust pressure.}}$$

Hence from equation 44

for the nozzle (fig 7B)

$$\eta_N = \frac{H_1 - H_2}{H_1 - H_{2s}} = \frac{1}{1 + \frac{H_2 - H_{2s}}{H_1 - H_2}} \quad (66).$$

For the rotor blade (fig 7D)

$$\zeta_R = \frac{H_2 - H_3}{H_2 - H_{3s}} = \frac{1}{1 + \frac{H_3 - H_{3s}}{H_2 - H_3}} \quad (67).$$

and for the stage (fig 7A)

$$\zeta_s = \frac{H_1 - H_3}{H_1 - H_{3ss}} = \frac{1}{1 + \frac{H_3 - H_{3ss}}{H_1 - H_3}} \quad (68).$$

Expression for the stage efficiency of expansion in terms of the losses in the elements.

The increase in entropy for the stage is

$$\phi_3 - \phi_{3ss} = \phi_3 - \phi_{3s} + \phi_2 - \phi_{2s}$$

Hence from equation 56

$$H_3 - H_{3ss} = H_3 - H_{3s} + \frac{T_3}{T_2} (H_2 - H_{2s}) \quad (69).$$

Hence from 68 and 69

$$\zeta_s = \frac{1}{1 + \frac{\frac{T_3}{T_2} (H_2 - H_{2s}) + H_3 - H_{3s}}{H_1 - H_3}} \quad (70).$$

and from 67, 68, and 70

$$\zeta_s = \frac{1}{\frac{T_3}{T_2} \left(\frac{1}{\zeta_N} - 1 \right) (1 - R) + \left(\frac{1}{\zeta_R} - 1 \right) R} \quad (71).$$

where R is the degree of reaction for the stage

$$\text{defined as } R = \frac{H_2 - H_3}{H_1 - H_3} \quad (72).$$

alternatively from 70 and 50

$$\zeta_s = \frac{1}{\frac{T_3}{T_2} \left(\frac{\epsilon_N \frac{v_2^2}{2}}{H_1 - H_3} \right) + \frac{\epsilon_R \frac{v_{r3}^2}{2}}{H_1 - H_3}} \quad (73).$$

(2) The total head efficiency of expansion.

In many instances one is more concerned with the final high grade energy available at the end of a process rather than with the energy released during the process.

The final available high grade energy is obtained by rearranging equation 44 as

$$H_{o1} - H_2 = WD + \frac{v_2^2}{2} \quad \text{--- (74).}$$

H_{o1} being the enthalpy corresponding to the state point reached after isentropic diffusion of the inlet absolute velocity.

The total head efficiency of expansion for the nozzle rotor blade, or stage, may be defined as

$$\zeta_o = \frac{\text{Final available high grade energy obtained in adiabatic expansion from the inlet total head state to the exhaust pressure.}}{\text{Final available high grade energy obtained in isentropic expansion from the inlet total head state to the exhaust pressure.}}$$

This gives

for the nozzle (fig 7B).

$$\zeta_{oN} = \frac{H_{o1} - H_2}{H_{o1} - H_{2s}} = \frac{1}{1 + \frac{H_2 - H_{2s}}{H_{o1} - H_2}} \quad \text{--- (75).}$$

for the rotor blade (fig 7D).

$$\zeta_{oR} = \frac{H_{o2} - H_3}{H_{o2} - H_{3s}} = \frac{1}{1 + \frac{H_3 - H_{3s}}{H_{o2} - H_3}} \quad \text{--- (76).}$$

and for the stage (fig 7A).

$$\zeta_{os} = \frac{H_{o1} - H_3}{H_{o1} - H_{3ss}} = \frac{1}{1 + \frac{H_3 - H_{3ss}}{H_{o1} - H_3}} \quad \text{--- (77).}$$

Hence from 69

$$\zeta_{os} = \frac{1}{1 + \frac{\frac{T_3}{T_2} (H_2 - H_{2s}) + H_3 - H_{3s}}{H_{o1} - H_3}} \quad (78).$$

from 75 this gives

$$\zeta_{os} = \frac{1}{1 + \frac{\frac{T_3}{T_2} \left(\frac{1}{\zeta_{oN}} - 1 \right) (1 - Ro) + \frac{H_3 - H_{3s}}{H_{o1} - H_3}}{}} \quad (79).$$

Where Ro , the "total head" degree of reaction is defined as

$$Ro = \frac{H_2 - H_3}{H_{o1} - H_3}, \quad (80).$$

From 67

$$\zeta_{os} = \frac{1}{1 + \frac{\frac{T_3}{T_2} \left(\frac{1}{\zeta_{oN}} - 1 \right) (1 - Ro) + \left(\frac{1}{\zeta_R} - 1 \right) Ro}{}} \quad (81).$$

Alternatively from 78 and 50

$$\zeta_{os} = \frac{1}{\frac{\frac{T_3}{T_2} \left(\frac{\epsilon_N \frac{v_2^2}{2}}{H_{o1} - H_3} \right) + \frac{\epsilon_R \frac{v_{r3}^2}{2}}{H_{o1} - H_3}}{}} \quad (82).$$

In figure 70 the appropriate relative total head enthalpies for the expansion process in the rotor blade are shown.

It will be noted that the definition of total head efficiency of expansion for the moving blade, given by equation 76, is not the same as the relative total head efficiency (ζ_{or}) which is related to the loss coefficients for the blade in equation 50. As has been pointed out previously the enthalpy drop $H_{o1r} - H_2$ cannot be expressed in terms of the release of high grade energy and the relative total head efficiency should be regarded as the total head efficiency of expansion obtained in a simulated static test rig.

(3) Stage efficiency - the turbine as a producer of mechanical work energy.

The efficiencies of expansion in the stage, which are related above to the irreversibilities in the flow through the elements of the stage, are concerned with the production of high grade energy. This high grade energy is a combination of mechanical work energy and kinetic energy and in the design of the stage one tries to ensure that as much as possible of the high grade energy appears as mechanical work.

The stage efficiency (distinct from the efficiency of expansion in the stage) is defined as

$$\eta = \frac{\text{Actual mechanical work output}}{\text{Ideal mechanical work output}}$$

The actual mechanical work output is given from equation 40 as $H_{o1} - H_{o3} = WD$. The ideal mechanical work output depends on the history of the exhaust kinetic energy after the working fluid leaves the moving row. This kinetic energy ($\frac{v_3^2}{2}$) is known as the leaving kinetic energy, or carry over kinetic energy. The total to static stage efficiency.

For single stage turbines which are not fitted with an exhaust diffuser, or for partial admission stages of steam turbines, where in each case the exhaust kinetic energy is degraded by friction, the final condition of the working fluid is given by the state point 3x (figure 8). The stage enthalpy loss is increased by $\frac{v_3^2}{2}$ and the ideal work output is $H_{o1} - H_{3ss}$.

For this case the stage efficiency is known as the "total to static" efficiency (η_{ts}) and is given by

$$\eta_{ts} = \frac{WD}{WD_{(ideal)}} = \frac{H_{o1} - H_{o3}}{H_{o1} - H_{3ss}} = \frac{1}{1 + \frac{H_3 - H_{3ss}}{H_{o1} - H_{o3}} + \frac{v_3^2}{2(H_{o1} - H_{o3})}}$$

or

$$\eta_{ts} = \frac{1}{1 + \frac{T_3}{T_2} \left(\frac{\xi_N \frac{v_2^2}{2}}{H_{01} - H_{03}} \right) + \frac{\xi_R \frac{v_{r3}^2}{2}}{H_{01} - H_{03}} + \frac{\frac{v_3^2}{2}}{H_{01} - H_{03}}} \quad (84).$$

The total to total stage efficiency.

For cases where the exhaust kinetic energy is not degraded, e.g. in a single stage turbine fitted with an exhaust diffuser, or in a multistage turbine where the nozzle blades are designed to absorb the leaving kinetic energy, the effective stage exhaust pressure is P_{03} . (fig. 8).

The ideal work output is then given by an isentropic expansion from state point 01 to the total head exhaust pressure P_{03} . This is given approximately by $H_{01} - H_{3ss} - \frac{v_3^2}{2}$

and the stage efficiency which is known as the "total to total" efficiency is given by

$$\eta_{tt} = \frac{H_{01} - H_{03}}{H_{01} - H_{3ss} - \frac{v_3^2}{2}} = \frac{1}{1 + \frac{H_3 - H_{3ss}}{H_{01} - H_{03}}} \quad (85).$$

or

$$\eta_{tt} = \frac{1}{1 + \frac{T_3}{T_2} \left(\frac{\xi_N \frac{v_2^2}{2}}{H_{01} - H_{03}} \right) + \frac{\xi_R \frac{v_{r3}^2}{2}}{H_{01} - H_{03}}} \quad (86).$$

This definition of total to total stage efficiency in terms of the loss coefficients of the elements is due to Hawthorne²⁷.

Special application of the total to total efficiency.

For the particular case of a typical stage in a multistage turbine, which is designed for a constant carry over velocity, the total to total efficiency given by 85 reduces to

$$\eta_{tt} = \frac{H_1 - H_3}{H_1 - H_{3ss}} = \eta_s \quad (87).$$

i.e. the total to total efficiency is then identical with the efficiency of expansion in the stage.

(4) The blading or diagram efficiency.

For a given ideal stage isentropic heat drop, $H_{o1} - H_{3ss}$, the total head efficiency of expansion in the stage determines the high grade energy made available. It is the function of the rotor blade to convert some of this high grade energy into mechanical work energy. The blading or diagram efficiency is defined here as

$$\eta_B = \frac{\text{Mechanical work energy produced}}{\text{Total high grade energy available to the rotor blade.}}$$

i.e.

$$\eta_B = \frac{WD}{H_{o1} - H_3} = \frac{H_{o1} - H_{o3}}{H_{o1} - H_3} = 1 - \frac{\frac{v_3^2}{2}}{H_{o1} - H_3} \quad \text{--- (88).}$$

This definition of blading efficiency differs somewhat from that normally used for impulse stages, but is considered by the writer to have a wider application for both turbine and compressor stages. A comparison with the usual impulse definition is given in subsection 6.

(5) Relationships between the expansion efficiency, the blading efficiency and the stage efficiencies.

From 83, 87 and 77

$$\eta_{ts} = \frac{H_{o1} - H_{o3}}{H_{o1} - H_{3ss}} = \frac{H_{o1} - H_{o3}}{H_{o1} - H_3} \times \frac{H_{o1} - H_3}{H_{o1} - H_{3ss}}$$

$$\therefore \eta_{ts} = \eta_B \times \eta_{os} \quad \text{--- (89).}$$

From 85 and 77

$$\eta_{tt} = \frac{H_{o1} - H_{o3}}{H_{o1} - H_{3ss} - \frac{v_2^2}{2}} = \frac{\eta_{os} - \frac{v_3^2/2}{H_{o1} - H_{3ss}}}{1 - \frac{v_3^2/2}{H_{o1} - H_{3ss}}} \quad \text{--- (90).}$$

and from 88 and 77

$$(1 - \zeta_B) \zeta_{os} = \frac{v_3^2/2}{H_{o1} - H_{3ss}} \quad (91).$$

Hence from 90 and 91

$$\zeta_{tt} = \frac{\zeta_{os} - (1 - \zeta_B) \zeta_{os}}{1 - (1 - \zeta_B) \zeta_{os}} \quad (92).$$

or from 89

$$\zeta_{tt} = \frac{\zeta_{ts}}{1 - \zeta_{os} + \zeta_{ts}} = \frac{\frac{1}{\zeta_B} \zeta_{os}}{(1 - \zeta_{os}) + \zeta_{os}} \quad (93).$$

(6) Design parameters and the "impulse" stage.

Consider an axial flow turbine stage where the axial velocity is constant. (figure 7).

Design Parameters. Important design parameters for the stage are :-

The total head degree of reaction, $R_o = \frac{H_2 - H_3}{H_{o1} - H_3}$

The blade speed to jet speed ratio, $\rho = \frac{s}{v_2}$

The work done factor or loading factor, $Z = \frac{WD}{s^2/2}$

The blading or diagram efficiency, $\zeta_B = \frac{WD}{H_{o1} - H_3}$

If values of R_o and ρ are chosen for the stage then the stage velocity triangles may be drawn to an unknown scale. Thus the initial choice of R_o and ρ determines all the velocity ratios in the stage, from which the loading factor and blading efficiency may also be obtained. The total head degree of reaction may be negative, zero or positive corresponding to the velocity ratio v_3/v_{r2} being < 1 , $= 1$ or > 1 respectively.

Enthalpy changes in the stage. If any one of the stage velocities or any one of the energy quantities involved in the design parameters (e.g. the blade speed or the specific

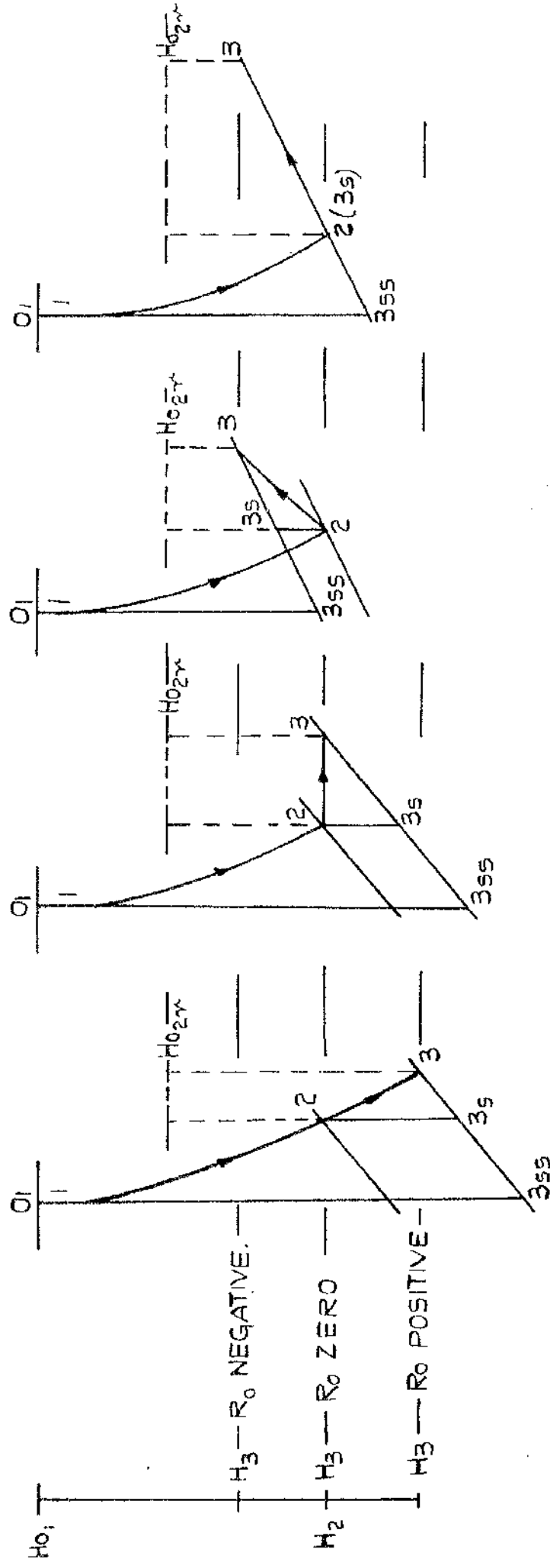


FIGURE 9A.

FIGURE 9B.

FIGURE 9C.

FIGURE 9D.

FIGURE 9E.

POSSIBLE PRESSURE CHANGES IN THE TURBINE STAGE

CORRESPONDING TO POSITIVE, NEGATIVE AND ZERO DEGREES OF REACTION.

FIG. 9.

work output) is chosen, then the magnitude of all velocities and energy quantities for the stage are determined. This being so the enthalpy changes across the nozzle row and moving blade row are known. In figure 9A enthalpy levels corresponding to positive, negative and zero degrees of reaction are shown. When the degree of reaction is positive the quantity $H_2 - H_3$ is known as the reaction effect. For negative degrees of reaction the quantity $H_3 - H_2$ is called here the compression effect.

Pressure changes in the stage. The pressure changes across the nozzle and blade row depend in the first instance on the location of the process in the H / ϕ field. When however the initial state point is known the enthalpy changes and element losses are the controlling factors. Possible pressure changes corresponding to positive and zero degree of reaction are shown in figures 9B and 9C respectively. For negative degrees of reaction possible pressure changes are shown in figures 9D and 9E. To encompass these possibilities the total head efficiency of expansion for the stage is best retained in the form of equation 79. i.e. as

$$\zeta_{os} = \frac{1}{1 + \frac{T_3}{T_2} \left(\frac{1}{\zeta_{oN}} - 1 \right) (1 - Ro) + \frac{H_3 - H_{3s}}{H_{o1} - H_3}} \quad (79).$$

In this equation the expression

$$\frac{H_3 - H_{3s}}{H_{o1} - H_3} = Ro \left(\frac{H_2 - H_{3s}}{H_2 - H_3} - 1 \right) \quad (94).$$

is the fractional stage loss occurring in the moving blade.

Ro positive figure 9B. For positive values of Ro equation 94 gives

$$\frac{H_3 - H_{3s}}{H_{o1} - H_3} = Ro \left(\frac{1}{\zeta_R} - 1 \right) \quad (95).$$

where ζ_R is the efficiency of expansion in the moving blade.

Ro = 0, figure 9C. For zero degree of reaction equation 94 gives

$$\frac{H_3 - H_{3s}}{H_{o1} - H_3} = \frac{H_2 - H_{3s}}{H_{o1} - H_3} \quad \text{--- (96).}$$

where $H_2 - H_{3s}$ is the isentropic enthalpy drop in the moving blade. This enthalpy drop corresponds to the pressure drop required to maintain a constant relative velocity in the moving blade passage. The zero reaction stage may be regarded as a special case of a stage with a pressure drop in the moving blade where the efficiency of expansion in equation 95 is zero.

Ro negative, figure 9D. Where Ro is negative there is a pressure rise in the moving blade passage and equation 94 may be written

$$\frac{H_3 - H_{3s}}{H_{o1} - H_3} = -Ro \left(1 - \frac{H_{3s} - H_2}{H_3 - H_2}\right) = -Ro (1 - \zeta_{cR}) \quad \text{--- (97).}$$

where ζ_{cR} is the efficiency of compression in the rotor blade. When the degree of reaction is negative it is better to work in terms of a degree of compression defined as

$$R_{oc} = \frac{H_3 - H_2}{H_{o1} - H_3} \quad \text{--- (98).}$$

in which case equation 97 reduces to

$$\frac{H_3 - H_{3s}}{H_{o1} - H_3} = R_{oc} (1 - \zeta_{cR}) \quad \text{--- (99).}$$

If the efficiency of compression in the blade passage is zero then there is no pressure rise in the blade passage and we are dealing with the zero pressure drop impulse stage. (figure 9E). Equation 99 then gives

$$\frac{H_3 - H_{3s}}{H_{o1} - H_3} = \frac{H_3 - H_2}{H_{o1} - H_3} = R_{oc} \quad \text{--- (100).}$$

The zero pressure drop impulse stage should therefore

be regarded as a special case of a stage designed to have a compression effect in the blade passage, where the efficiency of compression is zero.

In such an impulse stage the blade passage loss is often expressed in terms of a blade velocity coefficient defined

as $K = v_{r3}/v_{r2}$.

It will be noted that this definition for the zero pressure

drop blade is identical with $K = v_{r3}/v_{r3s}$ which is the

general definition used in equation 50. For the zero pressure drop impulse stage the usual definition of blading efficiency is

$$\eta'_B = \frac{H_{o1} - H_{o3}}{H_{o1} - H_2} \quad \text{--- (101). (Kearton}^{28}\text{).}$$

$H_{o1} - H_2$ being the kinetic energy available to the moving blade.

For the total to static efficiency in the stage this gives

$$\eta_{ts} = \eta_{oN} \times \eta'_B \quad \text{--- (102)}$$

This relationship is similar in form to the expression given here for total to static efficiency (equation 89) which may also be applied to the zero pressure drop impulse stage. This is

$$\eta_{ts} = \eta_{os} \times \eta_B \quad \text{--- (89).}$$

Equation 101 may be shown to give

$$\eta'_B = \frac{1}{1 + \frac{\epsilon_R \frac{v_{r3}^2}{2} + \frac{v_3^2}{2}}{H_{o1} - H_{o3}}} \quad \text{--- (103). (Horlock}^{24}\text{).}$$

while from equation 88

$$\eta_B = \frac{1}{1 + \frac{v_3^2/2}{H_{o1} - H_{o3}}} \quad \text{--- (104).}$$

It will be seen from equation 103 that the usual definition of blading efficiency for the impulse stage includes a term to account for the blade passage loss. Thus when using this definition it is assumed at the outset that it will not be possible to recover, as useful pressure rise, some of the energy associated with the compressor effect available to the rotor blade, so that all of the available compression effect becomes irreversible enthalpy loss.

Section 1 - Summary.

Definitions of efficiency of expansion (equation 68) and of total head efficiency of expansion (equation 77) for a turbine stage are given, which account for the irreversibilities of the flow process in the stage and which are independent of the application for which the turbine is intended. Since the definitions are for the flow process they may be applied to the individual elements of the stage. The efficiency of expansion for the stage is given in terms of the element efficiencies and degree of reaction in equation 71 and is related to the loss coefficients of the elements in equation 73. For the total head efficiency of expansion in the stage the corresponding relationships are given in equations 81 and 82, where equation 81 involves the total head degree of reaction.

Thus for a given total head stage isentropic heat drop ($H_{01} - H_{3ss}$, figure 7) the total head efficiency of expansion determines the total amount of high grade energy made available to the rotor blade. The blading or diagram efficiency, defined in equation 88, then determines the proportion of this high grade energy which appears as mechanical work energy, the remainder being retained by the working fluid as leaving kinetic energy.

Two definitions of stage efficiency (as distinct from efficiency of expansion in the stage) are given. Here one is concerned with the ratio of actual to ideal work obtained in the stage. In applications where the leaving kinetic energy is degraded the total to static stage efficiency is the criterion of performance and where the exhaust kinetic energy is not degraded the total to total stage efficiency is used. The relationship between the total to total stage efficiency and the loss coefficients in the elements is due to Hawthorne²⁷ and is given here in equation 86.

The total to static and total to total stage efficiencies are related to the blading efficiency and total head stage

VARIATION IN TOTAL TOTAL AND TOTAL TO STATIC STAGE EFFICIENCY WITH BLADING
EFFICIENCY FOR DIFFERENT VALUES OF THE TOTAL HEAD EFFICIENCY OF
EXPANSION IN THE STAGE

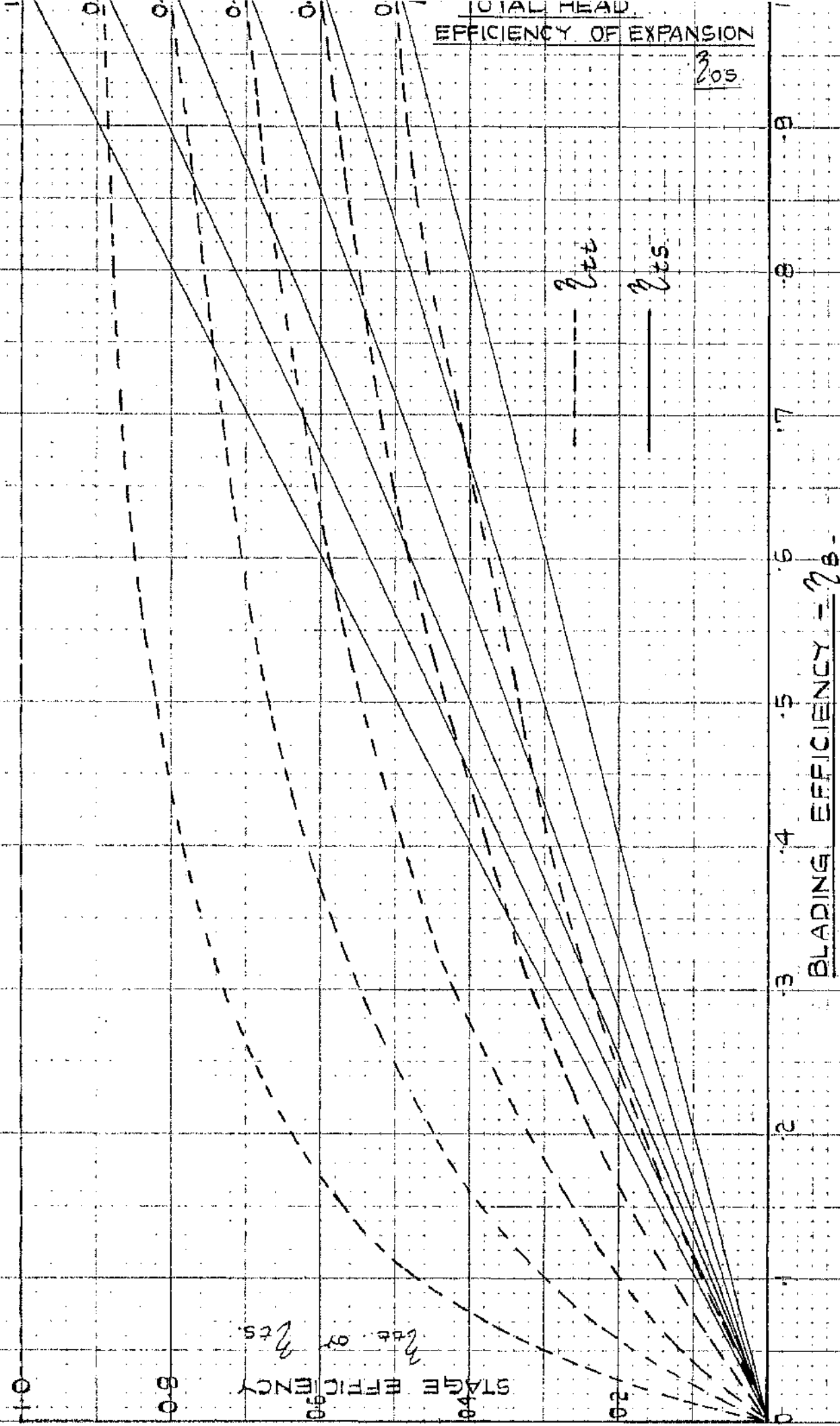


FIG. 10.

efficiency of expansion in equations 89 and 93. It will be seen that if the total head efficiency of expansion is assumed constant then as the blading efficiency increases both stage efficiencies also increase. Hence from the point of view of stage efficiency it is desirable to design the turbine stage for maximum blading efficiency.

The actual variation in the stage efficiencies with blading efficiency, for different values of the total head efficiency of expansion, is shown in figure 10. It will be noted that, whereas the total to static stage efficiency varies directly with the blading efficiency, the rate of change of total to total stage efficiency depends on the blading efficiency range. For high values of blading efficiency (above say 0.6) the variation in total to total efficiency is small. This variation does however increase as the efficiency of expansion decreases.

It has been shown that a choice of total head degree of reaction and of blade speed to jet speed ratio determine the form of the stage velocity triangles and the blading efficiency. It follows from this that as the blading efficiency varies, the deflection suffered by the gas in the blading elements will change. The effect of this variation in gas deflection on the loss coefficients in the elements, should be taken account of in assessing the variation in stage efficiencies with blading efficiency.

There are two possible definitions of an impulse stage. The "pure" impulse stage should be taken as one where the degree of reaction is zero. In practice this means that a pressure drop across the blade passage is necessary to maintain the relative velocity constant within the passage. The traditional impulse stage, where there is no pressure drop across the moving blade, should be regarded as a special case of a blade

which is designed to utilize an increase in enthalpy (or compression effect) in the blade passage, but where the efficiency of the compression process is zero.

Section 2, - The Axial Flow Compressor Stage.

The axial flow compressor stage as a "reversed" turbine stage.

Consider the axial flow turbine stage shown in figure 11A. As discussed in the previous section a choice of total head degree of reaction, blade speed to jet speed ratio and specific work done determines all the velocities and enthalpy changes in the stage. If all the stage velocities are somehow maintained in magnitude but reversed in direction the stage will operate as a compressor stage in which the enthalpy increases in the rotor and stator blades will be equal in magnitude to the corresponding enthalpy drops in the turbine stage. Using the nomenclature of the turbine stage the velocities of the corresponding compressor stage are shown in figure 11B. It will be noted that the enthalpy increases in the elements of the compressor stage are determined by the choice of total head degree of reaction, blade speed to jet speed ratio and specific work output for the turbine stage. The pressure changes in the elements of the stages depend on the element losses as well as on the enthalpy changes in the elements. Thus, while we may consider that the velocities of the compressor stage are the reverse of those in the turbine stage, neither stage is reversible in the thermodynamic sense.

A complete comparison between the stages is obtained if the turbine is fitted with an exhaust diffuser to utilize the leaving kinetic energy $v_3^2/2$. The exhaust diffuser of the turbine stage is equivalent to the inlet guide or nozzle blades, which precede the rotor blade, in the compressor stage.

It will be noted that (a) the velocity (v_3) entering the compressor stage rotor blade is equivalent to the velocity entering the turbine stage diffuser and (b) the velocity (v_1) leaving the compressor stage diffuser is equivalent to the velocity of approach to the turbine stage nozzles. This

H

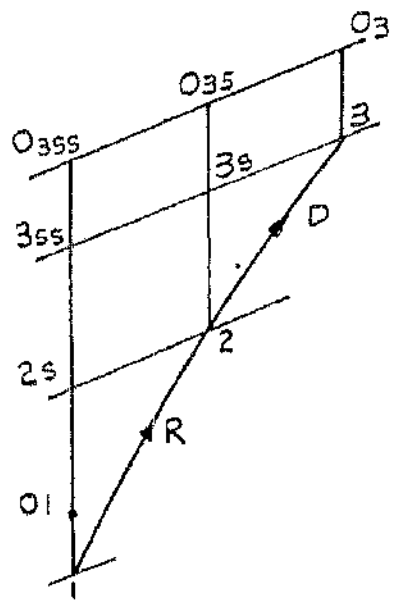


FIGURE 12A
(THE STAGE.)

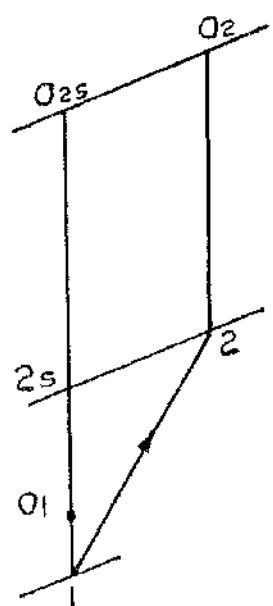


FIGURE 12B.
(THE ROTOR
BLADE)

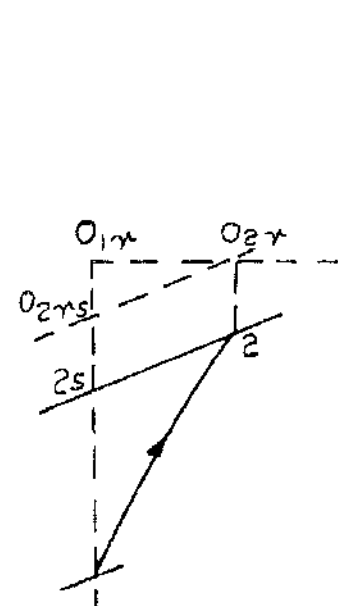


FIGURE 12C.
(THE ROTOR BLADE
RELATIVE
ENTHALPIES)

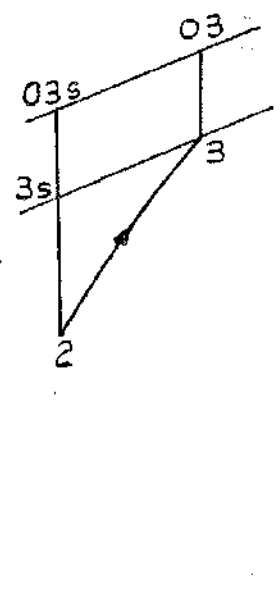


FIGURE 12D.
(THE STATOR
OR DIFFUSER
BLADE)

ϕ

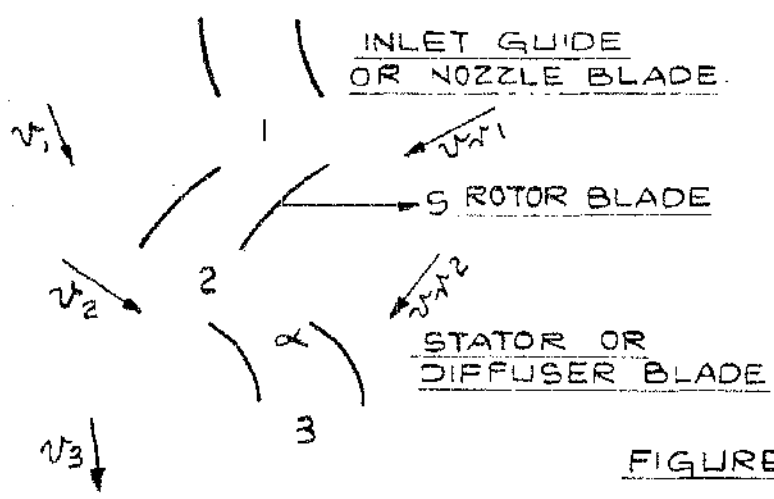


FIGURE 12 E

THE AXIAL FLOW COMPRESSOR STAGE.

FIG. 12.

velocity does not appear in the velocity triangles.

Efficiencies in the axial flow compressor stage.

Consider the axial flow compressor stage shown in figure 12. The working fluid enters the rotor blade (R) at condition 1, and leaves at condition 2. The fluid passes through the diffuser blade (D) leaving this blade at condition 3. In the rotor blade, stator blade or in the stage we are interested in the efficient utilization of available high grade energy. The high grade energy available to the rotor blade or to the stage is the kinetic energy at 1 plus the work input to the rotor blade. The high grade energy available to the diffuser blade is the kinetic energy leaving the rotor blade. In either of the elements or in the stage part of the total high grade energy initially available remains at outlet as directional kinetic energy when the compression process ceases.

(1) Efficiency of compression.

For any one element or for the stage the efficiency of the compression process may be defined as

$$\eta_c = \frac{\text{Total high grade energy absorbed during isentropic compression from the inlet condition to the exhaust pressure.}}{\text{Actual total high grade energy absorbed in adiabatic compression from the inlet condition to the exhaust pressure.}}$$

Hence from 43

for the diffuser blade (figure 12D)

$$\eta_{cD} = \frac{H_{3s} - H_2}{H_3 - H_2} = 1 - \frac{H_3 - H_{3s}}{H_3 - H_2} \quad (66c).$$

for the rotor blade (figure 12B)

$$\eta_{cR} = \frac{H_{2s} - H_1}{H_2 - H_1} = 1 - \frac{H_2 - H_{2s}}{H_2 - H_1} \quad (67c).$$

and for the stage (figure 12A)

$$\eta_{cs} = \frac{H_{3ss} - H_1}{H_3 - H_1} = 1 - \frac{H_3 - H_{3ss}}{H_3 - H_1} \quad (68c).$$

2. Total head efficiency of compression.

If at outlet of either of the elements or of the stage the remaining kinetic energy is absorbed in a reversible manner the pressure attained is the maximum actual pressure possible from the process. The actual exhaust total head pressure is thus the maximum pressure which can be reached in the actual process when all of the available high grade energy at inlet is absorbed. In the total head efficiency of compression a comparison is made between the actual available high grade energy at inlet and the ideal high grade energy, which should be available at inlet, to attain the same total head pressure.

Thus the total head efficiency of compression for either element or for the stage is defined as

$$\eta_{oc} = \frac{\text{Total high grade energy required at inlet to attain in isentropic compression the total head exhaust pressure of the actual process.}}{\text{Actual total high grade energy required at inlet to attain in adiabatic compression the actual exhaust total head pressure.}}$$

Thus for the diffuser blade (figure 12D)

$$\eta_{ocD} = \frac{H_{o3s} - H_2}{H_{o3} - H_2} = 1 - \frac{H_{o3} - H_{o3s}}{H_{o3} - H_2} \quad (75c).$$

for the rotor blade (figure 12B)

$$\eta_{ocR} = \frac{H_{o2s} - H_1}{H_{o2} - H_1} = 1 - \frac{H_{o2} - H_{o2s}}{H_{o2} - H_1} \quad (76c).$$

and for the stage (figure 12A)

$$\eta_{ocs} = \frac{H_{o3ss} - H_1}{H_{o3} - H_1} = 1 - \frac{H_{o3} - H_{o3ss}}{H_{o3} - H_1} \quad (77c).$$

Relationships between the element efficiencies of compression and the stage efficiencies of compression.

Using equations 65 and 56c it may be shown that approximately

$$H_3 - H_{3ss} = H_3 - H_{3s} + \frac{T_3}{T_2} (H_2 - H_{2s})$$

and

$$H_{o3} - H_{o3ss} = H_{o3} - H_{o3s} + \frac{T_{o3}}{T_2} (H_2 - H_{2s}) \quad (69c).$$

Hence for the efficiency of compression in the stage 68c and 69c give

$$\eta_{cs} = 1 - \frac{H_3 - H_{3s} + \frac{T_3}{T_2} (H_2 - H_{2s})}{H_3 - H_1} \quad (70c).$$

This may be expressed in terms of the element efficiencies given in equations 66c and 67c as

$$\eta_{cs} = 1 - ((1 - \eta_{oD}) (1 - R_c) + \frac{T_3}{T_2} (1 - \eta_{oR}) R_c) \quad (71c).$$

where R_c is the degree of compression for the stage defined as

$$R_c = \frac{H_2 - H_1}{H_3 - H_1} \quad (72c).$$

alternatively η_{cs} may be expressed in terms of the total head enthalpy loss coefficients (equation 50c). It is shown in equation 65 that approximately

$$H_2 - H_{2s} = \frac{T_2}{T_{o2r}} (H_{o2r} - H_{o2sr}) = \frac{T_2}{T_{o2r}} \epsilon_{cR} \frac{v_{r1}^2}{2}$$

and

$$H_3 - H_{3s} = \frac{T_3}{T_{o3}} (H_{o3} - H_{o3s}) = \frac{T_3}{T_{o3}} \epsilon_{oD} \frac{v_2^2}{2}$$

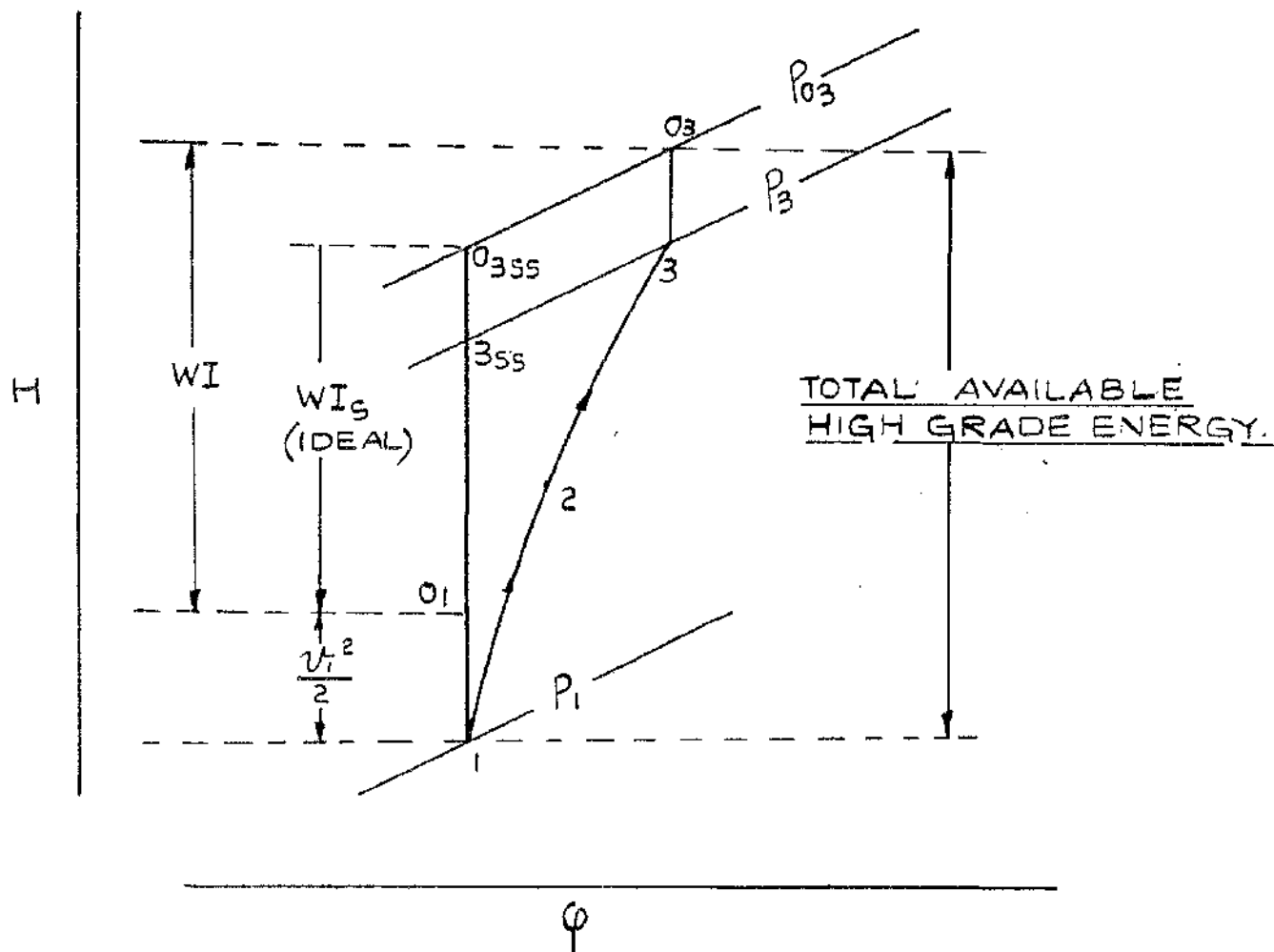
Hence from 70c

$$\eta_{cs} = 1 - \left[\frac{T_3}{T_{o3}} \left(\frac{\epsilon_{oD} v_2^2/2}{H_3 - H_1} \right) + \frac{T_3}{T_2} \left(\frac{T_2}{T_{o2}} \left(\frac{\epsilon_{cR} v_{r1}^2/2}{H_3 - H_1} \right) \right) \right] \quad (73c).$$

By similar methods the corresponding relationships may be obtained for the total head efficiency of compression.

These are

$$\eta_{ocs} = 1 - \frac{H_{o3} - H_{o3s} + \frac{T_{o3}}{T_2} (H_2 - H_{2s})}{H_{o3} - H_1} \quad (78c).$$



IDEAL WORK INPUT IN "TOTAL TO TOTAL"
STAGE EFFICIENCY DEFINITION FOR A COMPRESSOR.

FIG. 13.

$$\text{or } \zeta_{ocs} = 1 - \left[(1 - \zeta_{ocD}) (1 - R_{oc}) + \frac{T_{o3}}{T_2} (1 - \zeta_{cR}) R_{oc} \right] \quad (81c)$$

where the total head degree of compression is defined as

$$R_{oc} = \frac{H_2 - H_1}{H_{o3} - H_1} \quad (80c)$$

$$\text{and } \zeta_{ocs} = 1 - \left[\left(\frac{\zeta_{ocD} \frac{v_2^2}{2}}{H_{o3} - H_1} \right) + \frac{T_{o3}}{T_2} \left(\frac{T_2}{T_{o2r}} \left(\frac{\zeta_{cR} \frac{v_{r1}^2}{2}}{H_{o3} - H_1} \right) \right) \right] \quad (82c)$$

3. Blading efficiency, total to total and total to static efficiency in the compressor stage.

Blading efficiency. In the design of a turbine stage it is desirable to arrange for a high value of the blading efficiency. The velocity triangles for the stage and the blading efficiency are fixed by a choice of total head degree of reaction, blade speed to jet speed ratio, and specific work done, the blading efficiency being a function of degree of reaction and blade speed to jet speed ratio only. Thus for a given specific work output a choice of blading efficiency for the stage in effect means choosing a value for the stage leaving velocity. If this same design is used as a compressor stage, by maintaining the magnitude of the velocities but reversing their directions, the work input in the compressor stage will be equal in magnitude to the work output in the turbine stage, and the inlet absolute velocity (v_1 figure 13) to the compressor stage rotor blade will be determined by the initial choice of blading efficiency.

The blading or diagram efficiency for the compressor stage is defined as

$$\zeta_B = \frac{WI}{WI + \frac{v_1^2}{2}} = \frac{H_{o3} - H_{o1}}{H_{o3} - H_1} \quad (88c).$$

Thus the blading efficiency for the compression stage gives

the proportion of the total high grade energy, available at inlet to the stage, which is mechanical work energy. The total to total efficiency for the compressor stage.

While the efficiencies of the compression process in the stage have involved the total high grade energy available to the stage, it is with the efficient use of mechanical work energy that we are mainly concerned.

The total to total efficiency for the compressor stage is defined as

$$\eta_{\text{ctt}} = \frac{\text{Minimum work input required to attain the actual outlet total head pressure of the stage.}}{\text{Actual work input required to reach the same total head pressure.}}$$

Thus $\eta_{\text{ctt}} = \frac{W_{\text{is}}}{W_{\text{I}}} \quad (\text{see figure 13}).$

$$\text{or } \eta_{\text{ctt}} = \frac{H_{o3ss} - H_{o1}}{H_{o3} - H_{o1}} = 1 - \frac{H_{o3} - H_{o3ss}}{H_{o3} - H_{o1}} \quad (85c).$$

and the efficiency may be expressed in terms of the loss coefficients in the elements as

$$\eta_{\text{ctt}} = 1 - \left(\frac{\epsilon_{cD} \frac{v_2^2}{2}}{H_{o3} - H_{o1}} + \frac{T_{o3}}{T_2} \left(\frac{T_2}{T_{o2r}} - \frac{\epsilon_{cR} \frac{v_{r1}^2}{2}}{H_{o3} - H_{o1}} \right) \right) \quad (86c).$$

If the total to total stage efficiency is applied to a typical stage in a multistage compressor where the "carry over" velocity is constant then

$$\eta_{\text{ctt}} = \frac{H_{o3ss} - H_{o1}}{H_{o3} - H_{o1}} = \frac{H_{3ss} - H_1}{H_3 - H_1} = \eta_{\text{cs}} \quad (87c).$$

i.e. the total to total stage efficiency is the same as the efficiency of compression in the stage.

The total to static efficiency in the compressor stage.

In the case of a single stage turbine one has a choice of fitting or not fitting an exhaust diffuser. For the single stage compressor however the inlet nozzle or guide vanes

are an essential part of the stage. The roll of these nozzle vanes for a typical stage in a multistage compressor is assumed by the preceeding stage. Hence there is no parallel in the compressor stage for the total to static efficiency of the turbine stage.

Relationship between blading efficiency, total to total stage efficiency and total head efficiency of compression in the compressor stage.

From 85c and 77c

$$\eta_{ott} = \frac{1 - \frac{v_1^2/2}{H_{o3ss} - H_1}}{\eta_{ocs} - \frac{v_1^2/2}{H_{o3ss} - H_1}} \quad (90c).$$

and from 88c and 77c

$$\therefore \frac{1 - \eta_B}{\eta_{ocs}} = \frac{v_1^2/2}{H_{o3ss} - H_1} \quad (91c).$$

This gives

$$\eta_{ott} = 1 - \frac{(1 - \eta_{ocs})}{\eta_B} \quad (93c).$$

Hence from the stage efficiency view-point it is desirable to work with high values of blading efficiency, which means in effect operating the stage with a low approach velocity at inlet to the rotor blade.

Section 2 - Summary.

An analogy between the axial flow turbine and compressor stage is given, which is a useful tool with which to study the effect in the compressor stage of the stage design parameters. The compressor stage is considered as a similar turbine stage where the velocity vectors of the turbine stage are reversed in direction. If the two design parameters, the total head degree of reaction and the blade speed to jet speed ratio are chosen for the turbine stage then the form of the velocity triangles, the blading efficiency and the loading factor are determined for both the turbine stage and its compressor counterpart. This approach facilitates the interpretation of the role of the compressor stage elements. For example, it is evident that the inlet guide or nozzle blades of the compressor stage are equivalent to the exhaust diffuser of the turbine stage. The analogy would be complete for a turbine and similar compressor stage where there were no losses in the elements, so that each stage was also reversible in the thermodynamic sense. Then the pressure drops associated with the turbine stage would be equal in magnitude to the corresponding pressure increases in the compressor stage.

In dealing with efficiencies in the compressor stage, the procedure adopted is the same as that used in the turbine stage. Definitions are given of the efficiencies of the compression process in the elements and in the stage, and the interrelationships between the stage and element efficiencies are developed. The total head efficiency of compression in the stage is given in equation 97c and is related to the element losses in equations 81c and 82c.

In the total head efficiency of compression we are concerned with the high grade energy available at inlet to the stage to effect a pressure rise. This high grade energy is the sum of the work input to the stage and the kinetic energy generated in the inlet nozzle blades, which precede

the stage. The proportion of kinetic energy to work energy in the available high grade energy depends on the initial choice for the blading efficiency of the stage. Since however we are particularly concerned with the work energy absorbed, a definition of total to total stage efficiency is given which is the ratio of the minimum to the actual work required to attain the maximum possible stage pressure. (equation 85c). A relationship between the total to total stage efficiency, the blading efficiency and the total head efficiency of compression in the stage is given in equation 93c. It will be seen that, for a constant total head efficiency of compression, the stage efficiency increases as the blading efficiency increases.

With regard to the total to total stage efficiency it will be noted that the definition given here is similar to one which is sometimes called the "total head efficiency of the stage". This latter efficiency is however usually applied from the state point at inlet to the stationary nozzle blades and would therefore take account of losses in these blades.

In a turbine stage the total to static efficiency is the criterion of performance where there is no exhaust diffuser. In a compressor stage however, kinetic energy must be generated at inlet to the rotor blade and hence the equivalent in the compressor stage of the turbine exhaust diffuser must always be present. There is thus no parallel in the compressor stage for the total to static efficiency of the turbine stage.

PART 1 (d).

Conditions for maximum blading efficiency in axial flow turbines and compressors - factors affecting the choice of design parameters for the stage.

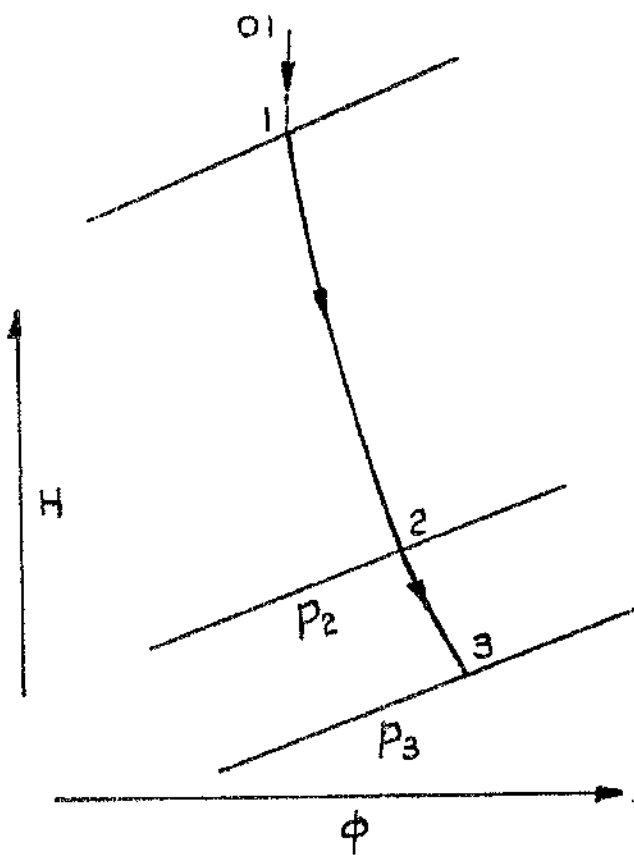
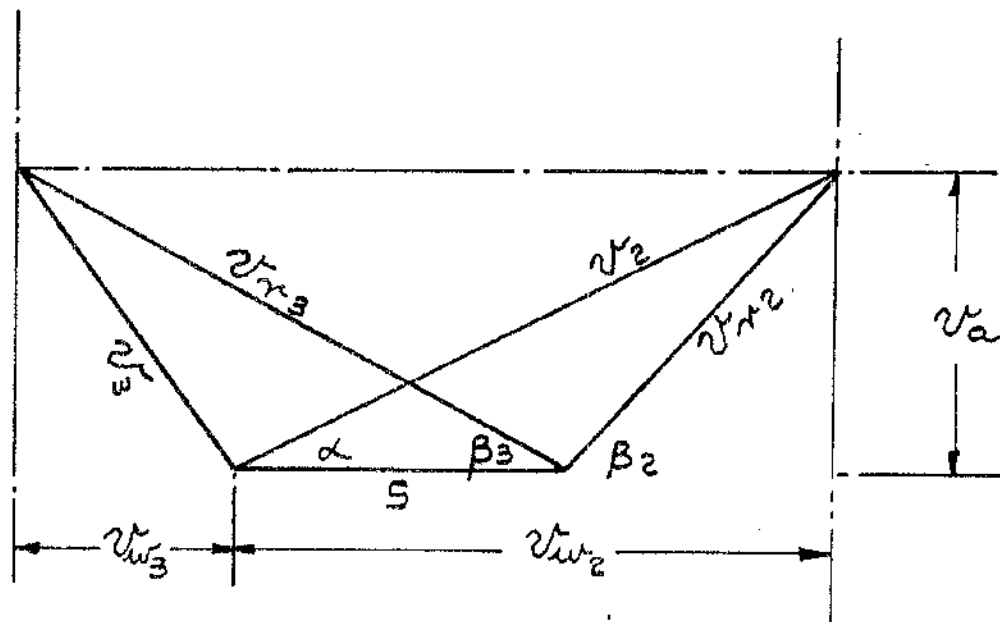
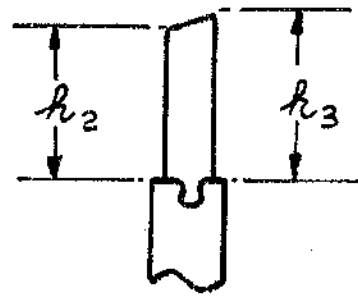
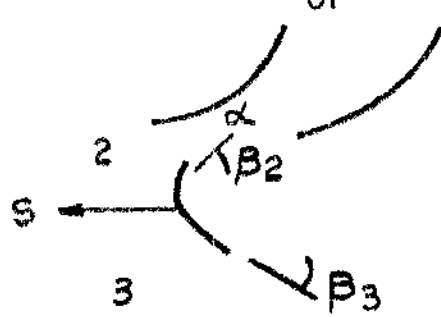


FIG. 14.

Part 1 (d).

Conditions for maximum blading efficiency in axial flow turbines and compressors - factors affecting the choice of design parameters for the stage.

(1). The blading efficiency. Consider the axial flow turbine stage shown in figure 14. We shall presume that the stage axial velocity is constant, which means that the blade heights at inlet and outlet are adjusted to nullify the effect of the change in specific volume across the moving blade. The reaction effect in the moving blade is

$H_2 - H_3 = \frac{v_{r3}^2 - v_{r2}^2}{2}$ and we shall define a reaction coefficient (G) given by

$$G = \frac{H_2 - H_3}{H_{01} - H_2} = \frac{\frac{v_{r3}^2 - v_{r2}^2}{2}}{\frac{v_2^2}{2}} \quad \text{---(105).}$$

The work done is given by

$$WD = s (v_{r3} \cos \beta_3 + v_{w2} - s) \quad \text{---(106).}$$

From 105

$$v_a^2 + (v_{r3} \cos \beta_3)^2 - (v_a^2 + (v_{w2} - s)^2) = G v_2^2$$

$$\therefore v_3 \cos \beta_3 = \sqrt{\frac{G v_{w2}^2}{\cos^2 \alpha} + (v_{w2} - s)^2} \quad \text{---(107).}$$

Hence from 106

$$WD = s \left(\sqrt{\frac{G v_{w2}^2}{\cos^2 \alpha} + (v_{w2} - s)^2} + v_{w2} - s \right) \quad \text{---(108).}$$

using the blade speed to tangential jet speed ratio

$$\bar{v} = s/v_{w2} \text{ this gives}$$

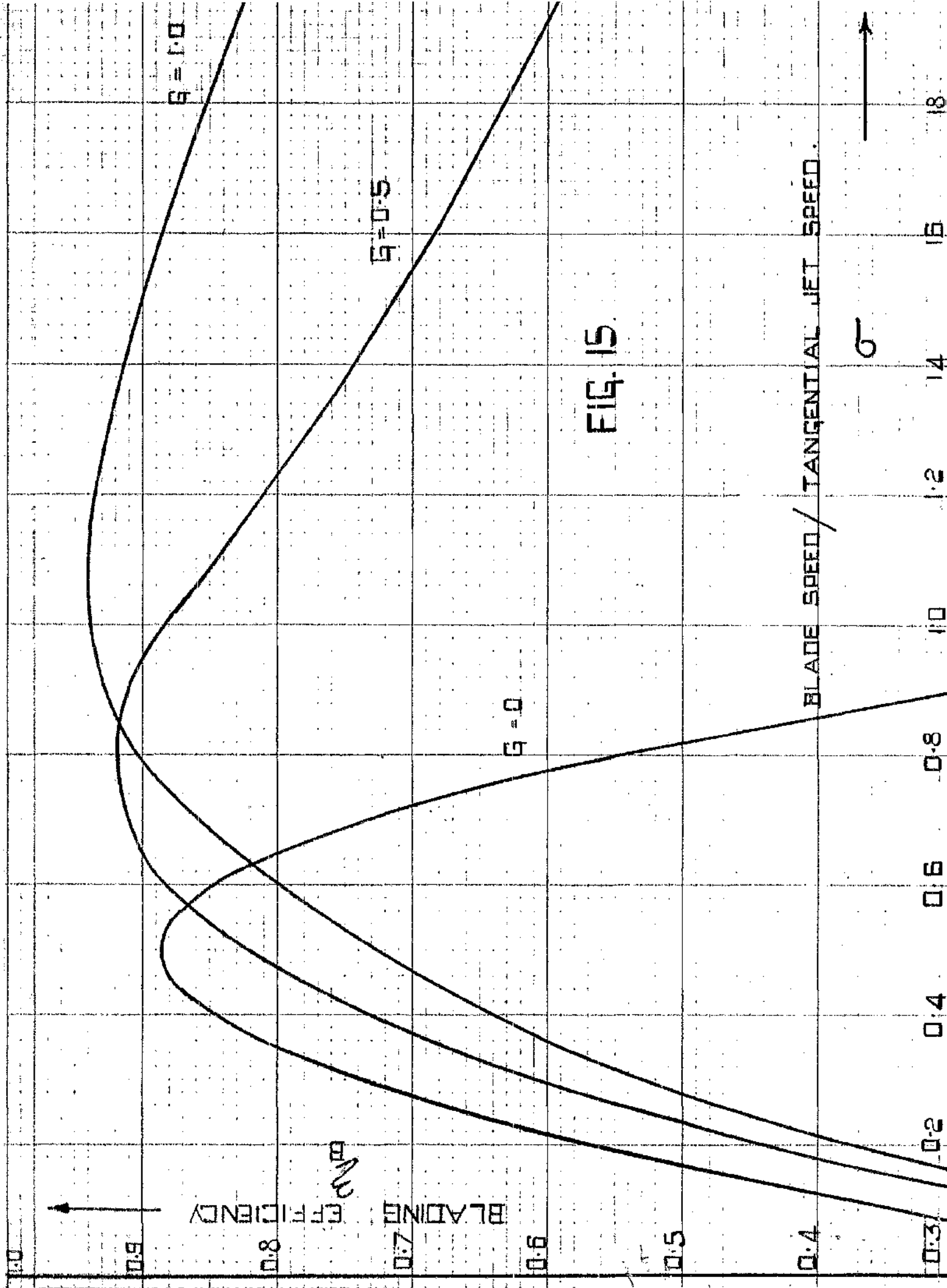


FIG. 15.

$\frac{1}{B}$ MAX.

FIG. 16

REACTION COEFFICIENT C_r

$\frac{1}{B}$ MAX.

1.0
0.95
0.90
0.85
0.80

4.5
4.0
3.5
3.0
2.5
2.0
1.5
1.0
0.5

$$\begin{aligned}
 WD &= \sqrt{v_{W2}^2} \left(\sqrt{\frac{G}{\cos^2 \alpha} + (1 - \sqrt{})^2} + 1 - \sqrt{} \right) \quad \text{---(109).} \\
 &= \frac{s^2}{\sqrt{}} \left(\sqrt{\frac{G}{\cos^2 \alpha} + (1 - \sqrt{})^2} + 1 - \sqrt{} \right)
 \end{aligned}$$

The high grade energy available to the moving blade is

$$H_{01} - H_3 = \frac{v_2^2}{2} (1 + G) = \frac{v_{W2}^2}{2 \cos^2 \alpha} (1 + G) \quad \text{---(110).}$$

Hence from 109 and 110 the blading or diagram efficiency is given by

$$\eta_B = \frac{2 \sqrt{} \cos^2 \alpha}{1 + G} \left(\sqrt{\frac{G}{\cos^2 \alpha} + (1 - \sqrt{})^2} + 1 - \sqrt{} \right) \quad \text{---(111).}$$

Thus the blading efficiency depends on $\sqrt{}$, α and G and we shall henceforth treat the nozzle angle α as a constant, (taken as 20° throughout). Hence for a given value of G ,

η_B is a function of $\sqrt{}$ only and we can find the speed ratio for maximum blading efficiency ($\eta_{B\max}$) by differentiating η_B with respect to $\sqrt{}$ and equating to zero. Hence for maximum blading efficiency for a given reaction coefficient

$$\left(\text{for } \sqrt{}_{\max} \eta_B \right) = \frac{1 + \frac{G}{\cos^2 \alpha}}{2} \quad \text{---(112).}$$

The maximum value of the blading efficiency is obtained by substituting 112 for $\sqrt{}$ in 111, this gives

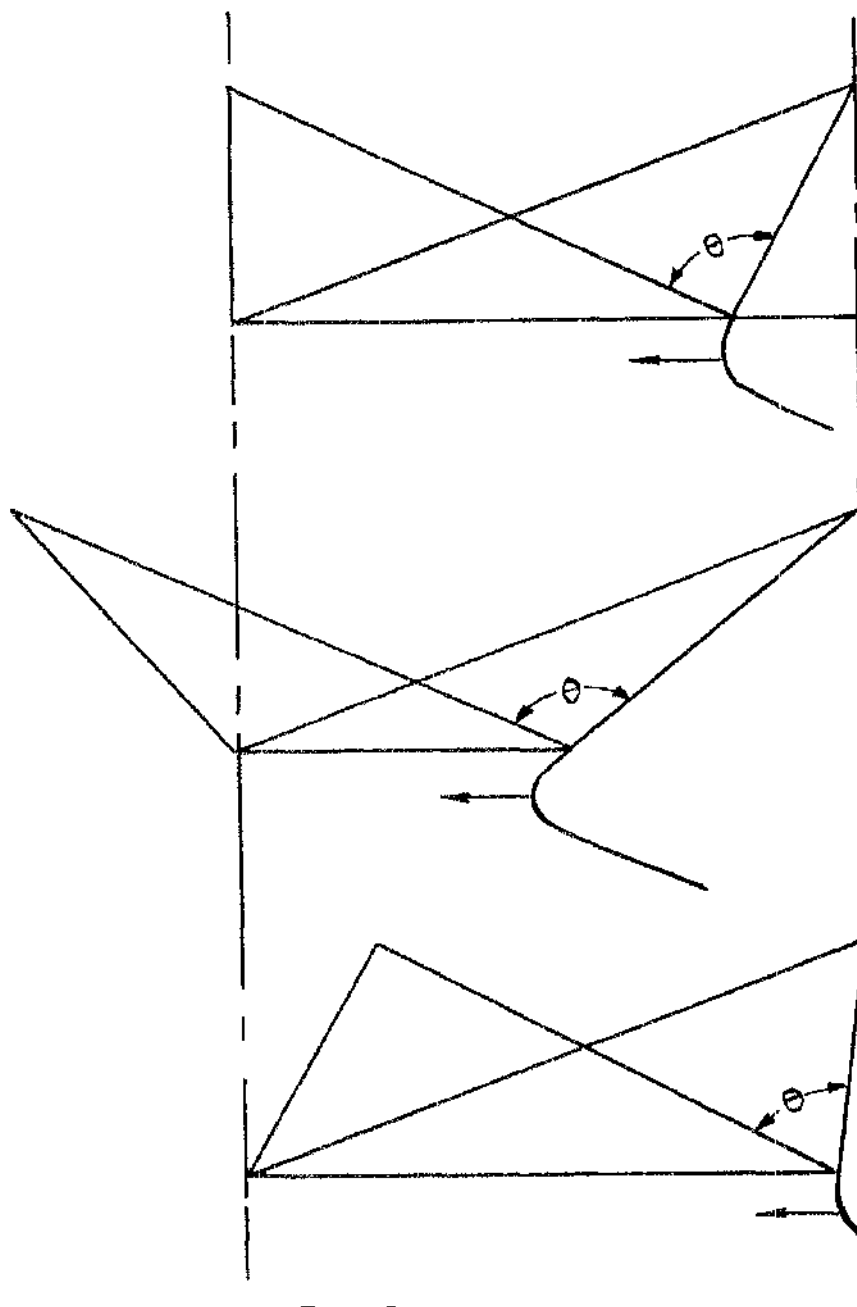
$$\eta_{B\max} = \frac{G + \cos^2 \alpha}{1 + G} \quad \text{---(113).}$$

The variation of η_B and $\sqrt{}$ for various values of G is shown in figure 15. The maximum value of the blading efficiency increases with increasing values of the reaction coefficient and the variation is shown in figure 16.

(2). Form of the velocity triangles when the stage is designed for maximum blading efficiency.

From equation 107,

$$v_{r3} \cos \beta_3 = v_{W2} \sqrt{\frac{G}{\cos^2 \alpha} + (1 - \sqrt{})^2} \quad \text{---(114).}$$



$$\begin{aligned} z_B^{\text{MAX.}} \\ G &= 0.5 \\ \sigma &= 0.79. \end{aligned}$$

$$\begin{aligned} z_B < z_B^{\text{MAX.}} \\ G &= 0.5 \\ \sigma &= 0.53. \end{aligned}$$

$$\begin{aligned} z_B < z_B^{\text{MAX.}} \\ G &= 0.5 \\ \sigma &= 0.95. \end{aligned}$$

θ = GAS DEFLECTION.

FIG. 17.

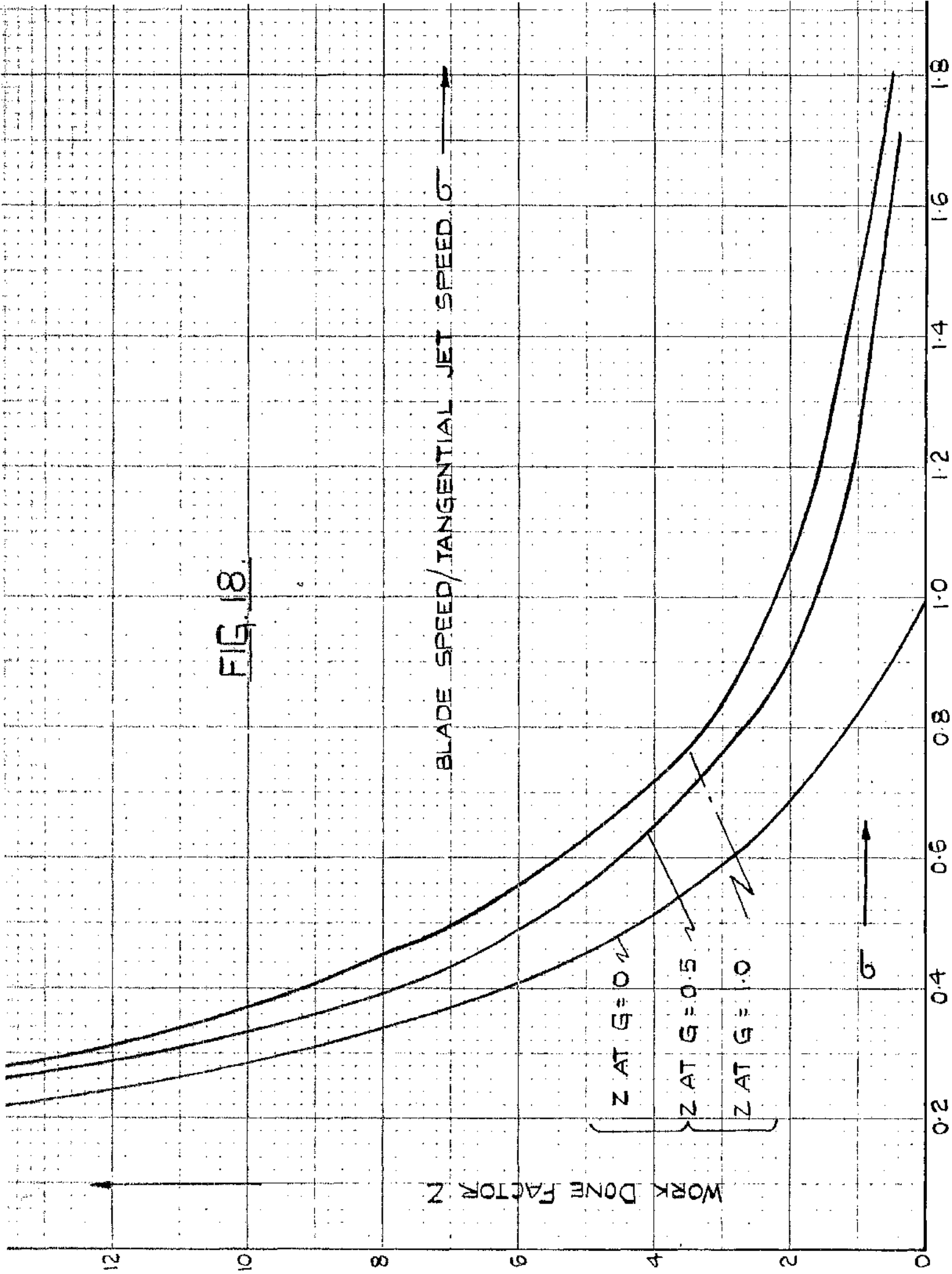


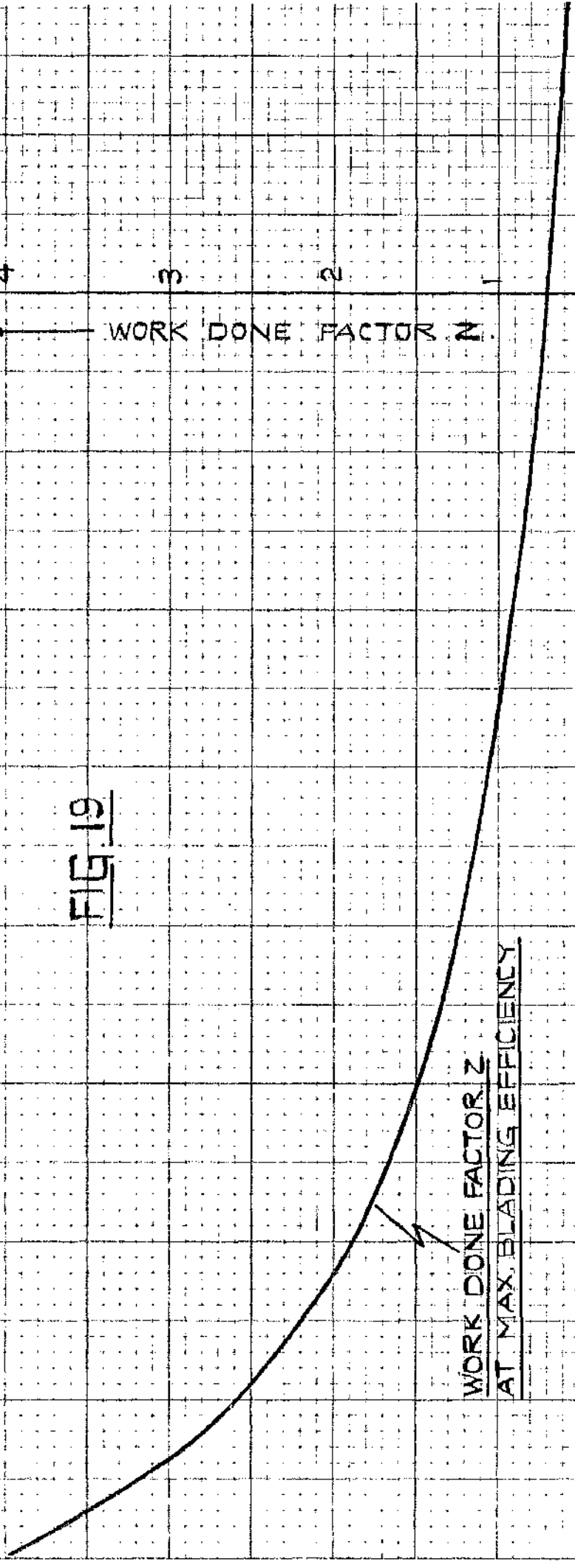
FIG. 19

WORK DONE FACTOR N .

WORK DONE FACTOR Z
AT MAX. BLADING EFFICIENCY

REACTION COEFFICIENT G .

0 0.5 1.0 1.5 2.0 2.5 3.0 3.5 4.0 4.5 5



and at maximum blading efficiency \bar{U} is given in 112 as a function of G . Substituting in 114 for \bar{U} gives

$$v_{r3} \cos \beta_3 = v_{w2} \sqrt{\frac{G}{\cos^2 \alpha} + \left(\frac{1 - \frac{G}{2 \cos^2 \alpha}}{2}\right)^2} = s. \quad (115).$$

Thus at maximum ζ_B the outlet whirl velocity v_{w3} is zero and only the inlet whirl component v_{w2} is removed. The form of the velocity triangles when the stage is designed to operate above and below $\bar{U} = \frac{1 + \frac{G}{\cos^2 \alpha}}{2}$ is shown in

figure 17 for a given reaction coefficient.

(3). The work done factor or loading factor for the stage.

The work done or loading factor for the stage is defined

$$\text{as } Z = \frac{WD}{\frac{s^2}{2}}$$

from 109 this gives

$$Z = \frac{2}{\bar{U}} \left(\sqrt{\frac{G}{\cos^2 \alpha} + (1 - \bar{U})^2} + 1 - \bar{U} \right) \quad (116).$$

i.e. Z is a function of G and \bar{U} . The variation in Z with \bar{U} is shown in figure 18 for different reaction coefficients. When the stage is designed for maximum blading efficiency the value of the work done factor is obtained by substituting 112 for \bar{U} in 116, this gives,

$$\begin{aligned} Z_{\text{at max } \zeta_B} &= \frac{2}{\bar{U}} \left(\frac{1 + \frac{G}{\cos^2 \alpha}}{2} + 1 - \bar{U} \right) = \frac{2}{\bar{U}(\text{for max } \zeta_B)} \\ &= \frac{2}{\frac{G}{(1 + \frac{G}{\cos^2 \alpha})}} \end{aligned} \quad (117).$$

The work done factor at maximum blading efficiency is a function of G only and is twice the reciprocal of the blade speed to tangential jet speed ratio for maximum blading efficiency. The relationship of equation 117 is given in graphical form in figure 19.

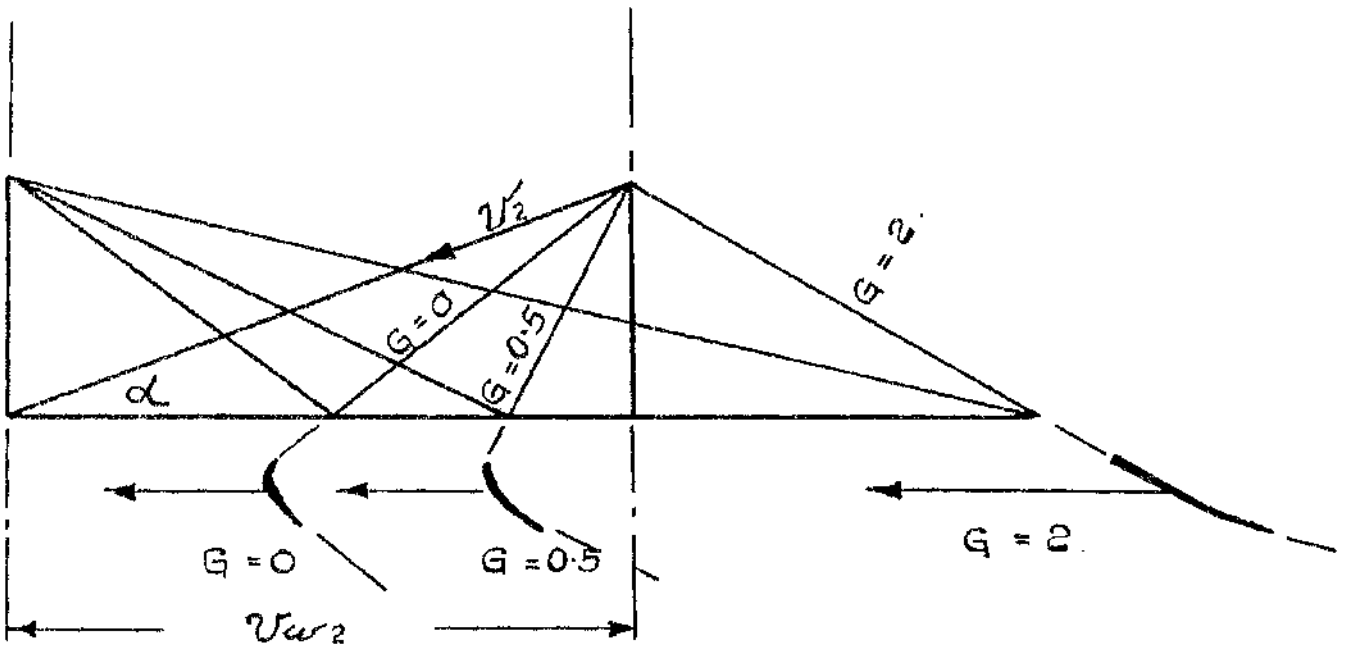


FIG. 20.

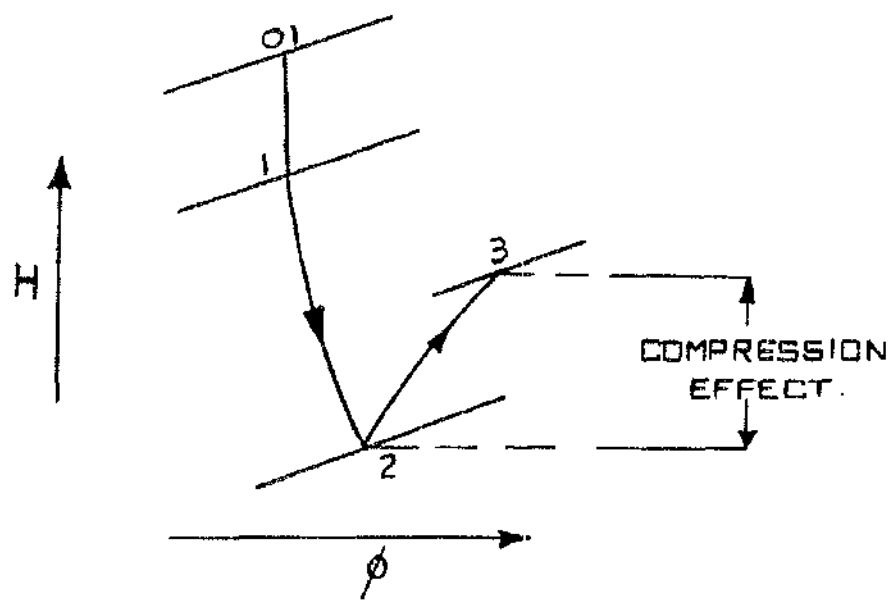
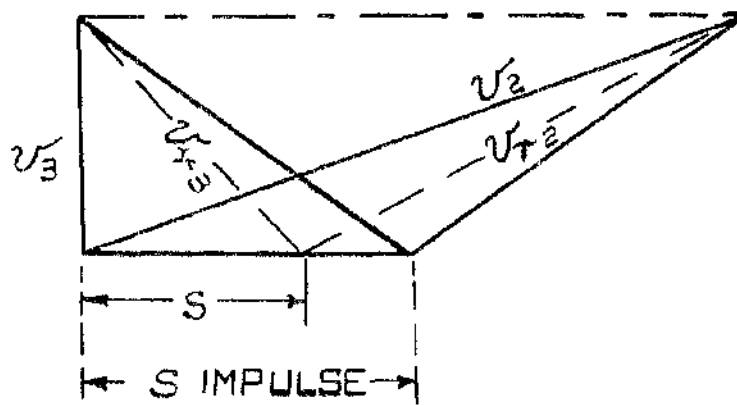


FIG. 21.

Thus when the stage is designed for maximum blading efficiency for a given reaction coefficient, the work done factor decreases with increasing reaction coefficient, and hence when efficiently utilizing a given blade speed the specific work output decreases as the reaction coefficient rises. An impulse blade therefore gives a large specific work output with a low blading efficiency, and a reaction blade gives a small specific work output with a higher blading efficiency, when each is operating at the same blade speed.

At maximum blading efficiency the work output given in equation 109 reduces to

$$WD = s v_{W_2}^2 = v_{W_2}^2 \left(\frac{1 + \frac{G}{2 \cos^2 \alpha}}{2} \right) \quad (118).$$

If the whirl velocity at inlet to the moving blade is maintained constant, then as the reaction coefficient increases we get more output work per pound but this also means a progressively increasing blade speed. (see figure 20).

(4). Compression in the rotor blade passages of a turbine stage.

The effect of various amounts of compression in the rotor blade passage can be studied from figure 21, where the blade speed is reduced below that required for zero degree of reaction. For negative degrees of reaction, where $v_{r_3} < v_{r_2}$, a compression coefficient (G_c) may be defined as

$$G_c = \frac{v_{r_2}^2 - v_{r_3}^2}{v_2^2 / 2} \quad (119).$$

As before it may be shown that the blading efficiency is given by

$$\eta_B = \frac{2 \sqrt{\cos^2 \alpha}}{1 - G_c} \left(\sqrt{(1 - \sqrt{\cos^2 \alpha})^2 - \frac{G_c}{\cos^2 \alpha}} + 1 - \sqrt{\cos^2 \alpha} \right) \quad (120).$$

FIGS. 22 & 23.

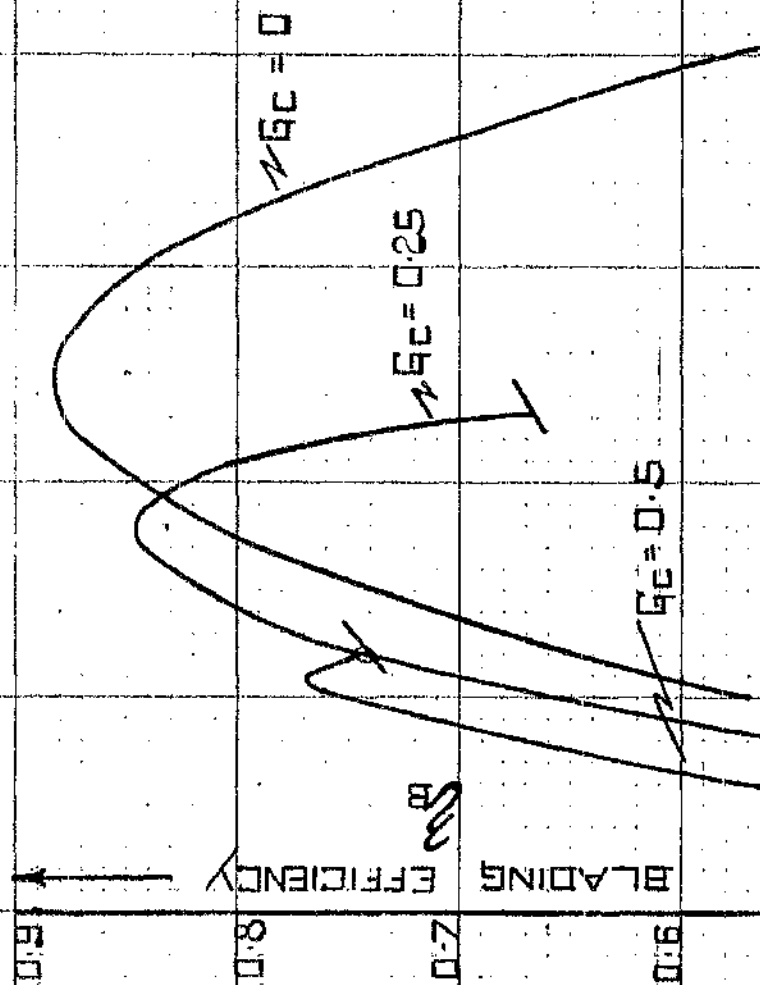


FIG. 22.

WORK DONE FACTOR Z AT MAX η_B

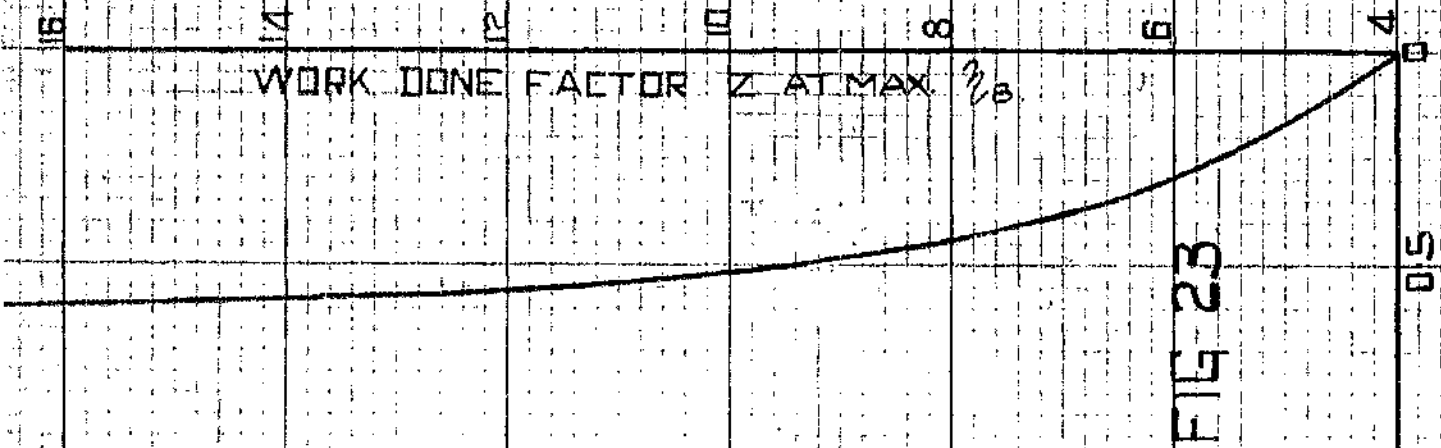


FIG. 23.

BLADE SPEED / TANGENTIAL JET SPEED, σ

G_c

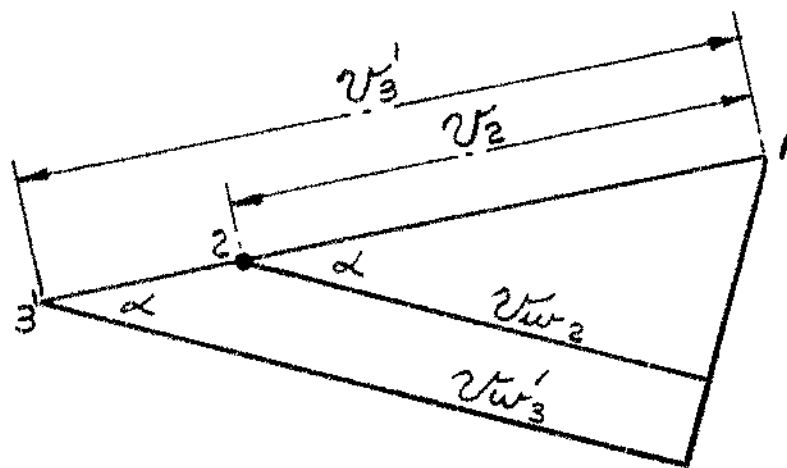
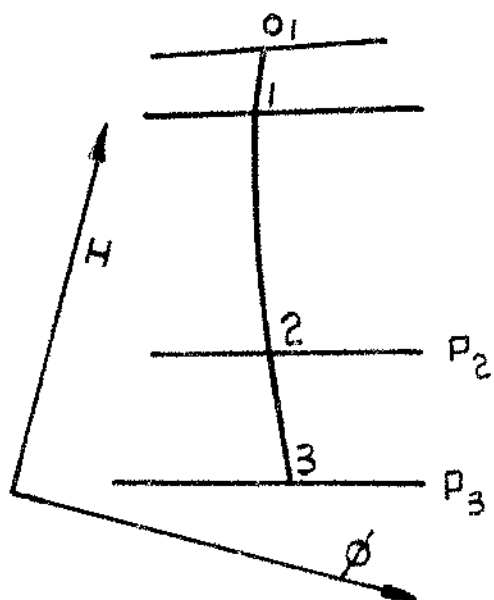


FIG. 24.

The condition for maximum blading efficiency is

$$\bar{U} = \frac{1 - \frac{G_o}{\cos^2 \alpha}}{2} \quad (121).$$

and the work done factor at maximum blading efficiency is given by

$$Z = \frac{4 \cos^2 \alpha}{\cos^2 \alpha - G_o} \quad (122).$$

The variation of η_B with \bar{U} for various values of G_o is shown in figure 22 and it will be observed that the maximum blading efficiency reduces substantially as G_o increases. In addition, as G_o is increased, the permissible variation in \bar{U} , about

\bar{U} (for max η_B), to avoid a serious fall in blading efficiency is considerably reduced. The work done factor at maximum blading efficiency is shown in figure 23 and increases as the compression coefficient increases.

(5). Relationship between the reaction coefficient (G), the total head degree of reaction (Ro) and the degree of reaction (R).

Consider the stage enthalpy changes shown in figure 24. The total head degree of reaction is defined as,

$$R_o = \frac{H_2 - H_3}{H_{o1} - H_3} \quad (80).$$

and the reaction coefficient as

$$G = \frac{H_2 - H_3}{H_{o1} - H_2} \quad (105).$$

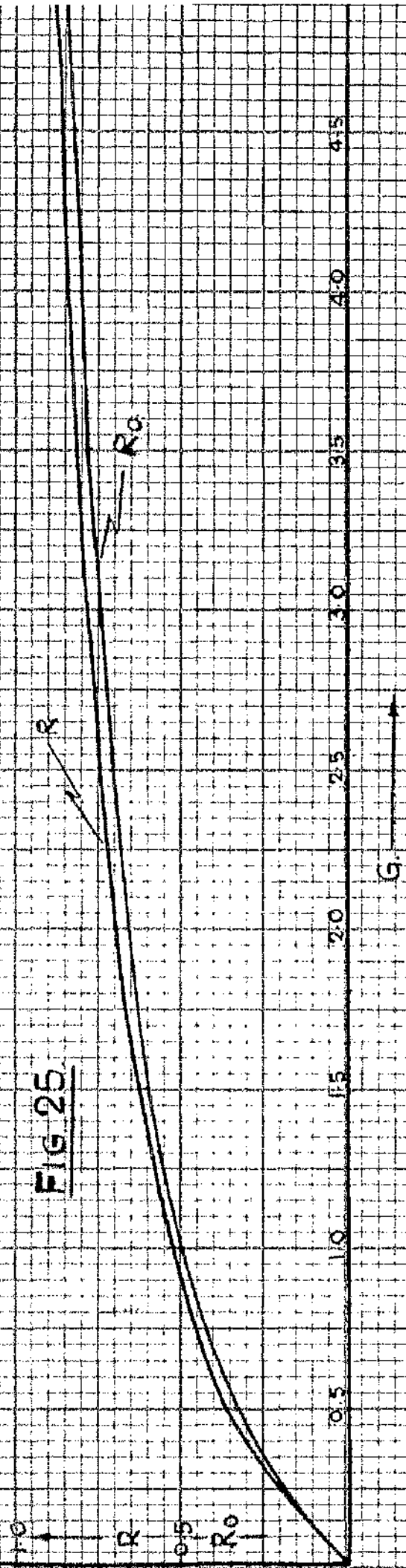
Thus the reaction coefficient and total head degree of reaction are related by the expression

$$G = \frac{R_o}{1 - R_o} \text{ or } R_o = \frac{G}{1 + G} \quad (123).$$

The usual definition of degree of reaction is

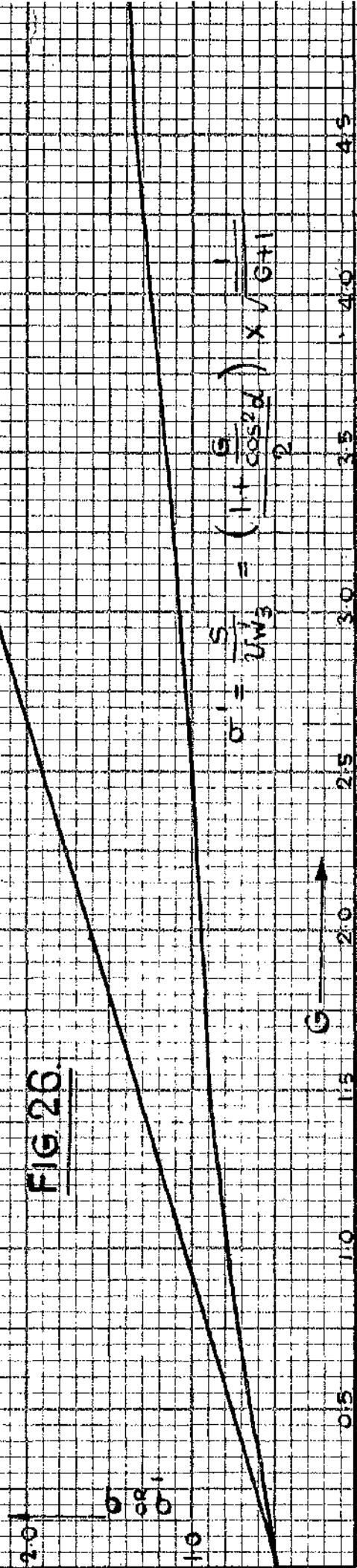
$$R = \frac{H_2 - H_3}{H_1 - H_3} \quad (72).$$

FIG 25



$$\sigma = 1 + \frac{G \cos^2 \alpha}{2} = \frac{S}{W_2}$$

FIG 26



$$\sigma' = \frac{S}{W_3} = \left(1 + \frac{G \cos^2 \alpha}{2} \right) \times \sqrt{\frac{1}{G+1}}$$

This definition is useful only when applied to a typical stage in a multistage turbine where the carry over velocity is constant. In such a case the stage enthalpy change $H_1 - H_3$ is identical with the stage work output. Thus from equations 105 and 109,

$$R = \frac{H_2 - H_3}{WD} = \frac{G \frac{v_2^2}{2}}{\sigma \cos^2 \alpha \frac{v_2^2}{2} \left(\sqrt{\frac{G}{\cos^2 \alpha}} + (1 - \sigma)^2 + 1 - \sigma \right)} \quad (124).$$

Thus R is in general a function of G and σ .

When designing at maximum blading efficiency however equation 124 gives

$$\left(\text{for max } \zeta_B \right) R = \frac{G}{\cos^2 \alpha + G} \quad (125).$$

For a "50 degree" reaction blade, $R = 0.5$, $G = 0.884$ and hence

$$\sigma \left(\text{for Max } \zeta_B \right) = \frac{1 + \frac{G}{\cos^2 \alpha}}{2} = 1$$

The relationships between R , G and R given in equations 123 and 125 are shown in graphical form in figure 25.

(6). The blade speed to jet speed ratio.

The blade speed to jet speed ratio, $\rho = \frac{s}{v_2}$ is related to the blade speed to tangential jet speed ratio by

$$\rho = \sigma \cos \alpha \quad (126).$$

A speed ratio defined by

$$\rho' = \frac{s}{v_3'} \quad (127).$$

is however sometimes used, where the velocity v_3' is the velocity which would be attained in expansion in a nozzle, in which the nozzle heat drop is equal to the stage total head heat drop $H_{01} - H_3$. i.e. $v_3' = 223.8 \sqrt{H_{01} - H_3}$.

The equivalent blade speed to tangential jet speed ratio would be defined as

$$\sigma' = \frac{s}{v_{W3}'} \quad (128).$$

where v_{w3}' is the tangential component of the velocity v_3'

assuming that the nozzle outlet angle is the same as that for the nozzle of the stage under consideration (see figure 24).

The speed ratios given in equations 126, 127 and 128 may be related to the total head degree of reaction for the stage.

$$\text{Thus } \frac{\rho'}{\rho} = \frac{\sqrt{v'}}{\sqrt{v}} = \frac{v_2}{v_3'} = \sqrt{1 - R_o} \quad (129).$$

Hence when the stage is designed for maximum blading efficiency equation 129 gives

$$\sqrt{v'} = \left(\frac{1 + \frac{G}{2 \cos^2 \alpha}}{2} \right) \sqrt{1 - R_o} = \left(\frac{1 + \frac{G}{2 \cos^2 \alpha}}{2} \right) \frac{1}{\sqrt{1 + G}} \quad (130).$$

This form of the speed ratio is useful in a number of applications. For example, if the stage heat drop and blade speed are determined, equation 130 gives the total head degree of reaction for maximum blading efficiency and so determines the best way to split the available stage heat drop between the static and moving rows. The relationships between \sqrt{v} , $\sqrt{v'}$ and G for maximum blading efficiency are shown in figure 26.

(7). Conditions for maximum blading efficiency in the axial flow compressor stage.

For the compressor stage shown in figure 12, a compression coefficient may be defined as

$$G_c = \frac{H_2 - H_1}{H_{o3} - H_2} = \frac{\frac{v_{r1}^2}{2} - \frac{v_{r2}^2}{2}}{\frac{v_2^2}{2}} \quad (105c).$$

and the blade speed to tangential jet speed ratio as

$$\sqrt{s} = \frac{s}{v_{w2}} \quad \text{where } v_{w2} \text{ is the whirl component of the absolute velocity entering the stator blade.}$$

velocity entering the stator blade.

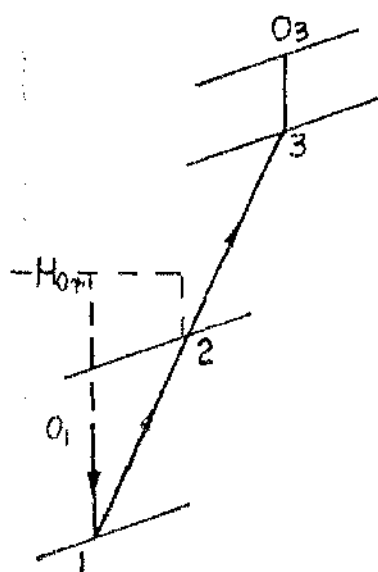


FIGURE 27A

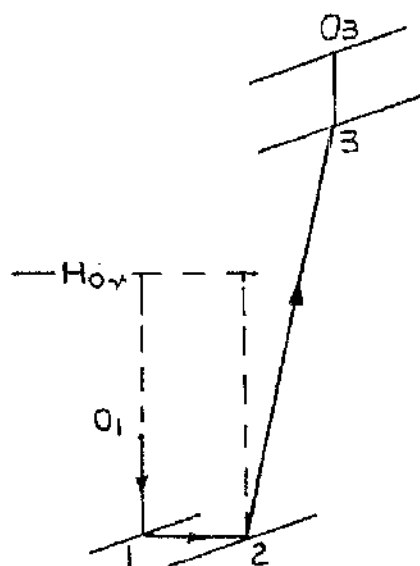


FIGURE 27B

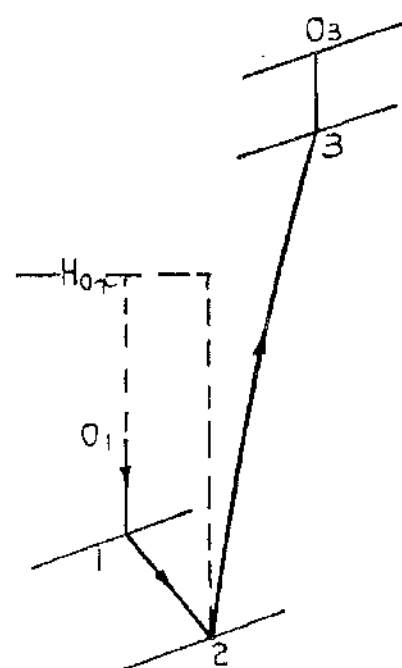


FIGURE 27C

φ

COMPRESSOR STAGES WITH POSITIVE,
ZERO AND NEGATIVE DEGREES OF COMPRESSION.

FIG. 27.

In a similar manner to that of the turbine stage it may be shown that the work input is given by

$$WI = \sqrt{v_{W_2}^2} \left(\sqrt{\frac{G}{\cos^2 \alpha} + (1 - \sqrt{v})^2} + 1 - \sqrt{v} \right) \quad (109c).$$

and the blading efficiency is

$$\eta_B = \frac{WI}{H_{03} - H_1} = \frac{2 \sqrt{v} \cos^2 \alpha}{1 + \frac{G_c}{G}} \left(\sqrt{\frac{G_c}{\cos^2 \alpha} + (1 - \sqrt{v})^2} + 1 - \sqrt{v} \right) \quad (111c).$$

where α is the stator blade inlet angle.

Thus for a given stator blade inlet angle maximum blading efficiency is obtained when

$$\sqrt{v} = \frac{1 + \frac{\frac{G_c}{\cos^2 \alpha}}{2}}{\frac{G_c}{\cos^2 \alpha}} \quad (112c).$$

The analogy between the compressor stage and the turbine stage, discussed in Part 1(c), may be used to determine the effect in the compressor stage of varying the stage design parameters. Thus the conclusions reached regarding the variation of blading efficiency and loading factor, with reaction coefficient and speed ratio for the turbine stage, may be applied to the compressor stage. These conclusions are summarized in figures 15, 16, 18, 19, 22 and 23 and when they are applied to the compressor stage it is only necessary to replace the reaction coefficient G with the compression coefficient G_c .

The H/ϕ diagrams for compressor stages corresponding to turbine stages with positive, zero and negative degrees of reaction are shown in figure 27. They are

- (a) a conventional compressor with compression effect in the rotor blade.
- (b) a zero degree of compression stage.
- and (c) a stage with expansion effect in the rotor blade.

While from the point of view of stage efficiency a turbine with compression in the rotor blade is liable to be inefficient, because of the greater losses associated with a diffusion process, a compressor with expansion in the rotor blade could give a more efficient compressor with a large loading factor. Shepherd²⁹ indicates that this type of compressor stage is only possible where the stage velocities are low, otherwise the operating Mach number will be such that flow separation may occur in the stator blade.

Part 1 (d) - Summary.

For an axial flow turbine stage the blading efficiency and loading factor are derived as functions of the blade speed to tangential jet speed ratio ($\sqrt{}$), and of the reaction coefficient (G), (Equations 111 and 116). The reaction coefficient is defined as the reaction effect in the moving blade divided by the kinetic energy at inlet to the blade and is given in equation 123 as a function of the total head degree of reaction for the stage. For a given reaction coefficient and nozzle outlet angle the blading efficiency is a maximum when

$$\sqrt{} = \frac{1 + \frac{G}{2 \cos^2 \alpha}}{2}$$

where α is the nozzle outlet angle.

The variation of blading efficiency with $\sqrt{}$ and G is shown in figure 15. It will be noted that there is a limited range of $\sqrt{}$, about that for maximum blading efficiency, within which $\sqrt{}$ may be chosen without incurring a serious fall in blading efficiency. This range of $\sqrt{}$, along with the value of the maximum blading efficiency increase with increase in reaction coefficient. For a given reaction coefficient, the loading factor increases with decreasing values of $\sqrt{}$, (figure 18), but the choice of loading factor is in general limited to the range of $\sqrt{}$ within which there is no serious fall in blading efficiency. When the stage is designed for maximum blading efficiency, the value of the maximum blading efficiency and the loading factor are functions of reaction coefficient only, the value of the loading factor being twice the reciprocal of the blade speed to tangential jet speed ratio. As the reaction coefficient rises the maximum blading efficiency increases (figure 16) while the loading factor decreases (figure 19). In choosing a reaction coefficient for the stage therefore, a compromise must be made between these conflicting factors.

If the stage is designed with a small compression effect in the rotor blade a considerable rise in loading factor can be obtained. This is however accompanied by a serious fall in blading efficiency. In addition, the position with regard to blading efficiency is further aggravated if the blade speed to tangential jet speed ratio is only slightly removed from that which gives maximum blading efficiency.

The variation in the stage efficiencies with speed ratio and reaction coefficient may be studied using the results derived in this section. The total to static, and total to total stage efficiencies are related to the blading efficiency and total head efficiency of expansion in the stage by the expressions

$$\eta_{ts} = \eta_B \times \eta_{os} \quad \text{--- (89).}$$

and

$$\eta_{tt} = \frac{\eta_{os}}{\frac{1}{\eta_B} (1 - \eta_{os}) + \eta_{os}} \quad \text{--- (93).}$$

where

$$\eta_{os} \text{ is given by}$$

$$\eta_{os} = \frac{1}{1 + \frac{T_3}{T_2} \left(\frac{1}{\eta_{ON}} - 1 \right) (1 - R_o) + \left(\frac{1}{\eta_R} - 1 \right) R_o} \quad \text{--- (81).}$$

or

$$\eta_{os} = \frac{1}{1 + \frac{T_3}{T_2} \left(\frac{\epsilon_N \frac{v_2^2}{2}}{H_{o1} - H_3} \right) + \frac{\epsilon_R \frac{v_{r3}^2}{2}}{H_{o1} - H_3}} \quad \text{--- (82).}$$

It will be seen from equation 89 that the plots of blading efficiency, given in figure 15, may be regarded as design plots of total to static efficiency against $\sqrt{\eta_{os}}$ where η_{os} is unity.

It has been shown that the blading efficiency and loading factor depend primarily on the choice of reaction coefficient for the stage. (figures 16 and 19). In making this choice of reaction coefficient, the effect on the stage efficiencies may be obtained by assuming constant element

efficiencies and using ζ_{os} in the form of equation 81. When the reaction coefficient is thus determined, a comparison of a number of stage designs may be made, each corresponding to a blade speed to jet speed ratio within the range where the blading efficiency is sensibly constant. By this means the optimum design from the loading factor and stage efficiency viewpoint may be determined. In assessing the stage efficiencies at this point, account should be taken of the variation in the loss coefficients of the elements as the gas deflection varies. An example of the way in which gas deflection varies with $\sqrt{}$ at constant reaction coefficient is given in figure 17. It may be shown that equation 82 can be expressed as

$$\zeta_{os} = \frac{1}{1 + \frac{T_3}{T_2} \frac{\epsilon_N}{1+G} + \frac{\epsilon_R}{1+G} (G + \sin^2 \alpha + (1 - \sqrt{})^2 \cos^2 \alpha)}$$

and to determine ζ_{tt} and ζ_{ts} it only remains to substitute experimental figures for ϵ_N and ϵ_R .

Typical such results for the variation in loss coefficients with gas deflection, for blading which is designed for optimum pitch to chord ratio, are given by Soderburg³⁰. The gas deflection and loss coefficient decrease as the blade speed to jet speed ratio rises. Thus the total head efficiency of expansion in the stage will rise continuously as the speed ratio is increased. The variation of stage efficiency with speed ratio may then be deduced from the blading efficiency graphs in figure 15 using the relationships given in equations 89 and 93. For a given reaction coefficient the total to static stage efficiency will exhibit a steeper characteristic at speed ratios below that for maximum blading efficiency and flatter characteristic above, compared with the corresponding blading efficiency curve. Rogers and Mayhew³¹ have considered the effect of friction losses on the stage efficiency characteristic and have suggested that the

speed ratio for maximum stage efficiency may differ somewhat from that for maximum blading efficiency.

The total to total stage efficiency has been shown to be much less dependant on the blading efficiency, especially at high values of the blading efficiency. (figure 10). At values of the blade speed about that for maximum blading efficiency the total to total stage efficiency will exhibit a much flatter characteristic than the total to static efficiency.

Equation 93 may be shown to give

$$\eta_{tt} = 1 - \frac{1 - \eta_{os}}{\eta_{ts}}$$

from which the total to total stage efficiency curve may be determined once the total to static characteristic has been established.

With regard to the definitions of degree of reaction given in this section, Shepherd³² used a different approach. He defines the degree of reaction as the reaction effect in the moving blade divided by the work output in the stage, thus :-

$$R_{sh} = \frac{H_2 - H_3}{WD}$$

This is a general definition which is not restricted to stages where the velocity entering and leaving the stage is the same. The relationship between R_{sh} and G is obtained by substituting R_{sh} for R in equation 124. This gives R_{sh} as a function of speed ratio and reaction coefficient. At maximum blading efficiency R_{sh} is a function of reaction coefficient only and is given by

$$R_{sh} = \frac{G}{\cos^2 \alpha + G}$$

Shepherd gives the blade speed to jet speed ratio for maximum blading efficiency as

$$\phi = \frac{\cos \alpha}{2(1 - R_{sh})}$$

and the value of the maximum blading efficiency as

$$\eta_{B_{\max}} = \frac{\cos^2 \alpha}{1 - R_{sh} \sin^2 \alpha}$$

Using the relationship between R_{sh} and G for maximum blading efficiency it may be shown that these latter expressions are identical with the corresponding expressions given here in equations 112 and 113.

For the axial flow compressor stage maximum blading efficiency is obtained when

$$\sqrt{v} = \frac{1 + \frac{G_c}{2 \cos^2 \alpha}}{2}$$

Here \sqrt{v} is the ratio of blade speed to the tangential component of the absolute velocity leaving the rotor blade,

α is the stator blade inlet angle and G_c , the compression coefficient, is the ratio of the compression effect in the rotor blade to the kinetic energy at inlet to the stator blade. The way in which the blading efficiency and loading factor for the compressor stage vary with the compression coefficient and speed ratio, can be obtained by using the analogy, between the compressor stage and similar turbine stage, discussed in the previous section.

Part 2.

- (a) The Determination in a static test rig of Local Total Head Efficiency of Expansion and of Stream Condition by means of an Impact Tube.

The measurement in a static test rig of the local efficiency of expansion and of stream condition in a subsonic or supersonic stream by means of an impact tube.

The loss of high grade energy in a turbine or compressor element may vary from point to point in the exit plane of the element. The impact tube when set at zero incidence to a stream records the local value of the total head or stagnation pressure. Thus if the total head condition of the working fluid entering a nozzle or diffuser is known the tube may be used to give local losses in total head pressure at the exit plane of the element. The function of the following section is to relate the recorded value of total head pressure to the local total head efficiency of expansion in a nozzle or blade element and to the local state of the fluid when the element is examined in a static test rig used to simulate the actual operating conditions. The equations developed allow for the case where the fluid stream approaching the impact tube is supersonic, in which case the recorded stagnation pressure is less than the actual stagnation pressure of the stream due to the loss in the total head pressure across the detached shock front up-stream of the tube. The relationships allow one to determine whether the local flow is subsonic or supersonic and in either case the local total head efficiency of expansion and local specific volume is then given in graphical form as a function of the local outlet stagnation pressure of the stream and of the theoretical Mach number after expansion. The graphs are drawn for the theoretical Mach numbers at outlet from the nozzle or blade which were used in the experimental work.

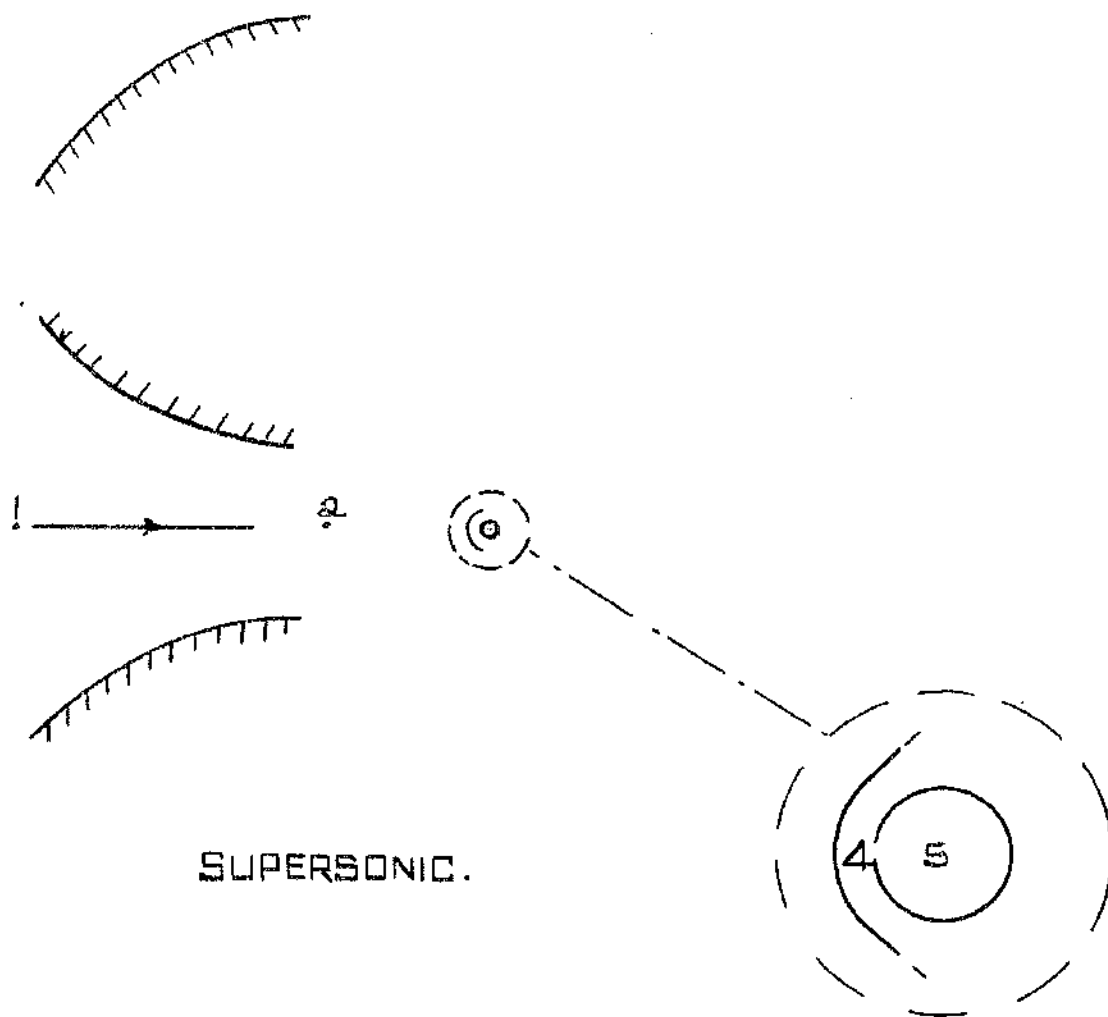
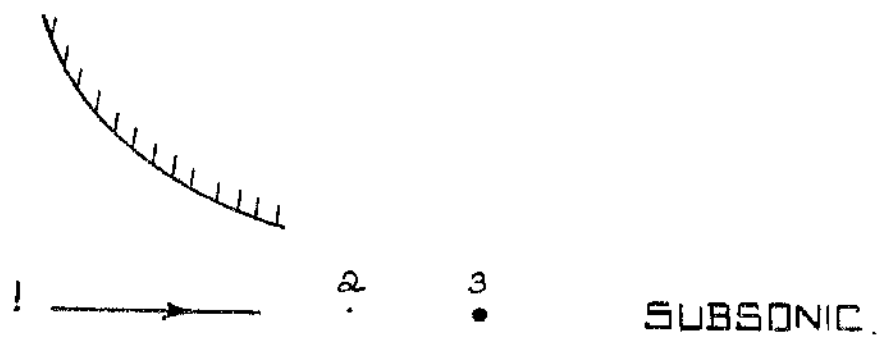


FIG. 30.

The measurement, in a static test rig, of the local efficiency of expansion and of steam condition in a subsonic or supersonic stream by means of an impact tube.

Let M denote Mach No.

"	v	"	velocity ft/sec.
"	V	"	specific volume ft ³ /lb.
"	P	"	pressure lb/ft ² .
"	v_a	"	acoustic velocity.
"	γ	"	isentropic index.
"	η	"	local total head efficiency of expansion.
"	DH	"	heat drop B.T.U./lb.
"	g	"	acceleration due to gravity.

Referring to figures 28, 29 & 30, consider an expansion from the total head condition (1) (Total head pressure P_1) to the static pressure P_2 . Thus an isentropic expansion from (1) gives the state point 2ϕ after expansion and an adiabatic expansion gives the point 2 with corresponding total head pressure P_3 .

$$\begin{aligned}
 \text{Hence } \frac{v_{2\phi}^2}{2g} &= \frac{\gamma}{\gamma-1} (P_1 V_1 - P_2 V_{2\phi}) \\
 \therefore v_{2\phi}^2 &= \frac{2g\gamma}{\gamma-1} P_1 V_1 \left(1 - \left(\frac{P_2}{P_1} \right)^{\frac{\gamma-1}{\gamma}} \right) \\
 &= \frac{2g\gamma}{\gamma-1} P_2 V_{2\phi} \left(\left(\frac{P_1}{P_2} \right)^{\frac{\gamma-1}{\gamma}} - 1 \right) \quad \text{--- (1)} \\
 \therefore v_{2\phi}^2 &= g \gamma P_2 V_{2\phi}
 \end{aligned}$$

$$\therefore M_{2\phi}^2 = \frac{v_{2\phi}^2}{v_a^2} = \frac{2}{\gamma-1} \left(\left(\frac{P_1}{P_2} \right)^{\frac{\gamma-1}{\gamma}} - 1 \right) \quad (2).$$

$$\begin{aligned} \text{also } v_2^2 &= \frac{2g\gamma}{\gamma-1} P_3 V_3 \left(1 - \left(\frac{P_2}{P_3} \right)^{\frac{\gamma-1}{\gamma}} \right) \\ &= \frac{2g\gamma}{\gamma-1} P_2 V_2 \left(\left(\frac{P_3}{P_2} \right)^{\frac{\gamma-1}{\gamma}} - 1 \right) \end{aligned} \quad (3).$$

$$\therefore v_{a2}^2 = g\gamma P_2 V_2$$

$$\therefore M_2^2 = \frac{2}{\gamma-1} \left(\left(\frac{P_3}{P_2} \right)^{\frac{\gamma-1}{\gamma}} - 1 \right) \quad (4).$$

Since $P_1 V_1 = P_3 V_3$ then from (1) and (3)

$$\zeta = \frac{DH}{DH_\phi} = \frac{v_2^2}{v_{2\phi}^2} = \frac{1 - \left(\frac{P_2}{P_3} \right)^{\frac{\gamma-1}{\gamma}}}{1 - \left(\frac{P_2}{P_1} \right)^{\frac{\gamma-1}{\gamma}}} \quad (5).$$

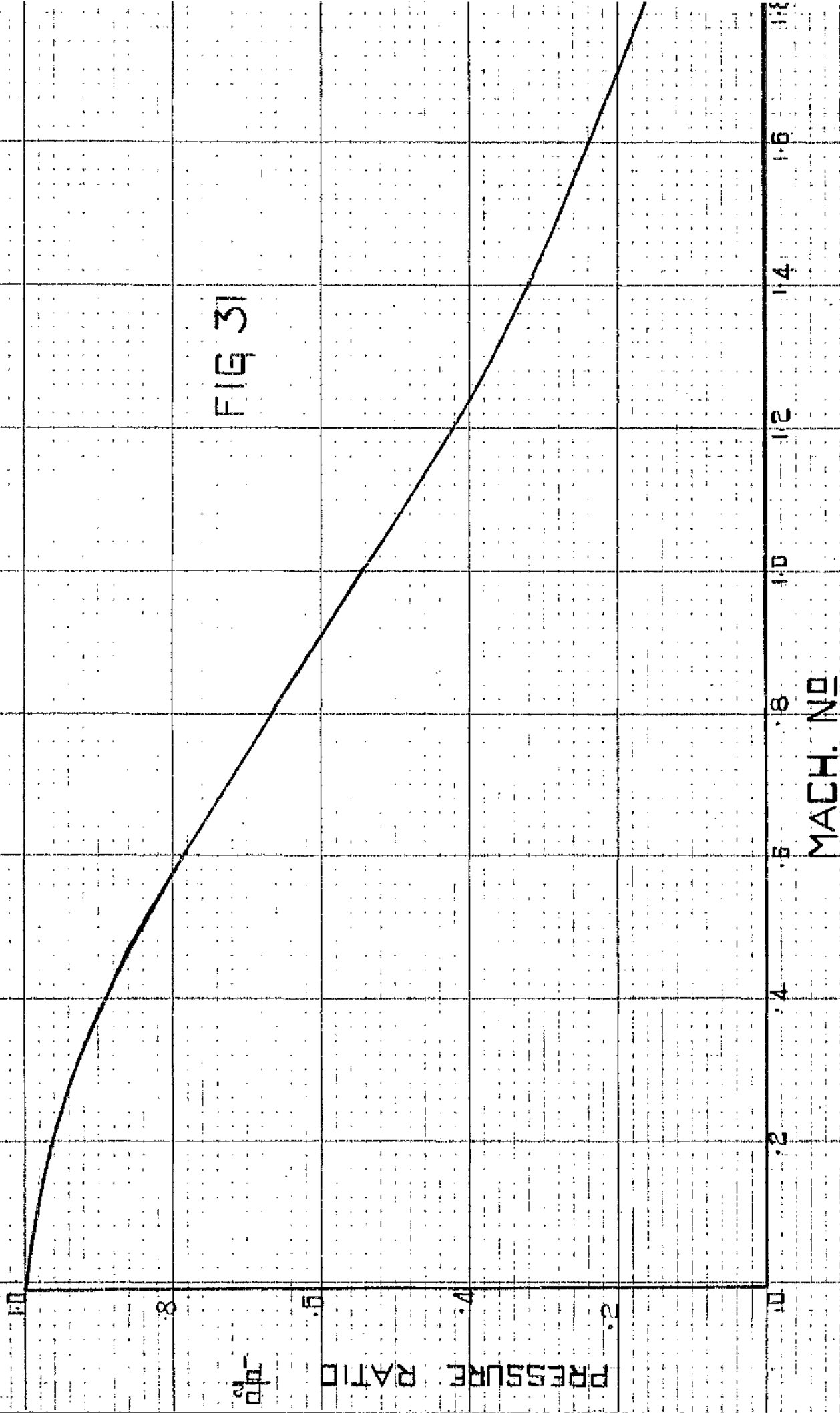
$$\text{from (2)} \quad \frac{P_2}{P_1} = \left(\frac{\gamma-1}{2} M_{2\phi}^2 + 1 \right)^{\frac{\gamma}{\gamma-1}}$$

$$\therefore \text{from (5)} \quad \zeta = \frac{1 - \left(\frac{P_2}{P_3} \right)^{\frac{\gamma-1}{\gamma}}}{1 - \left(\frac{\gamma-1}{2} M_{2\phi}^2 + 1 \right)^{-\frac{\gamma}{\gamma-1}}} \quad (6).$$

also from (1) and (3)

$$\zeta = \frac{v_2^2}{v_{2\phi}^2} = \frac{\left(\left(\frac{P_3}{P_2} \right)^{\frac{\gamma-1}{\gamma}} - 1 \right)}{\left(\left(\frac{P_1}{P_2} \right)^{\frac{\gamma-1}{\gamma}} - 1 \right)} \quad (7).$$

FIG 31



MACH NO M_2

.5

.6

.7

.8

.9

.97

1.0

.8

.6

.4

.2

0

EFFICIENCY η

FIG. 32.

1.0

.9

.8

.7

.6

.5

.4

PRESSURE RATIO $\frac{P_2}{P_3}$

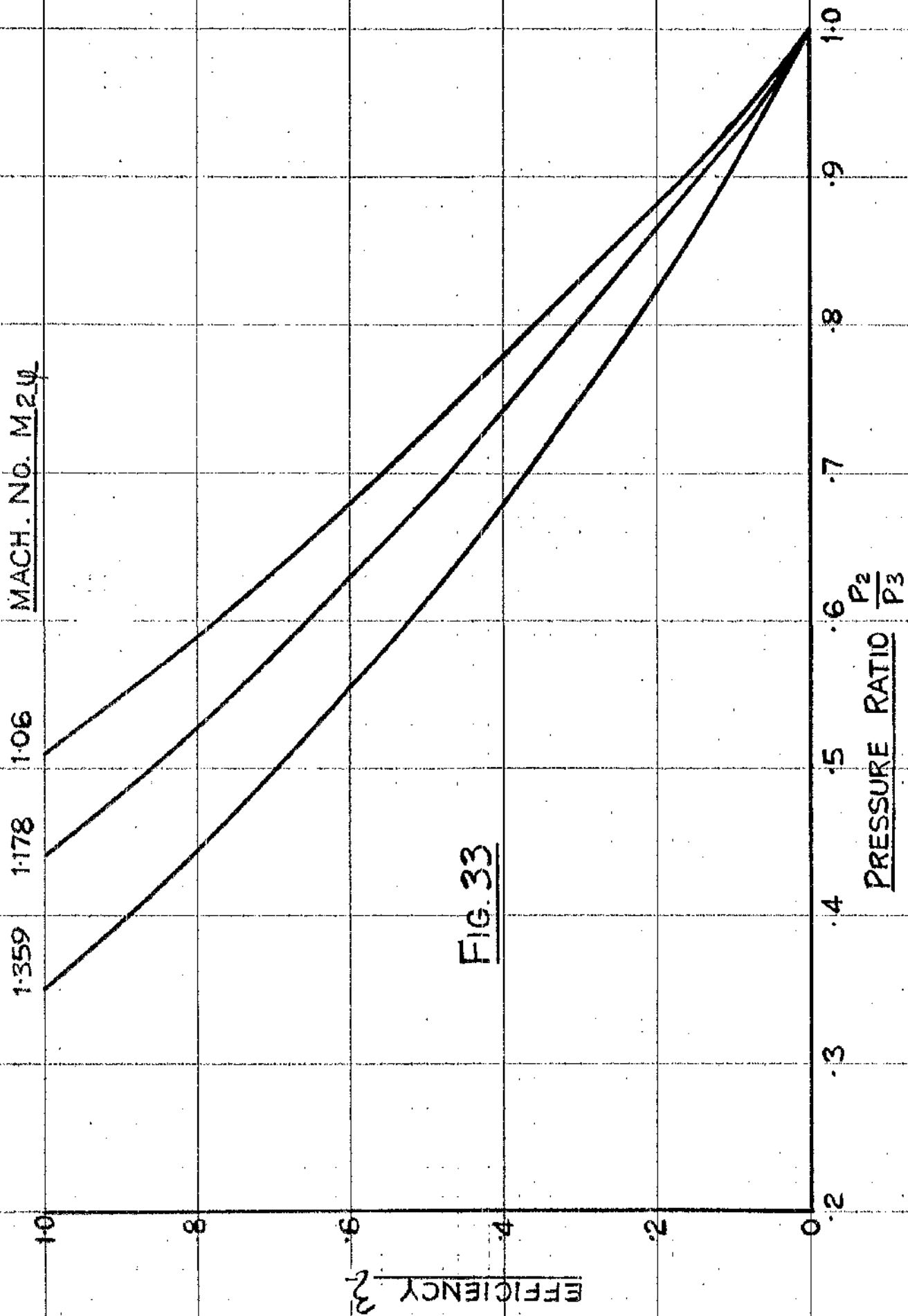


FIG. 33

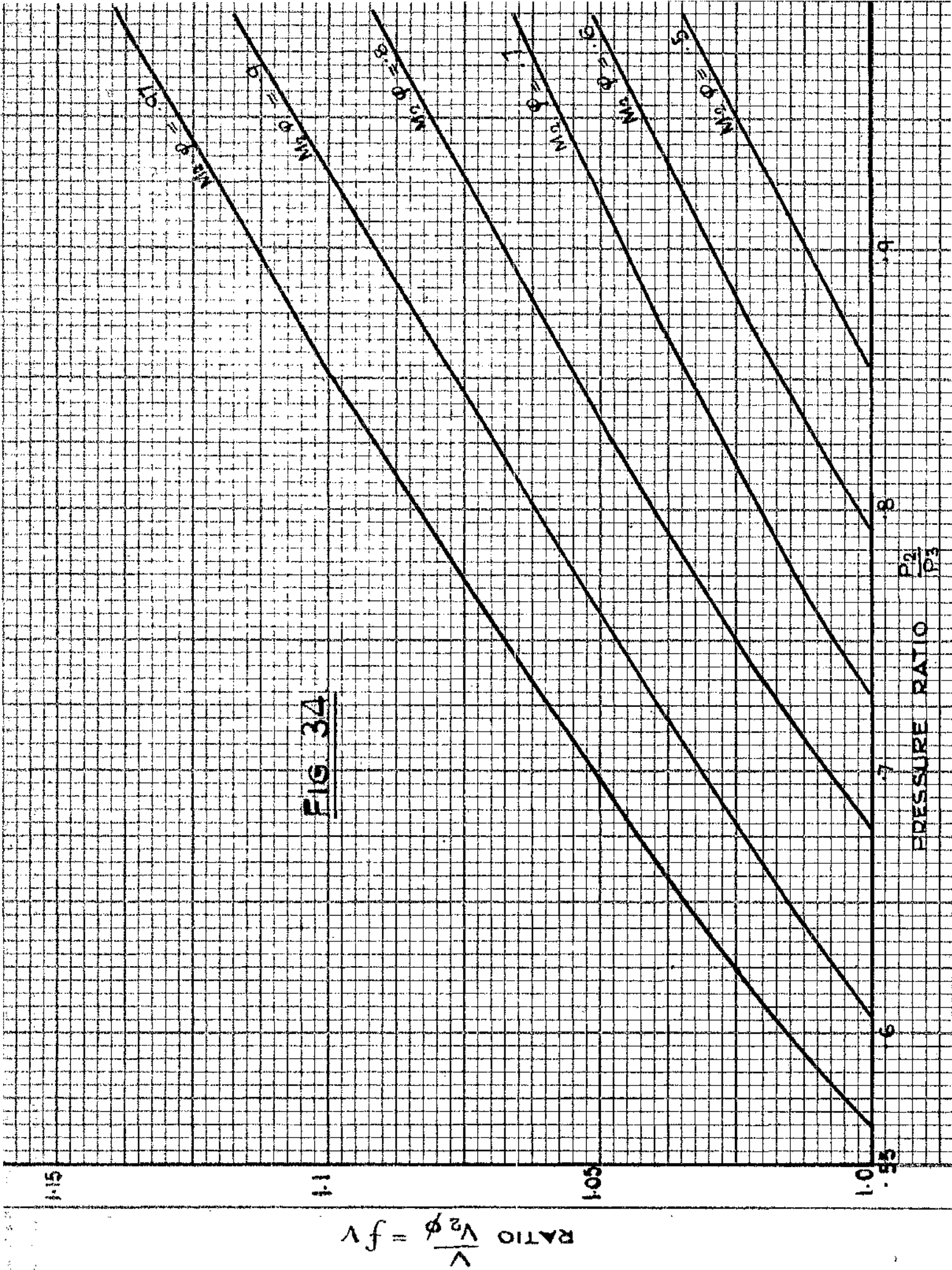


FIG 34

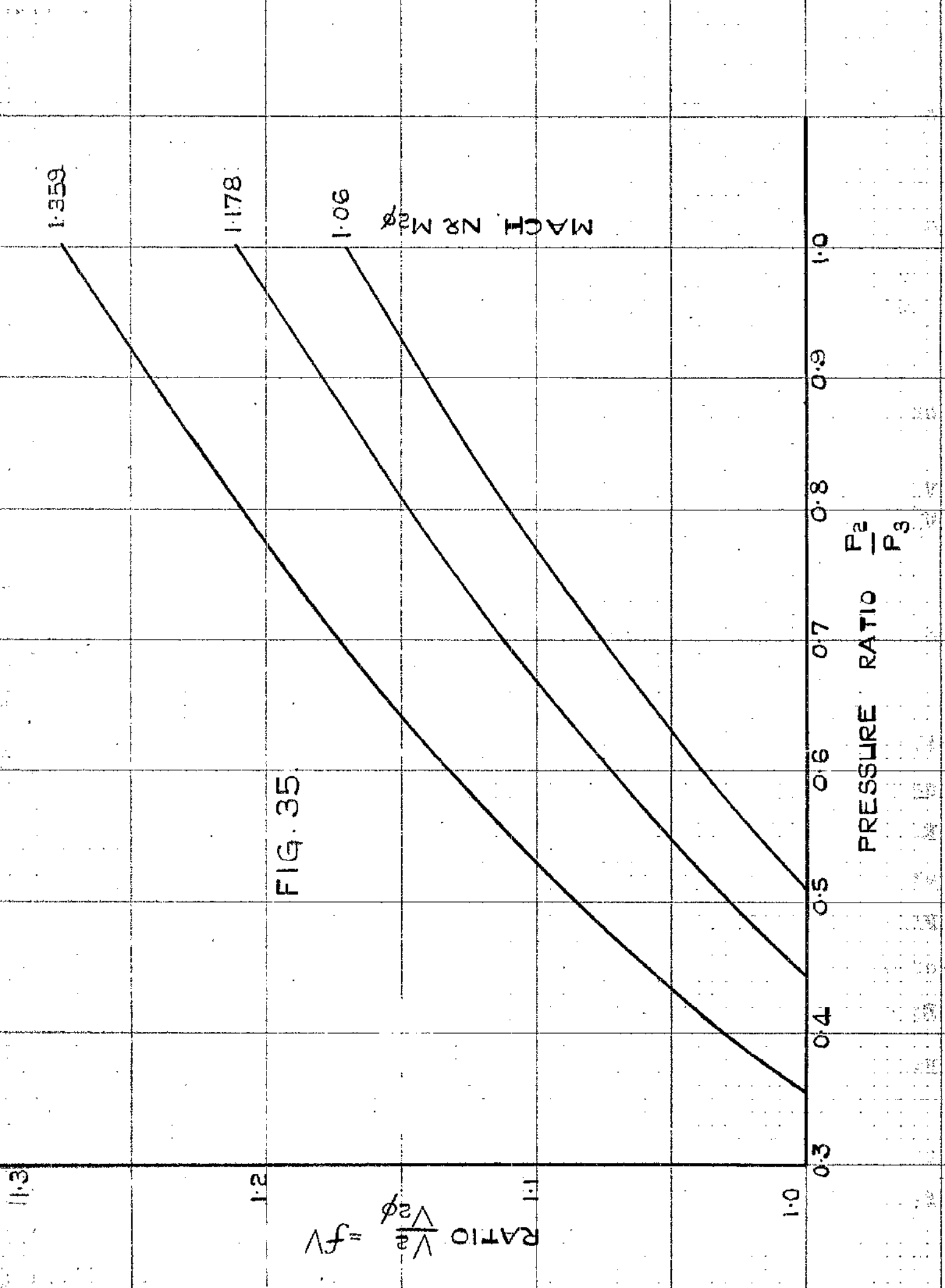


FIG. 35

$$\therefore \frac{V_2}{V_{2\phi}} = \frac{\left(\frac{P_1}{P_2} \right)^{\frac{\gamma-1}{\gamma}} - 1}{\left(\frac{P_3}{P_2} \right)^{\frac{\gamma-1}{\gamma}} - 1}$$

\therefore from 5

$$\frac{V_2}{V_{2\phi}} = \frac{1 - \left(\frac{P_2}{P_3} \right)^{\frac{\gamma-1}{\gamma}}}{1 - \left(\frac{P_2}{P_1} \right)^{\frac{\gamma-1}{\gamma}}} \times \frac{\left(\frac{P_1}{P_2} \right)^{\frac{\gamma-1}{\gamma}} - 1}{\left(\frac{P_3}{P_2} \right)^{\frac{\gamma-1}{\gamma}} - 1}$$

on simplifying this gives

$$\frac{V_2}{V_{2\phi}} = \frac{\left(\frac{P_2}{P_3} \right)^{\frac{\gamma-1}{\gamma}}}{\left(\frac{P_2}{P_1} \right)^{\frac{\gamma-1}{\gamma}}}$$

$$\therefore \frac{V_2}{V_{2\phi}} = \left(\frac{P_2}{P_3} \right)^{\frac{\gamma-1}{\gamma}} \left(\frac{\gamma-1}{2} M_{2\phi}^2 + 1 \right) \quad \text{_____ (8).}$$

The above relationships apply with subsonic or supersonic flow at point 2. Equation (2) is plotted in Fig. 31 as $\frac{P_2}{P_1}$ against Mach number.

Equation (6) relates ζ , $\frac{P_2}{P_3}$ and theoretical Mach No. after expansion $M_{2\phi}$.

Figs. 32 and 33 give ζ to a base of $\frac{P_2}{P_3}$ for various values of $M_{2\phi}$.

Equation (8) relates $\frac{V_2}{V_{2\phi}}$, $\frac{P_2}{P_3}$ and $M_{2\phi}$ and these are shown in Figs 34 and 35 for various values of $M_{2\phi}$.

Hence by obtaining the total head pressure P_3 the local total head efficiency and local specific volume can be obtained from the above relationships.

In subsonic flow the total head pressure is equal to the observed impact tube pressure, in supersonic flow however this is not so and a correction has to be made to the impact tube pressure to obtain the actual total head pressure of the stream.

Referring to Figs. 28, 29 and 30, for supersonic flow at 2 the impact tube acts like a large angled wedge so that a detached shock front forms up-stream of the impact tube. The total shock front is made up of a series of oblique shocks at various angles to the stream. However when the impact tube hole is aligned to be in the direction of the fluid stream, the changes of state experienced by the fluid approaching the hole correspond to those of a normal shock front.

For supersonic flow then P_4 and P_5 are the static pressure and total head pressure respectively after a normal shock jump from a stream Mach no. M_2 , and P_5 is equal to the observed impact tube pressure.

Hence from the theory of the normal shock wave the Rayleigh Supersonic Pitot - Tube relationship is

$$\frac{P_2}{P_5} = \frac{\left(\frac{2}{\gamma+1} M_2^2 - \frac{\gamma-1}{\gamma+1} \right)^{\frac{1}{\gamma-1}}}{\left(\frac{\gamma+1}{2} M_2^2 \right)^{\frac{\gamma}{\gamma-1}}} \quad (9).$$

(Shapiro³³).

also we have that $\frac{P_2}{P_3} = \left(1 + \frac{\gamma-1}{2} M_2^2 \right)^{\frac{\gamma}{\gamma-1}}$ (10).

Equation 9 relates the static pressure at outlet with the impact tube pressure for supersonic flow and is shown in Fig. 36. Superimposed on this graph is the relationship given by equation

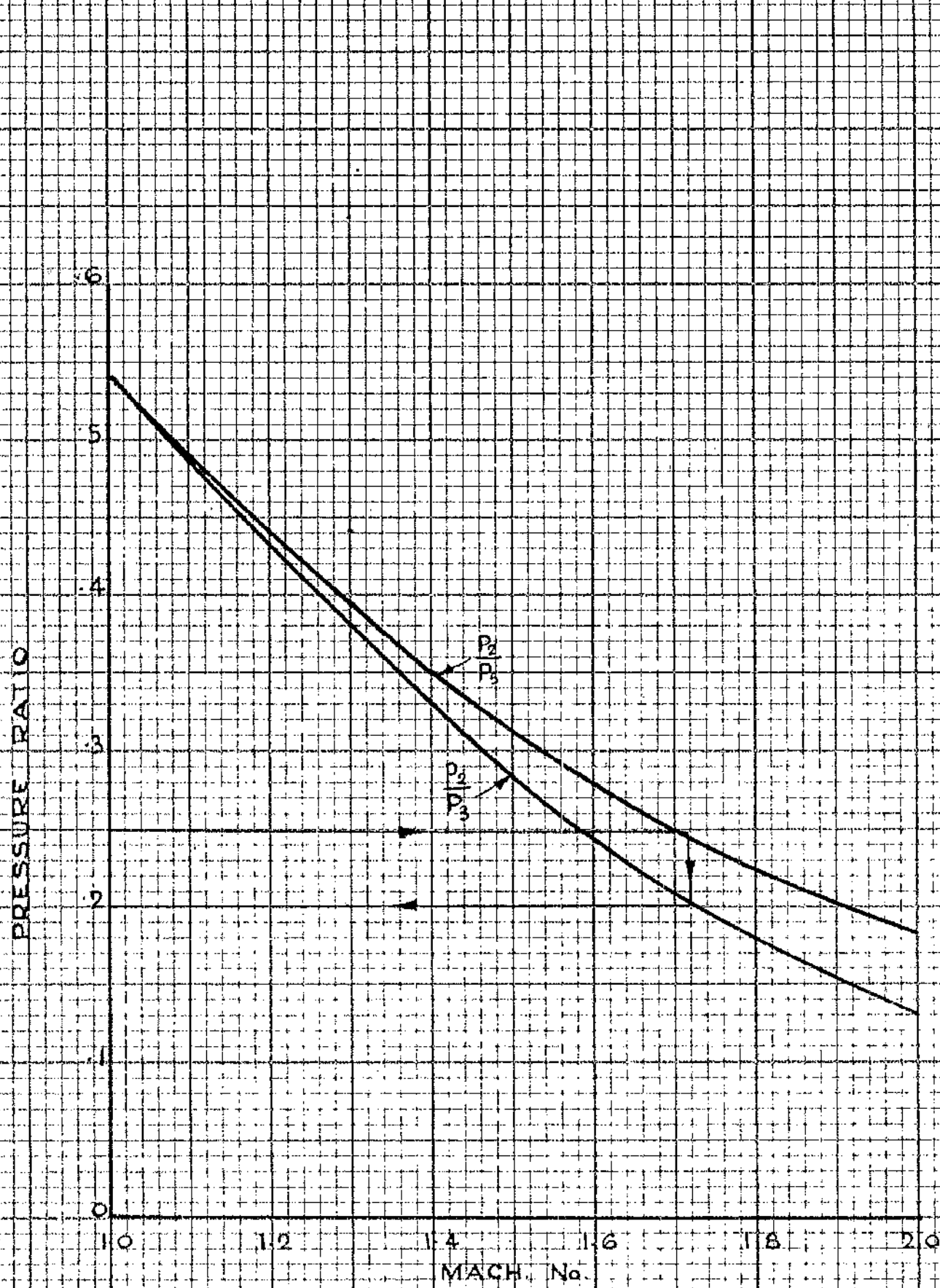


FIG No. 36

10 which is general for subsonic or supersonic flow.

Fig. 36 enables one to determine if the flow is supersonic or subsonic and if supersonic to obtain from the observed impact tube pressure the actual total head pressure of the stream.

Fig. 36 is drawn for superheated steam taking $\gamma = 1.3$, and has been reduced in size from its more accurate and larger original for presentation here. Thus if the ratio stream static pressure/ Impact tube pressure is less than 0.545 the stream Mach number is greater than unity and the ratio P_2/P_3 can be obtained as indicated. This ratio can then be used in Figs. 32 - 35 to obtain local efficiency and specific volume.

When plotting the relationships given in this section use may be made of Keenan and Kayes Gas Tables.³⁴ Table 34 for isentropic compressible flow with $\gamma = 1.3$ gives values of total head to static temperature ratio and total head to static pressure ratio for stream Mach numbers ranging from 0 to 10 and may be used to obtain the plots of pressure ratio, total head efficiency, and volume ratio in figures 31 to 35. Table 52 gives normal shock functions from which the plot of the Rayleigh pitot tube relationship in fig 36 may be made.

Summary of Part 2(a)

In subsonic flow the impact tube, if placed correctly in the stream at the exit plane of a nozzle or of a nozzle and blade pair, will record local values of the total head pressure of the stream. If locally the flow is supersonic a correction must be made to the observed impact tube pressure to obtain the actual total head pressure of the stream. The determination of whether or not the local flow is supersonic and the subsequent correction should this prove necessary are obtained using figure 36. The local total head efficiency of expansion and the ratio of the actual to the theoretical specific volume after expansion are shown to be functions of the pressure ratio, stream static pressure/stream total head pressure, and of the theoretical Mach number after expansion. Hence if one plots the local efficiency and volume ratio to a base of the above pressure ratio, for the various theoretical outlet Mach numbers at which an investigation is to take place, the local total head efficiency and state point of the fluid may be readily and expressly obtained. These relationships are shown in figures 31 - 35.

Part 2.

- (b) The Conversion of Local Values of Efficiency and of Efflux Angle into Mean Effective Values.

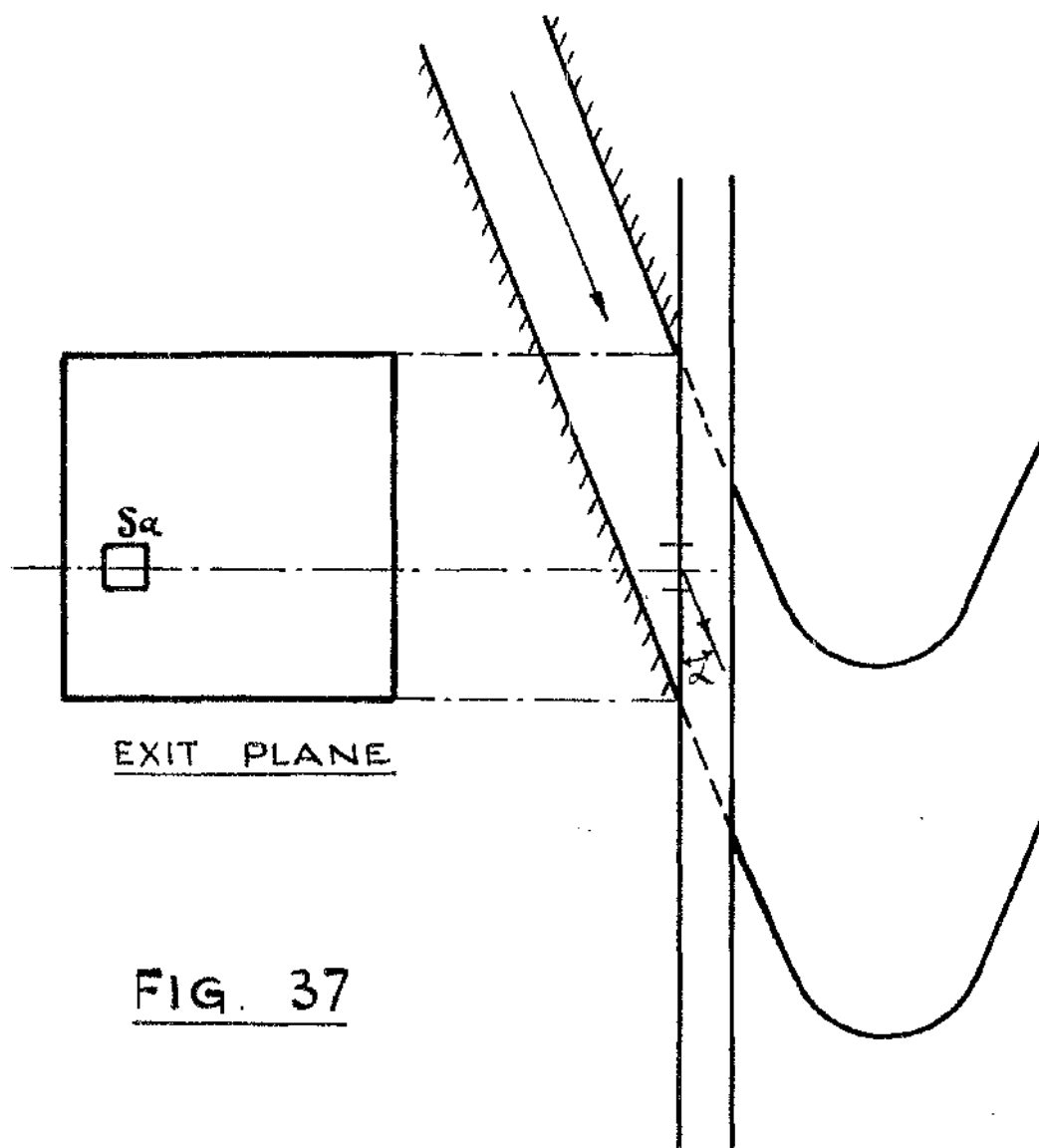
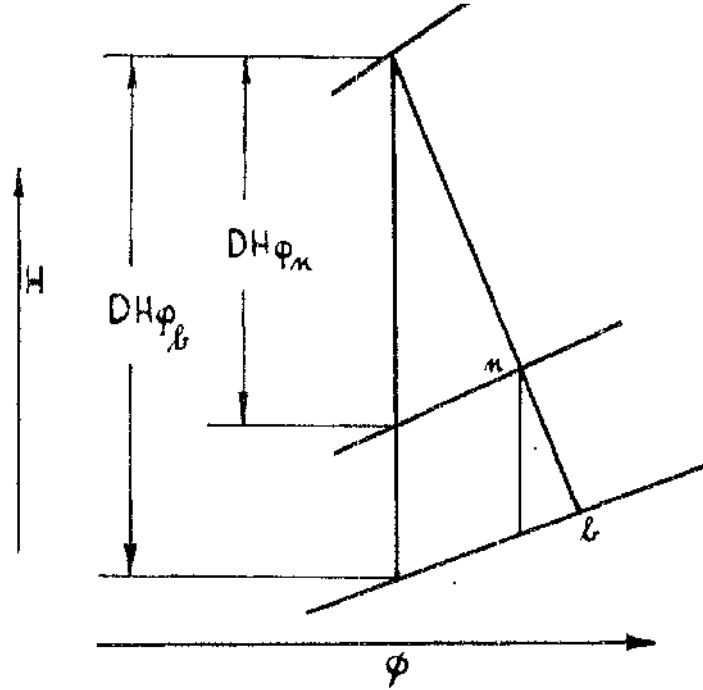


FIG. 37

Determination of the Mean or Effective Values of Efficiency of Expansion etc. from Traverses over the Exit Planes of a Nozzle and Blade Pair.

It will be appreciated that spot centre line readings of efficiency and efflux angle have to be modified to take account of two dimensional effects obtained from centre line traverses. The work of Howell⁷ and Ainley¹¹ further emphasised the need for three dimensional traverses to account for secondary losses. Having obtained the local values of efficiency, specific volume and efflux angle from the recorded impact tube readings at any cross-section of the flow in a nozzle or diffuser it is necessary to reduce these local values to a mean effective value which will apply to the whole cross-section.

This is done below with particular reference to the nozzle and blade pair used in the experimental work but the same general method would be used in any turbine or compressor element. In terms of local values, expressions are developed for the mean total head efficiency of expansion in the nozzle or in the nozzle and blade pair. The mean efficiency in the blade itself may then be obtained and for the particular case where there is no reaction in the blading a mean blade velocity coefficient is derived. The theory is further extended to give mean efflux angles for the nozzle and blade.

Referring to figure 37, consider a nozzle and blade pair in which the isentropic heat drop in the nozzle is DH_{ϕ_n} and in the nozzle and blade pair DH_{ϕ_b} . Suppose that traverses of the

nozzle and blade exit planes have been made and the values of local total head efficiency, specific volume and angle obtained over the areas.

Let DH = heat drop BTU./lb.

" m = mass flow lb. per sec.

" v = local velocity ft. per sec.

" α = local flow angle degrees.

" V = local specific volume ft^3/lb .

" η = local total head efficiency of expansion.

" da = local elemental area ft^2 .

" fV = the volume ratio V/V_ϕ .

" Σ = summation.

" K = blade velocity coefficient.

" \bar{x} = a mean value of x .

also let subscripts n and b denote the nozzle and blade outlet respectively.

Then at either plane the elemental mass flow at area da is given by $dm = \frac{v \sin \alpha da}{V}$

The total mass flow is then $m = \Sigma \frac{v \sin \alpha da}{V}$

But $\frac{v^2}{2} = \eta \frac{DH}{fV}$ and $\frac{v}{V_\phi} = fV$.

$$\begin{aligned} \therefore m &= \frac{V_\phi}{V} \Sigma \eta^{\frac{1}{2}} \sin \alpha \frac{da}{fV} \\ &= \frac{223.8}{V} DH^{\frac{1}{2}} \sin \alpha \frac{da}{fV} \end{aligned} \quad (1).$$

Hence at the nozzle exit

$$m = \frac{223.8}{V_{\phi n}} \sqrt{DH_{\phi n}} \Sigma \left(\eta^{\frac{1}{2}} \sin \alpha \frac{da}{fV} \right)_n \text{ lb/sec.} \quad (2).$$

and at the blade exit

$$m = \frac{223.8 \sqrt{DH \phi_b}}{v \phi_b} \leq \left(\gamma^{\frac{1}{2}} \sin \alpha \frac{da}{FV} \right)_b \text{ lb/sec.} \quad (3).$$

Kinetic energy at the exit planes.

At any plane the total flux of kinetic energy is

$$\leq \frac{v^2}{2g} \frac{v \sin \alpha da}{v} \text{ ft lb/sec.}$$

∴ Total flux of kinetic energy

$$= \frac{223.8^3 DH \phi^{\frac{3}{2}}}{2g v \phi} \leq \left(\gamma^{\frac{3}{2}} \sin \alpha \frac{da}{FV} \right) \text{ ft lbs/sec.} \quad (4).$$

Hence for one lb,

$$\text{K.E.} = \frac{223.8^2 DH \phi}{2g} \frac{\leq \gamma^{\frac{3}{2}} \sin \alpha \frac{da}{FV}}{\leq \gamma^{\frac{1}{2}} \sin \alpha \frac{da}{FV}} \text{ ft lbs/lb.}$$

$$\therefore DH = DH \phi \frac{\leq \gamma^{\frac{3}{2}} \sin \alpha \frac{da}{FV}}{\leq \gamma^{\frac{1}{2}} \sin \alpha \frac{da}{FV}} \text{ B.T.U./lb.}$$

∴ The mean total head efficiency of expansion is given by

$$\bar{\gamma} = \frac{\leq \gamma^{\frac{3}{2}} \sin \alpha \frac{da}{FV}}{\leq \gamma^{\frac{1}{2}} \sin \alpha \frac{da}{FV}} \quad (5).$$

$$\text{Thus } \bar{\gamma}_n = \left(\frac{\leq \gamma^{\frac{3}{2}} \sin \alpha \frac{da}{FV}}{\leq \gamma^{\frac{1}{2}} \sin \alpha \frac{da}{FV}} \right)_n \quad (6).$$

$$\text{and } \bar{\gamma}_b = \left(\frac{\leq \gamma^{\frac{3}{2}} \sin \alpha \frac{da}{FV}}{\leq \gamma^{\frac{1}{2}} \sin \alpha \frac{da}{FV}} \right)_b \quad (7).$$

The mean exit velocities for the nozzle and blade are given by

$$\bar{v}_n = 223.8 \sqrt{\bar{\gamma}_n DH \phi_n} \text{ and } \bar{v}_b = 223.8 \sqrt{\bar{\gamma}_b DH \phi_b}$$

It should be noted that $\bar{\gamma}_b$ is the mean total head efficiency of expansion for the nozzle and blade pair. The efficiency of the expansion process in the blade itself is given by

$$\bar{z}_b = \frac{H_n - H_b}{DH \phi_b - DH \phi_n}$$

$$\bar{z}_b = \frac{DH \phi_b \left(\frac{\sum z^{\frac{3}{2}} \sin \alpha \frac{da}{FV}}{\sum z^{\frac{1}{2}} \sin \alpha \frac{da}{FV}} \right)_b - DH \phi_n \left(\frac{\sum z^{\frac{3}{2}} \sin \alpha \frac{da}{FV}}{\sum z^{\frac{1}{2}} \sin \alpha \frac{da}{FV}} \right)_n}{DH \phi_b - DH \phi_n} \quad (8).$$

and the loss of high grade energy within the blade passage is

$$DH \phi_b - DH \phi_n - (H_n - H_b) \text{ B.T.U.}$$

∴ blade passage reheat loss is

$$DH \phi_b - DH \phi_n - \left[DH \phi_b \left(\frac{\sum z^{\frac{3}{2}} \sin \alpha \frac{da}{FV}}{\sum z^{\frac{1}{2}} \sin \alpha \frac{da}{FV}} \right)_b - DH \phi_n \left(\frac{\sum z^{\frac{3}{2}} \sin \alpha \frac{da}{FV}}{\sum z^{\frac{1}{2}} \sin \alpha \frac{da}{FV}} \right)_n \right] \quad (9)$$

For an impulse (zero pressure drop) blade this becomes

$$DH \phi_n \left[\left(\frac{\sum z^{\frac{3}{2}} \sin \alpha \frac{da}{FV}}{\sum z^{\frac{1}{2}} \sin \alpha \frac{da}{FV}} \right)_n - \left(\frac{\sum z^{\frac{3}{2}} \sin \alpha \frac{da}{FV}}{\sum z^{\frac{1}{2}} \sin \alpha \frac{da}{FV}} \right)_b \right] \quad (10)$$

For the impulse blade the loss in the blade passage may be expressed as

$$\text{Loss} = (1 - K^2) \frac{\bar{v}_n^2}{2gJ} = (1 - K^2) \bar{z}_n DH \phi_n \quad (11)$$

where K is the blade velocity coefficient.

Substituting for \bar{z}_n from (6) in (11) and equating to (10) gives

$$K = \sqrt{\left(\frac{\sum z^{\frac{3}{2}} \sin \alpha \frac{da}{FV}}{\sum z^{\frac{1}{2}} \sin \alpha \frac{da}{FV}} \right)_b \div \left(\frac{\sum z^{\frac{3}{2}} \sin \alpha \frac{da}{FV}}{\sum z^{\frac{1}{2}} \sin \alpha \frac{da}{FV}} \right)_n} \quad (12).$$

Effective mean exit angles.

Let the mean exit angles for the nozzle and blade be $\bar{\alpha}_n$ and $\bar{\alpha}_b$ respectively.

Tangential force on the blade = $\frac{m}{g} \times$ (change of tangential velocity) lbs.

$$= \frac{m}{g} (\text{inlet tangential velocity} + \text{outlet tangential velocity}) \text{ lbs.}$$

Hence the inlet tangential momentum flux is

$$= \frac{1}{g} \left\langle \frac{v_n}{v_n} \sin \alpha_n da \times v_n \cos \alpha_n \right\rangle \text{ lbs.}$$

$$= \frac{223.8^2 DH \phi_n}{g v_n} \sum \left(\int \sin \alpha_n \cos \alpha_n \frac{da}{rV} \right) \text{ lbs.}$$

$$= \frac{m}{g} \bar{v}_n \cos \bar{\alpha}_n \text{ lbs.}$$

$$\therefore \cos \bar{\alpha}_n = \left(\frac{\sum \int \sin \alpha \cos \alpha \frac{da}{rV}}{\left(\sum \int^{\frac{1}{2}} \sin \alpha \frac{da}{rV} \right) \sqrt{\frac{1}{2}}} \right)_n \quad \text{_____ (13).}$$

$$\text{similarly } \cos \bar{\alpha}_b = \left(\frac{\sum \int \sin \alpha \cos \alpha \frac{da}{rV}}{\left(\sum \int^{\frac{1}{2}} \sin \alpha \frac{da}{rV} \right) \sqrt{\frac{1}{2}}} \right)_b \quad \text{_____ (14).}$$

Summary of Part 2 (b).

In Part 2 (b) local values of efficiency and efflux angle are converted to mean effective values taking account of variations in mass flow per unit area throughout the exit plane element. Equation 8 gives the mean efficiency of the expansion process based on the static state of the fluid entering the element. Equation 5 may be applied generally to obtain the mean total head efficiency of expansion in a static test on a stator or rotor blade element. In the derivation of equation 5, it is assumed that the inlet total head state of working fluid is constant over the entire inlet flow area and the ideal final kinetic energy is that which would be obtained after isentropic expansion from this total head state to the static pressure at exhaust from the element. When testing cascades of blades in a wind tunnel, the total head state at inlet to the cascade is usually uniform and the reference total head pressure is often taken as the static pressure in the settling chamber upstream of the tunnel or nozzle.

In equations 6 and 7 the relationship for mean total head efficiency is applied at the exit plane of the tunnel or nozzle ($\bar{\eta}_n$) or at the exit plane of the blade cascade ($\bar{\eta}_b$). If there is a tunnel loss $\bar{\eta}_n$ will be less than unity and to calculate $\bar{\eta}_b$ the total head pressure at the immediate inlet to the cascade should be used. If the reference total head pressure is however taken as the static pressure in the settling chamber then the mean efficiency will include an allowance for the tunnel loss.

Expressions for the mean efflux angle at the nozzle or at the

blade exit are given in equations 13 and 14. These angles may be used in conjunction with the mean efflux velocities at the nozzle and blade exit to obtain the tangential blade force, the mean velocities being obtained using the appropriate mean total head efficiency.

In the experimental work described here, loss characteristics over a range of Reynolds and Mach numbers were obtained for a small nozzle and blade pair. The nozzle acted as a "wind" tunnel for a blade section which was essentially of impulse design and the test arrangement was such that the blade was forced to operate with zero pressure drop across the blade passage. Pitot traverses were made at the nozzle and blade exit planes and for the total head efficiency in each case the reference total head pressure was that at inlet to the nozzle. Since there was a small nozzle loss, this loss is included in the mean total head efficiency of the expansion for the blade. For this type of impulse blade the mean blade velocity coefficient, is given in equation 12, in terms of the mean total head nozzle and blade efficiencies.

Part 3.

An experimental investigation into the flow of superheated steam through a small nozzle and impulse blade pair yielding results on flow pattern and efficiency with varying Reynolds number and Mach number.

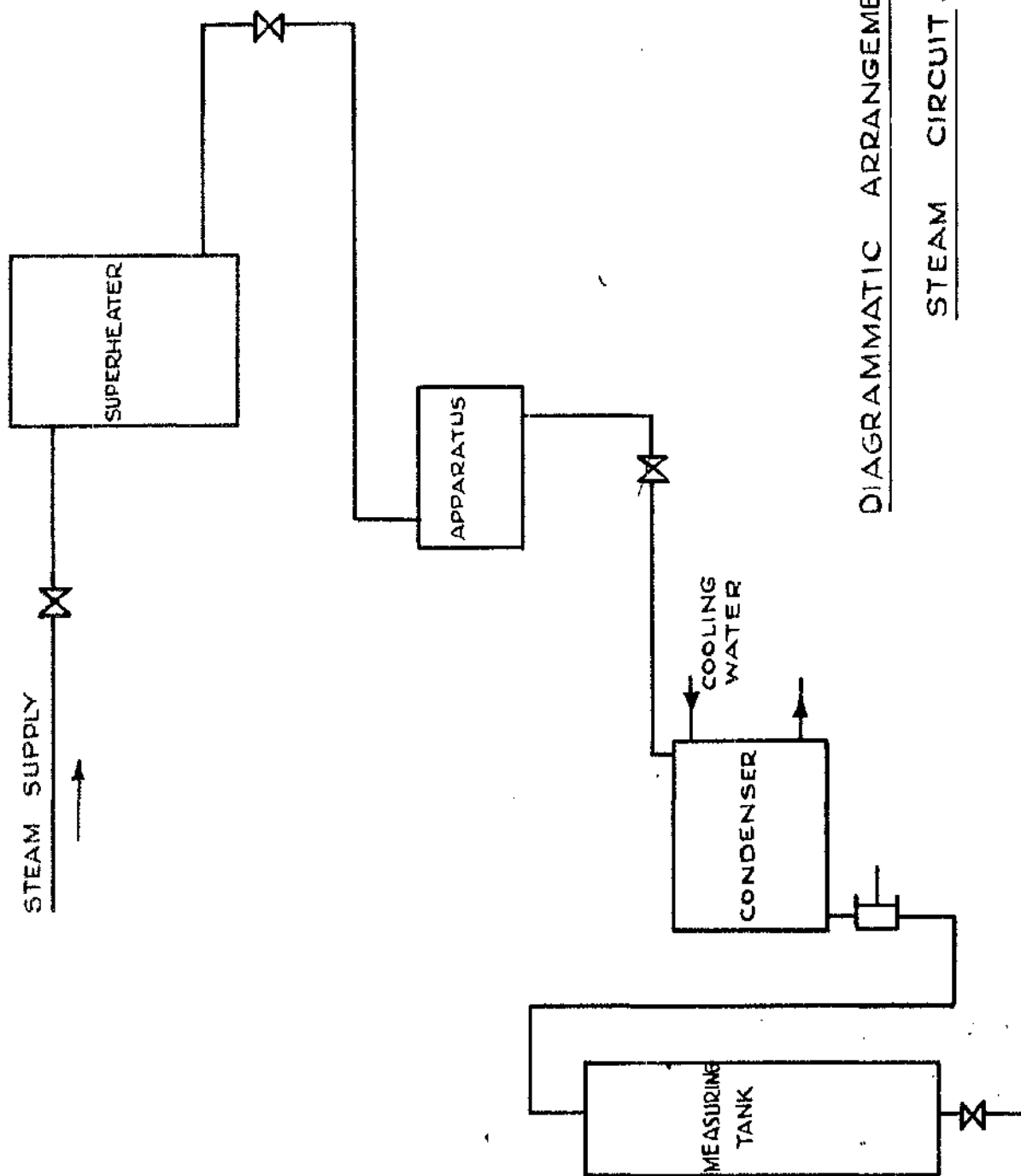
Object of the Experimental Work.

The underlying object is to develop an apparatus in which the methods of previous sections may be applied to typical machine elements and of course to examine these elements for flow patterns and friction factors.

It was decided to use superheated steam as the working fluid because of its availability and also due to the ease with which its density in a test section may be controlled and varied.

A nozzle of rectangular cross-section was manufactured to suit a standard set of blading which were essentially of impulse design. An impact tube and its associated traversing gear was then developed by means of which the flow patterns at either the nozzle or blade exit could be examined as near to true working conditions as possible. For this reason the tube and the traversing gear had to be of fairly robust construction so that they would operate efficiently in an atmosphere of relatively high pressure and temperature.

Description of the Apparatus.



DIAGRAMMATIC ARRANGEMENT OF THE
STEAM CIRCUIT.

FIG. 38.

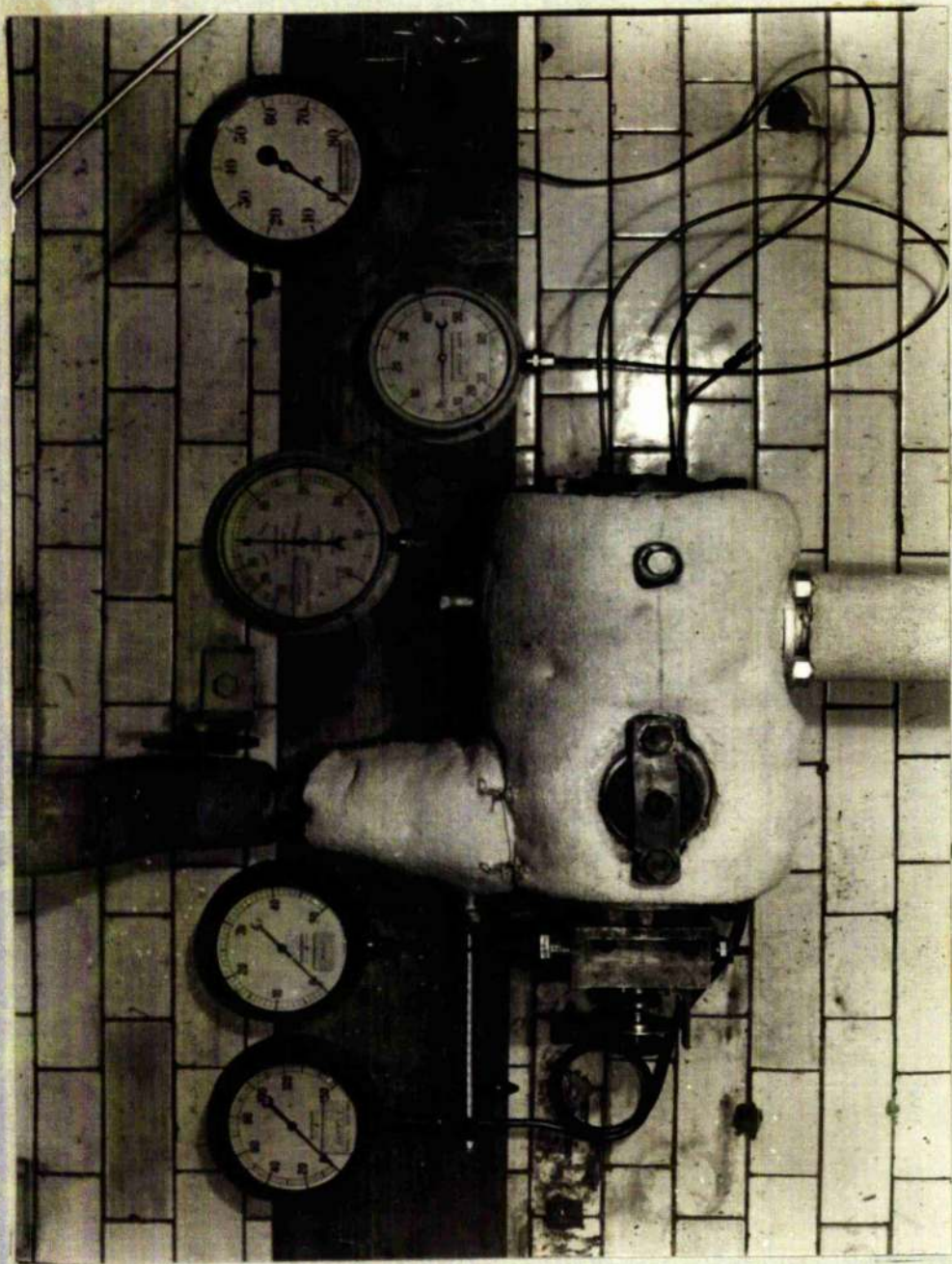


Plate 1.

General View of the Apparatus.

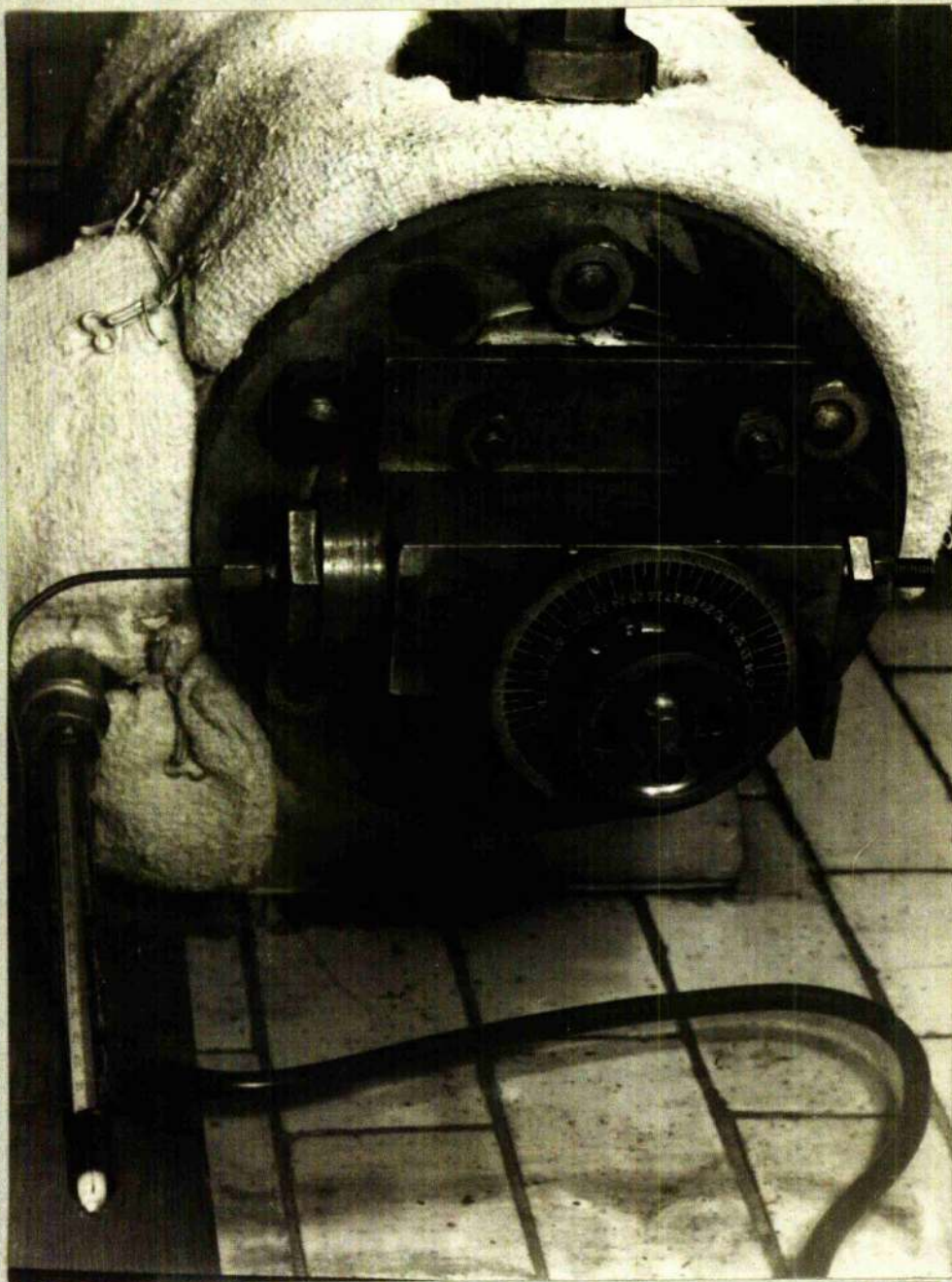


Plate 2.
Traversing Gear Mounted on End Cover.

Thermometer

Impact Tube

Pressure
Connection.

Protractor

Horizontal Scale
Bracket.

Inspection
Port.

Nut for Vertical Movement.

Main Lock.

End Cover.

Plate 3.

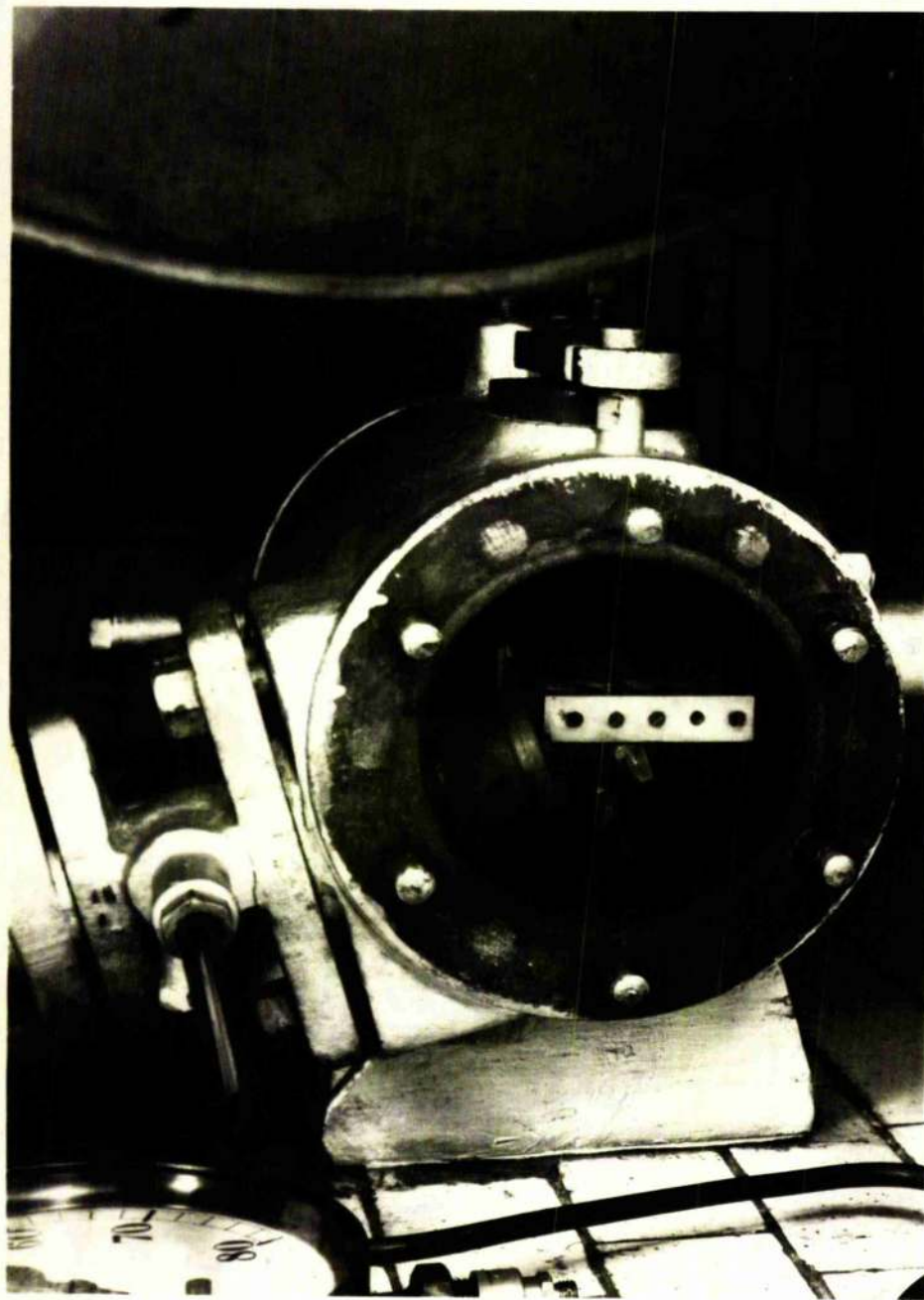


Plate 4.
Casing Interior.

Description of the Apparatus.

A diagrammatic arrangement of the steam circuit is shown in Fig. 38 (Page. 99). Wet steam is passed from a boiler through a gas fired superheater to a casing which contains the nozzle and blade elements. After passing through this test section the steam is exhausted to a surface condenser and the condensate may be measured in a graduated vessel. Throttle control valves are fitted before and after the superheater and between the casing and the condenser. By this arrangement considerable variation of the inlet state of the steam and of the exhaust pressure may be obtained.

The principal parts are:-

- (1) The casing.
- (2) The nozzle and blades.
- (3) The impact tube traversing gear.

The casing is shown on Plates 1, 2, 3, & 4, and is a cast iron pipe eight inches internal diameter by fourteen inches long fitted with a nozzle box, two end cover plates, a side inspection port, an exhaust opening and an arrangement for mounting the blades known as the blade carrier.

The nozzle box attaches to the steam supply pipe and is offset from the vertical at an angle of 15° . It is fixed to the casing by four studs which, passing through elongated holes, allow lateral movement of the nozzle box and hence of the nozzle position within the casing. The nozzle box is fitted with a thermometer.

f

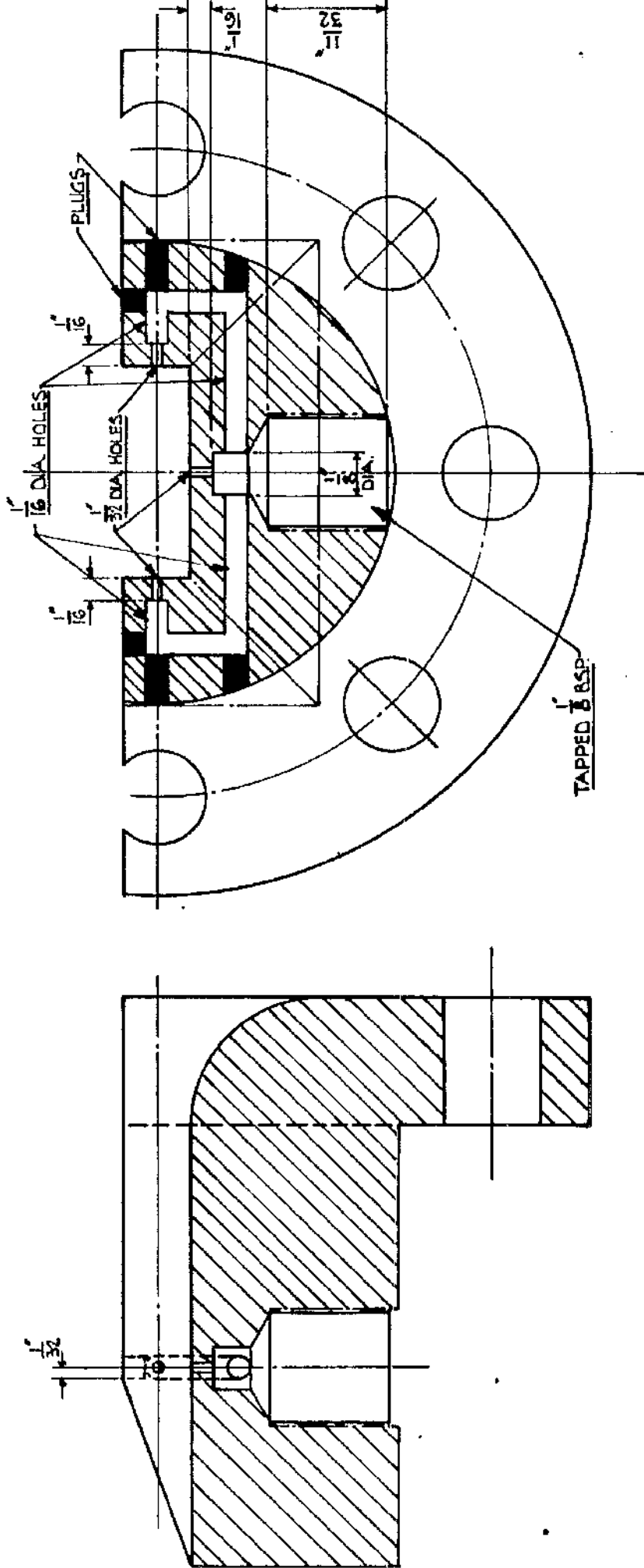


FIG 39 DETAIL OF PRESSURE TAPPING

SCALE:- TWICE FULL SIZE

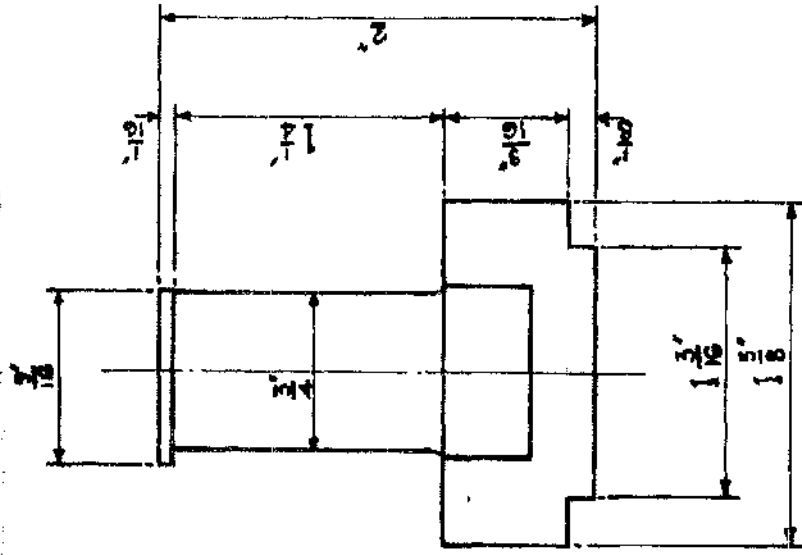
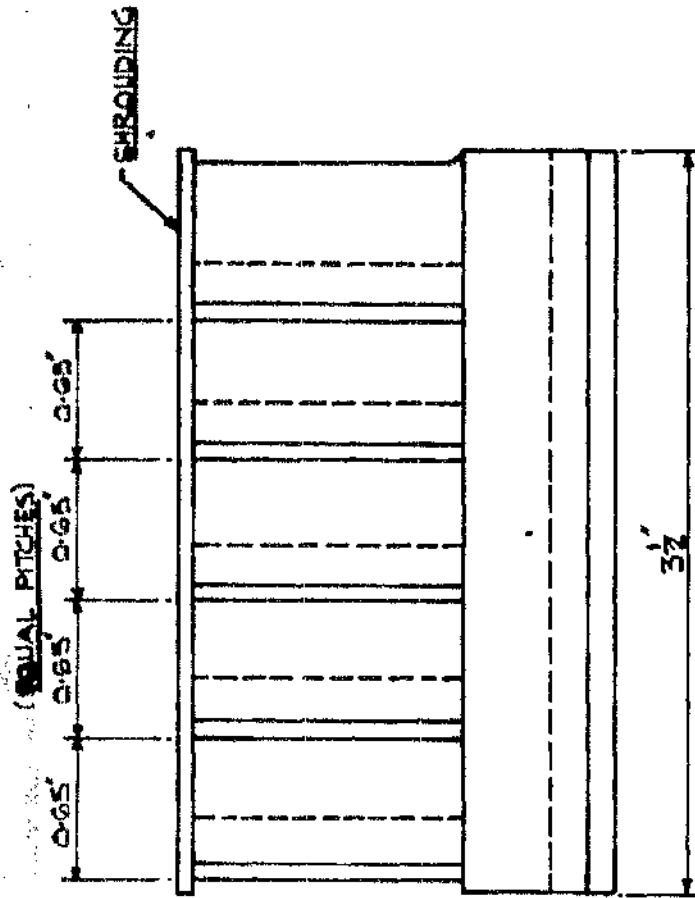
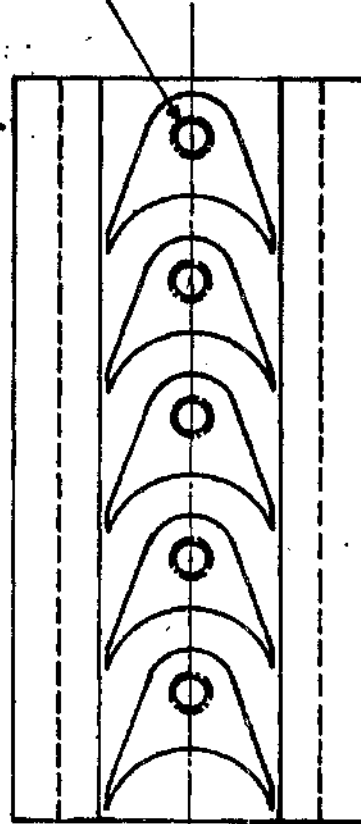


FIG-42



TAPPED HOLES FOR FIXING SCREWS
FROM SHROUDING

ARRANGEMENT OF BLADE ROW SEGMENT

SCALE: FULL SIZE

NOTE: FOR PASSAGE DIMENSIONS SEE SEPARATE DETAIL

PLAN WITH SHROUDING
REMOVED

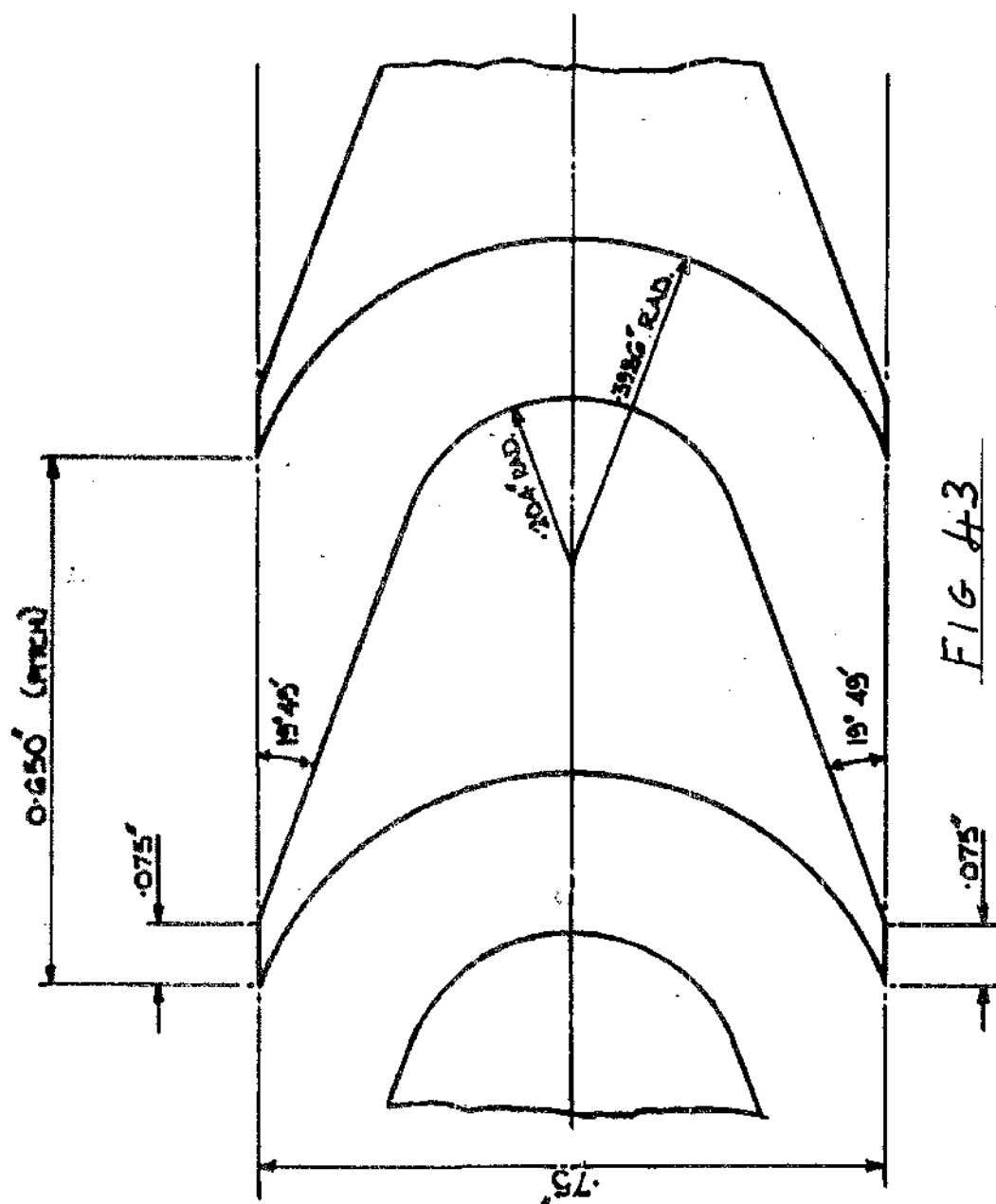


FIG #3

DETAIL OF BLADE PASSAGE (PARSONS SG30)

SCALE: 4 TIMES FULL SIZE



Packing Pieces.

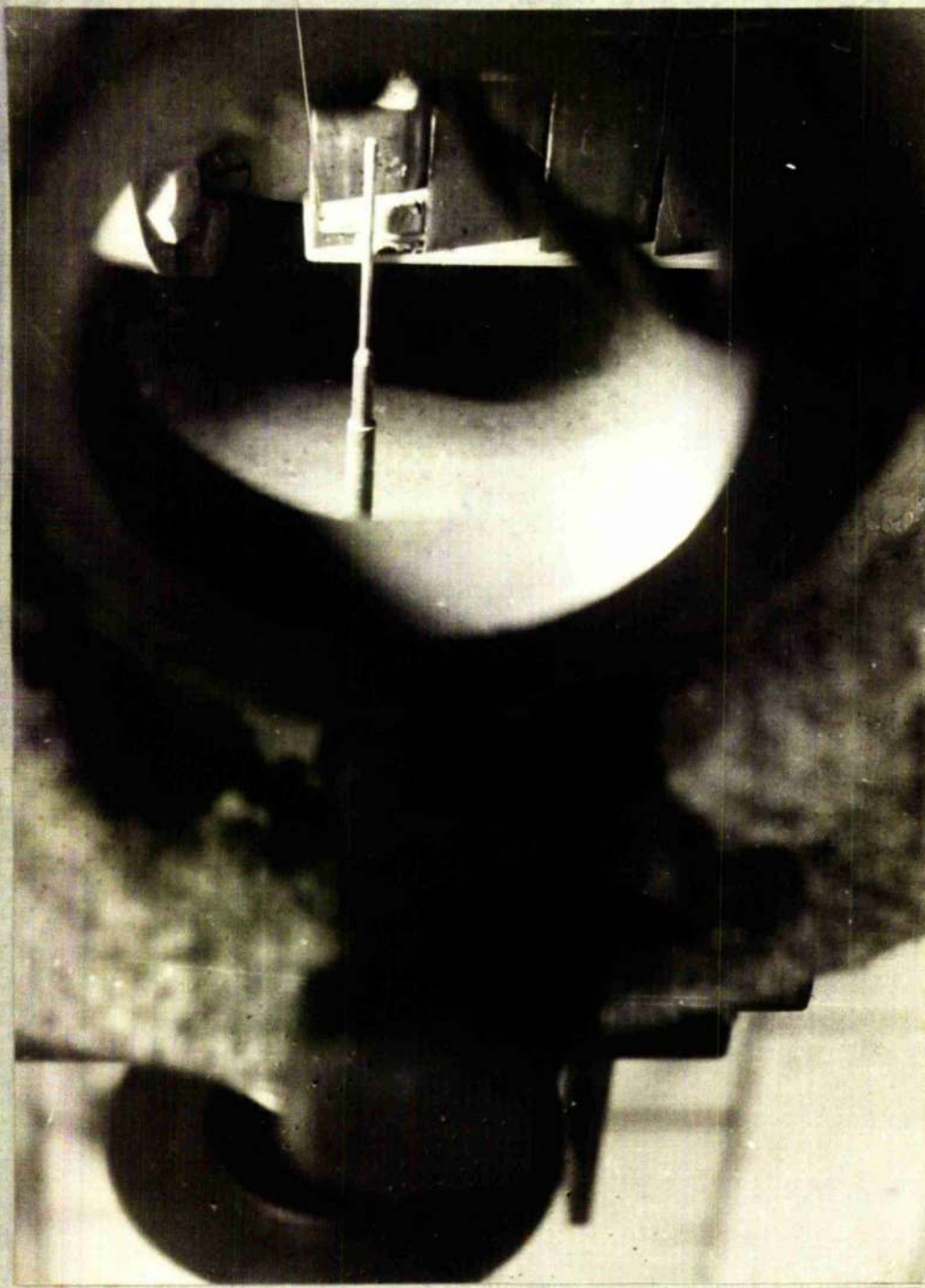


Plate 5.

View Through Inspection Port.

One end cover has a rectangular opening and four studs for mounting the traversing gear. The other cover has pipe connections for pressure tapplings from the nozzle.

The blade carrier, Plate 4, is a lever arrangement mounted within the casing and pivoted on screwed trunnions, which pass through the wall of the casing.

The other end of the lever has a vertical face on which the blading is fixed by friction plates fastened by four screws. Lateral movement of the blading is obtained by varying the relative position of the two trunnions while the vertical position depends on where the blades are clamped to the carrier face.

The nozzle is convergent parallel of rectangular section and is shown on Plate 4, and on Figs. 39 & 40, (Pages 105 & 106). It was manufactured in two parts to facilitate machining. The nozzle is mounted onto the nozzle box through an adapter piece so that the nozzle outlet angle is equal to the blade inlet angle of $19^{\circ} - 49'$. The adapter piece Fig. 41, (Page 107) is fitted with a static wall pressure tapping and with a tube which measures the total head pressure at inlet to the nozzle. Tappings of pressure are taken from three of the nozzle passage walls at exit and lead to one chamber. Thus the average nozzle exit pressure is obtained.

The blading used was a Parsons set of essentially impulse design and is shown on Plates 4 & 5 and on Figs. 42 & 43.

Packing pieces were introduced into the blade passages

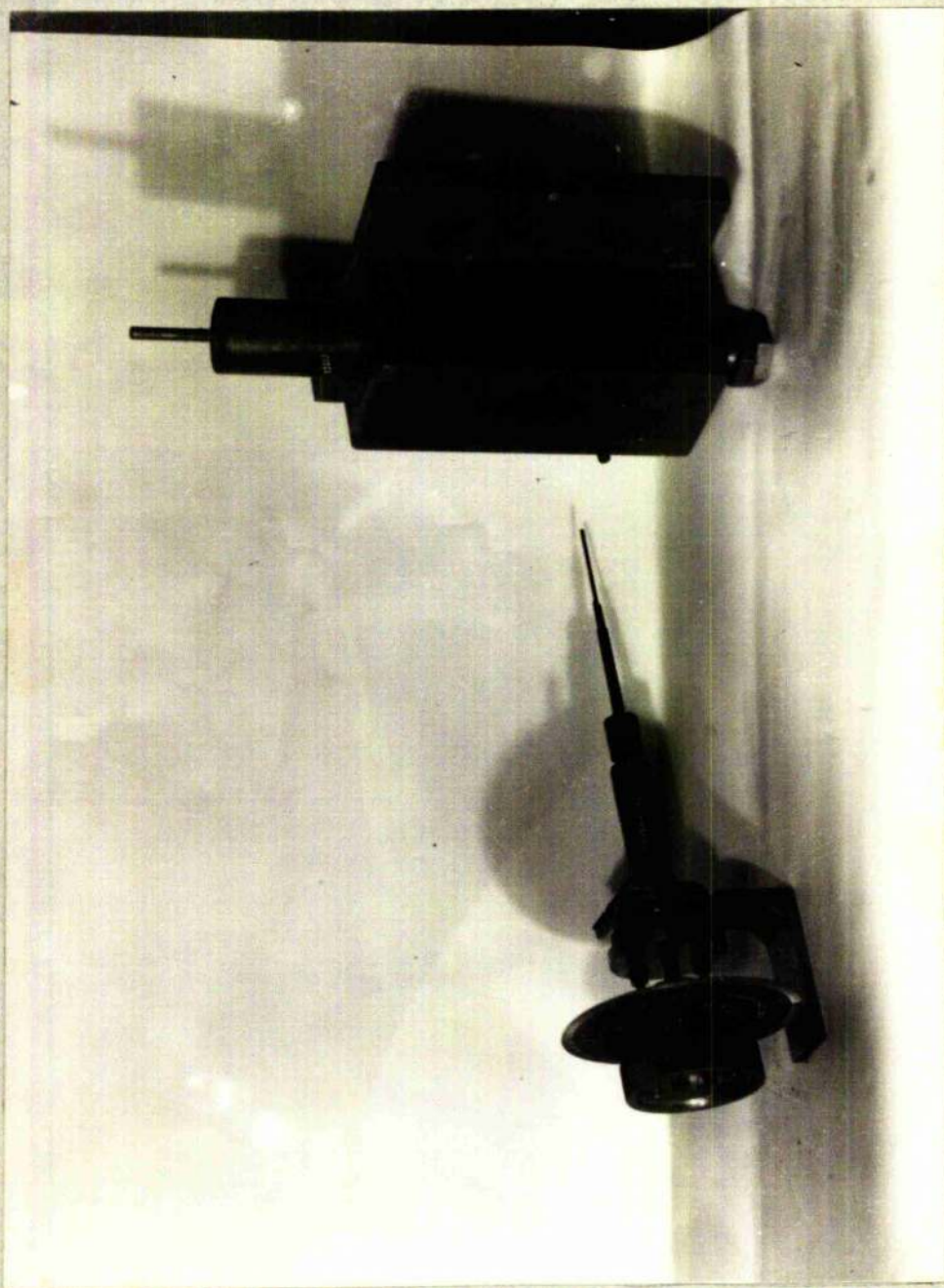
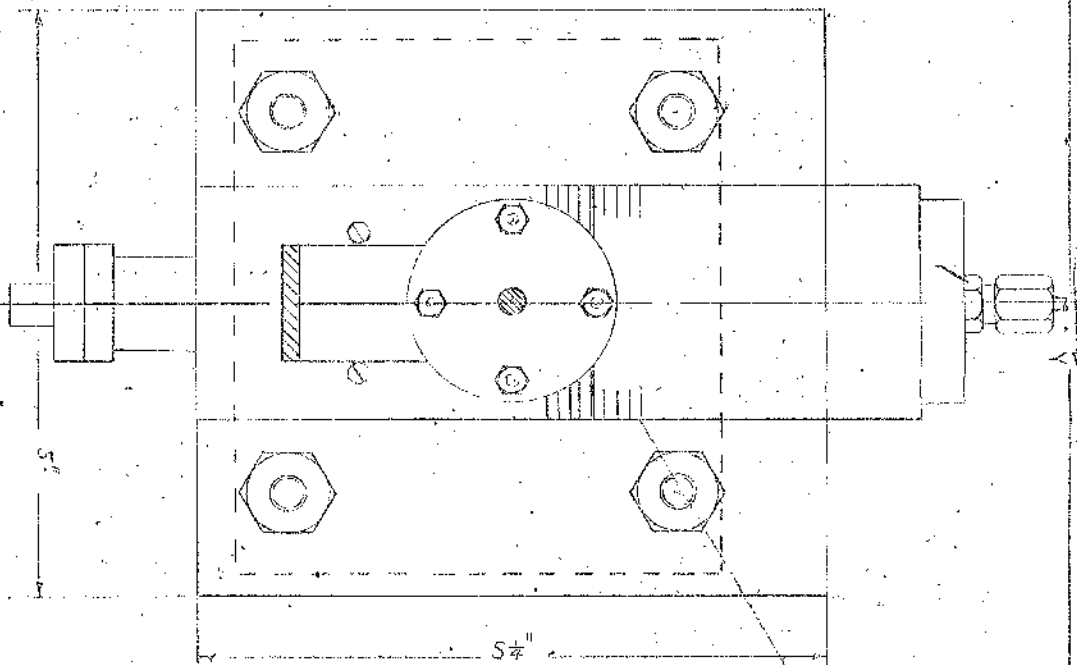


Plate 6.
Traversing Gear.

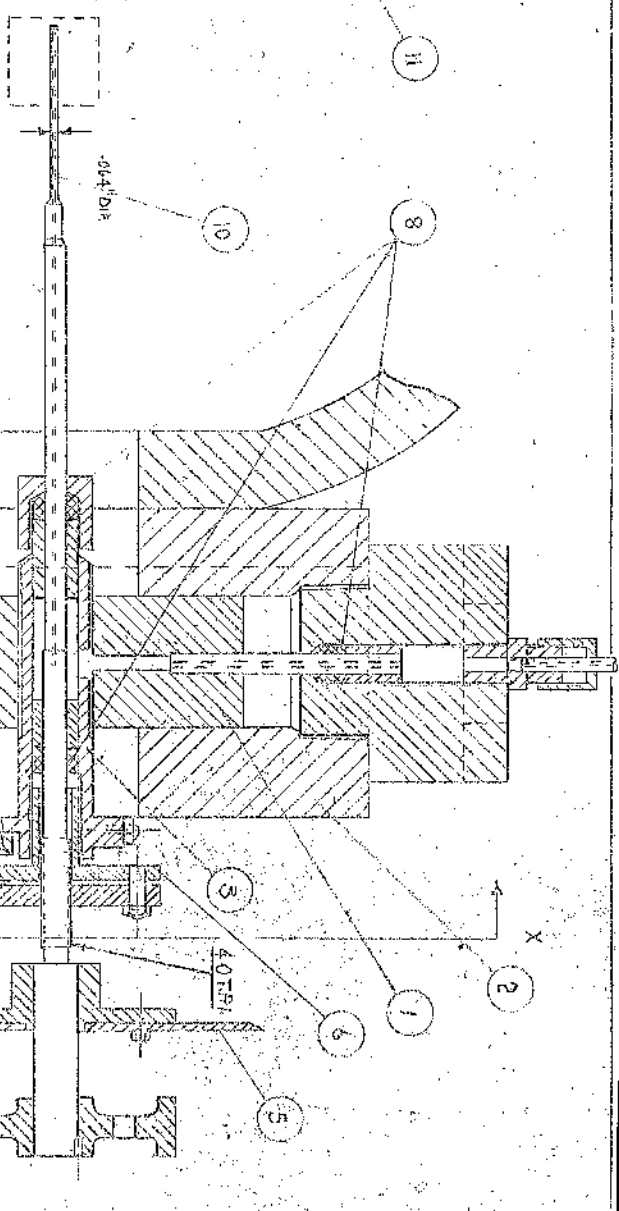
VIEW ON XX



SCALE — FULL SIZE

FIG 4-4

ITEM NO.	DESCRIPTION
1	PISTON
2	MAIN BLOCK
3	CARRIER
4	CARRIER BRACKET
5	GEORIGATOR
6	CARRIER NUT
7	DISC
8	PACKED GLANDS
9	VERT. ADJUSTMENT BOLTS
10	IMPACT TUBE
11	VERTICAL SCALE



SECTION ON YY

so that the effective blade height could be varied. The packing pieces are shown in position on Plate. 5. The impact tube traversing gear is shown on Plate 6 (Page 112) and in the drawing on Fig. 44. The traversing gear is designed so that the impact tube hole can be located at any point in the exit plane of the nozzles or blades. Thus it must be capable of vertical and horizontal movement as well as being able to rotate.

The main block (item 2) is clamped to the end cover facing the nozzle and has a vertical hole machined in it into which a piston (item 1) is lapped. At right angles to the axis of the piston near the middle of its length there is a screwed hole. This hole takes the impact tube carrier (item 3). The impact tube runs through the carrier and is located centrally in the carrier by sleeves. Pressure packing glands (item 8) are fitted at both ends of the carrier. Item 6, the carrier nut is screwed into the carrier and controls the pressure on the gland packing. Bolted to the carrier nut is a disc (item 7) which is screwed internally with 40T.P.I. and which engages with a screwed portion of the impact tube. Thus rotation of the impact tube causes a horizontal movement of the tube. This movement is measured on a scale scribed on the face of the carrier bracket (item 4).

A protractor is fitted to measure the angular position of the impact tube hole and a knurled nut is used to rotate the tube.

Vertical movement is obtained by two nuts (item 9) which can be arranged to push up or pull down the piston. The piston,

carrier, impact tube and carrier bracket move as one unit.

The impact tube (item 10) consists of four lengths of tubing of increasing diameter brazed together. The largest is a length of steel bar screwed for a part of its length with a 40 T.P.I. thread. The portion of the tube within the fluid stream is made of hypodermic tubing 0.0625" external diameter and with an impact hole 0.010" diameter at $\frac{3}{8}$ " from its end.

The pressure at the impact hole is communicated through the tubing to approximately the centre of impact tube and is released into a chamber within the carrier. This chamber is pressure sealed by packing glands mentioned previously. The chamber is connected through a vertical hole in the piston to a tube brazed to the top of the piston. The tube is pressure sealed in a large nut which screws into the top of the main block. Hence the impact tube pressure can be taken off from a simplex coupling at the top of the large nut. By this means the impact tube pressure may be observed without any direct pipe coupling onto the impact tube itself. In addition the parts of the tube used in the operation remain cool for handling.

Considerable attention was paid to the alignment of the protractor relative to the impact tube hole. The protractor was set so that when the impact tube hole was at T.D.C. the zero mark on the protractor was at B.D.C. The impact tube was then clamped in a V-block and placed in a Hilger projector with the hole at approximately 90° from T.D.C. The outline of the tube was magnified on the screen 50 times and the impact hole

showed up clearly. The tube was then rotated until the reflection on the screen showed the hole to be equidistant from the edges of the tube. Thus the hole was accurately positioned at 90° to T.D.C. The V-block was then placed on a surface table and by means of a height gauge the protractor was set so that the 0° and 180° marks were at 90° to T.D.C. The protractor was then clamped to the tube by the three screws provided.

The pressures recorded were taken from wall tapplings at the nozzle inlet and at the nozzle outlet, and also from the impact tube and from a tapping in the casing. In addition a fixed impact tube was placed upstream of the nozzle inlet but it was found that the velocity head here could be neglected and readings from the inlet nozzle wall tapplings were taken to give the inlet total head pressure.

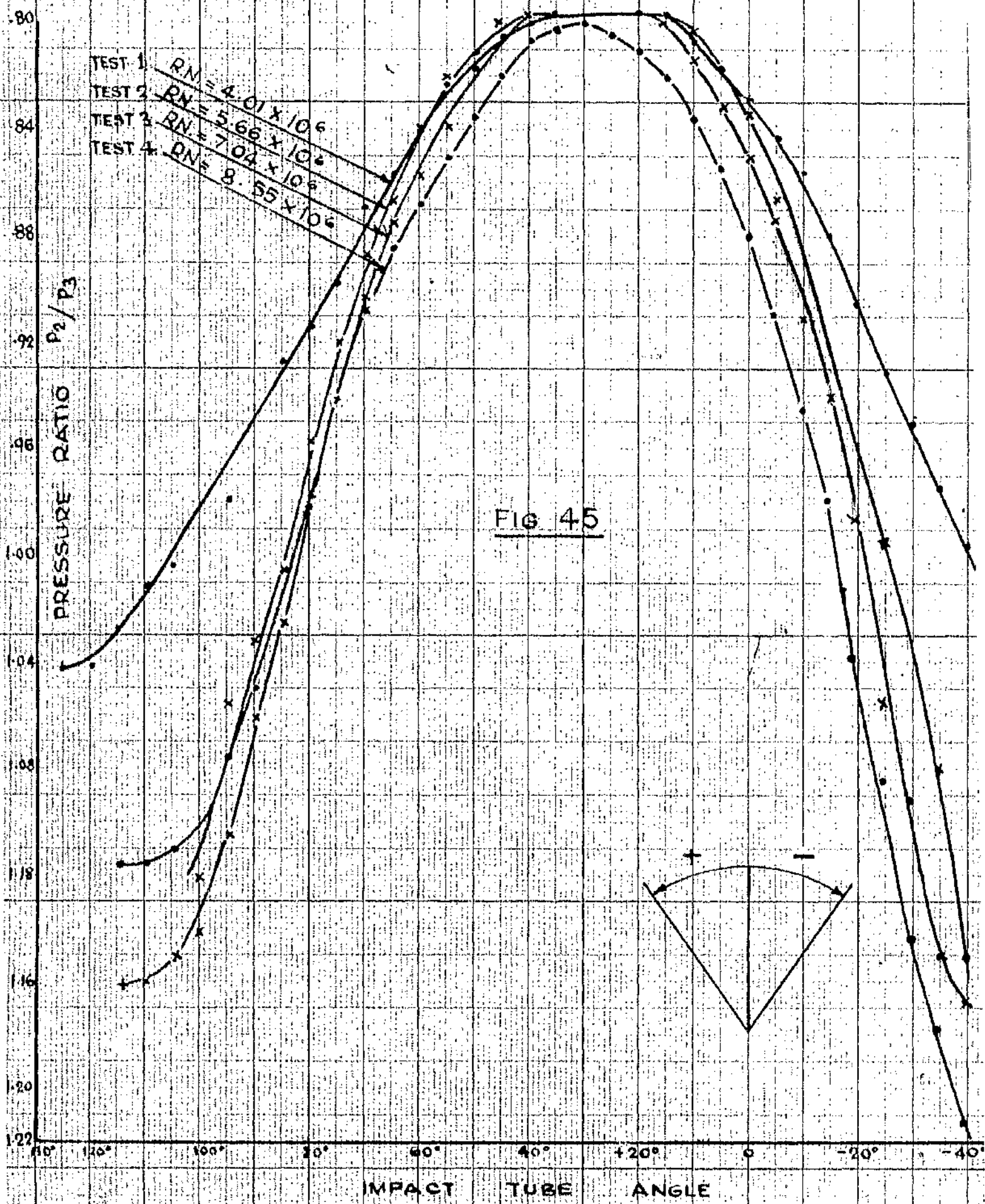
Preparation of the apparatus for testing.

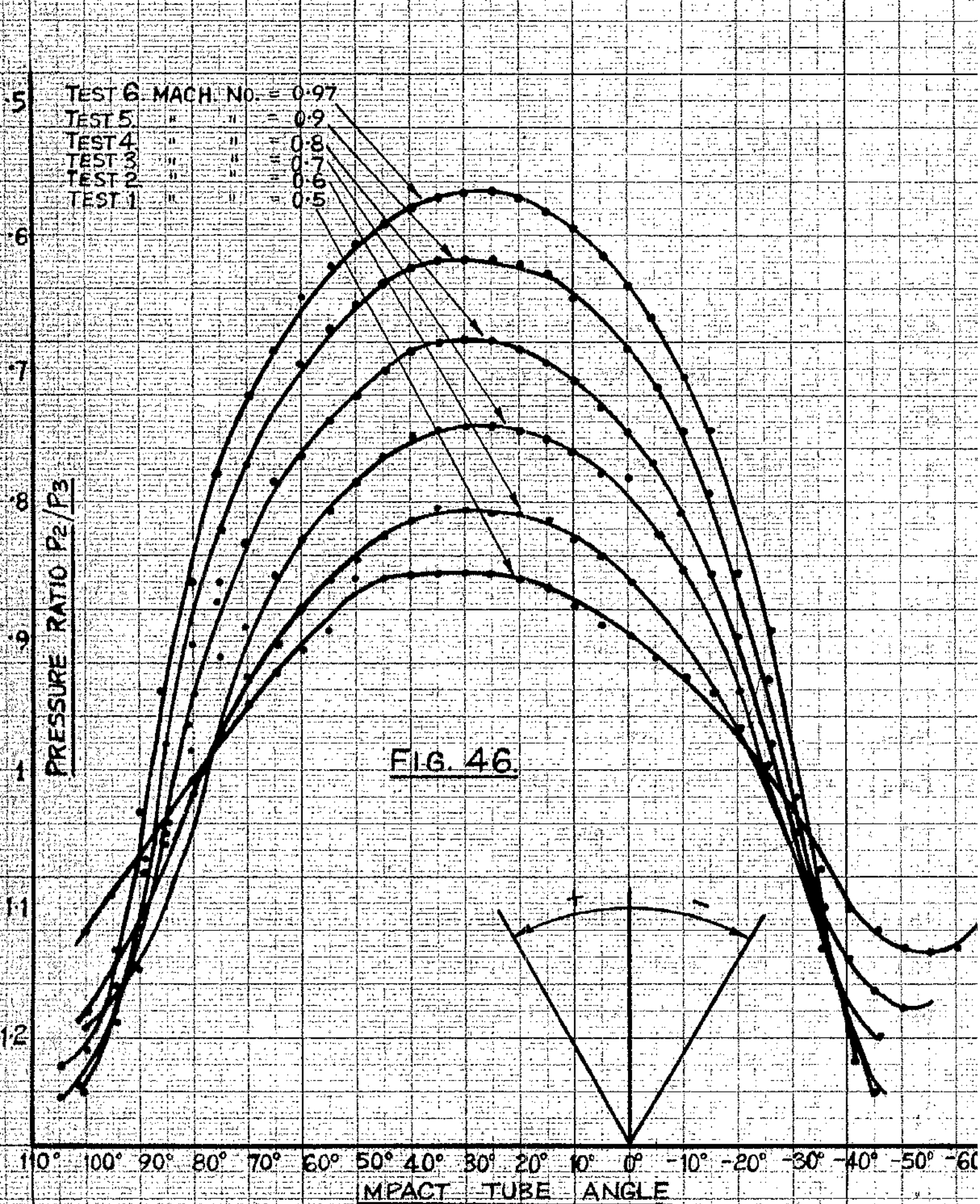
The nozzle was screwed into position so that the exit plane of the nozzle was vertical and parallel to the axis of the casing. Horizontal and vertical lines $0.10''$ apart were scribed on the nozzle face to divide the exit area regularly. Allowance was made for the fact that the actual flow area to be traversed would be lower than the exit face of the nozzle due to the clearance between the face and the hypodermic tubing. The traversing gear was then bolted to the end cover and corresponding horizontal and vertical lines were scribed on the carrier bracket and on the main block. The pressure gauges were accurately calibrated and a special large scale test gauge was used for the impact tube pressure. The procedure for examining the flow at the blade exit was similar to that at the nozzle exit.

Limitations set by the experimental rig on the applicability of the experimental results.

(a). It should be noted that the packing pieces which control the effective blade height were adjusted at each blade test so that the static pressure at the nozzle outlet was equal to that at the blade outlet. Thus the blade passage is forced to operate as a zero pressure drop impulse blade (figure 9E). The observed variation of loss with Reynolds number and Mach number will therefore apply to such a zero pressure drop impulse stage, one example of which is the partial admission stage in a steam turbine. Here the turbine disc runs in a constant pressure medium, the static pressure on either side of the disc being maintained the same by drilling balance holes through the disc.

(b). The nozzle outlet pitch was made equal to the blade pitch so that the steam flow covers one blade pitch only and the whole blading cascade does not therefore run full in the pitchwise direction. This is particularly important when considering the observed variation in efflux angle in the pitchwise direction, as the variation would be influenced by neighbouring blades running full of steam.





ONE DIMENSIONAL TRAVERSE AT CENTRE OF NOZZLE EXIT

Test Programme

A preliminary investigation of the characteristics of the impact tube was first made with the impact tube hole situated at the centre of the nozzle exit. Figures 45 and 46 show experimental readings of the variation of pressure round the impact tube, for various Reynolds numbers and Mach numbers, as the position of the hole is varied by rotating the tube. The correct alignment of the impact tube hole with the absolute direction of the stream is essential if the maximum impact tube pressure is to be observed.

The local direction of the stream was found by rotating the tube in one direction and observing an angle at some suitable arbitrary pressure. The tube was then rotated in the opposite direction until the same pressure was obtained, the new angle being noted. The direction of the stream is then the mean of these two angles and by positioning the tube at this angle the correct total head pressure is obtained.

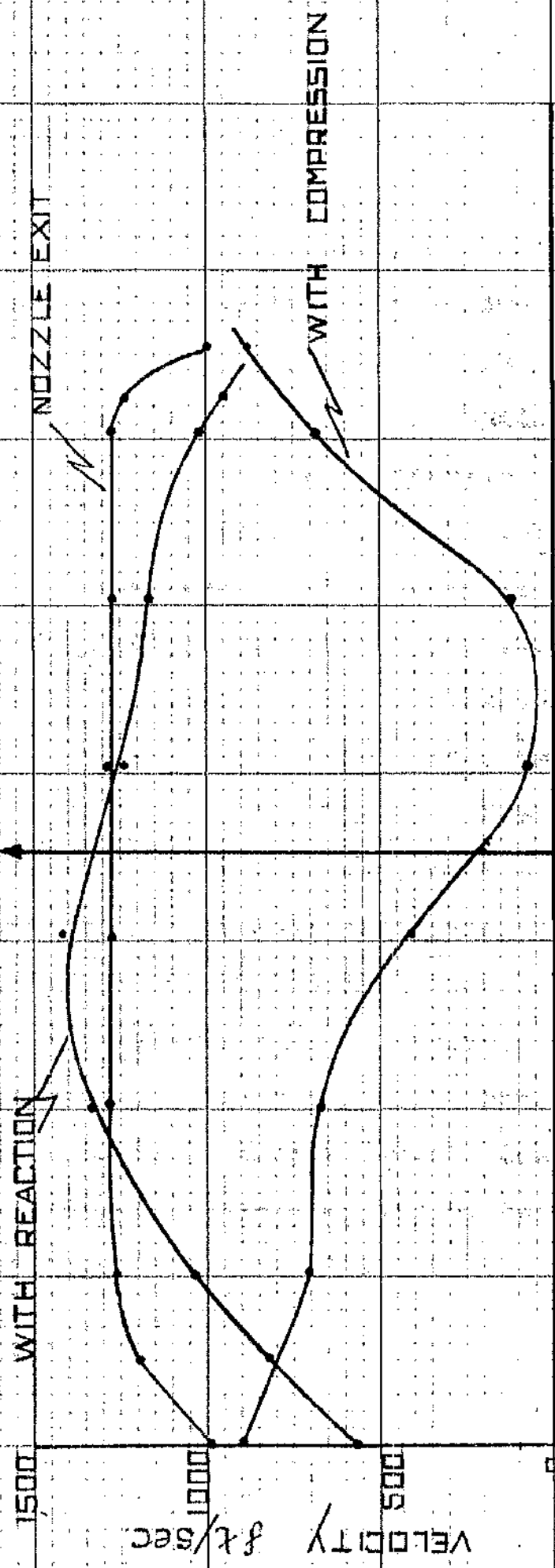
This is more accurate than rotating the tube until the maximum pressure is observed due to the relative flatness of the top of the curve and the time necessary for the fluid pressure to build up inside the tube.

The dependance of loss on Reynolds number and Mach number indicates a main test series which would show the variation of loss with these parameters. Since the blades were essentially impulse in design, it was decided to test as near to pure impulse conditions as possible. Thus a preliminary test was

COMPARISON OF BLADE EXIT VELOCITY DISTRIBUTION FOR SMALL

AMOUNTS OF COMPRESSION AND REACTION ACROSS THE BLADE PASSAGE.

FIG. 47.



NOZZLE INLET PRESSURE	NOZZLE ALONE	WITH REACTION	WITH COMPRESSION
34.7 LB/IN. ²	34.7 LB/IN. ²	34.7 LB/IN. ²	34.7 LB/IN. ²
NOZZLE EXIT PRESSURE	22.7 "	22.7 "	21.7 "
BLADE EXIT PRESSURE	22.7 "	20.7 "	22.7 "

arranged during which the blade packing pieces which control the effective height of the blades were adjusted so that there was no pressure drop within the blade passage. During this operation the flow pattern at the blade outlet was observed with firstly a small amount of reaction in the blade passage and secondly with a small amount of compression in the passage. The test conditions along with graphs of exit velocity distribution along a horizontal centre line for the nozzle and blade are shown on Fig. 47 for this preliminary test.

The main tests are grouped into three series and for simplicity test conditions, results and calculations for each series are given separately.

Series 1 on page 124.

Series 2 on page 151.

Series 3 on page 164.

In all the series the steam remains superheated during expansion to avoid the complication of either supersaturation³⁵ or wetness. In each series specimen experimental observations, calculations and derived tables only are given here. A complete set of experimental and derived tables is given in appendix 2.

The symbolism used in the presentation of the test results is the same as that in Part 2 (a) (page 75) and in Part 2 (b) (page 90).

Series 1.

In this series the exit Mach number was kept constant at 0.6 and the Reynolds number varied by changing the inlet nozzle pressure. There are in total eight three dimensional tests, four at the nozzle and four at the blade exit flow area. The nozzle tests are numbered 1 - 4 and the blade tests 1A - 4A.

The nozzle test conditions are given in the following table. The blade test conditions vary only slightly from these due to daily variations in barometric pressure.

Test 1	Test 2	Test 3	Test 4
$P_1 = 24.3 \text{ lb/in}^2$	$P_1 = 35.15 \text{ lb/in}^2$	$P_1 = 44.15 \text{ lb/in}^2$	$P_1 = 54.32 \text{ lb/in}^2$
$P_2 = 19.3 \text{ lb/in}^2$	$P_2 = 28.0 \text{ lb/in}^2$	$P_2 = 35.15 \text{ lb/in}^2$	$P_2 = 43.25 \text{ lb/in}^2$
$H_1 = 1229.2 \text{ BTU/lb}$	$H_1 = 1229.2 \text{ BTU/lb}$	$H_1 = 1229.2 \text{ BTU/lb}$	$H_1 = 1229.2 \text{ BTU/lb}$
$T_1 = 380^\circ\text{F}$	$T_1 = 383.6^\circ\text{F}$	$T_1 = 386.7^\circ\text{F}$	$T_1 = 389.8^\circ\text{F}$
$M_{2\phi} = 0.6$	$M_{2\phi} = 0.6$	$M_{2\phi} = 0.6$	$M_{2\phi} = 0.6$
Reynolds number 4.01×10^6	Reynolds number 5.66×10^6	Reynolds number 7.04×10^6	Reynolds number 8.55×10^6

On the following pages the results and calculations for tests 1 and 1A are given in detail. The remaining tests results and tables of calculations are given in appendix 2 (pages 2-32).

The calculations are concerned with the determination of the effective values as described in Part 2.

Specimen Results and Calculations ----- Series 1.Test 1

Barometric pressure 29.22 ins Hg = 14.3 lb/in²

$$P_1 = 24.3 \text{ lb/in}^2$$

$$P_2 = 19.3 \text{ lb/in}^2 \quad \frac{P_2}{P_1} = 0.796 \therefore M_{2\phi} = 0.6 \text{ from Fig 3E.}$$

$$H_1 = 1229.2 \text{ BTU/lb}$$

$$DH_{\phi} = 20.74 \text{ BTU/lb}$$

$$T_1 = 380^{\circ}\text{F}$$

$$T_{2\phi} = 334.5^{\circ}\text{F}$$

$$V_{2\phi} = \frac{1.253 (H_1 - DH_{\phi} - 835)}{P_2} = 24.25 \text{ ft}^3/\text{lb}$$

$$v_{2\phi} = 223.8 \sqrt{DH_{\phi}} = 1020 \text{ ft/sec.}$$

viscosity $\mu_{2\phi} = 3.26 \times 10^{-7} \text{ lb sec/ft}^2$ from appendix 1 Fig. 66
(also ref. 36).

$$\text{Reynolds number } R_n = \frac{1 \times 1020 \times 10^7}{24.25 \times 32.2 \times 3.26} = 4.01 \times 10^6$$

Test 1A

Barometric pressure 29.32 ins Hg = 14.37 lb/in²

$$P_1 = 24.37 \text{ lb/in}^2$$

$$P_2 = 19.39 \text{ lb/in}^2 \quad \frac{P_2}{P_1} = 0.796 \therefore M_{2\phi} = 0.6$$

$$H_1 = 1229.25 \text{ BTU/lb}$$

$$DH_{\phi} = 20.58 \text{ BTU/lb}$$

$$T_1 = 380^{\circ}\text{F}$$

$$T_{2\phi} = 334.9^{\circ}\text{F}$$

$$V_{2\phi} = 24.15 \text{ ft}^3/\text{lb}$$

$$v_{2\phi} = 1015 \text{ ft/sec}$$

$$\mu_{2\phi} = 3.27 \times 10^{-7} \text{ lb. sec/ft}^2 \quad R_n = 3.99 \times 10^6$$

Measured flow 14.1 gallons in 1 $\frac{1}{4}$ hours.

The observed readings of impact tube pressure P_3 and efflux angle are given on pages 126 and 127 for tests 1 and 1A, in Table 1.

TABLE 1 TEST 1. HORIZONTAL STATIONS.

VERTICAL STATIONS.

STATION	$-3\frac{1}{4}$	-3	-2	-1	0	1	2	3	$3\frac{1}{4}$									
	$p_3 \propto \frac{\text{lbs}}{\text{in}^2}$	$p_3 \propto \frac{\text{lbs}}{\text{in}^2}$	$p_3 \propto \frac{\text{lbs}}{\text{in}^2}$	$p_3 \propto \frac{\text{lbs}}{\text{in}^2}$	$p_3 \propto \frac{\text{lbs}}{\text{in}^2}$	$p_3 \propto \frac{\text{lbs}}{\text{in}^2}$	$p_3 \propto \frac{\text{lbs}}{\text{in}^2}$	$p_3 \propto \frac{\text{lbs}}{\text{in}^2}$	$p_3 \propto \frac{\text{lbs}}{\text{in}^2}$									
3	21.5	51	22.3	56	23.3	58	23.6	50	23.6	53	23.7	50	23.7	50	22.4	55	21.3	52.5
$2\frac{1}{2}$	20.5	37	22.7	36.5	24.1	40	24.3	35	24.0	38	23.9	37	23.8	37.5	23.5	38	22.6	37.5
$1\frac{1}{2}$	21.0	31	22.8	29	24.0	30.5	24.3	32	24.3	32	24.3	31	24.3	30.5	23.8	29.5	22.9	29.5
$\frac{1}{2}$	21.0	23	24.1	26	24.3	27	24.3	28	24.3	29	24.1	28.5	24.1	26	24.0	25.5	22.9	25
$-\frac{1}{2}$	21.8	23	23.0	26	24.1	26	24.3	27	24.3	29	24.1	29	24.1	27	23.4	25.5	22.9	24
$-1\frac{1}{2}$	21.8	19	22.9	20	24.2	20	24.3	21	24.1	21.5	24.1	20.5	23.4	19	23.1	18	22.1	18
$-2\frac{1}{2}$	20.1	10	21.3	10	24.1	11.5	24.1	10.5	24.1	12	24.2	10	23.8	11	22.3	12	21	18.5
-3	20.0	3	20.5	3	24.1	9.5	23.8	6.5	23.5	4.5	23.4	5	23.4	8.5	21.6	9	20.3	8.5

TABLE 1 TEST 1A.

HORIZONTAL STATIONS →

VERTICAL STATIONS ↓

STATION	-3	$-2\frac{3}{4}$	$-2\frac{1}{2}$	-2	-1	0	1	2	3	$3\frac{1}{4}$
	$P_3 \propto \frac{1 \text{ lb}}{\text{in}^2}$	$P_3 \propto \frac{1 \text{ lb}}{\text{in}^2}$	$P_3 \propto \frac{1 \text{ lb}}{\text{in}^2}$	$P_3 \propto \frac{1 \text{ lb}}{\text{in}^2}$	$P_3 \propto \frac{1 \text{ lb}}{\text{in}^2}$	$P_3 \propto \frac{1 \text{ lb}}{\text{in}^2}$	$P_3 \propto \frac{1 \text{ lb}}{\text{in}^2}$	$P_3 \propto \frac{1 \text{ lb}}{\text{in}^2}$	$P_3 \propto \frac{1 \text{ lb}}{\text{in}^2}$	$P_3 \propto \frac{1 \text{ lb}}{\text{in}^2}$
2				20.47 10	20.57 3	20.7 5				
$1\frac{1}{2}$	19.77 10	19.87 10	20.27 10	22.37 10	21.87 6	21.37 2.5	20.67 2.5	20.27 3	20.57 3	20.97 24.5
1	20.07 7	20.37 7	21.07 7	23.17 12.5	23.17 13	23.07 12	22.47 10.5	20.97 7	20.77 10	21.97 24
$\frac{1}{2}$	20.47 7	21.27 7.5	23.07 19	24.07 21	24.07 24	24.17 24	23.87 24	23.57 18	23.37 20	23.27 24
$-\frac{1}{2}$	21.07 33	22.77 33	23.57 35	24.07 37	24.17 37	23.97 36.5	23.97 36	24.07 37.5	22.97 37.5	22.87 40
$-1\frac{1}{2}$	20.27 64	21.07 64	22.57 61	22.87 61	23.87 55	23.97 54	23.67 54	23.47 54	23.37 53.5	22.07 52
-2				19.67 82	20.7 82	20.97 82.5	21.27 81	21.47 80	20.57 81	19.77 81

Measured Flow = 14.1 galls. / $1\frac{1}{4}$ hrs.

Table 2 is shown for tests 1 and 1A on pages 129 and 130.

In this table the observed readings are converted to pressure ratio $\frac{P_2}{P_3}$ and to local values of efficiency of expansion.

The values of efficiency are obtained from the pressure ratio using the graph for $M_{2\phi} = 0.6$ in Fig 32 (page 78).

Flow area covered by each impact tube reading.

Typical diagrams or maps of the nozzle and blade exit flow areas are given in Figs 48 and 49 (pages 134 & 135). In a locality where the rate of change of impact tube pressure was large it was necessary to take more readings. Hence the flow area is split up into smaller areas each represented by one impact tube reading. Where the stations are close together an area factor $f(da)$ is introduced. These area factors are shown in the diagrams. Since the basic stations are 0.1 inches apart the basic elemental area is $da = 0.01 \text{ in}^2$ and any smaller elemental area is given by $f(da) \times 0.01 \text{ in}^2$.

On pages 131 and 132, table 3 for tests 1 and 1A are given.

This table gives the figures for the calculations of $\xi \frac{1}{2} \sin \alpha \frac{f da}{fV}$ which is proportional to the mass flow given by equation 1 page 90.

The table shows local values of

- (1) $\xi \frac{1}{2}$ ----- from table 2
- (2) $\sin \alpha$ ----- from table 1
- (3) $f(da)$ ----- from the area factor diagram.
- (4) fV ----- from Fig. 34. (page 80).

TEST 1 TABLE 2

STATION	-3 1/4	-3	-2	-1	0	1	2	3	3 1/4
	P ₂ /P ₃	P ₂ /P ₃	P ₂ /P ₃	P ₂ /P ₃	P ₂ /P ₃	P ₂ /P ₃	P ₂ /P ₃	P ₂ /P ₃	P ₂ /P ₃
3	.898	.865	.828	.818	.883	.815	.899	.862	.906
2 1/2	.941	.850	.801	.796	.913	.807	.920	.821	.854
1 1/2	.919	.847	.804	.796	.916	.801	.913	.804	.843
1/2	.885	.839	.774	.801	.973	.801	.973	.825	.843
-1 1/2	.885	.843	.752	.798	.988	.796	1.0	.801	.874
-2 1/2	.960	.946	.900	.801	.973	.801	.973	.865	.919
-3	.965	.941	.801	.811	.920	.811	.920	.844	.950

TEST 1C TABLE 2

STATION	-3	$-2\frac{3}{4}$	$-2\frac{1}{2}$	-2	-1	0	1	2	3	$3\frac{1}{4}$
	$\frac{P_2}{P_3}$ η	$\frac{P_2}{P_3}$ η	$\frac{P_2}{P_3}$ η	$\frac{P_2}{P_3}$ η	$\frac{P_2}{P_3}$ η	$\frac{P_2}{P_3}$ η	$\frac{P_2}{P_3}$ η	$\frac{P_2}{P_3}$ η	$\frac{P_2}{P_3}$ η	$\frac{P_2}{P_3}$ η
Z				.948	.260 .964 .259	.962 .174				
$1\frac{1}{2}$.981 .087 .976	.110 .956 .202	.867 .632 .887	.535 .908 .430	.939 .283 .956	.202 .964 .259	.926 .343			
1	.966 .155 .953	.216 .921 .367	.837 .783 .837	.783 .841 .762	.864 .668 .926	.363 .935 .300	.883 .555			
$\frac{1}{2}$.968 .260 .912	.411 .841 .762	.806 .966 .806	.946 .806 .946	.803 .961 .813	.909 .823 .857	.830 .820 .834	.800		
$-\frac{1}{2}$.921 .367 .852	.706 .823 .857	.806 .946 .806	.961 .810 .924	.810 .924 .810	.924 .810 .924	.810 .924 .810	.924 .810 .924	.808 .727	
$-1\frac{1}{2}$.956 .202 .921	.367 .860 .667	.868 .727 .813	.909 .810 .924	.820 .871 .827	.835 .830 .820	.879 .574			
-2				.986 .065 .962	.174 .926 .343	.912 .411 .904	.450 .944 .259	.981 .087		

TEST 1 TABLE 3

STATION	-3 1/4	-3	-2	-1	0	1	2	3	3 1/4
$\eta^2 \sin^2 fda$	$\eta^2 \sin^2 fda$	$\eta^2 \sin^2 fda$	$\eta^2 \sin^2 fda$	$\eta^2 \sin^2 fda$	$\eta^2 \sin^2 fda$	$\eta^2 \sin^2 fda$	$\eta^2 \sin^2 fda$	$\eta^2 \sin^2 fda$	$\eta^2 \sin^2 fda$
$f.v$	$f.v$	$f.v$	$f.v$	$f.v$	$f.v$	$f.v$	$f.v$	$f.v$	$f.v$
3	.692 .777 1/4	.803 .829 1/4	.911 .808 1/2	.941 .766 1/2	.941 .799 1/2	.949 .766 1/2	.949 .766 1/2	.810 .819 1/2	.664 .793 1/4
	1.028 .131	1.019 .1635	1.009 .383	1.006 .358	1.006 .374	1.005 .362	1.005 .362	1.018 .163	1.03 .128
2 1/2	.522 .602 3/8	.846 .595 3/8	.987 .663 3/4	1 .574 3/4	.980 .616 3/4	.970 .602 3/4	.960 .609 3/4	.931 .616 3/8	.835 .609 3/8
	1.039 .1135	1.015 .186	1.001 .675	1 .4305	1.002 .652	1.003 .637	1.004 .637	1.007 .2155	1.016 .188
1 1/2	.644 .515 1/2	.856 .685 1/2	.980 .508 1	1 .530 1	.530 1	.515 1	1 .508 1	.960 .642 1/2	.847 .692 1/2
	1.033 .153	1.014 .205	1.002 .497	1 .530 1	.530 1	.515 1	1 .508 1	1.004 .235	1.012 .211
1/2	.644 .391 1/2	.987 .638 1/2	1 .454 1	1 .670 1	.685 1	.687 .477 1	.687 .439 1	.980 .430 1/2	.869 .623 1/2
	1.033 .116	1.001 .216	1 .454 1	.470 1	.485 1	.471 1	1.001 .432	1.002 .210	1.013 .1815
-1 1/2	.738 .391 1/2	.880 .628 1/2	.987 .638 1	1 .654 1	.685 1	.687 .485 1	.687 .454 1	.920 .430 1/2	.808 .607 1/2
	1.024 .141	1.012 .1905	1.005 .432 1	.454 1	.485 1	.478 1.001	1.001 .448	1.008 .196	1.013 .174
-1 1/2	.738 .326 1/2	.868 .342 1/2	.905 .342 1	.358 1	.367 1	.387 .350 1	.420 .326 1	.892 .309 1/2	.773 .309 1/2
	1.024 .1175	1.013 .1465	1.001 .340 1	.358 1	.362 1.001	1.001 .345	1.008 .258	1.011 .136	1.021 .117
-2 1/2	.628 .174 3/8	.664 .174 3/8	.987 .199 3/4	.987 .182 3/4	.987 .208 3/4	.995 .174 3/4	.980 .191 3/4	.865 .208 3/8	.646 .317 3/8
	1.063 .027	1.03 .042	1.001 .147	1.001 .135	1.001 .154	1.001 .130	1.004 .137	1.019 .0615	1.023 .071
-3	.400 .652 1/4	.522 .052 1/4	.987 .165 1/2	.960 .115 1/2	.931 .079 1/2	.960 .087 1/2	.940 .108 1/2	.767 .154 1/4	.680 .128 1/4
	1.065 .405	1.039 .0065	1.001 .081	1.004 .054	1.007 .0365	1.004 .042	1.004 .071	1.027 .023	1.001 .017
Σ	0.804	1.156	2.809	2.7895	2.8785	2.780	2.693	1.842	1.0875

$$\Sigma \frac{\eta^2 \sin^2 fda}{f.v} = 18.2395$$

TEST 1a TABLE 3

STATION	-3	-2 3/4	-2 1/2	-2	-1	0	1	2	3	3 1/2
$\eta^2 \sin \alpha \cdot fda$	$\eta^2 \sin \alpha \cdot fda$	$\eta^2 \sin \alpha \cdot fda$	$\eta^2 \sin \alpha \cdot fda$	$\eta^2 \sin \alpha \cdot fda$	$\eta^2 \sin \alpha \cdot fda$	$\eta^2 \sin \alpha \cdot fda$	$\eta^2 \sin \alpha \cdot fda$	$\eta^2 \sin \alpha \cdot fda$	$\eta^2 \sin \alpha \cdot fda$	$\eta^2 \sin \alpha \cdot fda$
$fV \eta^2 \sin \alpha \cdot fda$	$fV \eta^2 \sin \alpha \cdot fda$	$fV \eta^2 \sin \alpha \cdot fda$	$fV \eta^2 \sin \alpha \cdot fda$	$fV \eta^2 \sin \alpha \cdot fda$	$fV \eta^2 \sin \alpha \cdot fda$	$fV \eta^2 \sin \alpha \cdot fda$	$fV \eta^2 \sin \alpha \cdot fda$	$fV \eta^2 \sin \alpha \cdot fda$	$fV \eta^2 \sin \alpha \cdot fda$	$fV \eta^2 \sin \alpha \cdot fda$
2										
1 1/2										
1										
1/2										
-1/2										
-1 1/2										
-2										
Σ										

$$\Sigma \eta^2 \sin \alpha \cdot \frac{fda}{fV} = 10.367$$

For each station the products $z^{\frac{1}{2}} \sin \alpha \frac{fda}{fV}$ are obtained and the products are summated.

$$\text{Test 1} \quad \sum z^{\frac{1}{2}} \sin \alpha \frac{fda}{fV} = 18.239$$

$$\text{Test 1A} \quad \sum z^{\frac{1}{2}} \sin \alpha \frac{fda}{fV} = 10.367$$

36 3 2 1 0 -1 -2 -3

3	1/4	1/2	3/4	1	1/2	1/4	1/4	1/4
2 1/2	3/8	1/2	3/4	1	1/2	3/8	1/2	3/8
1 1/2	1/2	1	1	1	1	1/2	1	1/2
1/2	1/2	1	1	1	1	1/2	1	1/2
1/4	1/2	1	1	1	1	1/2	1	1/2
3/8	3/8	3/4	3/4	3/4	3/4	3/8	3/8	3/8
1/4	1/4	1/2	1/2	1/2	1/2	1/4	1/4	1/4

VERTICAL STATIONS

SCALE - 1" = 0.125'

HORIZONTAL STATIONS
NOZZLE EXIT FLOW AREA

IMPACT READINGS TAKEN AT POINTS MARKED

SERIES I

NUMBERS IN RECTANGLES ARE AREA FACTORS (F_{RA}) FOR SMALL AREAS SUM

FIG. 4-8.

On pages 137 and 138 table 4 for tests 1 and 1A are given. These enable one to calculate the mean values of nozzle efficiency, efficiency of expansion for the pair, blade velocity coefficient and blade loss.

The table gives local values of

(1) ζ from table 2.

(2) $\zeta^{3/2} \sin \alpha \frac{fda}{fv}$ from table 3.

For each station the product $\zeta^{3/2} \sin \alpha \frac{fda}{fv}$ is given and the products are summated.

$$\text{Test 1} \quad \sum \zeta^{3/2} \sin \alpha \frac{fda}{fv} = 16.407$$

From equation 6 page 91.

$$\bar{\zeta}_n = \left(\frac{\sum \zeta^{3/2} \sin \alpha \frac{fda}{fv}}{\sum \zeta^2 \sin \alpha \frac{fda}{fv}} \right)_n = \frac{16.407}{18.239} = 0.900$$

Similar calculations taking account only of variations along the vertical centre line give

$$\bar{\zeta}_n \phi = \frac{2.798}{2.878} = 0.972$$

$$\text{Test 1A} \quad \sum \zeta^{3/2} \sin \alpha \frac{fda}{fv} = 8.060$$

From equation 7 page 91 the mean efficiency of the pair $\bar{\zeta}_b$ is

$$\bar{\zeta}_b = \left(\frac{\sum \zeta^{3/2} \sin \alpha \frac{fda}{fv}}{\sum \zeta^2 \sin \alpha \frac{fda}{fv}} \right)_b = \frac{8.060}{10.367} = 0.778$$

$$\text{and } \bar{\zeta}_b \phi = \frac{1.441}{1.756} = 0.820$$

TEST 1 TABLE 4

STATION	-3 1/4	-3	-2	-1	0	1	2	3	3 1/4
	$\eta \frac{3}{4} \sin \alpha \frac{fda}{fV}$	$\eta \frac{3}{4} \sin \alpha \frac{fda}{fV}$	$\eta \frac{3}{4} \sin \alpha \frac{fda}{fV}$	$\eta \frac{3}{4} \sin \alpha \frac{fda}{fV}$	$\eta \frac{3}{4} \sin \alpha \frac{fda}{fV}$	$\eta \frac{3}{4} \sin \alpha \frac{fda}{fV}$	$\eta \frac{3}{4} \sin \alpha \frac{fda}{fV}$	$\eta \frac{3}{4} \sin \alpha \frac{fda}{fV}$	$\eta \frac{3}{4} \sin \alpha \frac{fda}{fV}$
3	.478	.131	.643	.1635	.830	.383	.883	.358	.883
	.0625	.105	.318	.316	.330	.325	.325	.362	.899
2 1/2	.272	.1135	.716	.186	.973	.475	.4305	.460	.452
	.031	.133	.462	.4305	.434	.411	.402	.867	.2135
1 1/2	.377	.153	.732	.205	.960	.497	.530	.1	.515
	.058	.150	.477	.530	.530	.515	.508	.920	.235
1/2	.377	.116	.973	.216	.1	.454	.1	.470	.1
	.044	.210	.454	.470	.485	.459	.420	.960	.210
-1/2	.544	.141	.774	.1905	.973	.432	.1	.485	.1
	.077	.1475	.420	.454	.485	.465	.436	.845	.196
-1 1/2	.544	.1175	.752	.1465	.988	.340	.1	.358	.973
	.066	.110	.336	.358	.352	.336	.252	.794	.136
-2 1/2	.183	.027	.440	.042	.973	.147	.973	.135	.988
	.005	.0185	.143	.131	.150	.1285	.126	.643	.0615
-3	.160	.005	.272	.0065	.973	.081	.920	.054	.920
	.001	.002	.079	.080	.032	.039	.065	.500	.027
Σ	0.3425	0.876	2.689	2.7395	2.798	2.6795	2.534	1.036	0.714

$$\Sigma \eta \frac{3}{4} \sin \alpha \frac{fda}{fV} = 16.4075$$

TEST 1a TABLE 4

Station	-3	-2 $\frac{3}{4}$	-2 $\frac{1}{2}$	-2	-1	0	1	2	3	3 $\frac{1}{4}$										
	$\eta \frac{1}{4} \sin \frac{fda}{fv}$	$\eta \frac{1}{4} \sin \frac{fda}{fv}$	$\eta \frac{1}{4} \sin \frac{fda}{fv}$	$\eta \frac{1}{4} \sin \frac{fda}{fv}$	$\eta \frac{1}{4} \sin \frac{fda}{fv}$	$\eta \frac{1}{4} \sin \frac{fda}{fv}$	$\eta \frac{1}{4} \sin \frac{fda}{fv}$	$\eta \frac{1}{4} \sin \frac{fda}{fv}$	$\eta \frac{1}{4} \sin \frac{fda}{fv}$	$\eta \frac{1}{4} \sin \frac{fda}{fv}$										
	$\eta \frac{3}{4} \sin \frac{fda}{fv}$	$\eta \frac{3}{4} \sin \frac{fda}{fv}$	$\eta \frac{3}{4} \sin \frac{fda}{fv}$	$\eta \frac{3}{4} \sin \frac{fda}{fv}$	$\eta \frac{3}{4} \sin \frac{fda}{fv}$	$\eta \frac{3}{4} \sin \frac{fda}{fv}$	$\eta \frac{3}{4} \sin \frac{fda}{fv}$	$\eta \frac{3}{4} \sin \frac{fda}{fv}$	$\eta \frac{3}{4} \sin \frac{fda}{fv}$	$\eta \frac{3}{4} \sin \frac{fda}{fv}$										
2				.240	.031	.259	.013	.174	.017											
				.008	.003		.003													
$1\frac{1}{2}$.087	.006	.110	.007	.202	.014	.632	.051	.535	.0375	.430	.014	.283	.011	.202	.011	.259	.008	.343	.046
	.0005	.000			.003		.032		.020		.006		.003		.002		.002		.015	
1	.155	.006	.216	.007	.367	.013	.783	.071	.783	.0985	.762	.0895	.648	.072	.343	.0345	.300	.029	.555	.05
	.001	.0015			.005		.0555		.077		.068		.398	.386	.857	.284	.820	.1915		
$1\frac{1}{2}$.240	.014	.411	.020	.762	.105	.946	.260	.946	.393	.961	.398	.909	.386	.857	.284	.820	.1915	.800	.735
	.003	.008			.080		.246		.372		.383		.351		.244		.157		.108	
- $1\frac{1}{2}$.367	.080	.706	.113	.857	.197	.946	.436	.961	.588	.924	.571	.924	.564	.946	.590	.708	.324	.727	.203
	.029	.080			.169		.414		.565		.527		.521		.558		.242		.167	
-1	.202	.048	.367	.066	.667	.132	.727	.276	.909	.388	.924	.387	.871	.375	.835	.366	.820	.227	.574	.109
	.097	.024			.088		.201		.352		.358		.326		.306		.186		.0625	
-2					.065	.090	.174	.198	.174	.198	.343	.280	.411	.307	.450	.322	.259	.151	.087	.05
					.006		.034		.034		.096		.1265		.105		.039		.0065	
Σ	.01305	.01135	.0345	.09625	1.423	1.441	1.3745	1.267	0.635	0.368										

$$\Sigma \eta^{\frac{3}{4}} \sin \propto \frac{fda}{fv} = 8.060$$

From equation 12 page 92 the mean blade velocity coefficient.

$$K = \sqrt{\frac{\left(\frac{\sum r^{3/2} \sin \alpha \frac{fda}{rV}}{\sum r^{3/2} \sin \alpha \frac{fda}{rV}} \right)_b}{\left(\frac{\sum r^{3/2} \sin \alpha \frac{fda}{rV}}{\sum r^{3/2} \sin \alpha \frac{fda}{rV}} \right)_n}}$$

$$\therefore K = \sqrt{\frac{0.778}{0.900}} = 0.920$$

$$\text{Similarly } K_{\phi} = \sqrt{\frac{0.820}{0.972}} = 0.920$$

$$\begin{aligned} \text{The blade loss} &= (1 - K^2) \bar{r}_n DH \phi \\ &= (1 - 0.865) \times 0.900 \times 20.58 = 2.50 \text{ BTU/lb} \end{aligned}$$

$$\text{and the blade loss } \phi = (1 - 0.844) \times 0.972 \times 20.58 = 3.12 \text{ BTU/lb} .$$

Table 5 for tests 1 and 1A are given on pages 141 and 142 .

These tables enable one to calculate mean efflux angles.

The tables show the local values of

(1) $\eta^{\frac{1}{2}}$ from table 2

(2) $\cos \alpha$ from table 1

(3) $\eta^{\frac{1}{2}} \sin \alpha \frac{fda}{fV}$ from table 3

for each station the product $\eta \cos \alpha \sin \alpha \frac{fda}{fV}$ is given and the products are summated.

Test 1

$$\sum \eta \cos \alpha \sin \alpha \frac{fda}{fV} = 14.512, \quad \sum \eta^{\frac{1}{2}} \sin \alpha \frac{fda}{fV} = 18.239.$$

$$\bar{\eta}_n = 0.900.$$

From equation 13 page 93.

$$\cos \bar{\alpha}_n = \left(\frac{\sum \eta \sin \alpha \cos \alpha \frac{fda}{fV}}{\sum \eta^{\frac{1}{2}} \sin \alpha \frac{fda}{fV} \sqrt{\bar{\eta}_n}} \right)_n$$

$$= \frac{14.512}{0.95 \times 18.239} = 0.838.$$

$$\therefore \bar{\alpha}_n = 33^\circ.$$

Test 1A

$$\sum \eta \cos \alpha \sin \alpha \frac{fda}{fV} = 6.505, \quad \sum \eta^{\frac{1}{2}} \sin \alpha \frac{fda}{fV} = 10.367$$

$$\bar{\eta}_b = 0.788$$

From equation 14 page 93.

$$\cos \bar{\alpha}_b = \frac{6.505}{0.883 \times 10.367} = 0.71.$$

$$\therefore \bar{\alpha}_b = 44.7^\circ$$

Mass flow calculations and results for tests 1A to 4A.

The table below gives experimental mass flow readings for tests 1A to 4A along with the function $\xi \sin \alpha \frac{fda}{fV}$ for each test from table 3.

Also shown are the calculated mass flow figures obtained as follows:-

For test 4A.

$$DH_{\phi} = 20.55 \text{ BTU/lb. } H_1 = 122925 \text{ BTU/lb.}$$

$$V_{2\phi} = \frac{1.253(H_1 - DH_{\phi} - 835)}{43.25} = 10.81 \text{ ft}^3/\text{lb.}$$

$$da = \frac{0.01}{144} \text{ ft}^2$$

From equation 3 page 91.

$$m = \frac{223.8 \sqrt{DH_{\phi}}}{V_{2\phi}} \times \xi \sin \alpha \frac{da}{fV}$$

$$\begin{aligned} m &= \frac{223.8 \sqrt{DH_{\phi}}}{V_{2\phi}} \times da \times \xi \sin \alpha \frac{fda}{fV} \\ &= \frac{223.8 \sqrt{20.55}}{V_{2\phi}} \times \frac{.01}{144} \times 10.6425 = .0692 \text{ lb/sec.} \end{aligned}$$

The actual measured flow is $\frac{31.5 \times 10}{1.25 \times 3600} = .0700 \text{ lb/sec.}$

Series 1 Mass flow measurements.

Test No.	1A	2A	3A	4A
Measured flow per 1½ hrs. (Galls)	14.1	20.1	25.2	31.5
$\xi \sin \alpha \frac{fda}{fV}$	10.367	10.906	10.591	10.6425
Measured flow lb/sec.	0.0313	0.0449	0.0560	0.0700
Calculated flow lb/sec.	0.0303	0.0464	0.0561	0.0692
% age difference	-3.20	+3.34	+0.18	-1.14

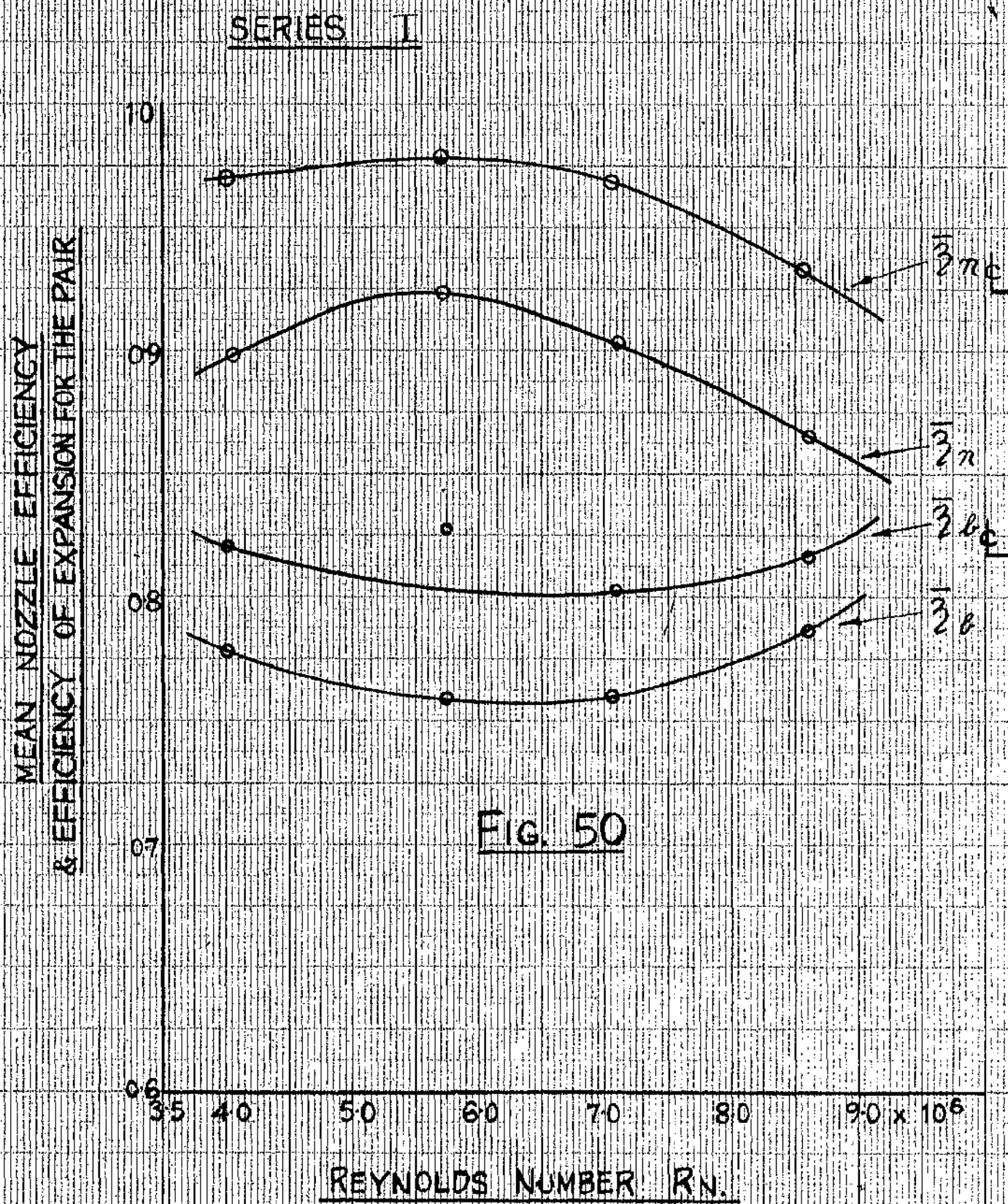
Series 1 ----- Final Results.

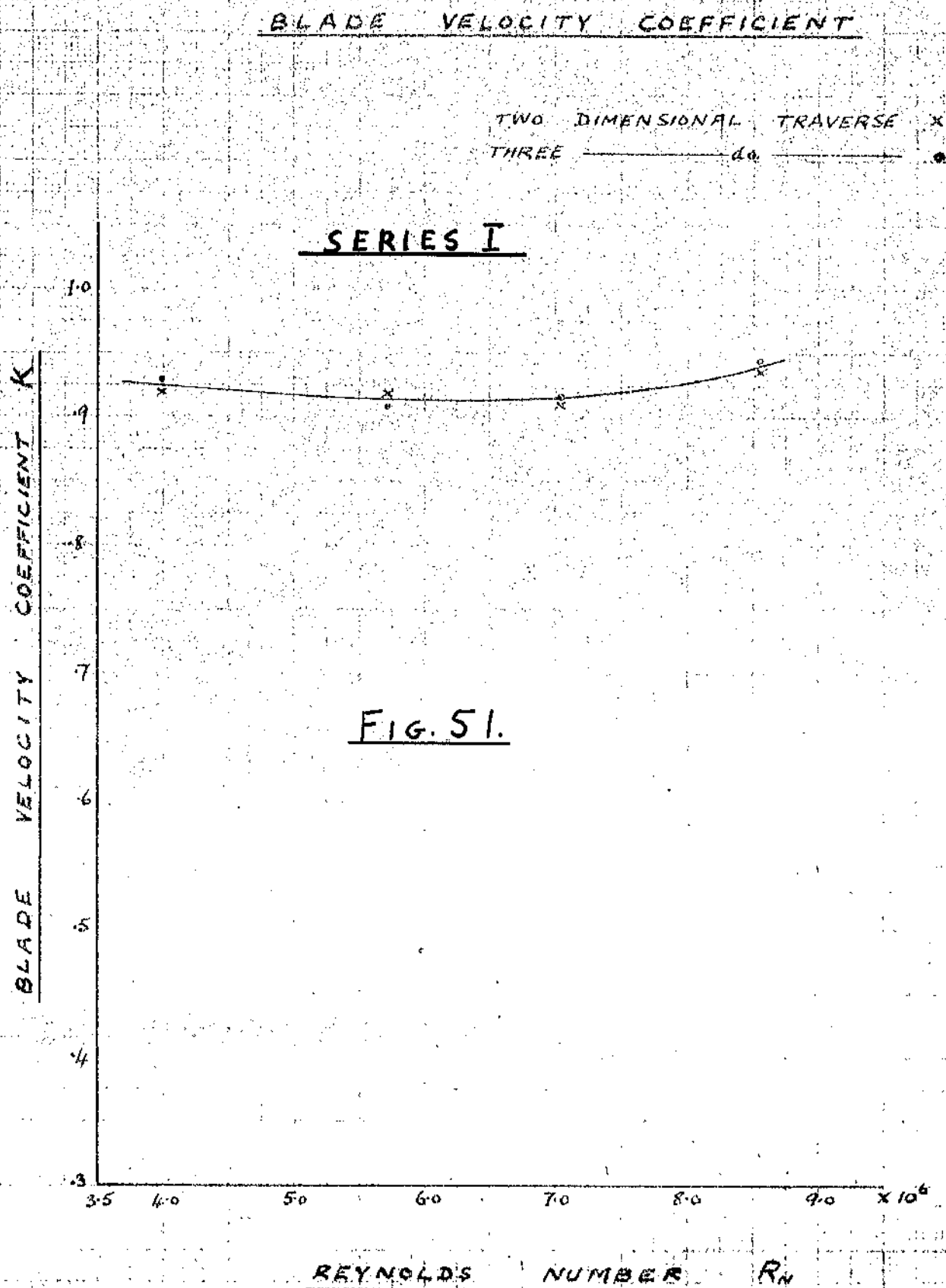
The results for the series 1 tests are shown in the table on page 145 . From these results the following graphs have been drawn and are shown in subsequent figures.

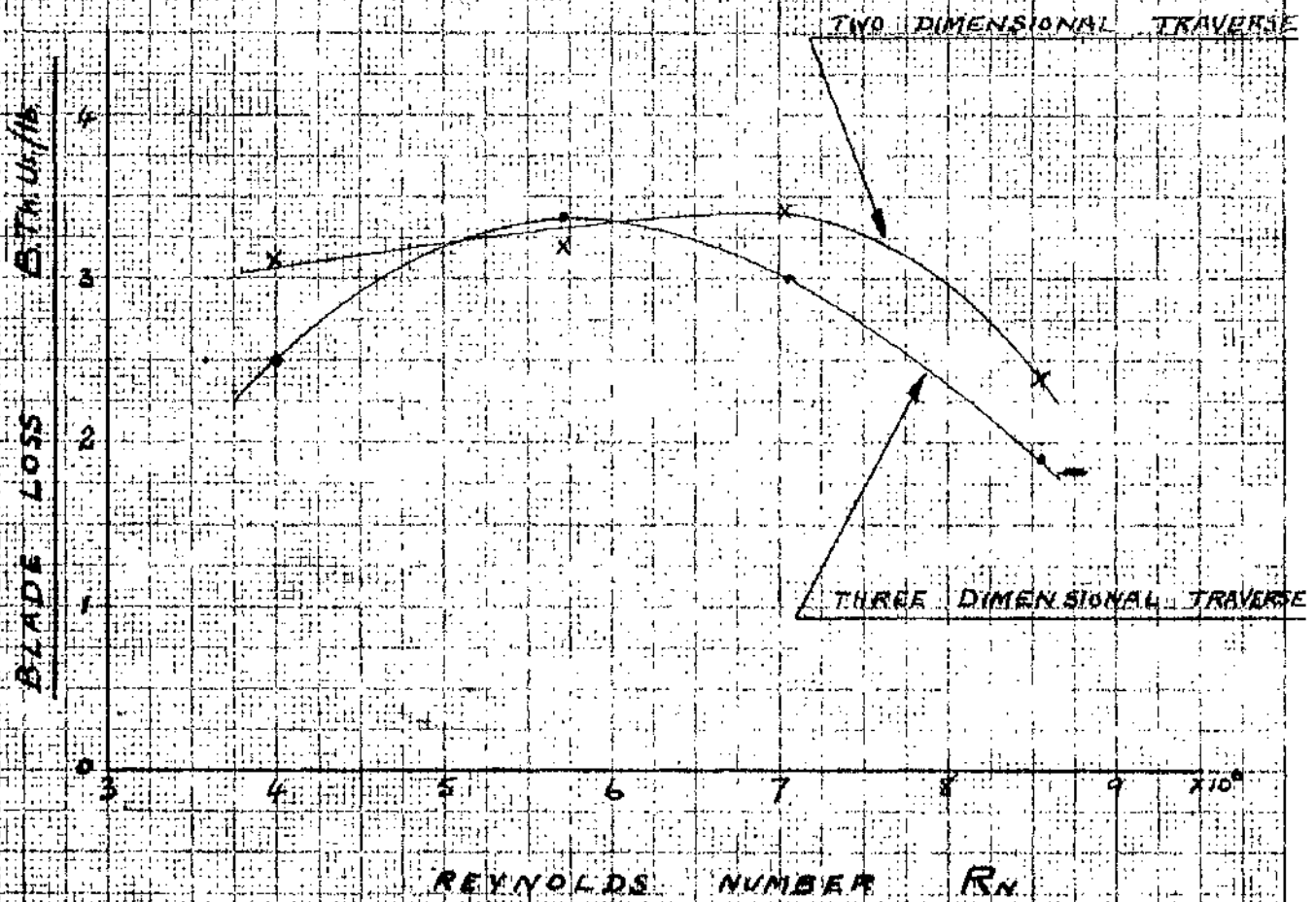
- (1) Mean nozzle efficiency and efficiency of expansion for the pair to a base of Reynolds number. Fig. 50 (page 146).
 - (2) The blade velocity coefficient to a base of Reynolds number. Fig. 51 (page 147).
 - (3) Blade passage loss to a base of Reynolds number. Fig. 52 (page 148).
 - (4) Typical graphs showing velocity distribution for the nozzle and blade exit along a vertical centre line. Figs. 53 and 54 (pages 149 & 150).
 - (5) Typical graphs shown variations of efflux angle at nozzle and blade exit along a vertical centre line. Figs. 53 and 54 (pages 149 & 150).
-

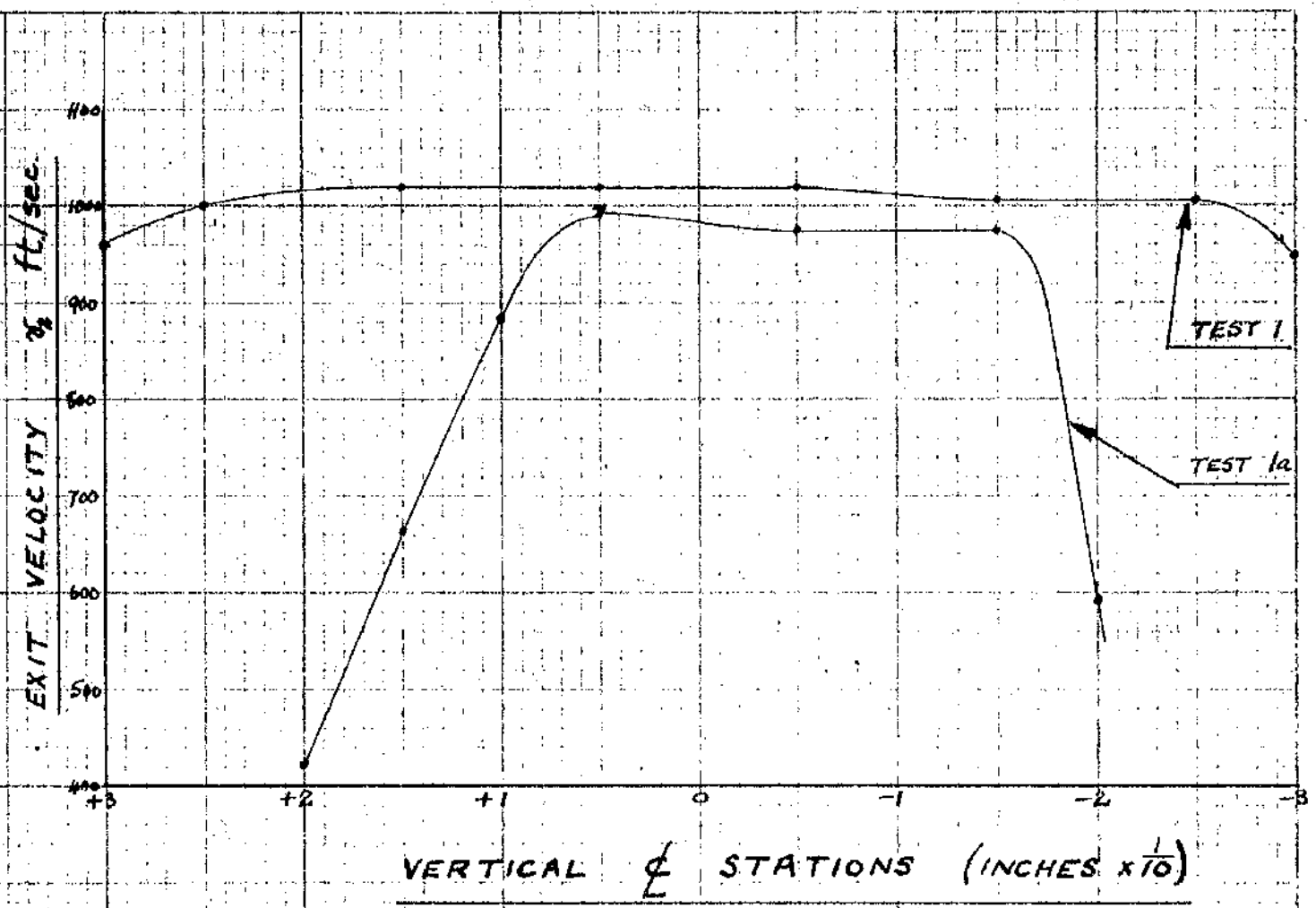
Series 1-Table of Final Results.

Test	1	1A	2	2A	3	3A	4	4A
Mach No. M_2	← 0.6 →							
Reynolds No. $\times 10^6$	4.01	3.99	5.66	5.72	7.04	7.04	8.55	8.55
$\bar{\eta}_n$.900		.926		.908		.872	
$\bar{\eta}_b$.778		.762		.762		.778
K		.930		.909		.916		.946
α	33°	44.7°	33°	44.4°	32.5°	44.6°	38°	44.1
Blade loss B.T.U./lb		2.50		3.38		3.00		1.19
$\bar{\eta}_{n\epsilon}$.972		.981		.971		.935	
$\bar{\eta}_{b\epsilon}$.820		.826		.805		.817
K_ϵ		.920		.919		.911		.936
Blade loss ϵ		3.12		3.20		3.41		2.41

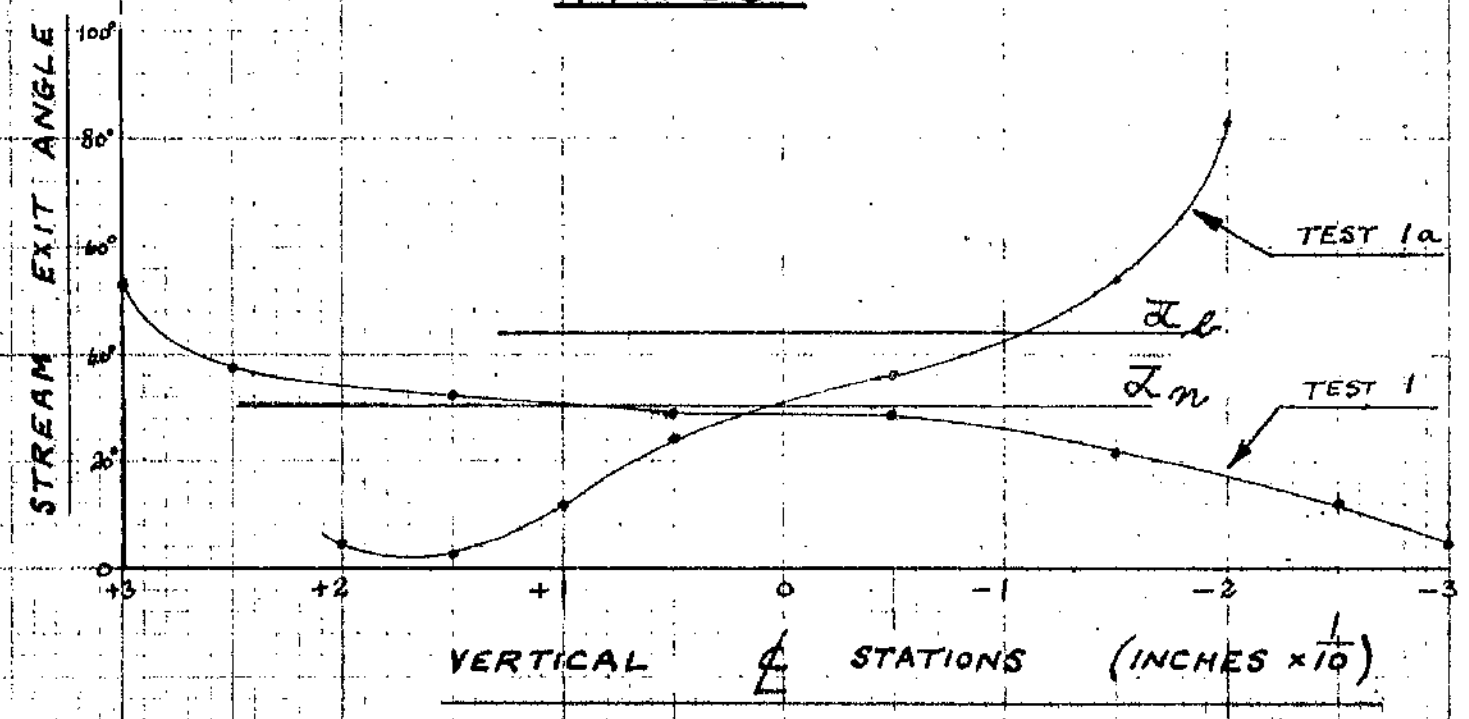


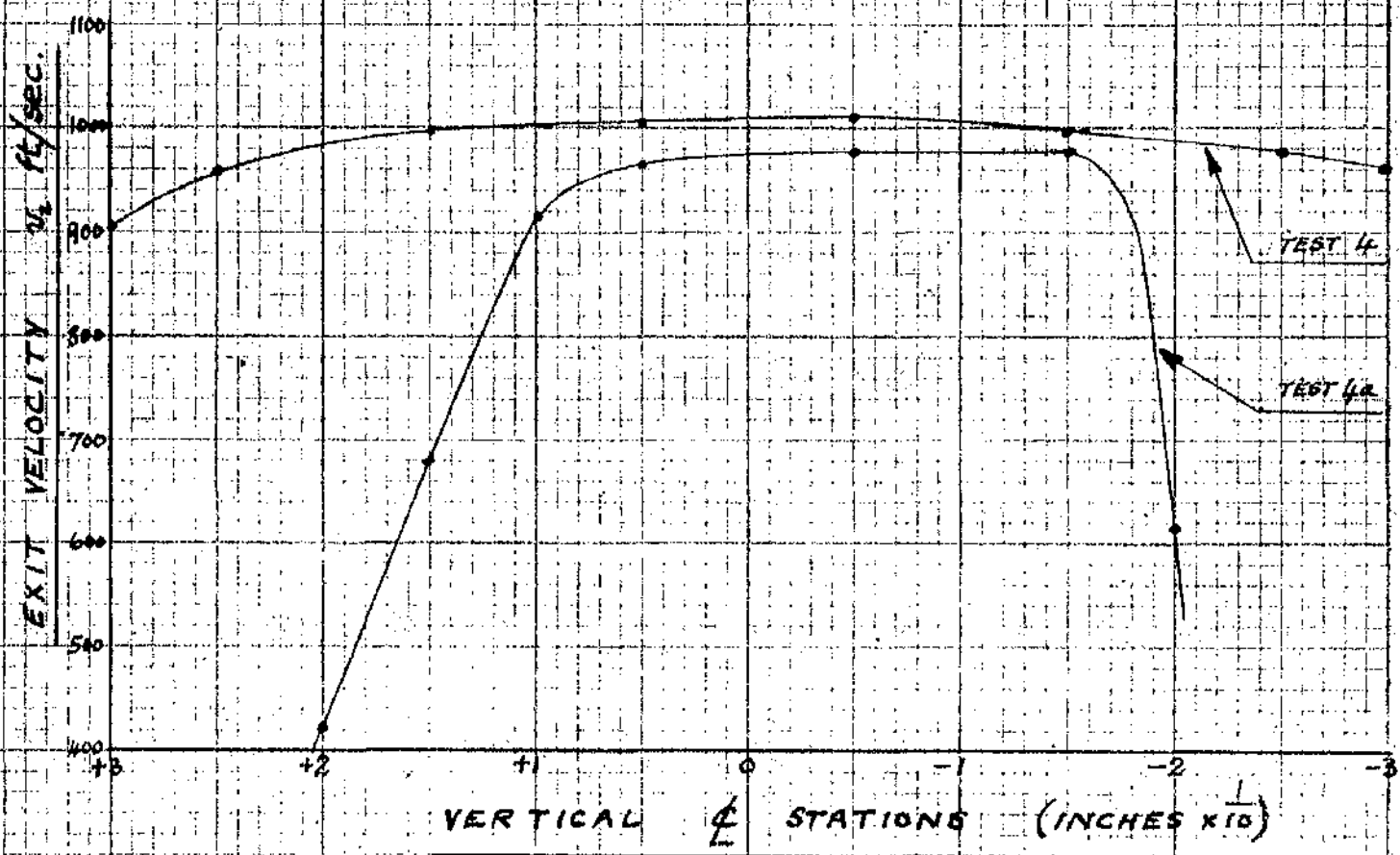


SERIES IBLADE LOSSFIG. 52.

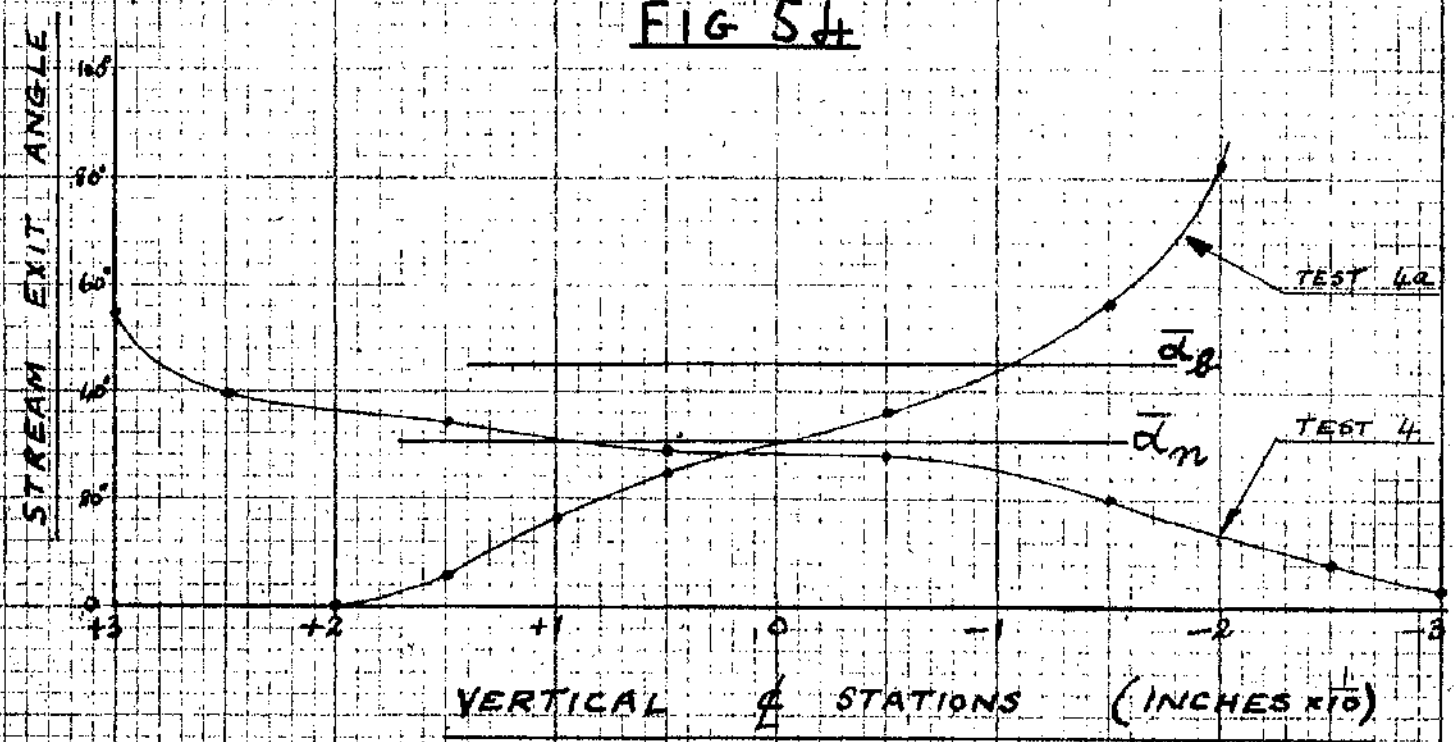


SERIES I.
FIG. 53.





SERIES I.
FIG 54



Series 2

Series 2.

In this test series the exit Mach number is varied within the subsonic region. There are twelve three dimensional tests, six at the nozzle and six at the blade exit. The nozzle tests are numbered 1 - 6 and the blade tests 1A - 6A. The exit Mach numbers taken are 0.5, 0.6, 0.7, 0.8, 0.9, and 0.97. For the tests in the range $M_{2\phi}$ equal to 0.5 to 0.8 the inlet nozzle pressure is 24.3 lb/in² which is the same as in test 1 series 1. The back pressures are chosen to give the correct exit Mach numbers from Fig. 31 (page 77). In the tests at $M_{2\phi} = 0.9$ and 0.97 the inlet pressure was raised above 24.3 lb/in² so as to prevent the expansion entering the wet field.

The test conditions are shown in the table on page 153.

The calculation of the effective values takes the same form as in series 1 except that for the values of local efficiency the graphs in Fig. 32 (page 78) must be used.

Specimen calculations for tests 1 and 1A are given in appendix 1 (page 197), and tables 1 to 5 for tests 1 and 1A are given in appendix 1 pages 199 to 210. The remaining tables of observed and derived results for tests 2 to 6 and 2A to 6A for series 2 are given in appendix 2 (pages 33 to 83).

The final results for series 2 are described on page 155.

Series 2 ----- Test Conditions.

Test No.	1	1A	2	2A	3	3A	4	4A	5	5A	6	6A
Inlet pressure P_1 lb/in. ²	24.3	24.3	24.3	24.3	24.3	24.3	24.3	24.3	30.0	30.0	32.5	32.6
Back pressure P_2 lb/in. ²	20.7	20.7	19.32	19.32	17.88	17.88	16.35	16.35	18.38	18.38	18.30	18.30
Inlet temperature T_1 °F.	←					380°F						→
Exit Mach No. M_2	0.5	0.5	0.6	0.6	0.7	0.7	0.8	0.8	0.9	0.9	0.97	0.97

Mass flows for tests 1A to 6A.

The table below gives a comparison between the actual measured flow and the flow figures calculated from the traverse readings for tests 1A to 6A. The calculations follows the same pattern as those for the mass flow figures in the series 1 tests.

Series 2 Mass flow results.

Test No.	1A	2A	3A	4A	5A	6A
Measured flow lb/sec.	0.0288	0.0343	0.0375	0.0384	0.0494	0.0539
Calculated flow lb/sec.	0.0284	0.0331	0.0352	0.0380	0.0501	0.0528
%age difference	-1.39	-3.50	-6.13	-1.04	+1.42	-2.04

Series 2 ----- Final Results.

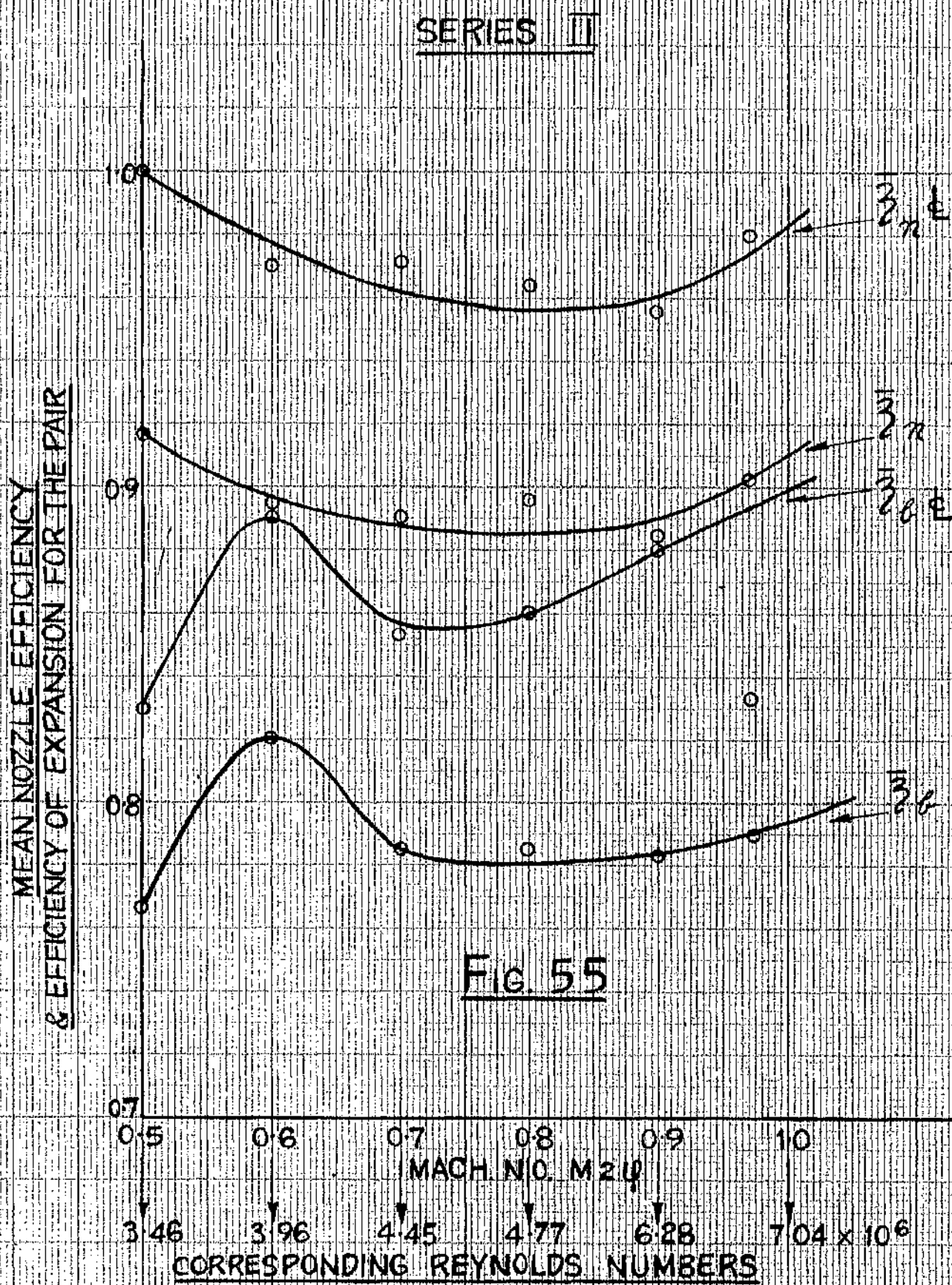
The final results for the series 2 tests are given in the table on page 156. From these results the following graphs have been drawn and these appear in subsequent figures.

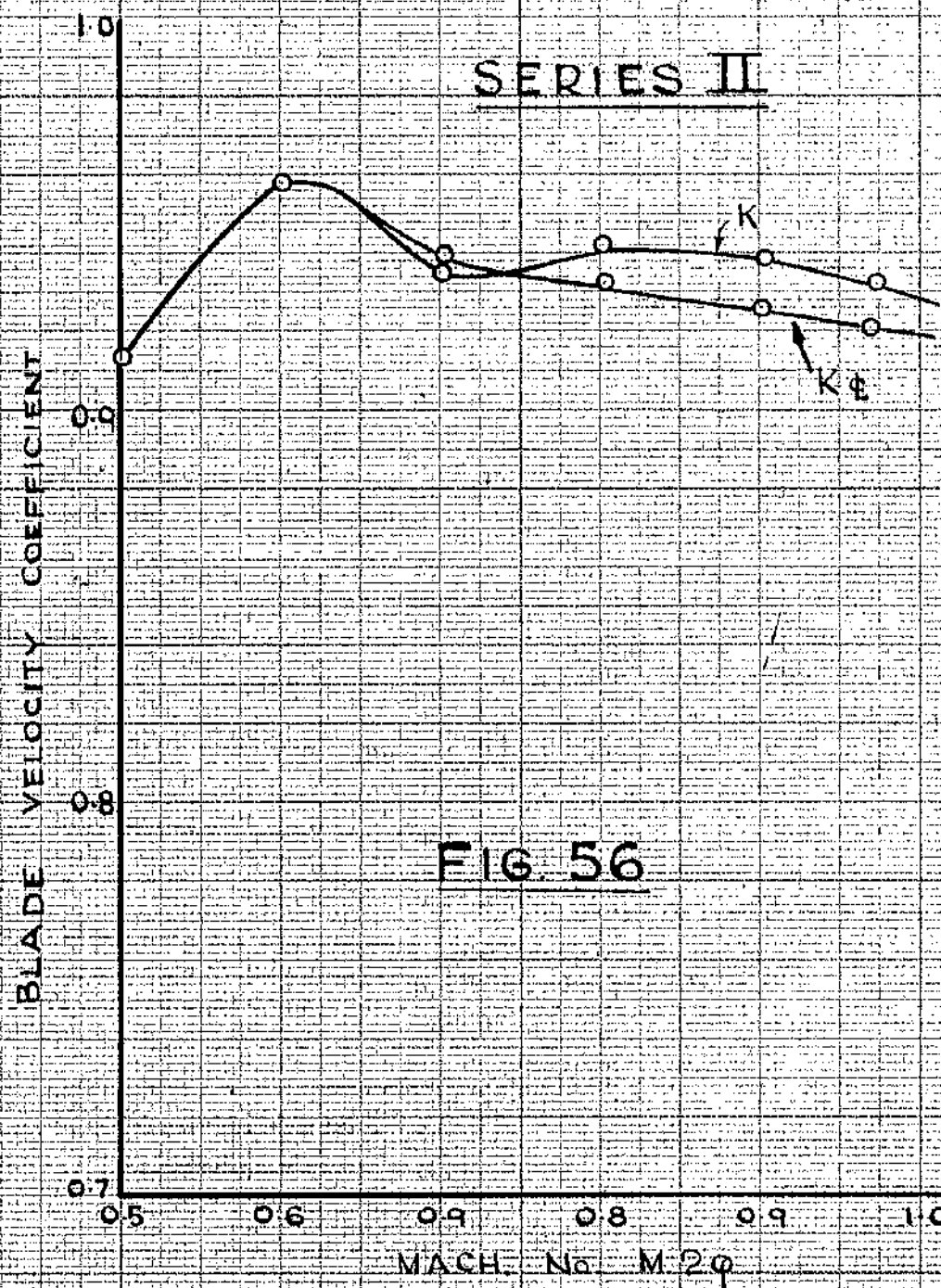
- (1) The mean nozzle efficiency and efficiency of expansion for the pair to a base of Mach number Fig. 55 (page 157).
 - (2) Blade velocity coefficient to a base of Mach number Fig. 56 (page 158).
 - (3) Blade loss to a base of Mach number Fig. 57 (page 159).
 - (4) Typical graphs of velocity distribution along a vertical centre line for the nozzle and blades Figs 58 and 59 (pages 160 and 161).
 - (5) Typical graphs of efflux angle along a vertical centre line for nozzle and blades Fig. 60 (page 162).
 - (6) Table 1 for test 1A to 6A show that as the impact tube traverses in a horizontal position, there is a considerable decrease in impact tube pressure on either side of the centre line. Velocity distributions for a horizontal traverse have been calculated for these tests and typical results appear in graphical form in Fig. 61 (page 163).
-

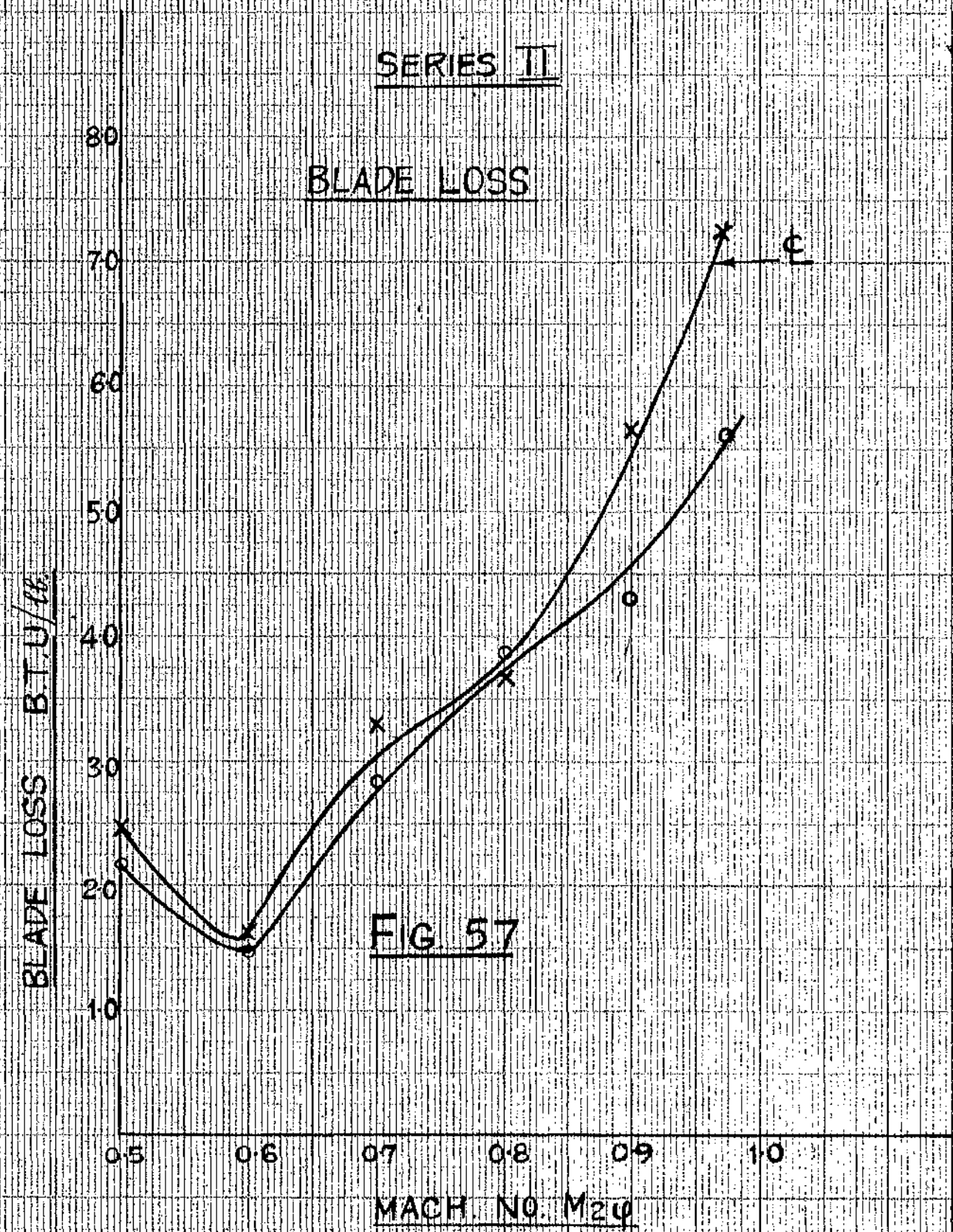
Series 2 ----- Table of final results.

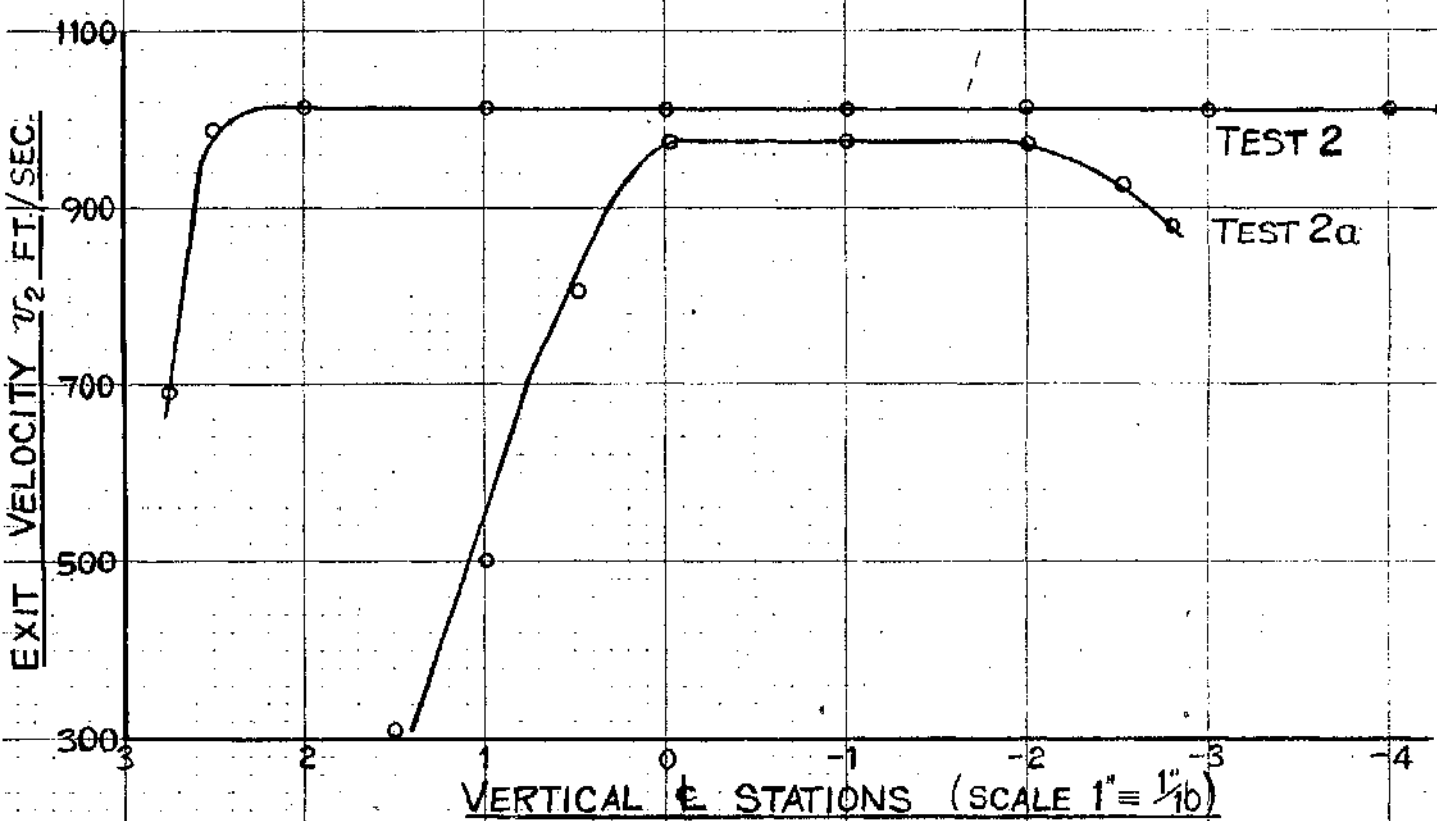
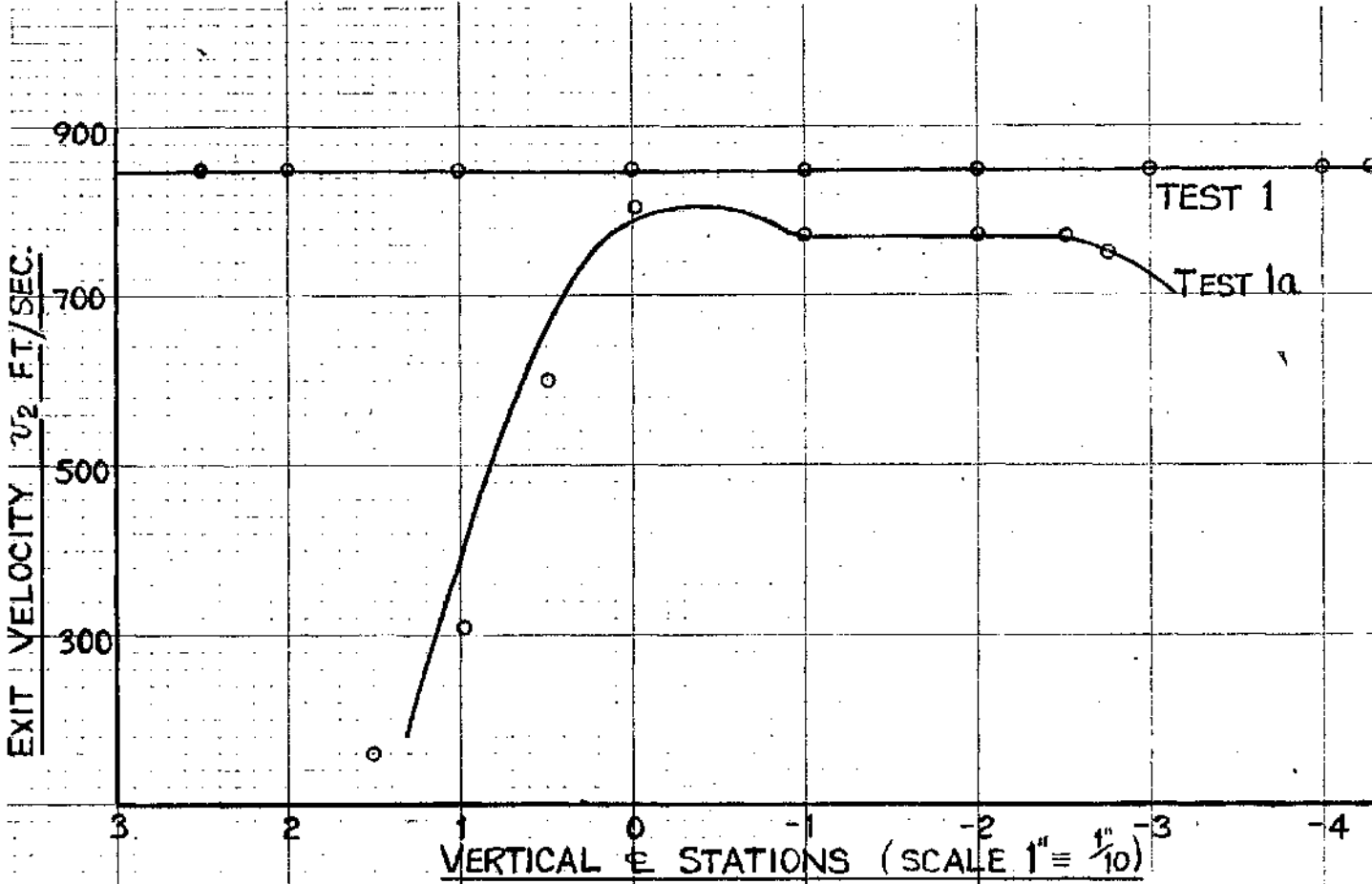
Series 2.

Test No.	1	1A	2	2A	3	3A	4	4A	5	5A	6	6A
Mach No. M_2	0.5	0.5	0.6	0.6	0.7	0.7	0.8	0.8	0.9	0.9	0.97	0.97
Reynolds No ($\times 10^6$)	3.46	3.46	3.96	3.96	4.45	4.45	4.77	4.77	6.28	6.28	7.04	7.04
\bar{z}_n	0.917		0.894		0.891		0.897		0.884		0.902	
\bar{z}_o		0.766		0.821		0.785		0.785		0.783		0.790
K		0.914		0.959		0.940		0.935		0.941		0.935
Blade loss BTU/lb.		2.185		1.455		2.860		3.900		4.310		5.570
α	33-11°	44-24°	34-0°	45-0°	35-6°	45-15°	35-24°	46-46°	36-58°	47-51°	35-6°	45-46°
$\bar{z}_n \phi$	1.0		0.97		0.973		0.965		0.957		0.98	
$\bar{z}_o \phi$		0.83		0.894		0.854		0.86		0.881		0.832
K ϕ		0.911		0.96		0.935		0.944		0.928		0.922
Blade loss BTU/lb. ϕ		2.46		1.585		3.33		3.70		5.68		7.26



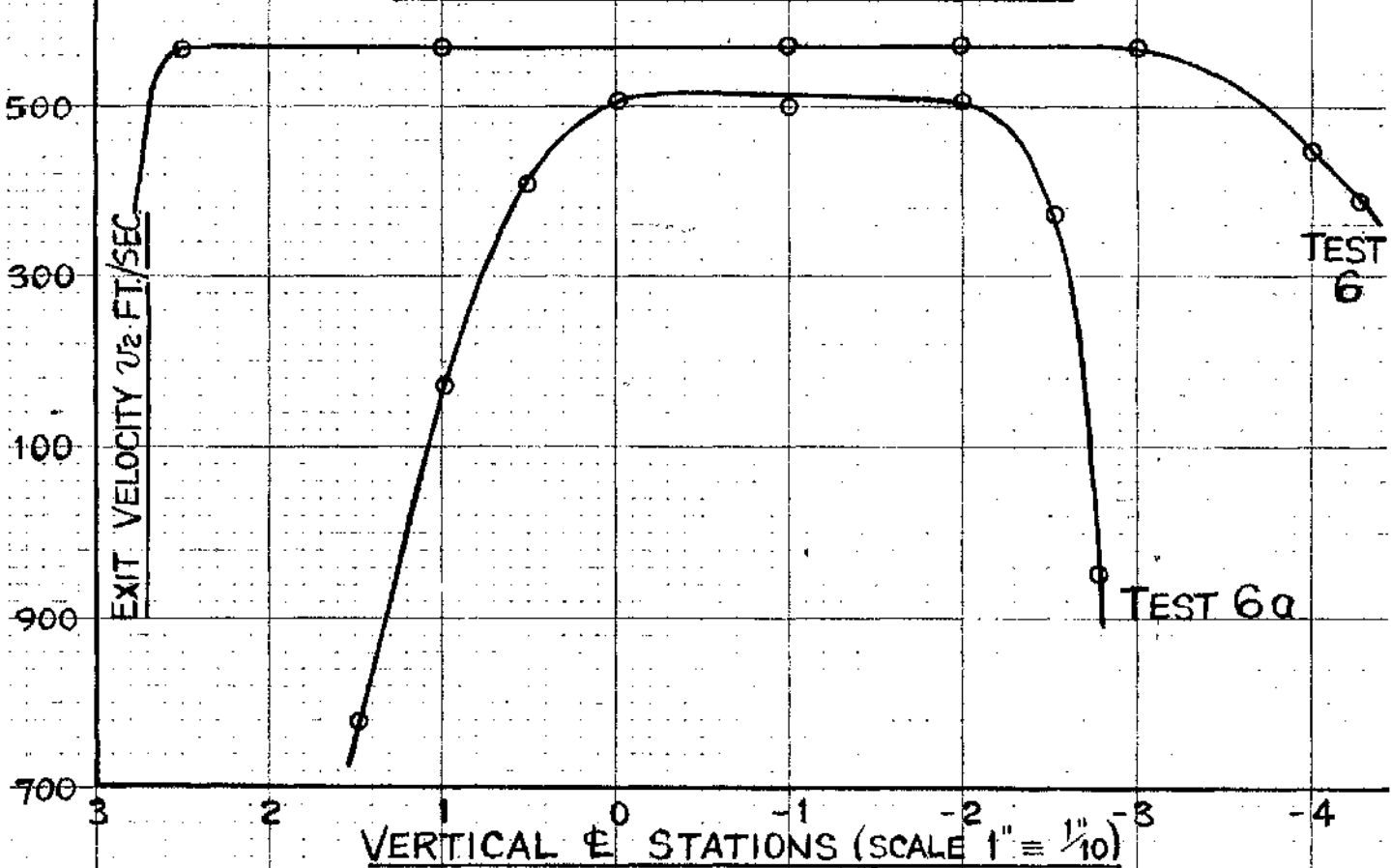
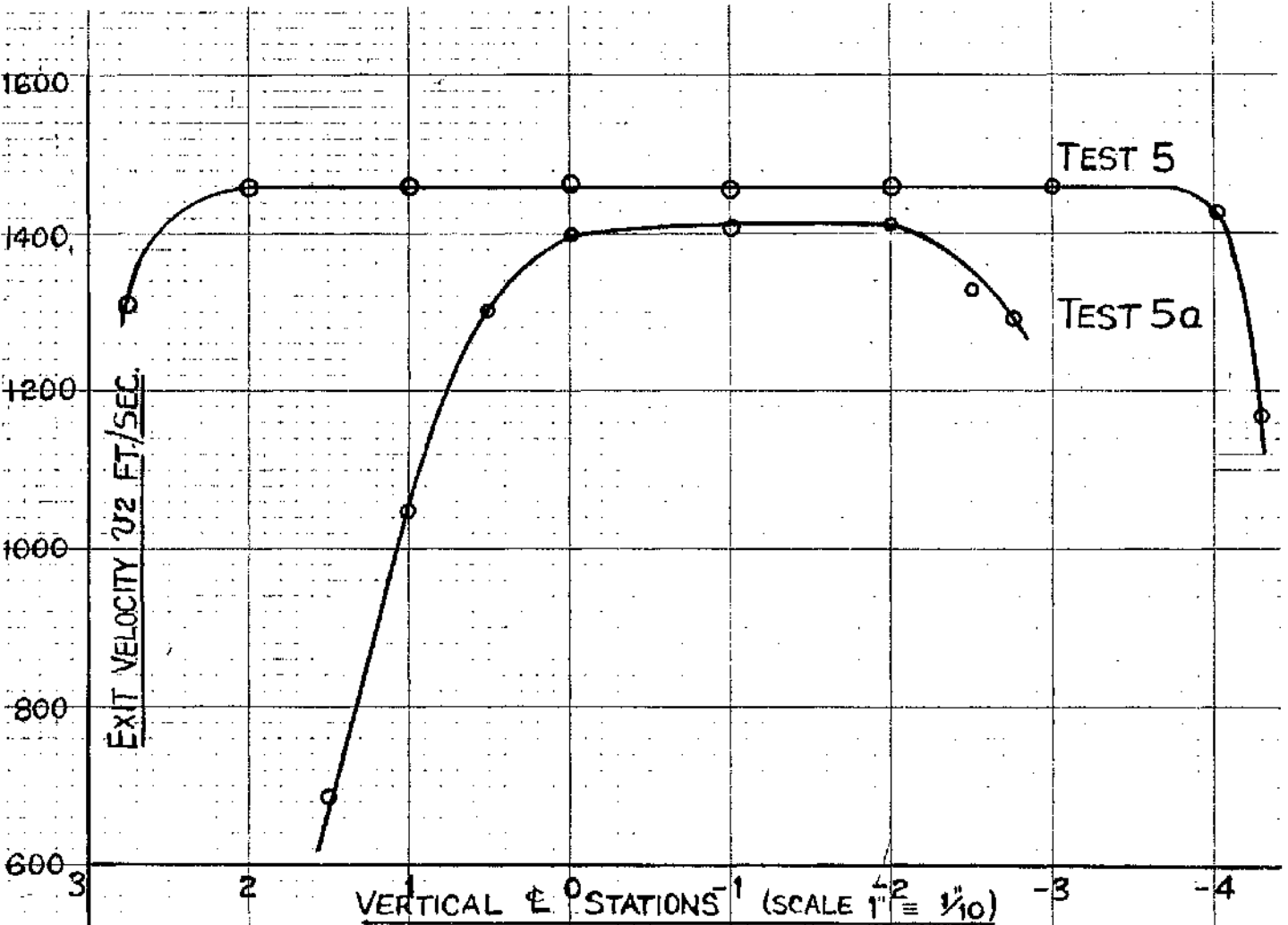






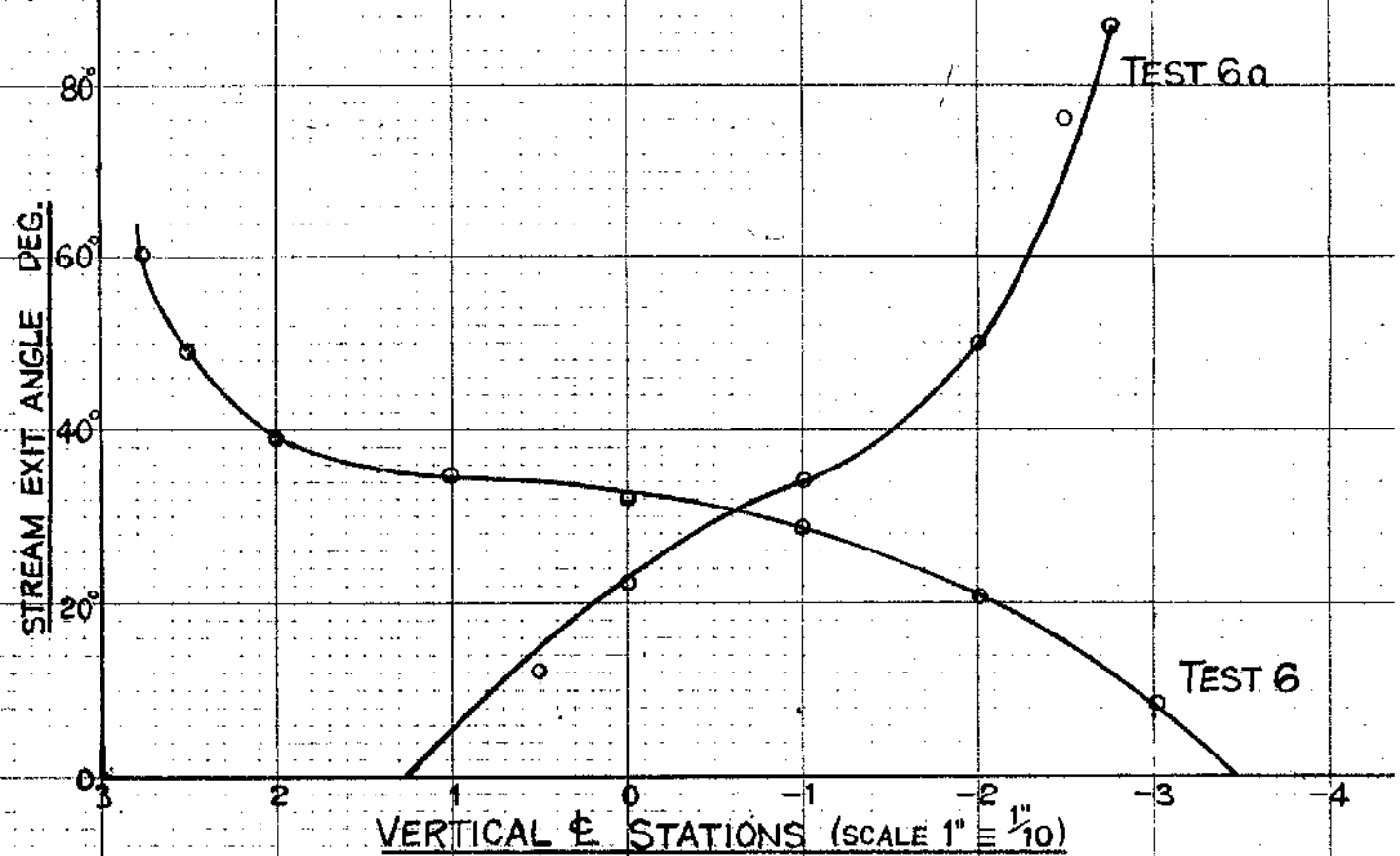
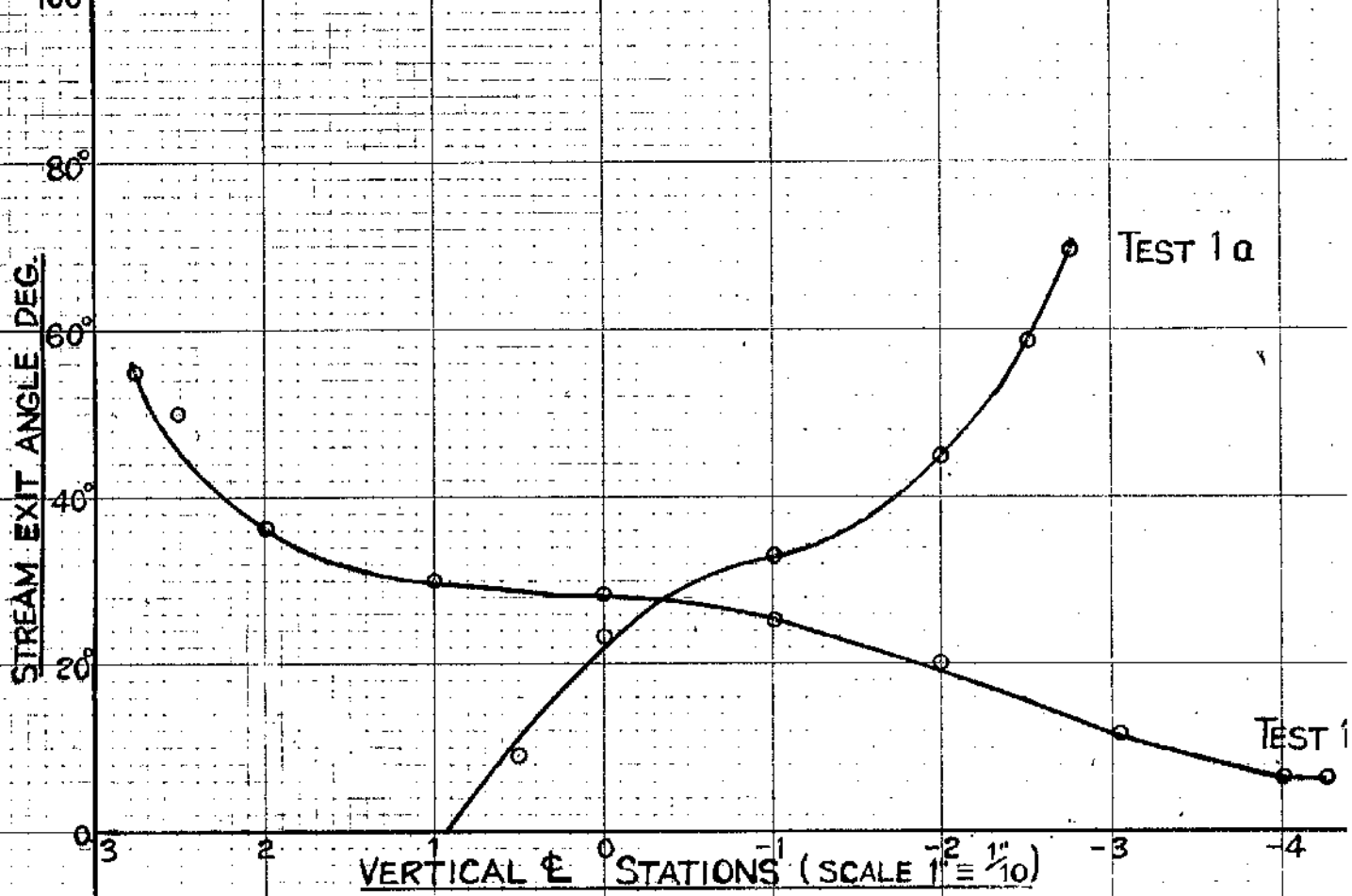
SERIES III

FIG. 58

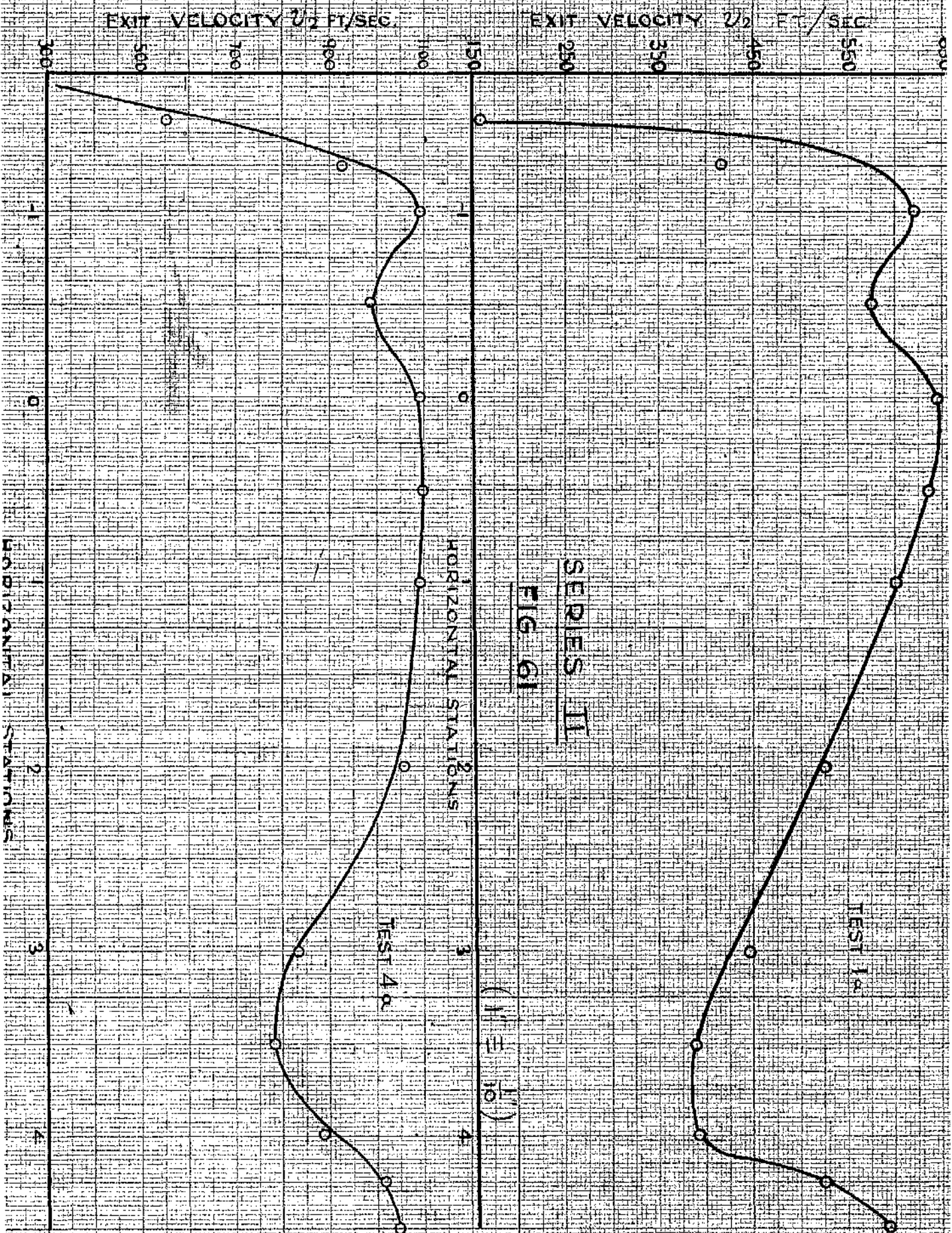


SERIES II

FIG. 59



SERIES II
FIG. 60



Series 3.

Series 3.

In this test series the range of outlet Mach number was extended into the supersonic field. The tests were carried out only at the blade exit and along a vertical centre line. There are three groups of tests with inlet pressures of 64.5, 53.37, and 44.45 lb/in². In each group the maximum Mach number is obtained with a back pressure of 1 lb/in²g. and the inlet temperature is chosen to avoid expansion into the wet field at maximum Mach number. In all tests, including those in series 1 and 2 where the Mach numbers is less than unity, the back pressure in the casing and the nozzle outlet pressure were as expected equal. For this test series, in the cases where the outlet Mach number was greater than unity the nozzle outlet pressure corresponded to the critical pressure.

The test conditions for series 3 are shown in the tables on pages 166, 167, 168 along with the final results. Specimen calculations are given on page 169 and the graphs of the final results are described on page 170.

Effect of supersonic Mach number on efflux angle.

An additional test in this series wherein the variation of nozzle efflux angle with supersonic Mach number was investigated is described on page 174.

Series 3 ----- Test conditions and final results.Group 1

Inlet pressure P_1 lb/in ²	← 64.5 →			
Back pressure P_2 lb/in ²	32.5	24.5	19.5	15.5
Mach No. $M_2 \phi$	1.075	1.298	1.46	1.6
Inlet Temp. T_1 °F	← 490 →			
Reynolds No. ($\times 10^6$)	11.4	11.75	11.55	11.5
$\bar{f} b \phi$	0.849	0.815	0.88	0.868
$K \phi$	0.921	0.903	0.938	0.931
Blade loss BTU/lb. ϕ	9.85	16.6	12.8	17.1

Series 3 ----- Test conditions and final results.

Group 2

Inlet pressure P_1 lb/in. ²	←				54.37								
Back pressure P_2 lb/in. ²	46.25	43.2	40.0		36.56	33.0	26.5	22.5	18.5	15.			
Mach No. M_2	0.5	0.6	0.7		0.8	0.9	1.08	1.228	1.37	1.5			
Inlet Temp. T_1 °F	←				450								
Reynolds No. ($\times 10^6$)	6.66	7.61	8.55		9.3	10.1	10.66	10.65	10.2	10.			
\bar{z}	0.733	.771	.794		.828	.81	.76	.744	.791	.78			
K	0.856	.879	.891		.910	.90	.872	.864	.891	.88			
Blade loss BTU/lb. ϕ	4.16	5.01	6.04		6.3	8.8	15.4	20.0	19.6	23.			

Series 3 ----- Test conditions and final results.

Group 3

Inlet pressure P_1 lb/in. ²	←					44.45						→
Back pressure P_2 lb/in. ²	37.6	35.2	32.43	29.7	26.84	24.84	22.45	19.45	15.45			
Mach No. M_2	0.5	0.6	0.7	0.8	0.9	0.97	1.06	1.178	1.359			
Inlet Temp. T_1 °F	←				408							→
Reynolds No. ($\times 10^6$)	5.91	6.76	7.55	8.14	8.7	8.89	9.24	9.36	9.32			
η	.7125	.762	.830	.871	.851	.841	.806	.755	.797			
K	.845	.875	.911	.935	.924	.916	.896	.869	.893			
Blade loss BTU/lb. ϕ	4.32	5.02	4.80	4.56	6.66		11.5	17.25	17.75			

Calculations. The calculations differ slightly from those in series 1 and 2 due to the possibility of the local outlet Mach number being greater than unity. The method described in detail on pages 83 and 85 is used for dealing with this. The specimen calculations given below are for the test in group 3, with $M_{2\phi} = 1.359$. The necessary tables for group 3 are given in appendix 1 pages 211 to 217. Those for group 1 and 2 are given in appendix 2 pages 84 to 103.

Group 3, $M_{2\phi} = 1.359$.

$$P_1 = 44.45 \text{ lb/in}^2$$

$$P_2 = 15.45 \text{ lb/in}^2$$

$$\therefore \frac{P_2}{P_1} = 0.347 \quad \therefore M_{2\phi} = 1.359$$

$$T_1 = 408^\circ\text{F}$$

$$H_1 = 1240 \text{ BTU/lb.}$$

$$\therefore T_{2\phi} = 214.64^\circ\text{F}, \quad DH_{\phi} = 87.55 \text{ BTU/lb.}$$

$$v_{2\phi} = 2094 \text{ ft/sec}, \quad V_{2\phi} = 25.7 \text{ ft}^3/\text{lb.}$$

$$\mu_{2\phi} = 2.71 \times 10^{-7}, \quad R_n = 9.32 \times 10^6.$$

$$\text{At station 0, } \frac{P_2}{P_5} = 0.415.$$

$$\therefore \frac{P_2}{P_3} = 0.4065 \quad \text{----- Fig. 36 (page 84).}$$

$$\therefore \bar{\gamma} = 0.88 \quad \text{----- Fig. 33 (page 79).}$$

$$\text{From table 3 } \bar{\gamma}^{\frac{1}{2}} \sin \alpha \frac{fda}{fV} = 1.8227 \quad \text{----- appendix 1 (page 216).}$$

$$\text{From table 4 } \bar{\gamma}^{\frac{3}{2}} \sin \alpha \frac{fda}{fV} = 1.4545 \quad \text{----- appendix 1 (page 217).}$$

$$\therefore \bar{\gamma}_b = \frac{1.4545}{1.8227} = 0.797$$

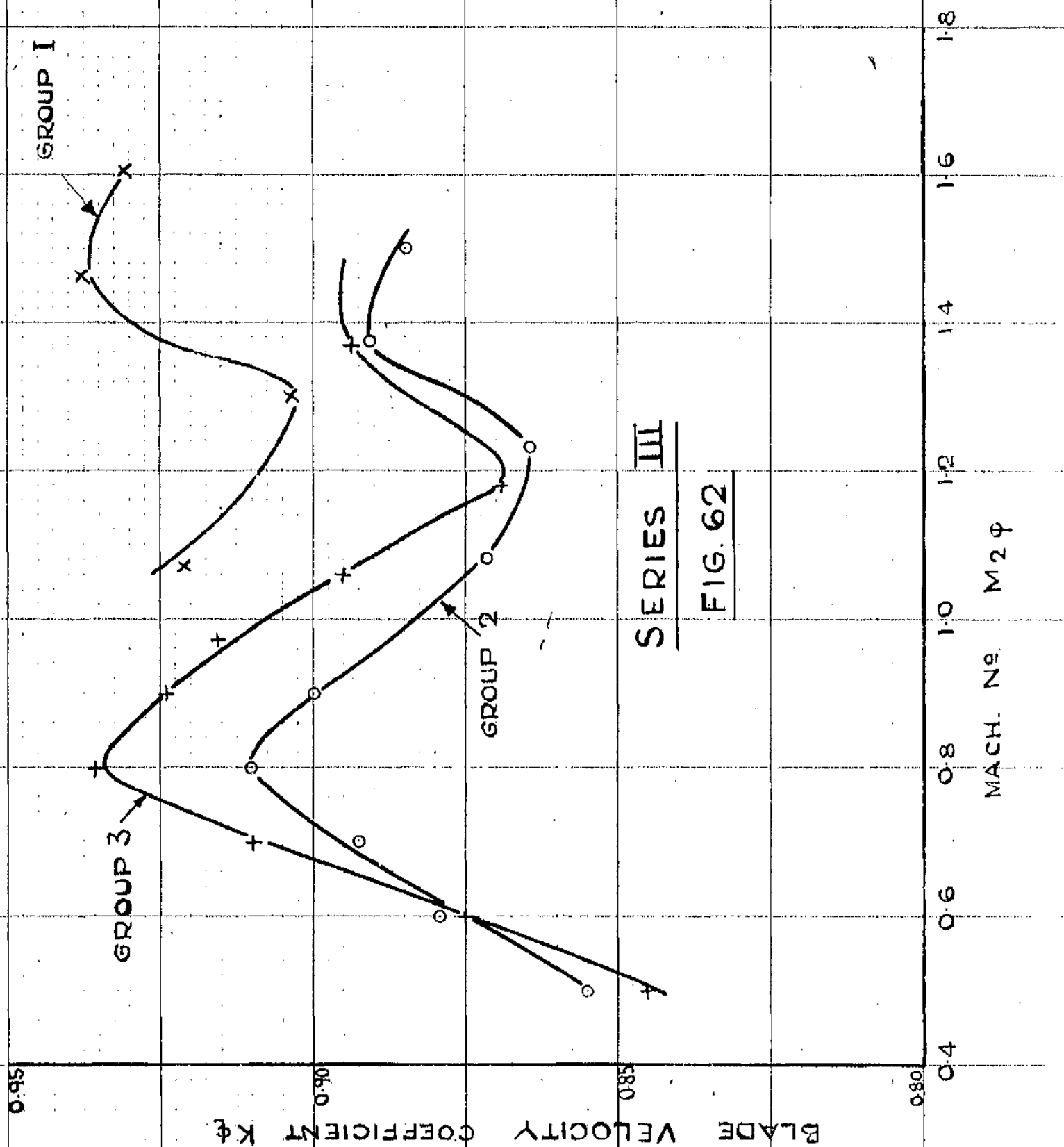
$$\text{Taking } \bar{\gamma}_n = 1 \quad \therefore K_{\phi} = \sqrt{.797} = 0.893.$$

$$\text{Blade loss } \phi = (1 - K^2) DH_{\phi} = (1 - .797) \times 87.55 = 17.75 \text{ BTU/lb.}$$

Series 3 ----- Final Results.

From the final average results the following graphs have been drawn.

- (1) The efficiency of expansion as $K_{\phi} (\sqrt{\gamma} v_{\phi})$ to a base of Mach number Fig. 62 (page 171).
- (2) Blade velocity coefficient K_{ϕ} to a base of Reynolds number. Fig. 63 (page 172).
- (3) Blade loss to a base of Mach number Fig. 64 (page 174).



SERIES III

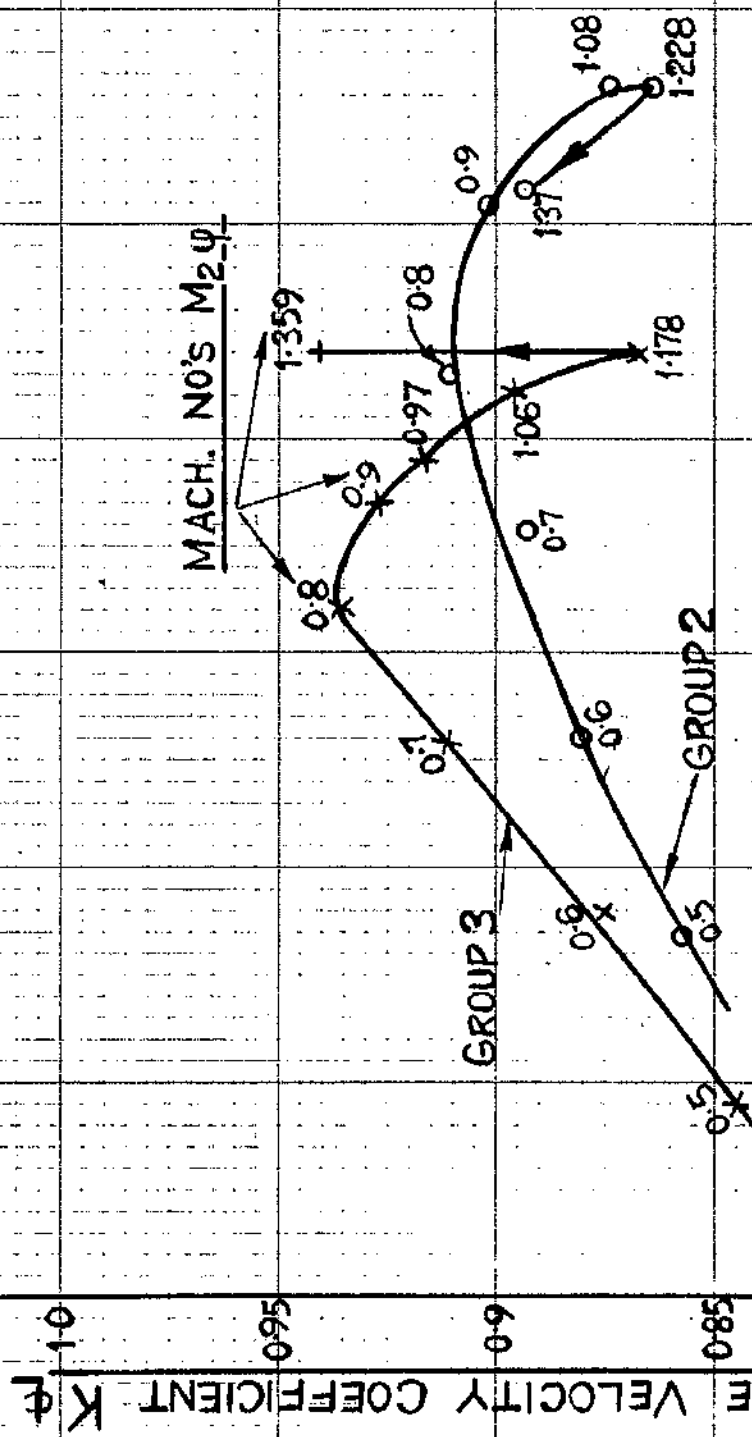
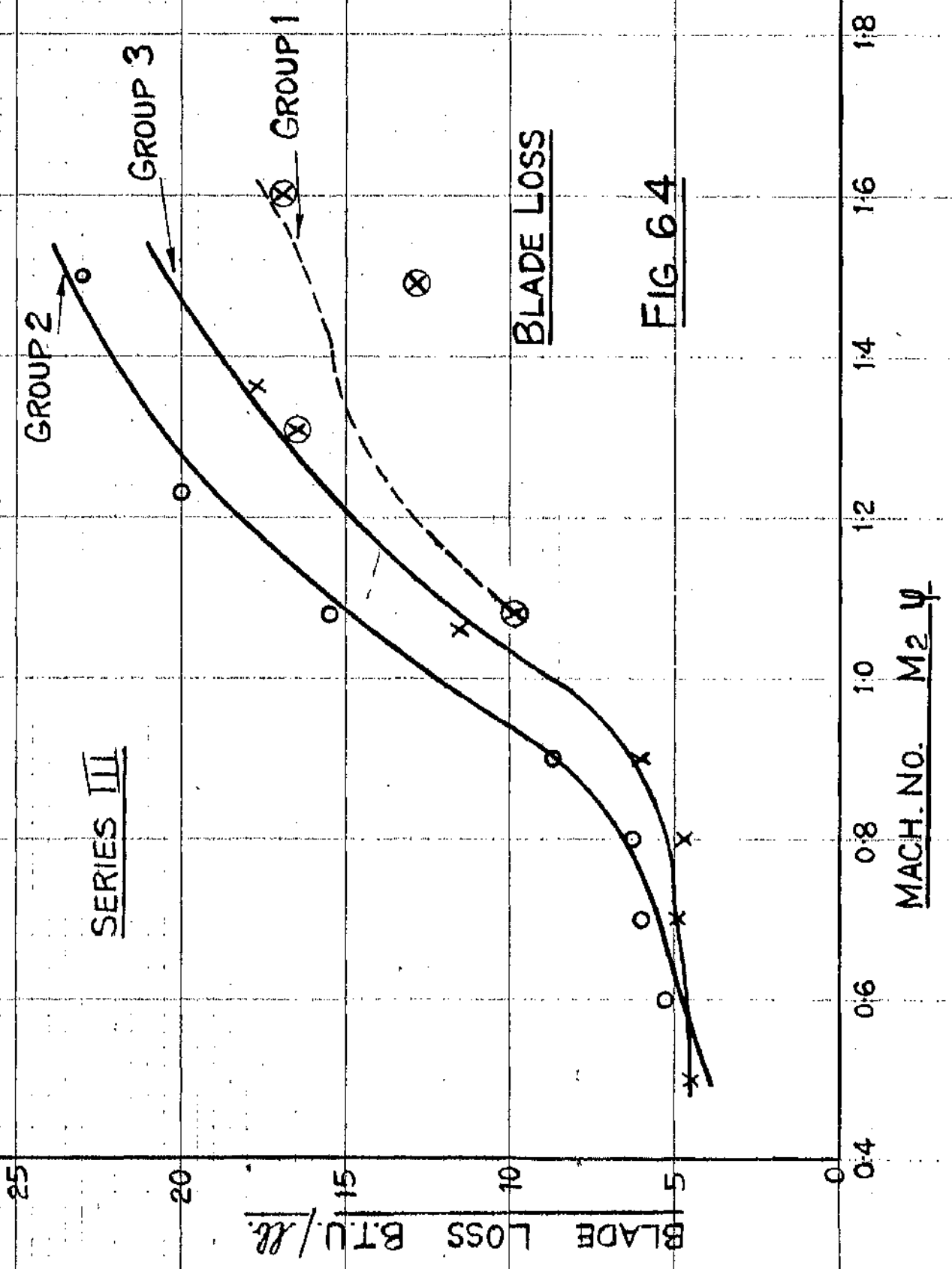


FIG. 63

REYNOLDS NO. RN.

12×10^6



Effect of Supersonic Mach Number on Efflux Angle.

It was observed in series 3 that the efflux angle at any given station varied considerably as the Mach number was increased into the supersonic field. To investigate this further a traverse was made along the vertical centre line of the nozzle outlet at values of Mach number greater than unity.

The results are given in Fig. 65 (page 175) and show the change of efflux angle with Mach number for various vertical stations.

Discussion of Results.

Discussion of Results.

Part 1.

The stage efficiency of a turbine or compressor has been shown to depend on two broad considerations. The first of these is the effect of friction in the stage elements which causes the degeneration of high grade energy and the second is the choice of such design parameters as the degree of reaction or loading factor for the stage. The enthalpy loss or loss of high grade energy in a static or moving element is shown to be a composite quantity comprising a basic friction work term plus an auxiliary loss term. The friction work is equal in magnitude to the high grade energy which is degenerated to low grade energy and the auxiliary loss term is due to the "heating" effect of the low grade energy thus created. For a compression process the auxiliary term is positive while for an expansion it is negative. Comparing similar expansion and compression processes therefore, where the friction work is the same, the compression process will be less efficient than the expansion process. The enthalpy loss is related to other ways of expressing the irreversibility in the blade element and the expressions developed may be applied to static or moving elements in axial flow turbines or compressors with high and low speed flow.

The stage efficiencies in turbines or compressors are shown to be dependant on the blading or diagram efficiency as well as on the friction losses in the elements. A comprehensive theory is developed giving the variation in blading efficiency with such stage design parameters as the degree of reaction, the blade speed to jet speed ratio and the loading factor. The analysis is developed for positive, zero, or negative degrees of reaction and the speed ratio for maximum blading efficiency is obtained for any given degree of reaction. It is shown that the value of the maximum blading efficiency increases as the degree of reaction increases. However the loading factor at maximum blading efficiency reduces as the degree of reaction increases and in

choosing design parameters for the stage account must be taken of these conflicting factors. For a turbine stage the total to static stage efficiency is used where the exhaust kinetic energy is degraded by friction and it is shown that this stage efficiency is directly proportional to the blading efficiency. The total to total stage efficiency, used where the exhaust kinetic energy is not degraded, also increases as the blading efficiency increases. It is shown however that where the friction losses in the elements are low and the blading efficiency high, the total to total stage efficiency is almost independent of blading efficiency. The characteristic variation of the two stage efficiencies with blade speed to jet speed ratio at a given degree of reaction may be deduced from the corresponding variation of blading efficiency and from the way in which the process efficiency varies as the velocity triangles change.

Part 2.

Having decided on the broad features of a design by determining the amount of reaction or compression, blade speeds and stream velocities to be used, it is then necessary to obtain experimentally the net friction loss in the proposed element and also the path taken by the working fluid as it passes through the element. In the section on the measurement of local efficiency by means of an impact tube, it has been shown how the tube may be used in either subsonic or supersonic flow to obtain local values of efficiency, specific volume, and efflux angle. The observed local total head pressures across a section must be converted to mean effective values at that section. To ease this transformation a method has been formulated using the theory, graphs and tables provided here. The calculations given for mean effective values represent a maximum requirement

and they may be modified to lessen the work involved in individual applications. For example, in many cases using cascades of blades in wind tunnels the variation of density across the traverse plane may be neglected and in calculating mean efficiency the local efficiency need not be weighted for mass flow.

Part 3.

The technique evolved for the measurement and calculation of loss represents a method which is applicable to all types of turbo machine elements with either compression or expansion in the elements and proves effective here in its application to a nozzle and blade pair. The inherent disadvantage in the method is the length of time required both for obtaining the impact tube readings and for completing the calculations. Some considerable amount of work has been done towards reducing the time factor by introducing automatic traversing gears and calculators. (See references 37 and 38).

The advantages of using steam as a working fluid in this type of testing lie in the ease with which the inlet condition and exhaust pressure can be varied giving a very flexible variable density tunnel and also in the simplicity of accurate flow measurement by condensation. The accuracy of the calculated mean values is difficult to assess due to the number of variables involved, but a check on the calculated mass flow rates is obtained by comparison with the observed flow figures and show

a good agreement.

With regard to the experimental results it should be emphasized that these apply to the type of machine element tested that is to a single nozzle and impulse blade pair and that the losses measured exclude incidence effects. This limits the variables making the experimental work an attempt to correlate loss and flow characteristics with Reynolds number and Mach number for a constant geometry system.

The general impressions from all the subsonic test results are that, while the losses change, the general flow pattern at the nozzle or blade exit remains substantially the same with varying Reynolds number and Mach number. For the nozzle we find isentropic flow throughout the major part of the outlet area with the region of low flow and high loss confined to a small wall boundary layer, while the variation of efflux angle in the vertical direction is considerable.

At the blade exit plane the isentropic condition is nowhere realized. On the vertical centre line the velocity (Figs 53 and 54 pages 149 and 150) reaches a constant maximum for only 40% of the outlet height and this region is flanked by large unsymmetrical boundary layers, the maximum loss being on the convex side of the blade passage. Whether these loss regions can be described as boundary layers is doubtful because they are probably caused by detachment of the true boundary layer due to the curvature of the blade passage walls. Centrifugal effects within the blade passage will result in the lowest static

pressure normal to the flow occurring at the convex surface of the blade. Hence at some subsonic Mach number a local Mach number of unity will appear firstly at the convex surface. This can result in a shock discontinuity stemming from the convex surface with consequent detachment or thickening of the boundary layer downstream from the point of origin of the shock.

In the horizontal direction the blade velocity distribution (Fig. 61 page 163) as well as showing the wall loss displays regions of low efficiency on either side of the vertical centre line. This is explained by the internal distribution of static pressure formed by the curvature of the blade passage which causes circulatory motion or vortices to be imposed on the main flow. Again vertically we find the same form of efflux angle distribution as for the nozzle.

The variation of mean nozzle efficiency with Reynolds number (Fig. 50 page 146) follows the same pattern for the two and three dimensional tests and show a maximum value at a Reynolds number of 5.7×10^6 . The variation of the mean pair efficiency with Reynolds number is however in the reverse direction to the nozzle efficiency. One would expect that in a region of high nozzle efficiency, that is with a good quality jet entering the blades passage, that the loss in the blade passage would be small. Remembering however that the loss regions in the nozzle are confined to the boundary layer, with good nozzle efficiency we then have a high energy stream

passing from the vicinity of the nozzle wall to the wall of the blading. A slower layer of fluid would be expected to conform more to the path dictated by the blade passage wall with consequently less disturbance to the rest of the flow. Thus we assume that regions of high velocity approaching a blade boundary will cause greater subsequent loss than regions of low velocity. The reverse would apply to the jet quality away from the boundaries. The blade velocity coefficient as would be expected follows the same pattern as the mean pair efficiency.

In the graphs of mean nozzle and mean pair efficiency with Mach number (Fig. 55 page 157) we see that the nozzle efficiency reduces with increase of Mach number up to 0.9 and then increases from 0.9 to 1.0. In the mean pair efficiency graphs, where the losses are greater, there is a similar tendency for the efficiency figures to increase as a Mach number of unity is approached. Ainley¹¹ and Todd¹⁰ have reported increase in efficiency as the Mach number approaches unity. They say that this is due to a local shock wave appearing first at some point on the convex surface of the blade and some way inside the passage and that as the free stream Mach number is increased the shock front moves towards the blade outlet leaving less surface in contact with the thickened boundary layer. For circular nozzles Guy⁴ and Giffen³ have each indicated a rise in efficiency at high steam speeds although they disagreed as to the form of the curve at low steam speeds.

The graphs of mean pair efficiency also indicate a rise of efficiency with increasing Reynolds number below a Mach number of 0.6 and again a rise of efficiency with increased Mach number above 0.7 with the range 0.6 to 0.7 as a transition zone. This to some extent confirms the observations of a number of observers to the effect that Reynolds number is the controlling parameter below a Mach number of 0.66 and Mach number the controlling parameter thereafter. This is again supported by the graphs of loss in Fig. 57 (page 159).

The series 3 test results plotted in Fig. 62 (page 171) show a regular pattern for the variation of centre line blade velocity coefficient with Mach number and indicate maximum values at 0.8 in the subsonic field and 1.4 in the supersonic field. To show the influence of Reynolds number the coefficients are again plotted to a base of Reynolds number in Fig. 63 (page 172). In the Mach number range 0.9 to 1.2 it will be observed that the variation in Reynolds number is small so that the reduction in blade velocity coefficient here must be solely due to Mach number effects. The effect of Reynolds number on the coefficient in this same range of Mach number can be seen by comparing the group 3 tests with the group 2 tests where the increase of Reynolds number from group 3 to group 2 reduces the coefficient. The variation of centre line loss with Mach number (Fig 64 page 173) shows a progressive increase of loss with Mach number.

As stated previously the pattern of efflux angles for the nozzles and blades varies very little with Reynolds number and

subsonic Mach number. In the efflux angle graphs in Figs. 53 and 54 (pages 149 and 150), the nozzle efflux angle steadies to a value of 28° over a large proportion of the vertical traverse and is almost constant with Reynolds number. In the graphs in Fig. 60 (page 162) the corresponding steady values are 28° at Mach number 0.5 rising to 32° at Mach number 0.97, and the mean calculated values of nozzle efflux angle agree very closely with these central steady values. This small variation in efflux angle with Mach number is consistent with the results obtained by Ainley¹¹. Ainley quotes variations in efflux angle with subsonic Mach number for various theoretical outlet angles. His results show that the jet is deflected towards the axial direction as the Mach number is increased from low subsonic values up to unity. The variation is about 6° for a theoretical outlet angle of 40° (measured from the axial direction) and the variation decreases as the theoretical axial outlet angle is increased. There is however a considerable difference of about 8° between the mean values quoted above and the geometric outlet angle and in addition the efflux angles of the nozzle or blade differ from those quoted by Guy where the formula \sin^{-1} opening/pitch was said to give the mean outlet angle. It should be remembered however that in Guy's experiments the nozzles being tested were supported on either side by other nozzles running full of steam.

The change in the pattern of the nozzle efflux angle distribution in the supersonic field (Fig. 65 page 175) is in

contrast to the small changes in the subsonic region. Considering the vertical centre line at the mid point of the nozzle, as the Mach number approaches unity the efflux angle is 32° with angles varying up to 56° and down to 10° at the boundaries. As the Mach number increases to 1.5 the flow is deflected away from the boundaries towards the main stream and with increasing Mach number the vertical variation of efflux angle is reduced. Hence with increasing supersonic Mach number the efflux angle tends to follow more closely the geometric outlet angle.

In all the tests the pressure at exhaust from nozzle or blades has been taken as equal to the pressure observed in the casing and the assumption is then made that this pressure is constant along the line of the traverse. This is justified provided the variation in pressure is small due to the relative difficulty of making accurate static pressure measurements in the free stream, reliance normally being placed on wall tapings. In the subsonic tests the casing pressure and nozzle wall tapings were found to coincide. In the supersonic tests the nozzle wall tapings, as would be expected, gave the critical back pressure and the casing pressure was again taken as the static pressure along the traverse line. Stodola³⁹ has shown that the variation in static pressure at the exhaust from a convergent parallel nozzle with super critical expansion is small and in any case the impact tube measures the total energy of the stream so that a slight departure of the local static pressure from the final

back pressure means only that a little of the total energy is retained as potential energy. The transformation to kinetic energy will be complete a little further downstream with only a slight effect on efficiency.

We have seen in the section on the analysis of losses that the effective loss in turbo machine elements can be divided into two parts. The first part is the friction work or the basic loss of high grade energy which is dissipated as low grade energy. The second part, which is positive or negative depending on the pressure gradient, represents the "heating" effect of the low grade energy on the specific volume. The internal heating will be equivalent to external heating of the same amount and is therefore distinct and separate from the basic friction work loss. One feels that it is this basic friction work loss and not the effective loss which should be related to Reynolds number and Mach number. Unfortunately the measurement of the basic loss is much more difficult than that of the effective loss, since it would entail traverse measurements through the whole expansion or compression process.

In the section on efficient mechanical energy transfer we saw, for a turbine stage, that the maximum blading or diagram efficiency rises as the degree of reaction increases. The comparative effects of a small amount of reaction and of a small amount of compression have shown in Fig. 47 (page 122) where the flow with compression appears to break down completely in the centre of the blade. Ainley¹¹ has stated for the turbine

blades with which he was dealing that the loss decreased with increased reaction. Hence from the point of view of increased efficiency both in expansion in the blading and in diagram efficiency high reaction is beneficial. The upper limit on reaction will be due only to the decrease in work done factor with increased reaction.

Conclusions.

It is well known that where friction is involved care must be exercised in applying thermodynamic principles. It has been shown here how the expressions for the energy inter-changed between the rotor blades and the working fluid in turbines and compressors are modified in a friction process. The loss of useful energy caused by friction is shown to comprise of two parts, one of which accounts for the degeneration by friction work of high grade energy into low grade energy and the other for the effect of this low grade energy on the specific volume of the fluid. Thus the nature of any friction process may be more readily examined and it is shown here how friction affects the efficiency of similar expansion and compression processes.

Some work has already been done on the choice of design parameters for the efficient operation of both the impulse blade and 50° reaction blade. The section on maximum blading efficiency, with its concept of Reaction Coefficient, forms a comprehensive theory which will fill the gap between these two as well as embracing the operation of the axial flow compressor. The flexibility of the theory will be apparent to those who are contemplating unorthodox designs. For example it is well known that in axial flow compressors the growth of the boundary layer from stage to stage reduces the efficiency. If occasionally a stage is introduced with a little reaction in say the moving blade, an improvement in the axial velocity distribution would result.

The determination of local efficiency and efflux angle and

The conversion of these local values into mean effective values is a necessary step in the analysis of the performance of machine elements. It is suggested that the methods herein developed will ease and simplify this transformation. These methods take account of variable density and supersonic flow and may therefore be used, in individual applications, to assess the errors involved in applying quicker but less rigorous procedures.

With regard to the flow pattern in the nozzle and blade pair, there was an unexpected variation in nozzle efflux angle about the centre of the nozzle, the stream apparently paying little heed to the geometric outlet angle except in a small central core. This flow pattern remained comparatively unchanged with varying Reynolds number and subsonic Mach number. When however the Mach number was increased to values greater than unity, there was a marked straightening of the stream lines, so that with progressively increasing Mach number the stream conformed more and more to the geometric outlet angle at all sections of the nozzle.

The variation of profile and total loss coefficients with Reynolds and Mach number for the writers zero pressure drop impulse blade is compared in appendix 3 with similar research by other workers, notably Armstrong⁴⁰, Ainley⁴¹ and Kearton⁴². Armstrong examined the profile loss characteristics for an impulse blade at high Reynolds number and found that above a Reynolds number of 2×10^5 , based on blade chord, the loss coefficient remains substantially constant. When however the Reynolds number is reduced from high values and approaches the 2×10^5 region there is a sudden increase in the loss coefficient. The writers work,

which covers a similar high Reynolds number range, helps to confirm that a chord Reynolds number of 2×10^5 is in fact a critical value of this parameter. The following conclusions regarding the variation of loss coefficients were found to be consistent with most of the experimental data given in appendix 3.

Below a Mach number of 0.66 the controlling parameter is the Reynolds number. As the Reynolds number is reduced below 2×10^5 both the profile and the total loss coefficient show a considerable increase and above this critical value they remain substantially constant. Where the Reynolds number is high (above 2×10^5) and the Mach number is above 0.66 then (a) the total enthalpy loss coefficient remains constant while the total stagnation pressure loss coefficient increases as the Mach number increases, and (b) the profile enthalpy and stagnation pressure loss coefficients are both Mach No. dependant and increase with increasing values of the Mach number.

The impact tube and traversing gear have been shown to be capable of use in relatively high pressure, temperature and density streams. Hence the arrangement may be used to test steam or gas turbine elements near to their actual working conditions, or indeed the gear may be adapted for use on actual turbines or compressors.

In general however the experimental and analytical procedures involved in testing turbo machinery elements are time consuming and repetitive. In future work it would be desirable to introduce more labour saving devices, such as automatic traversers and integrators, and certain suggestions along these lines by other workers have already been referred to.

Bibliography.

1. Briling. "Energy Losses in Steam Turbine Buckets".
Article in "Engineering" April 1910.
2. "Sixth and Final Report of the Steam Nozzle
Research Committee". Proc. I.Mech.E. Vol 1, 1930.
3. Giffen E. "Steam Flow in Nozzles; Velocity Coefficients
and at Low Steam Speeds". Proc. I.Mech.E. Vol, 155
Orang T.F. 1946.
4. Guy H.L. "Some Researches on Steam Turbine Nozzle
Efficiency". Journal of the Institute of Civil
Engineers. Vol 13, 1939.
5. Dollin F. "Investigation of Steam Turbine Nozzle
Efficiency and Blading Efficiency". Proc.
I.Mech.E. Vol 144, 1940.
- 6, 39. Stodola Steam and Gas Turbines Vol 1, 6 - Page 139;
39 - Page 136.
7. Howell A.R. "Fluid Dynamics of Axial Compressors".
Proc. I.Mech.E. Vol 153, 1945.
8. Howell A.R. "Design of Axial Compressors".
Proc. I.Mech.E. Vol 153, 1945.
9. Howell A.R. & "Overall Stage Characteristics for Axial Flow
Bonham R.P. Compressors". Proc.I.Mech.E. Vol 163, 1950.
10. Todd K.W. "Practical Aspects of Cascade Wind Tunnel
Research". Proc.I.Mech.E. Vol 157, 1947.
11. Ainley D.G. "The Performance of Axial Flow Turbines".
Proc.I.Mech.E. Vol 159, 1948.
12. Weske J.R. "Investigation of Blade Characteristics".
Transactions of the American Society of
Mechanical Engineers. Vol 66, 1944 PP. 413.
13. Carter A.D.S. "Three Dimensional Flow Theories for Axial
Compressors and Turbines". Proc.I.Mech.E.
Vol 159, 1948.
14. Todd K.W. "Some Developments in Instrumentation for Air
Flow Analysis". Proc.I.Mech.E. Vol 161, 1949.
15. Hodkinson B. "The Impact Tube". Proc.I.Mech.E. Vol 151, (No.3)

16. Bairstow L. "Applied Aero Dynamics". Longmans 1939.
17. Durand. "Aerodynamic Theory" Vol 3, Division H.
- 18, 20, & 31. Rogers "Engineering Thermodynamics". Longmans, Green, and Mayhew. 1957, 18 - Page 186; 20 - Page 387; 31 - Page 420.
- 19, 29, & 32. "Introduction to the Gas Turbine". Constable, Shepherd, D.G. 1960, 19 - Pages 125 - 128; 29 - Page 182; 32 - Chapter 7.
21. Hunsaker J.C. & "Engineering Applications of Fluid Mechanics". Rightmire B.G. McGraw - Hill 1947. Chapter 6.
- 22, 33. Shapiro A.H. The Dynamics and Thermodynamics of Compressible Fluid Flow. Volume 1 Ronald Press, New York 1953, 22 - Page 18; 33 - Page 154.
23. Kearton W.J. "Turbo Blowers and Compressors". Pitman, 1926, Pages 35 - 37.
24. Horlock J.H. "Losses and Efficiencies in Axial Flow Turbines". A Review of Experimental Data. Inst. J. Mech Sci, Pergamon Press. 1960, Vol 2 PP 48 - 75.
- 25, 26, 28 & 42. "Steam Turbine Theory and Practice". Pitman Kearton W.J. (Seventh Edition) 1958. 25 - Page 163; 26 - Pages 182 and 211; 28 - Page 176; 42 - Pages 253 - 259.
27. Hawthorne W.R. "Thermodynamics of Cooled Turbines". Part 1: The Turbine Stage, A.S.M.E. paper 55 - A - 186, 1955.
30. Soderburg C.R. Unpublished Note, Gas Turbine Laboratory, Massachusetts' Institute of Technology. - now reproduced in reference 24.
34. Keenan & Keyes Gas Tables, Wiley 1948.
35. Binnie A.M. & "The Pressure Distribution in a Convergent Woods M.W. Divergent Steam Nozzle". Proc.I.Mech.E. Vol 138, p. 229, 1938.
36. Keenan J.H. & Thermodynamic Properties of Steam. Keyes F.G.
37. Todd K.W. "The Auto Recorder". Aeronautical Quarterly. Vol 4, 1954.

38. Kraft H. & Berry T.M. "Automatic Integrating Pressure Traverse Recorder". The Transactions of the American Society of Mechanical Engineers. Vol 62, 1940.
40. Armstrong W.D. "The Non Uniform Flow of Air through Cascades of Blades". PhD. Thesis, Cambridge University 1954.
41. Ainley D.G. & Mathieson G.C.R. "A Method of Performance Estimation for Axial Flow Turbines". Aeronautical Research Council R. & M. 2974 (1957).
43. Cheshire L.J. "Axial Turbines" - Gas Turbine Principles and Practice, Ed. Sir H. Roxbee Cox. Newnes. 1955.
-

Appendix 1.

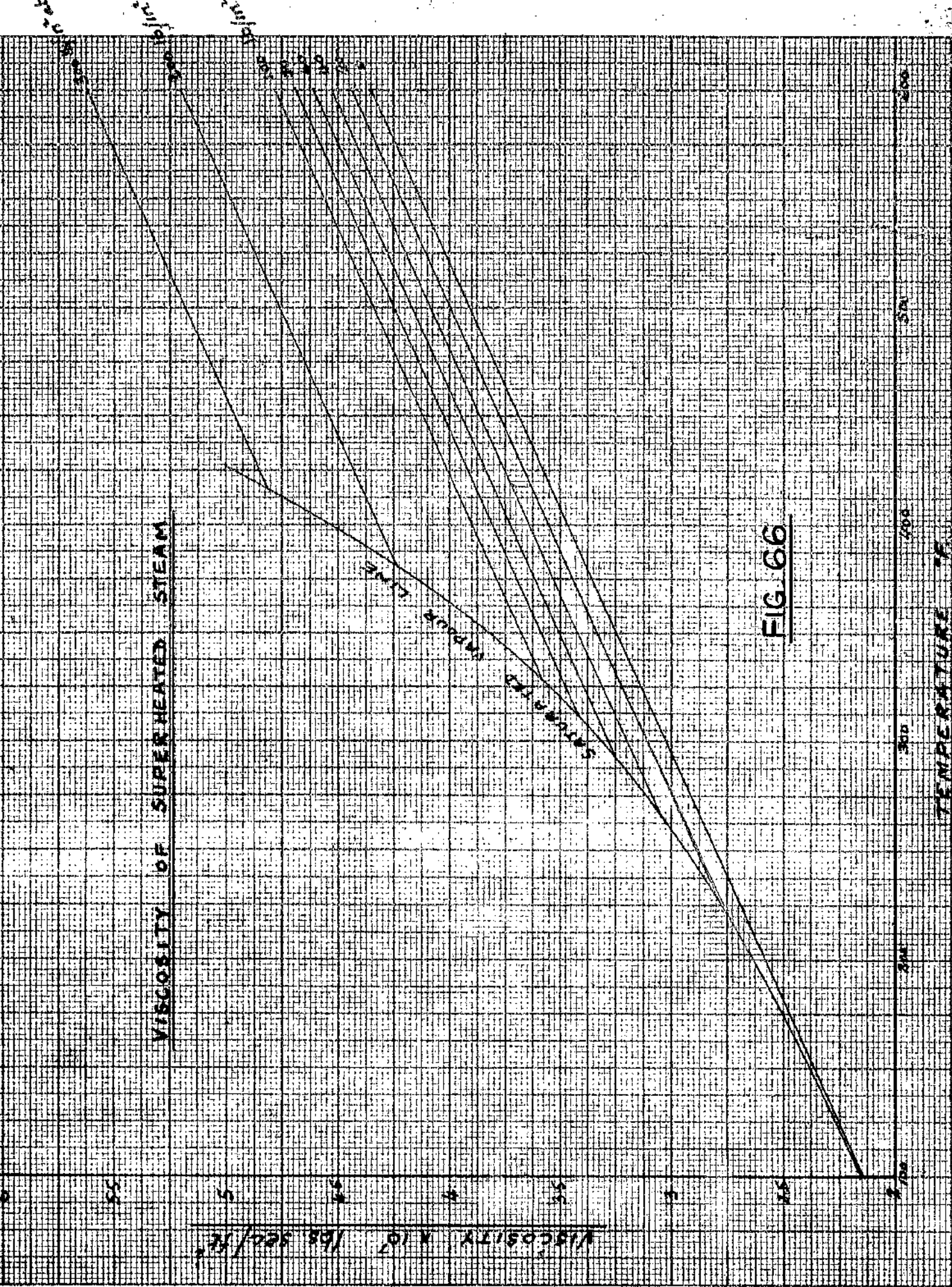


FIG. 66

Specimen tables of observed and derived results Series 2.

Tests 1 and 1A.

Specimen Calculations for test 1 and 1A Series 2.

$$P_1 = 24.3 \text{ lb/in}^2 \quad \therefore \frac{P_2}{P_1} = 0.852 \quad \therefore M_{2\phi} = 0.5.$$

$$P_2 = 20.7 \text{ lb/in}^2$$

$$H_1 = 1229.25 \text{ BTU/lb.} \quad DH_{\phi} = 14.45 \text{ BTU/lb.}$$

$$T_1 = 380^{\circ}\text{F} \quad T_{2\phi} = 348.5^{\circ}\text{F}$$

$$v_{2\phi} = 223.8 \sqrt{DH_{\phi}} = 851 \text{ ft/sec.} \quad v_{2\phi} = 23 \text{ ft}^3/\text{lb.}$$

$$\mu_{2\phi} = 3.325 \times 10^{-7} \text{ lb/sec/ft}^2$$

$$R_n = 3.46 \times 10^6$$

From Test 1 Table 3.

$$\Sigma \gamma^{\frac{1}{2}} \sin \alpha \frac{fda}{FV} = 19.129, \text{ and } \Sigma \epsilon \gamma^{\frac{1}{2}} \sin \alpha \frac{fda}{FV} = 2.992 \text{ (for vertical } \epsilon \text{)}$$

From Test 1A Table 3

$$\Sigma \gamma^{\frac{1}{2}} \sin \alpha \frac{fda}{FV} = 11.083 \text{ and } \Sigma \epsilon \gamma^{\frac{1}{2}} \sin \alpha \frac{fda}{FV} = 1.358 \text{ (for vertical } \epsilon \text{)}$$

From Test 1 Table 4.

$$\Sigma \gamma^{\frac{3}{2}} \sin \alpha \frac{fda}{FV} = 17.541 \text{ and } \Sigma \epsilon = 2.992.$$

From Test 1A Table 4.

$$\Sigma \gamma^{\frac{3}{2}} \sin \alpha \frac{fda}{FV} = 8.467 \text{ and } \Sigma \epsilon = 1.126.$$

$$\text{Hence } \bar{\gamma}_n = \frac{17.541}{19.129} = 0.917, \quad \bar{\gamma}_{n\epsilon} = \frac{2.992}{2.992} = 1.0.$$

$$\bar{\gamma}_e = \frac{8.467}{11.083} = 0.766, \quad \bar{\gamma}_{e\epsilon} = \frac{1.126}{1.358} = 0.83$$

$$\text{Blade velocity coefficient } K = \sqrt{\frac{0.766}{0.917}} = 0.914.$$

$$\text{and } K_{\epsilon} = \sqrt{\frac{0.83}{1}} = 0.911.$$

$$\text{Blade loss} = (1 - K^2) \bar{\gamma}_n DH_{\phi} = 2.185 \text{ BTU/lb.}$$

$$\text{Blade loss}_{\phi} = (1 - K_{\phi}^2) \bar{z}_n \phi_{DH} = 2.46 \text{ BTU/lb.}$$

From test 1 table 5.

$$\sum z \cos \alpha \sin \alpha \frac{fda}{FV} = 15.331.$$

From test 1A table 5.

$$\sum z \cos \alpha \sin \alpha \frac{fda}{FV} = 6.902.$$

Hence for the mean nozzle exit angle.

$$\cos \bar{\alpha}_n = \frac{\sum z \cos \alpha \sin \alpha \times \frac{fda}{FV}}{\sqrt{\bar{z}_n} \sum z^{\frac{1}{2}} \sin \alpha \frac{fda}{FV}} = \frac{15.331}{0.957 \times 19.129} = 0.837.$$

$$\therefore \bar{\alpha}_n = 33^{\circ} - 11'$$

and for the mean blade exit angle.

$$\cos \bar{\alpha}_b = \frac{6.902}{0.875 \times 11.083} = 0.714 \therefore \bar{\alpha}_b = 44^{\circ} - 24'$$

TABLE I

TEST No: - I
SERIES II

MACH No. .5

BAROMETRIC PRESS = 19.328/in² $P_1 = 24.3$ LB/IN² Ab. $P_2 = 20.7$ LB/IN² Ab.

TEMP. 300° F.

HORIZONTAL STATIONS →

STATIONS	-3 $\frac{3}{4}$	-3 $\frac{1}{2}$	-3 $\frac{1}{4}$	-3	-2	-1	0	1	2	3	3 $\frac{1}{4}$
	P_3	P_3	P_3	P_3	P_3	P_3	P_3	P_3	P_3	P_3	P_3
2 $\frac{3}{4}$	20.8 55	20.9 55	21.5 55	22.3 58	23.4 56	23.8 54	24.3 55	24.3 56.5	24.8 58	24.8 57	24.8 55
2 $\frac{1}{2}$	20.8 51	21.1 51	22.4 51.5	23.3 55	24.3 52	24.3 49	24.3 50	24.3 50	24.3 51	24.8 52.5	24.8 55
2	20.9 34	21.8 38	23.5 40	24.3 40.5	24.3 39.5	24.3 37	24.3 36.5	24.3 38	24.3 39	24.3 41.5	24.3 44
1	21.4 25	22.3 29	23.6 29	24.3 31	24.3 30	24.3 30	24.3 30	24.3 31.5	24.3 30.5	23.1 30	21.8 29
0	21.5 21	22.5 23	23.5 26	24.3 26.5	24.3 27	24.3 28	24.3 28	24.3 27	24.3 27	23.1 25	21.7 25
-1	21.3 21	22.4 23	23.6 24.5	24.3 23	24.3 23	24.3 26	24.3 25	24.3 25	24.3 26	22.8 23	21.4 22
-2	21.2 15.5	22.3 19	23.3 18	24.3 18	24.3 19	24.3 19	24.3 20	24.3 20	24.3 19.5	22.1 17	21.2 17
-3	21 5	21.4 6	22.2 9	23.4 10	24.3 11	24.3 11	24.3 12	24.3 11	24.3 12	21.2 11	20.9 11
-4		20.9 -3	21.1 -3	21.7 4	24.3 7.5	24.3 6.5	24.3 6.5	24.3 6.5	24 7	20.8 7	20.8 55
-4 $\frac{1}{4}$		20.9 -4	21 -4	21.5 0	24.3 5.5	24.3 6	24.3 6.5	24.3 6.5	23.6 6	20.7 6	20.7 6

VERTICAL STATIONS →

TEST No. - 1A
SERIES II

MACH. No. 5

TABLE I

BAROMETRIC PRESS = 14.4218 in Hg

$P_1 = 24.3 \text{ LB/IN}^2 \text{ AB}$

$P_2 = 20.7 \text{ LB/IN}^2 \text{ AB}$

TEMP. 380 °F

HORIZONTAL STATIONS →

STATIONS	-1 3/4	-1 1/2	-1 1/4	-1	-1/2	0	1/2	1	2	3	3 1/2	4	4 1/4	4 1/2
	P_3	P_3	P_3	P_3	P_3	P_3	P_3	P_3	P_3	P_3	P_3	P_3	P_3	P_3
1 1/2	-	-	-	20.82	21.42	21.32	21.22	20.82	-	-	-	20.82	20.82	20.82
1	20.62	20.82	21.02	21.12	21.42	21.52	21.52	21.22	20.82	20.42	-	20.82	20.82	20.82
1/2	20.42	20.82	21.02	21.12	21.22	21.22	21.02	20.82	20.42	20.42	-	20.82	20.82	20.82
0	21.22	21.02	21.32	21.42	21.52	21.52	21.22	21.02	20.82	20.42	20.42	20.82	20.82	20.82
-1	22.32	21.52	21.32	21.22	21.12	21.02	20.82	20.82	20.42	20.42	20.42	20.82	20.82	20.82
-2	22.42	21.42	21.22	21.12	21.02	20.82	20.82	20.82	20.42	20.42	20.42	20.82	20.82	20.82
-2 1/2	21.32	21.22	21.32	21.42	21.52	21.52	21.22	21.02	20.82	20.42	20.42	20.82	20.82	20.82
-2 3/4	-	21.22	21.42	21.52	21.52	21.22	21.02	20.82	20.42	20.42	20.42	20.82	20.82	20.82

VERTICAL STATIONS ↑

TEST No: - I
SERIES II

MACH No. 5

TABLE 2.

BAROMETRIC PRESS = 14.318/in²

$P_1 = 24.3$ LB./IN² Ab.

$P_2 = 70.7$ LB./IN² Ab.

TEMP 380°F.

STATIONS	-3 3/4	-3 1/2	-3 1/4	-3	-2	-1	0	1	2	3	3 1/4
	$\frac{P_1}{P_3}$	$\frac{P_1}{P_3}$	$\frac{P_1}{P_3}$	$\frac{P_1}{P_3}$	$\frac{P_1}{P_3}$	$\frac{P_1}{P_3}$	$\frac{P_1}{P_3}$	$\frac{P_1}{P_3}$	$\frac{P_1}{P_3}$	$\frac{P_1}{P_3}$	$\frac{P_1}{P_3}$
2 3/4	.995-.027	.99	.963-.232	.984-.462	.985-.76	.969-.872	.980-.995	.987	.982	.982-.91	.982
2 1/2	.995-.027	.982-.105	.979-.49	.987-.747	.988	.982-.995	.995	.995	.995	.982-.995	.982
2	.99	.949-.33	.88	.852-.995	.852	.852-.995	.995	.995	.995	.982-.995	.982
1	.967-.207	.925-.462	.877-.817	.852-.995	.852	.852-.995	.995	.995	.995	.982-.995	.982
0	.967-.24	.919-.52	.88	.852-.995	.852	.852-.995	.995	.995	.995	.982-.995	.982
-1	.9711-.82	.924-.69	.877-.817	.852-.995	.852	.852-.995	.995	.995	.995	.982-.995	.982
-2	.9777-.14	.928-.462	.885-.74	.852-.995	.852	.852-.995	.995	.995	.995	.982-.995	.982
-3	.986-.082	.965-.2	.9325-.43	.894-.765	.852	.852-.995	.995	.995	.995	.982-.995	.982
-4		.97	.955-.987	.912	.852-.995	.852	.852-.995	.995	.995	.982-.995	.982
-4 1/4		.99	.955-.985	.909	.852-.995	.852	.852-.995	.995	.995	.982-.995	.982

TEST NO: - 1A
SERIES II

MACH. No.

S

TABLE 2

BAROMETRIC PRESS = 14.42

$P_1 = 24.38 / \text{IN}^2 \text{ AB}$

$P_2 = 20.718 / \text{IN}^2 \text{ AB}$

TEMP. 380. °F

STATIONS	-1 3/4	-1 1/2	-1 1/4	-1	1/2	0	1/2	1	2	3	3 1/2	4	4 1/4	4 1/2
	P_1/P_2	P_1/P_2	P_1/P_2	P_1/P_2	P_1/P_2	P_1/P_2	P_1/P_2	P_1/P_2	P_1/P_2	P_1/P_2	P_1/P_2	P_1/P_2	P_1/P_2	P_1/P_2
1 1/2	S	S	S	974	975	973	975	974	975	S	S	974	974	974
1	S	974	975	974	975	973	975	974	975	S	S	974	974	974
1/2	S	974	975	974	975	973	975	974	975	S	S	974	974	974
0	974	974	975	974	975	973	975	974	975	S	S	974	974	974
-1	974	974	975	974	975	973	975	974	975	S	S	974	974	974
-2	974	974	975	974	975	973	975	974	975	S	S	974	974	974
-2 1/2	974	974	975	974	975	973	975	974	975	S	S	974	974	974
-2 3/4	974	974	975	974	975	973	975	974	975	S	S	974	974	974

[illegible]

SERIES II	TEST:-1a	TABLE :-3
1	2	3
4	5	6
7	8	9
10	11	12
13	14	15
16	17	18
19	20	21
22	23	24
25	26	27
28	29	30
31	32	33
34	35	36
37	38	39
40	41	42
43	44	45
46	47	48
49	50	51
52	53	54
55	56	57
58	59	60
61	62	63
64	65	66
67	68	69
70	71	72
73	74	75
76	77	78
79	80	81
82	83	84
85	86	87
88	89	90
91	92	93
94	95	96
97	98	99
100	101	102
103	104	105
106	107	108
109	110	111
112	113	114
115	116	117
118	119	120
121	122	123
124	125	126
127	128	129
130	131	132
133	134	135
136	137	138
139	140	141
142	143	144
145	146	147
148	149	150
151	152	153
154	155	156
157	158	159
160	161	162
163	164	165
166	167	168
169	170	171
172	173	174
175	176	177
178	179	180
181	182	183
184	185	186
187	188	189
190	191	192
193	194	195
196	197	198
199	200	201
202	203	204
205	206	207
208	209	210
211	212	213
214	215	216
217	218	219
220	221	222
223	224	225
226	227	228
229	230	231
232	233	234
235	236	237
238	239	240
241	242	243
244	245	246
247	248	249
250	251	252
253	254	255
256	257	258
259	260	261
262	263	264
265	266	267
268	269	270
271	272	273
274	275	276
277	278	279
280	281	282
283	284	285
286	287	288
289	290	291
292	293	294
295	296	297
298	299	300
301	302	303
304	305	306
307	308	309
310	311	312
313	314	315
316	317	318
319	320	321
322	323	324
325	326	327
328	329	330
331	332	333
334	335	336
337	338	339
340	341	342
343	344	345
346	347	348
349	350	351
352	353	354
355	356	357
358	359	360
361	362	363
364	365	366

[illegible]

SERIES II **TEST: -1**

TABLE :- 4

[illegible]

$$A = \eta^{\frac{1}{2}} \sin \alpha \frac{f da}{f v}$$

SERIES II TEST:- 1A.

TABLE :- 4

[illegible]

$$A = \eta_2 \sin \alpha \frac{f da}{f v}$$

SERIES II TEST:-1 TABLE:-5

[illegible]

$$A = \frac{1}{2} \sin \alpha \frac{f \, d\alpha}{f \, d\alpha}$$

SERIES II TEST:- 1A. TABLE:- 5

[illegible]

$$A = \frac{1}{2} \sin \frac{\pi}{5}$$

Specimen Tables of Observed and Derived Results

Series 3 (Group 3).

TABLE OF OBSERVED READINGS OF PRESSURE + ANGLE.

GROUP: - 3
SERIES III

BAROMETRIC PRESS = 14.45 lb/in^2
 $P_2 = \text{LB/IN}^2 \text{ AB.}$

$P_1 = 44 \text{ LB/IN}^2 \text{ AB.}$

TEMP.

STATIONS	-2 3/4		-2 1/2		-2 1/4		-2		-1		0		1/2		3/4		1		1 1/4		1 1/2		VERTICAL STATIONS			
	P_3	α	P_3	α	P_3	α	P_3	α	P_3	α	P_3	α	P_3	α	P_3	α	P_3	α	P_3	α	P_3	α	P_3	α	P_3	α
23.15	27.5	111	28.1	124	28	131	27.9	135	27.7	146	27.6	159	25.9	168	24.7	174	24	177	23.2	181	-	-				
20.75	27.1	108	28.1	122	27.9	131	27.9	135	27.6	147	27.4	160	25	169	23.5	172	22.4	178	21.3	181	20.9	184				
18.08	24.2	101	27.9	115	28.1	126	28.1	134	28	148	28.3	159	26	167	24	172	21.9	176	20	184	19.3	183				
15.25	23.9	101	27.4	117	27.9	126	27.7	133	27.3	147	27.3	160	24.1	169	21.8	173	19	177	18	182	16.1	186				
12.39	21.7	100	26	112	27.4	124	27.3	132	26.9	146	27	159	23.9	169	21.4	173	18	177	15.2	180	14	182				
10.39	18	95	24	106	26.9	123	27	131	26.5	146	26.7	159	23.1	169	20.8	173	17.3	178	13.8	183	12.7	183				
8	13	94	18.9	102	24.2	115	26.3	127	26	147	26.3	159	23.2	169	21	173	18.3	177	15	181	12.8	183				
5	7.1	95	12	103	17.1	111	21.6	119	25.2	145	25.1	158	24.2	168	22	173	20.4	175	17.9	178	15.6	180				
1	8	93	14.7	106	20.5	122	22.9	132	21.7	152	22.9	156	22.8	162	22	165	21.8	167	20.7	173	19.1	176				

RATIO OF BACK PRESSURE AND CONVERTED ANGLE PRESSURE READING.

GROUP: 3
SERIES III

TABLE I.

BAROMETRIC PRESS = 14.45 lb/in²
P_f = LB/IN² AB. TEMP.

P_f = 44.8 LB/IN² AB.

STATIONS	-2 3/4	-2 1/2	-2 1/4	-2	-1	0	1/2	3/4	1	1 1/4	1 1/2	1 3/4	VERTICAL STATIONS.											
	$\frac{P_2}{P_5} \propto \frac{P_2}{P_5}$	$\frac{P_2}{P_5} \propto \frac{P_2}{P_5}$	$\frac{P_2}{P_5} \propto \frac{P_2}{P_5}$	$\frac{P_2}{P_5} \propto \frac{P_2}{P_5}$	$\frac{P_2}{P_5} \propto \frac{P_2}{P_5}$	$\frac{P_2}{P_5} \propto \frac{P_2}{P_5}$	$\frac{P_2}{P_5} \propto \frac{P_2}{P_5}$	$\frac{P_2}{P_5} \propto \frac{P_2}{P_5}$	$\frac{P_2}{P_5} \propto \frac{P_2}{P_5}$	$\frac{P_2}{P_5} \propto \frac{P_2}{P_5}$	$\frac{P_2}{P_5} \propto \frac{P_2}{P_5}$	$\frac{P_2}{P_5} \propto \frac{P_2}{P_5}$	$\frac{P_2}{P_5} \propto \frac{P_2}{P_5}$											
	.898	.69	.888	.49	.889	.45	.892	.34	.894	.21	.911	.12	.936	.0	.955	.3	.972	.1	—	—	—	—	—	—
	.848	.72	.826	.58	.833	.49	.823	.45	.838	.33	.842	.20	.894	.11	.928	.8	.957	.2	.985	.1	.995	.4		
	.839	.79	.768	.65	.763	.54	.763	.46	.764	.32	.769	.21	.805	.13	.847	.8	.881	.4	.945	.4	.961	.2		
	.75	.79	.686	.63	.679	.54	.681	.47	.689	.33	.689	.20	.743	.11	.792	.7	.86	.3	.888	.2	.939	.6		
	.741	.80	.663	.68	.641	.56	.642	.48	.65	.39	.648	.21	.7	.11	.729	.7	.827	.3	.902	.0	.944	.2		
	.766	.85	.647	.74	.6	.57	.599	.49	.607	.34	.602	.21	.66	.11	.709	.7	.781	.2	.878	.3	.912	.3		
	.82	.86	.674	.78	.58	.65	.55	.53	.555	.33	.56	.21	.596	.11	.633	.7	.685	.3	.762	.1	.822	.3		
	.9	.85	.738	.77	.65	.69	.53	.61	.49	.35	.492	.22			.535	.7	.56	.5	.602	.2	.646	.0		
	.688	.87	.53	.74	.448	.58	.45	.48	.418	.28	.415	.24	.45	.18	.425	.15	.426	.13	.438	.7	.46	.4		

M₂₀ ↓

.5

.6

.7

.8

.9

.97

1.06

1.178

1.359

READINGS OF CONVERTED PRESSURE RATIO AND LOCAL EFFICIENCY

GROUP: -3

TABLE II

BAROMETRIC PRESS 14.45 lb/in²

SERIES III

 $P_1 = 44.45 \text{ lb/in}^2 \text{ AB.}$ $P_2 = \text{LB/IN}^2 \text{ AB}$

TEMP

STATIONS	$-2\frac{3}{4}$		$-2\frac{1}{2}$		$-2\frac{1}{4}$		-2		-1		0		$\frac{1}{2}$		$\frac{3}{4}$		1		$1\frac{1}{4}$		$1\frac{1}{2}$		\rightarrow VERTICAL STATIONS			
	$\frac{P_2}{P_3}$	η	$\frac{P_2}{P_3}$	η	$\frac{P_2}{P_3}$	η	$\frac{P_2}{P_3}$	η	$\frac{P_2}{P_3}$	η	$\frac{P_2}{P_3}$	η	$\frac{P_2}{P_3}$	η	$\frac{P_2}{P_3}$	η	$\frac{P_2}{P_3}$	η	$\frac{P_2}{P_3}$	η	$\frac{P_2}{P_3}$	η	$\frac{P_2}{P_3}$	η	$\frac{P_2}{P_3}$	η
5	.818	.665	.883	.766	.888	.734	.889	.733	.892	.718	.894	.697	.911	.58	.936	.42	.955	.29	.972	.175	—	—				
6	.818	.72	.828	.82	.833	.795	.833	.775	.838	.77	.842	.752	.894	.5	.928	.335	.957	.2	.985	.06	.995	.02				
7	.839	.58	.768	.843	.763	.884	.763	.884	.766	.872	.759	.9	.805	.717	.857	.552	.881	.42	.945	.18	.961	.126				
8	.75	.74	.688	.947	.679	.977	.681	.972	.684	.942	.689	.942	.743	.764	.712	.604	.86	.388	.858	.297	.939	.151				
9	.741	.629	.643	.84	.641	.91	.642	.9	.65	.88	.648	.885	.7	.736	.729	.66	.827	.412	.902	.228	.944	.12				
97	.766	.484	.647	.77	.6	.895	.591	.898	.607	.894	.602	.895	.66	.738	.704	.63	.781	.45	.878	.235	.912	.166				
106	.82	.311	.674	.612	.58	.81	.55	.89	.555	.883	.55	.89	.595	.78	.633	.711	.685	.585	.762	.427	.823	.307				
117B	.9	.139	.738	.396	.615	.616	.539	.77	.4818	.89	.4894	.88	.5016	.87	.5577	.785	.56	.722	.602	.646	.646	.562				
139	.688	.386	.527	.64	.4926	.8	.4065	.88	.421	.848	.4065	.88	.4065	.88	.476	.86	.4186	.855	.432	.826	.4554	.776				

AREA		STATION
Δa		
.25	o	$2\frac{1}{2}$
.25	o	$2\frac{1}{4}$
.25	o	2
.25	o	$1\frac{3}{4}$
.25	o	$1\frac{1}{2}$
.25	o	$1\frac{1}{4}$
.25	o	1
.25	o	$\frac{3}{4}$
.375	o	$\frac{1}{2}$
.75	o	0

1	o	-1
.625	o	-2
.25	o	$-2\frac{1}{4}$
.25	o	$-2\frac{1}{2}$
.25	o	$-2\frac{3}{4}$

FLOW AREA DIAGRAM FOR CENTRE-LINE TRAVERSE.

SERIES III

FIG. 69

SERIES II GROUP-3

TABLE 4, K and M_{18}

VERTICAL STATIONS

[illegible]

$$A = \eta^{\frac{1}{2}} \sin \alpha \frac{f da}{f v}$$

Appendix 3.

An examination of the variation of loss coefficients with Mach number and Reynolds number with particular reference to the existence of critical values of these parameters.

0.6
0.5
0.4
0.3
0.2
0.1
0

ENTHALPY LOSS COEFFICIENTS - SERIES S.1.

ARMSTRONG $\epsilon_h = \gamma_h$ LOW MACH. No.

AINLEY $\epsilon_h = \gamma_h$
LOW MACH. No.

SERIES S.1
MACH.
No. 0.8

ϵ_t

ϵ_h

REYNOLDS NUMBER (BLADE CHORD)

1×10^5

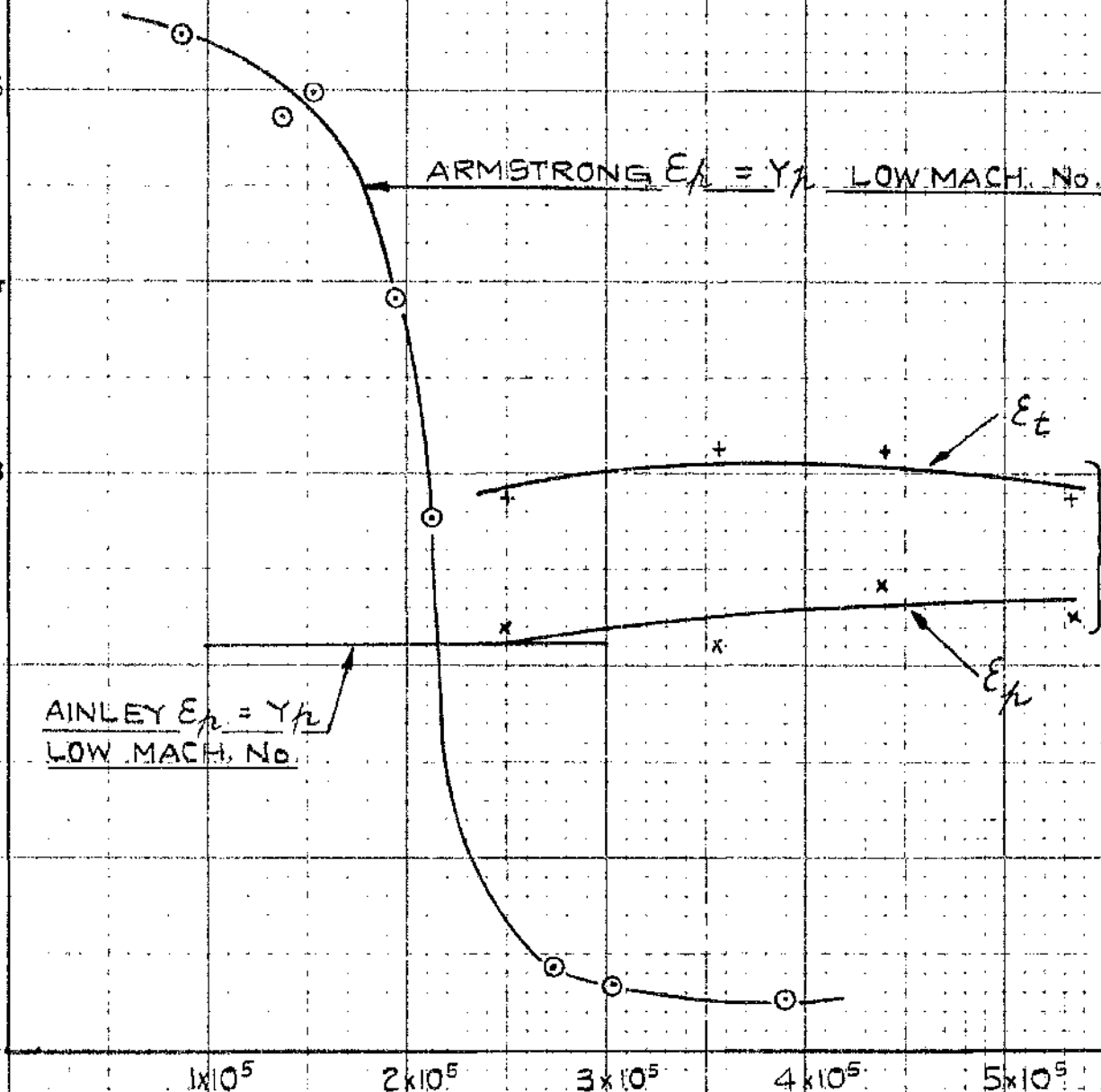
2×10^5

3×10^5

4×10^5

5×10^5

FIG. 70



TOTAL HEAD PRESSURE LOSS COEFFICIENT Y

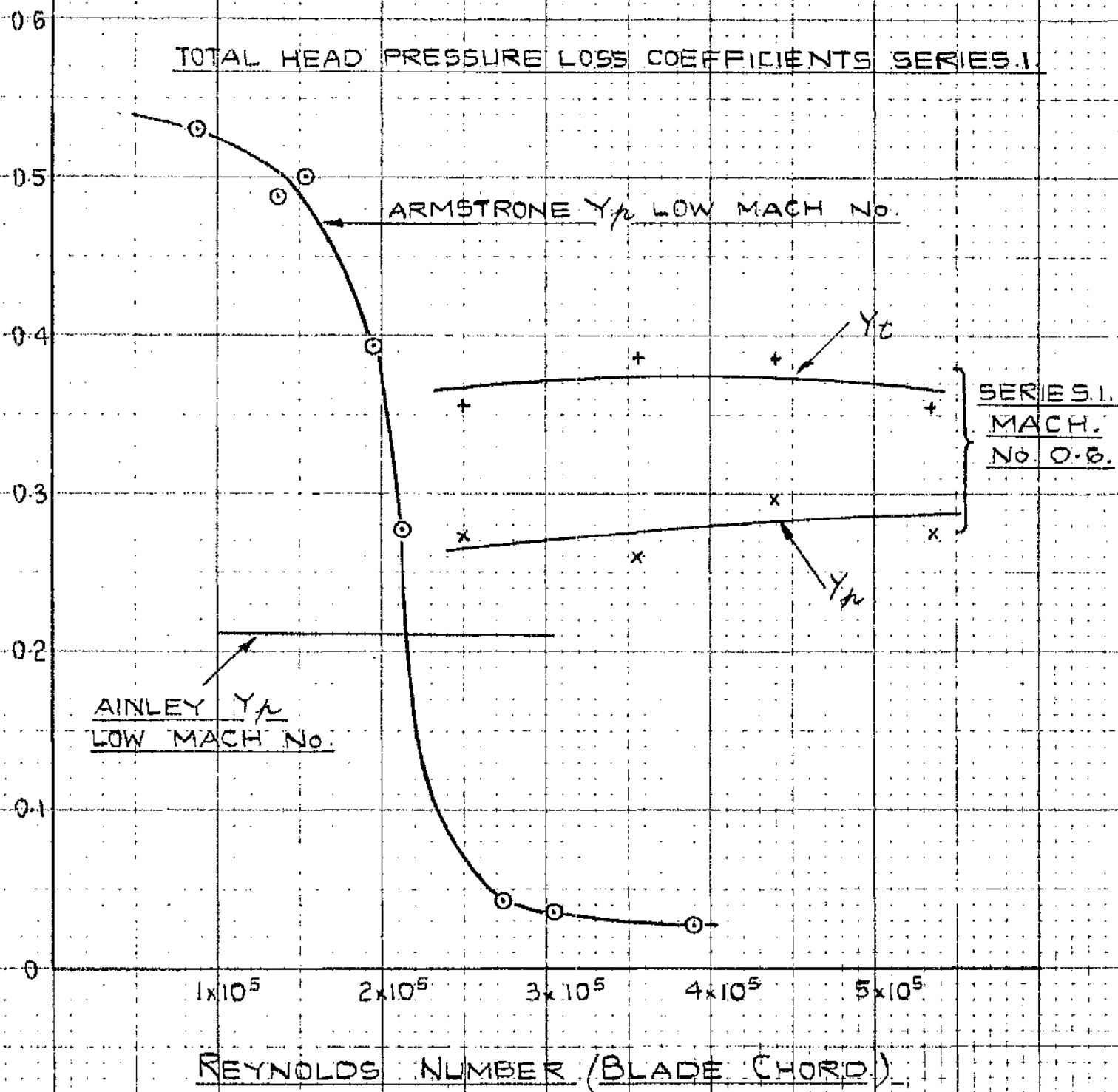


FIG. 71

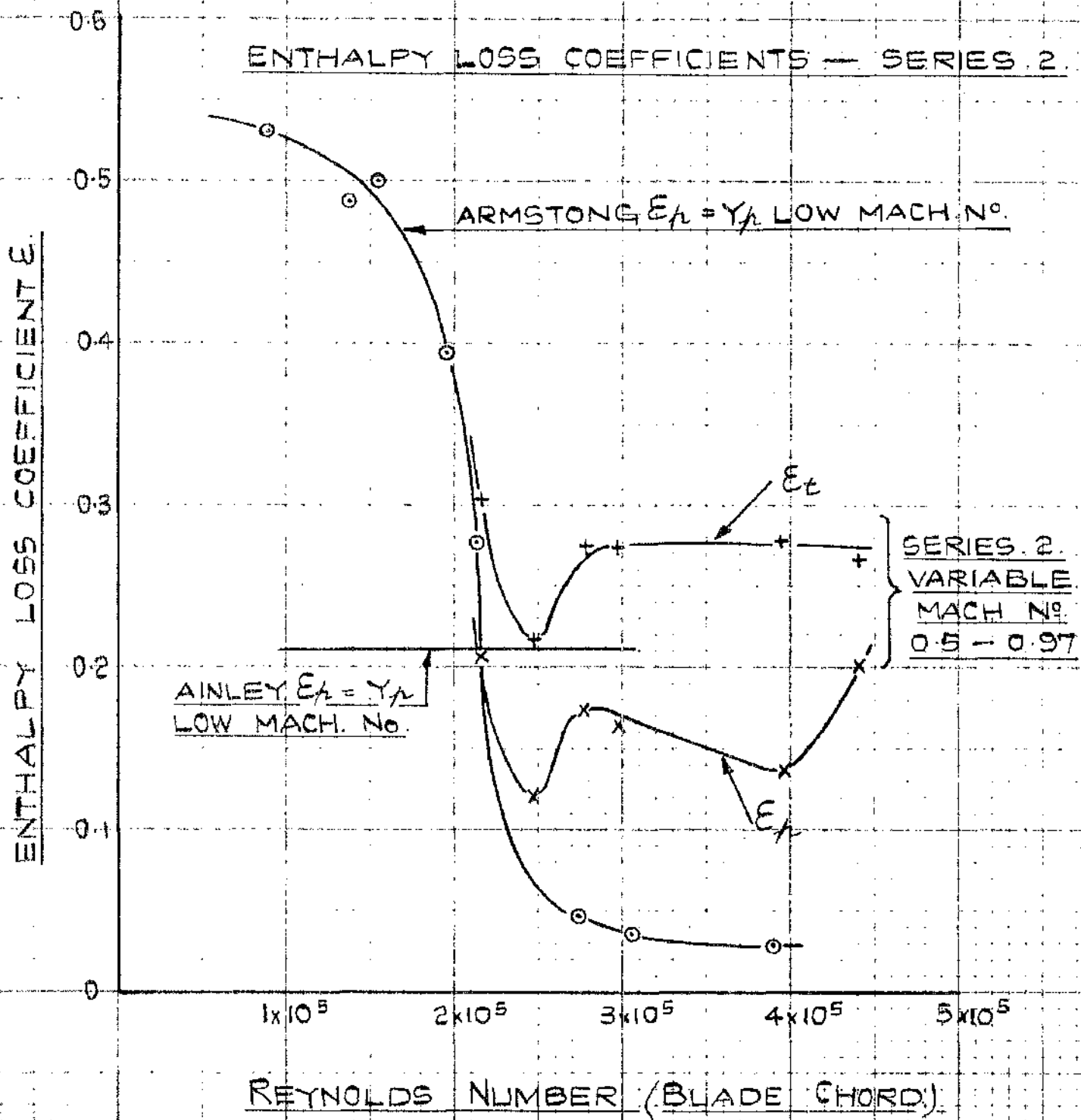


FIG. 72

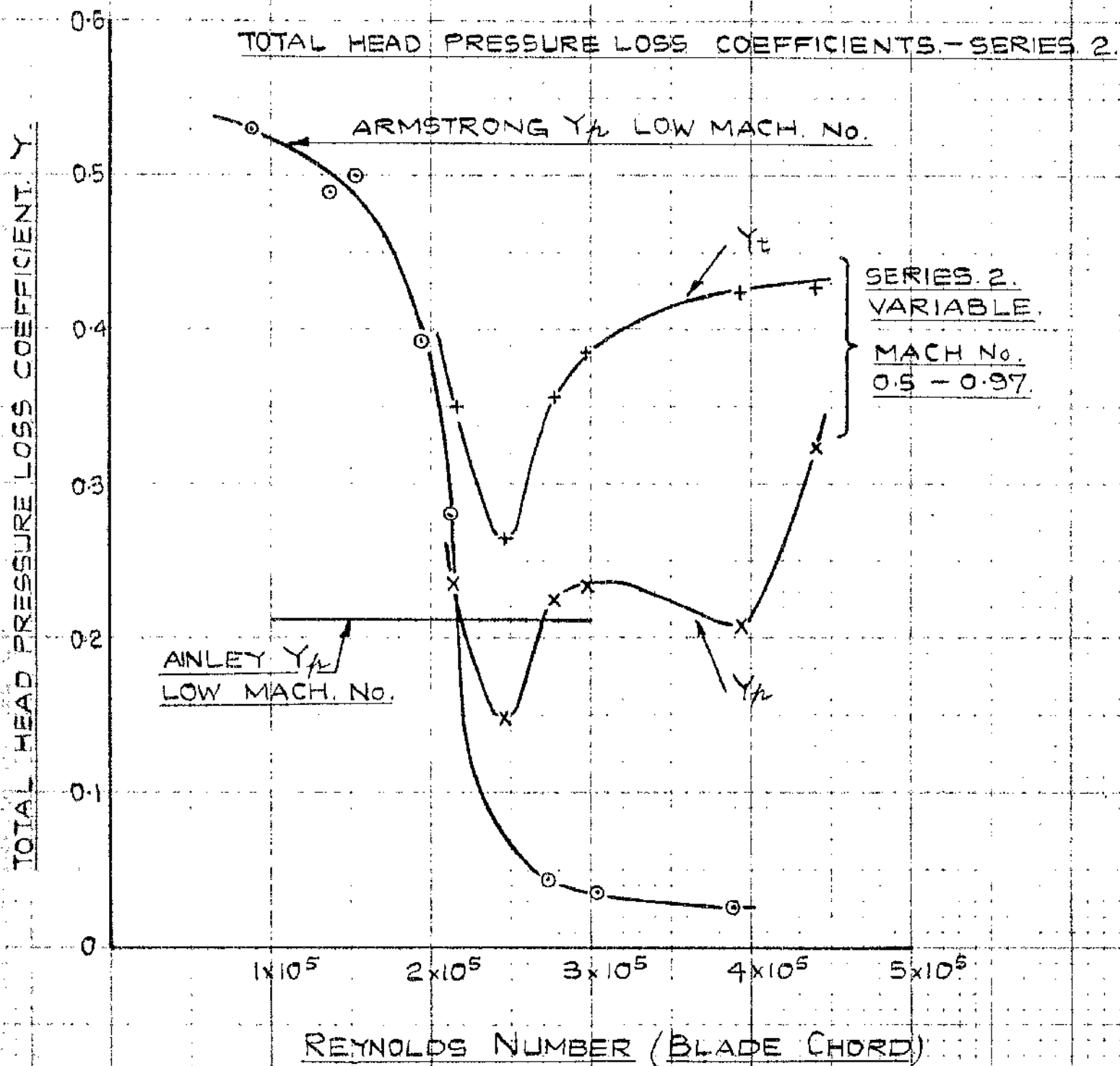


FIG. 73

Appendix 3.

An examination of the variation of loss coefficients with Mach number and Reynolds number with particular reference to the existence of critical values of these parameters.

A particular study of the variation of loss coefficients at high Reynolds number has been made by Armstrong⁴⁰, Ainley⁴¹ and Kearton⁴². To compare the writer's work with theirs, the results from test series 1 and 2 are given in the accompanying tables along with details of the geometry of the impulse blade used in the tests. The efficiencies of expansion for the blade have been converted to enthalpy loss coefficients (ξ) and to total head pressure loss coefficients (γ) by the relationships derived in Part 1. The coefficients are given as profile or centre line coefficients (ξ_p and γ_p) and as total loss coefficients (ξ_t and γ_t), where the total loss coefficients include the profile and secondary losses. The test Reynolds numbers (previously based on a length dimension of one foot) have been calculated on a basis of blade chord and on a characteristic dimension equal to four times the hydraulic mean depth at the outlet throat section of the blade passage.

For test series 1, where the outlet Mach number is constant at 0.6, ξ_p and ξ_t , and γ_p and γ_t are plotted in figures 70 and 71 respectively to a base of chord Reynolds number. The corresponding results for series 2, where the Mach number varies from 0.5 to 0.97 are given in figures 72 and 73.

Comparison with Armstrong's work.

In Armstrong's work air tests at low velocities were carried out on a cascade of large impulse blades. The blades were designed for good incidence characteristics with a well rounded inlet edge.

In the tests the air inlet angle was maintained constant at 35 degrees (from the axial direction) and total head profile pressure loss coefficients were obtained over a range

Geometry of the impulse blade used in test series 1 & 2 (see fig 43) pitch 0.65 ins; height 0.65 ins; blade chord = axial chord, 0.75 ins; hydraulic mean depth at the outlet throat section of the blade, 0.075 ins; hydraulic mean diameter 0.30 ins; aspect ratio 0.866; pitch/chord ratio 0.866; thickness to chord ratio 0.615; inlet and outlet angle 20° ; nominal fluid deflection 140° ; opening to pitch at blade outlet = 0.30.

Table 1.

Test results for the impulse blade from series 1 Constant Mach number 0.6.

Test No.	1A.	2A.	3A.	4A.
$R_n (L = 1ft) \times 10^6$	3.99.	5.27.	7.041.	8.55.
$R_n (\text{chord}) \times 10^5$	2.50.	3.58.	4.40.	5.35.
$R_n (\text{H.M.D.}) \times 10^5$	1.00.	1.43.	1.76.	2.14.
ζ_p profile	0.820.	0.826.	0.805.	0.817.
ε_p profile	0.220.	0.210.	0.242.	0.223.
Y_p profile	0.272.	0.259.	0.298.	0.275.
Y_p profile (Ainley)	-----	0.212-----	-----	-----
ζ_t^{TOTAL}	0.778.	0.762.	0.762.	0.778.
$\varepsilon_t^{\text{TOTAL}}$	0.287.	0.312.	0.312.	0.287.
Y_t^{TOTAL}	0.354.	0.385.	0.385.	0.354.
Y_t^{TOTAL} (Ainley)	-----	0.628-----	-----	-----

Table 2.

Test results for the impulse blade from series 2 - variable Mach number.

Test no.	1A.	2A.	3A.	4A.	5A.	6A.
Mach No.	0.5	0.6	0.7	0.8	0.9	0.97.
R_N (L = 1ft) $\times 10^6$	3.46	3.96	4.45	4.77	6.28	7.04
R_N (chord) $\times 10^5$	2.16	2.48	2.78	2.98	3.94	4.40
R_N (H.M.D.) $\times 10^5$	0.86	0.99	1.12	1.20	1.57	1.76
ζ_p profile.	0.83	0.894	0.854	0.860	0.881	0.832
ϵ_p profile.	0.204	0.120	0.171	0.164	0.133	0.200
Y_p profile.	0.236	0.148	0.225	0.232	0.203	0.322
Y_p profile. (Ainley)	-----	-----	0.212	-----	-----	-----
ζ_t TOTAL	0.766	0.821	0.785	0.785	0.783	0.750
ϵ_t TOTAL	0.302	0.215	0.271	0.271	0.277	0.266
Y_t TOTAL	0.350	0.265	0.356	0.383	0.422	0.429
Y_t TOTAL (Ainley)	-----	-----	0.628	-----	-----	-----

of chord Reynolds number varying from 0.8×10^5 to 4.0×10^5 . The average air deflection in the tests was approximately 68° , and since the tests were performed at low Mach numbers the enthalpy and pressure loss coefficients may be assumed identical.

The results are shown in figures 70 to 73 and indicate an abrupt rise in loss coefficients as the Reynolds number is reduced. The critical region lies between 1.8 and 2.3×10^5 , an average value of approximately 2.0×10^5 . In test series 1 the writer's Reynolds numbers are greater than 2.5×10^5 (figures 70 and 71) but in series 2 (figures 72 and 73) where the lower Reynolds numbers are approaching Armstrong's critical value, the loss coefficients rise sharply confirming Armstrong's result. Below the critical Reynolds number Armstrong also found that the boundary layer growth on the convex side of the blade surface was of such a magnitude that the blade channel acted like a convergent nozzle.

Ainley's loss correlation.

Ainley and Mathieson⁴¹ give the results of air cascade tests at low Mach numbers. For nozzle blades (fluid inlet angle \angle_1 zero) and for impulse blades (fluid outlet angle $\angle_2 = -$ fluid inlet angle \angle_1), they correlate the profile loss coefficient at zero incidence with the pitch to chord ratio (P/c) in the form of a series of graphs each corresponding to a different fluid outlet angle. The results are for a thickness to chord ratio (t/c) of 0.2.

A relationship is given between the opening to pitch ratio at blade outlet and the fluid outlet angle. For the writer's blade this gives a fluid outlet angle very close to the nominal inlet angle of 20° . Hence for comparison with Ainley's data, the impulse blade of series 1 and 2 has been assumed to have fluid inlet and outlet angles of 20° from the tangential direction, giving a fluid deflection of 140° .

Hence at $t/c = 0.2$, $P/c = 0.866$ and $\angle_2 = 70^\circ$ (axial direction), Ainley gives $Y_p = 0.170$

and for this impulse blade where $t/c = 0.25$

$$Y_p = 0.170 \left(\frac{0.25}{0.2} \right)^{-1} = 0.212.$$

For the secondary loss in the blade passage Ainley gives

$$Y_s = h \left(\frac{C_L}{P/c} \right)^2 \frac{\cos^2 \alpha_2}{\cos^3 \alpha_m}$$

where $\frac{C_L}{P/c} = 2 (\tan \alpha_1 - \tan \alpha_2) \cos \alpha_m$

$$\tan \alpha_m = \frac{\tan \alpha_1 + \tan \alpha_2}{2}$$

and h , an empirical coefficient is given in graphical form as a function of

$$\left(\frac{A_2}{A_1} \right)^2 \times \left(1 + \frac{D - h}{D + h} \right)^{-1}$$

Here A_1 is the inlet annulus area $\times \cos \alpha_1$

A_2 " " outlet " " $\times \cos \alpha_2$

D is the mean diameter of the blade and h is the blade height.

Hence for the writer's blade :- $\alpha_m = 0$.

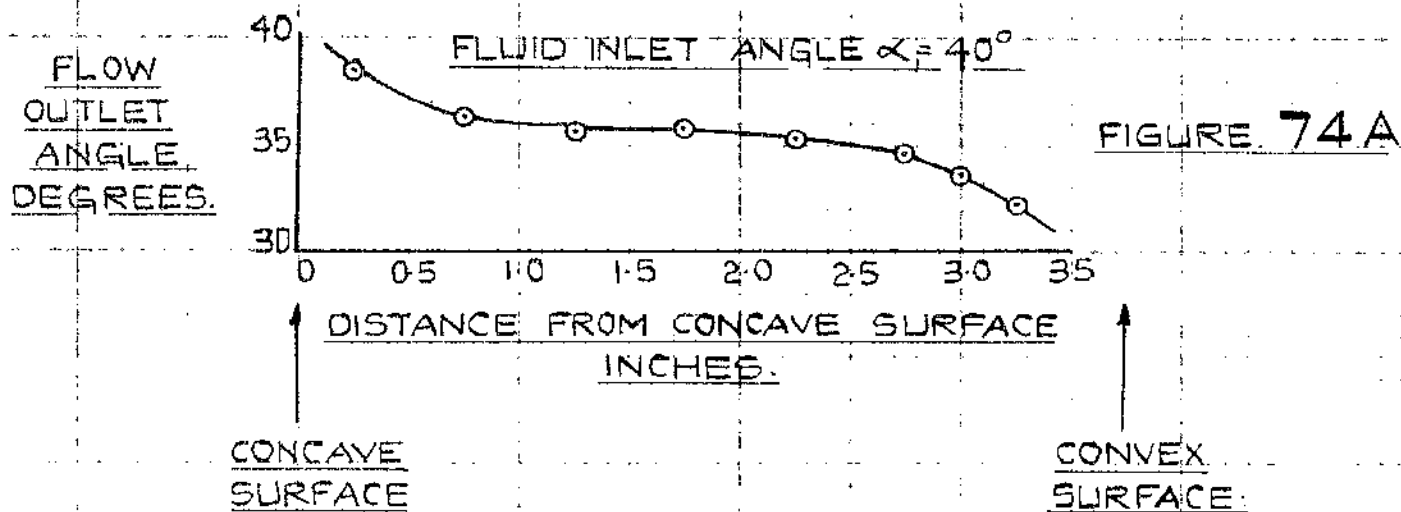
$$\left(\frac{C_L}{P/c} \right)^2 \times \frac{\cos^2 \alpha_2}{\cos^3 \alpha_m} = \left[2 (2 \tan 70^\circ) \right]^2 \cos^2 70^\circ = 14.10$$

and h is a function of $\left(1 + \frac{D - h}{D + h} \right)^{-1}$

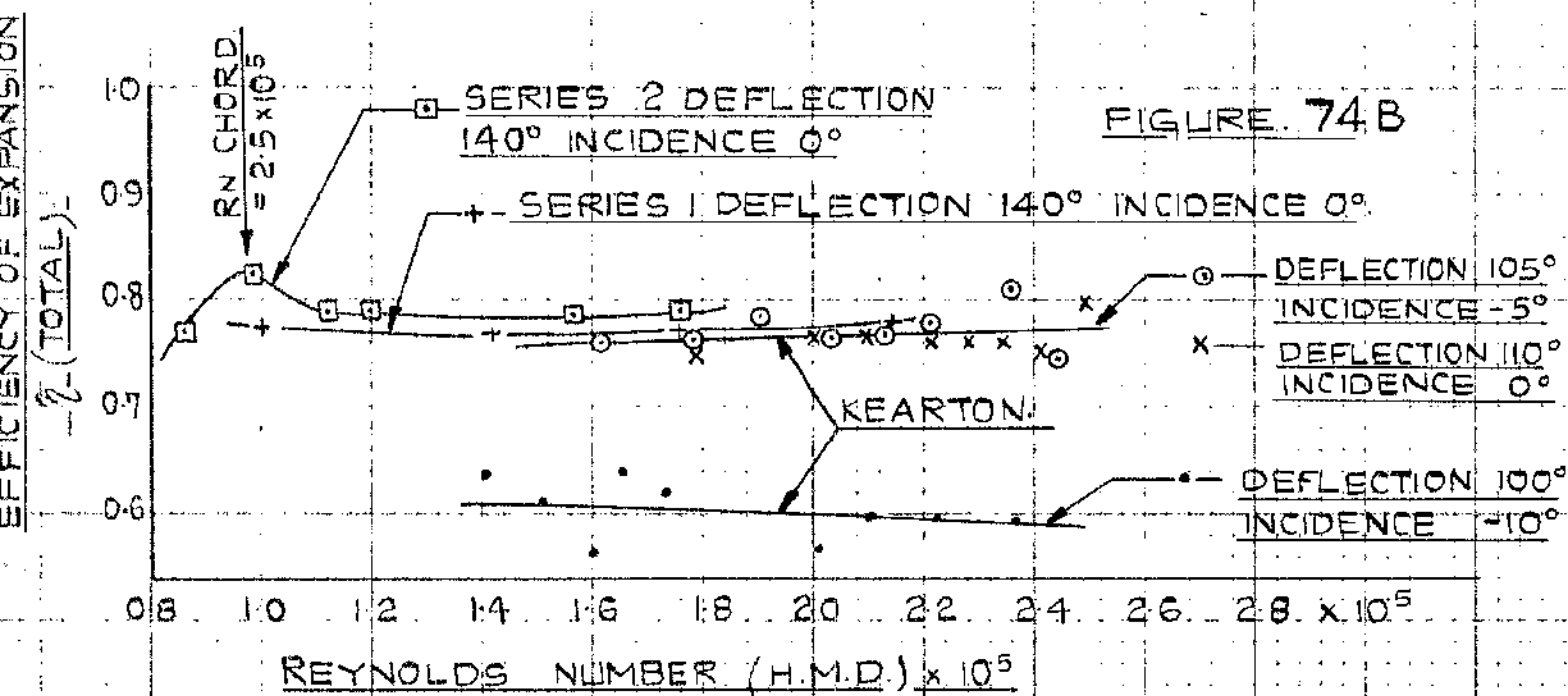
Using values of mean diameter from 10 in. to 40 in. and the blade height of 0.65 in., the quantity $\left(1 + \frac{D - h}{D + h} \right)^{-1}$ varies from 0.534 to 0.506. An average value of 0.52 has been used here, for which Ainley gives $h = 0.0295$.

Hence $Y_s = 0.0295 \times 14.1 = 0.416$ and therefore the estimated value of the total loss using Ainley's correlation is

$$Y_t = 0.416 + 0.212 = 0.628.$$



FLUID DIRECTION AT IMPULSE BLADE OUTLET KEARTON.



EFFICIENCIES OF PROFILE TYPE IMPULSE BLADES.

FIG. 74

In Ainley's cascade tests the operating Mach numbers were less than 0.5 and the chord Reynolds number varied from 1×10^5 to 3×10^5 . Ainley suggested that in this Reynolds number range there is little variation in loss coefficient but proposes however that, below his average Reynolds number of 2.0×10^5 , a correction should be applied to the overall efficiency of the turbine by assuming that the stage losses are proportional to $R_N^{-0.2}$.

Ainley's estimates of profile and total loss coefficient are shown in tables 1 and 2 and in figures 70 to 73. The prediction for profile loss corresponds favourably with the writer's value but for the total loss coefficient Ainley's method greatly overestimates the loss in this "profile type" of steam turbine impulse blade.

Comparison with Kearton's work.

Kearton⁴² has examined the flow and loss characteristics for model profile type impulse blades at high Reynolds numbers using air as the working fluid. The blade had inlet and outlet angles of 35° (from the tangential direction) and the tunnel was arranged so that tests could be made with air inlet angles of 30° , 35° , 40° and 45° . Direct measurements were made of the tangential blade force, by connecting the blade cascade to weights suspended from a pulley. Total head pressure and fluid direction measurements were made at a number of stations along the blade pitch at the mid height of the blade. Kearton found that, at an inlet angle of 45° , the average outlet angle was equal to the nominal outlet angle of 35° . For the other three tunnel settings the average outlet angle was slightly greater than 35° showing a positive deviation. A typical result is shown in figure 74 A. In the pitchwise direction the outlet angle is greatest at the concave surface (positive deviation) and is least at the convex surface (negative deviation).

Like Armstrong, Kearton also observed the greatest loss in total head pressure at the convex side of the blade passage.

The variation in fluid outlet angle observed by Kearton is very similar in form to that obtained by the writer and shown in figures 53 and 54 (test 1a and 4a). The maximum positive or negative deviation about the mean efflux angle for the writer's blade is however greater than that observed in Kearton's tests. This is because in Kearton's experimental rig the blades adjacent to the blade passage under test were also passing air, whereas in the writer's apparatus the adjacent blades do not run full of steam. (see page 117). From figures 53 and 54 it will also be observed that the biggest loss region is on the convex side of the blade.

From the measured blade force, the air flow and assuming an average fluid outlet angle of 35° , blade velocity coefficients were calculated over a range of Reynolds number, based on the hydraulic mean diameter at the blade outlet. Kearton's results are shown in figure 74B. The velocity coefficients have been converted to efficiencies for comparison with the results from test series 1 and 2 which are also shown in the figure. When calculating the blade velocity coefficients Kearton made a correction for a small reaction effect obtained during the tests. In the writer's experiments the arrangement was such that no pressure drop occurs across the blade passage. Kearton's results apply therefore to the zero reaction stage while the writer's pertain to the zero pressure drop impulse stage.

Kearton's figures are for total loss in the blade passage at low air velocities. The lower curve corresponds to a fluid deflection of 100° and the upper curve to deflections of 105° - 110° . One would have expected the efficiency to decrease with increase in fluid deflection but the main factor here is probably incidence effects and not fluid deflection. Both Kearton's impulse blade and that

PROFILE LOSS
PROFILE LOSS AT $R_N = 1.5 \times 10^5$

3.0
2.5
2.0
1.5
1.0

— IMPULSE BLADES.

- - - REACTION BLADES.

0.5 1.0 1.5 2.0 $\times 10^5$
REYNOLDS NUMBER $\times 10^5$

VARIATION OF PROFILE LOSS
WITH REYNOLDS No. - CHESHIRE

FIG. 75

used in series 1 and 2 are the same form of "profile" blade, where the sharp inlet edge results in poor incidence characteristics. It is Kearton's zero incidence results therefore which should be compared with those of series 1 and 2 where the incidence is also zero. It will be noted from figure 74B that these results do compare favourably, bearing in mind that Kearton's figures are for low Mach numbers and for Reynolds numbers well above Armstrong's critical Reynolds number, while those of series 1 and 2 are for high Mach numbers and that some of the figures are in the region of the critical Reynolds number.

It is worthwhile at this point to summarize the limits within which the above results are applicable.

- (1). Armstrong's data applies to profile pressure loss coefficients. Low Mach number. Chord Reynolds number range $0.8 \times 10^5 - 4 \times 10^5$. Exhibits a critical Reynolds number at approximately 2×10^5 .
- (2). Ainley's data applies to profile and total loss coefficients. Mach numbers less than 0.5. No critical Reynolds number in the range $1 \times 10^5 - 3.5 \times 10^5$ (chord). Suggests that below a Reynolds number of 2×10^5 the turbine loss is proportional to $R_n^{0.2}$.
- (3). Kearton's data applies to total loss coefficients only. Low Mach number. Reynolds number based on hydraulic mean diameter but above Armstrong's critical Reynolds number.
- (4). Series 1. For profile and total loss coefficients. Mach number constant at 0.6. Reynolds number range $2.5 \times 10^5 - 5.35 \times 10^5$ (chord).
- (5). Series 2. For profile and total loss coefficients. Mach number range 0.5 - 0.97. Reynolds number range $2.16 \times 10^5 - 4.4 \times 10^5$ (chord).

In addition to the work quoted above some results on the variation of losses with Reynolds number are given by Cheshire⁴³ and by Soderburg³⁰. These are:-

- (6). Cheshire. Cheshire's results are shown in figure 75.

They are for profile loss coefficients in the Reynolds number range $0.5 \times 10^5 - 2 \times 10^5$.

(7). Soderburg. Soderburg gives the following relationship for the variation in total loss coefficient with Reynolds number.

$$\xi = \left(\frac{10^5}{R_n}\right)^{0.25} \times \xi'$$

where ξ' is the total enthalpy loss coefficient at $R_n = 10^5$.

Appendix 3 - Summary.

Below a Reynolds number of 1×10^5 there seems to be general agreement that the loss coefficients rise. Above 1×10^5 on the other hand Ainley's results suggest that the coefficients remain constant, while Soderburg's indicate a continuous decrease. Cheshire's figures also exhibit a considerable decrease in coefficient as the Reynolds number rises above 1×10^5 . Armstrong's critical Reynolds number at 2×10^5 is confirmed by the results of series 2 for both profile and total loss coefficients at low Mach numbers. If this figure is used as the controlling Reynolds number parameter then Ainley's data, Cheshire's results and Soderburg's relationship would all confirm an increase in losses at Reynolds numbers below the critical value. Above 2×10^5 it would appear that, at low velocities, the losses are substantially constant. For example Ainley's data gives a constant loss coefficient, while Cheshire's results, in which the loss ratio curve flattens out as the Reynolds number approaches Armstrong's critical value, are not inconsistent with the losses remaining constant above 2×10^5 .

It will be noted that most of the loss coefficient results at high Reynolds numbers are obtained from tests at low Mach numbers. It has been suggested previously that a Mach number of 0.66 is a controlling parameter. Using a critical Reynolds number of 2×10^5 and a critical Mach number of 0.66 the following conclusions are consistent with most of the above data.

1. Below a Mach number of 0.66 the controlling parameter is the Reynolds number.

(a) below $R_n = 2 \times 10^5$ both the profile and total loss coefficients rise. (Ainley, Armstrong, Soderburg, Cheshire, Series 2).

(b) above $R_n = 2 \times 10^5$ both the profile and total loss coefficients remain substantially constant.

(Ainley, Armstrong, Series 1, Kearton, Cheshire).

2. Above a Mach number of 0.66 and above a Reynolds number of 2×10^5 .

- (a) the total enthalpy loss coefficient ξ_t remains constant while the total head pressure loss coefficient (Y_t) varies with Mach number. (Series 2).

For a constant enthalpy loss coefficient this variation in pressure loss coefficient is expected from the relationship.

$$Y = \xi \left(1 + \frac{\gamma}{2} M^2\right)$$

- (b) The profile enthalpy and total head pressure loss coefficients are both Mach number dependant.
-

Acknowledgments.

This research work was directed by Professor A.S.T. Thomson, D.Sc., Ph.D., A.R.C.S.T., M.I.C.E., M.I.Mech.E., whom the author respectfully thanks for the equipment and opportunity placed at his disposal.

Acknowledgment is also due to Dr. J.B.O. Sneeden, B.Sc., Ph.D., F.R.S.E., former principal lecturer in Mechanical Engineering and to Mr. A.M. Laird, B.Sc., A.R.C.S.T., M.I.Mech.E., principal lecturer in Applied Thermodynamics for their helpful guidance, advice and criticism during the progress of the work. The author also wishes to record his thanks to Professor A.W. Scott, B.Sc., Ph.D., A.R.C.S.T., M.I.Mech.E., M.I.Chem.E., for his suggestions and for the interest that he has taken in the work.



Appendix 2.


Series 1 ----- Page 2.

Series 2 ----- Page 33.

Series 3 (Groups 1 & 2)---- Page 84.



[Faint, illegible text, possibly bleed-through from the reverse side of the page.]



Series 1

Tests 2 - 4

and 2A - 4A




TABLE 1

77934 TEST 2

STATION	-3½	-3	-2	-1	0	1	2	3	3½
	$p_3 \propto$	$p_3 \propto$	$p_3 \propto$	$p_3 \propto$	$p_3 \propto$	$p_3 \propto$	$p_3 \propto$	$p_3 \propto$	$p_3 \propto$
	lbs/in ²	lbs/in ²	lbs/in ²	lbs/in ²	lbs/in ²	lbs/in ²	lbs/in ²	lbs/in ²	lbs/in ²
3	28.35 55	30.25 55.5	33.45 56	34.55 53	34.15 58	34.75 52	34.25 52	32.95 53	31.05 51
2½	24.65 42.5	32.15 41.5	35.15 40	35.15 38.5	35.15 39.5	35.15 39	35.15 39	34.25 41	32.65 40
1½	33.45 28	34.95 30	35.15 30.5	35.15 31	35.15 32	35.15 32	35.15 30.5	34.75 30	33.55 29
½	33.65 26	34.35 26	35.15 26	35.15 27	35.15 30	35.15 27.5	35.15 26.5	34.45 26.5	33.55 26
-½	31.75 24	33.75 25.5	35.15 25	35.15 27	35.15 27	35.15 26	35.15 25	34.65 23	33.35 22
-1½	31.05 19.5	33.25 19	35.15 19	35.15 20	35.15 20	35.15 19.5	35.15 19	34.15 18.5	32.55 18
-2½	24.25 7	31.35 9.5	35.15 10.5	35.05 9.5	35.15 9	35.15 9	34.85 10	32.65 8	30.25 7.5
-3	28.55 -3	29.55 +0.5	35.15 7.5	34.85 6	34.85 4.5	34.85 4	34.65 6.5	34.05 3.5	29.15 3

TABLE 1 TEST 2A

STATION	-3		$-2\frac{3}{4}$		$-2\frac{1}{2}$		-2		-1		0		1		2		3		3
	$P_3 \propto$		$P_3 \propto$		$P_3 \propto$		$P_3 \propto$		$P_3 \propto$		$P_3 \propto$		$P_3 \propto$		$P_3 \propto$		$P_3 \propto$		P_3
	lbs/in ²	°	lbs/in ²	°	lbs/in ²	°	lbs/in ²	°	lbs/in ²	°	lbs/in ²	°	lbs/in ²	°	lbs/in ²	°	lbs/in ²	°	lbs/in ²
2	28.6	4	29.0	4	29.0	4	30.6	4	30.6	8.5	29.8	8.5	29.3	5	28.8	5	29.6	24.5	29.7
$1\frac{1}{2}$	29.0	2	29.3	2	29.9	2	32.5	11	32.3	7	31.5	6	30.5	3	28.6	5.5	30.2	23	30.9
1	29.4	0	30.2	0	31.4	9.5	33.9	16	34.3	17	34.3	16.5	33.6	16.5	31.0	9	31.1	20	32.0
$\frac{1}{2}$	30.2	3.5	31.7	9	33.6	21	34.8	22	34.8	24	35.0	25	34.7	23.5	33.7	18	33.6	19.5	33.7
$-\frac{1}{2}$	30.9	32	33.2	33.5	34.4	35.5	34.8	36.5	34.9	35.5	34.9	36.5	34.6	37.5	34.5	42.5	34.3	36	34.0
$-1\frac{1}{2}$	29.3	63	31.2	63.5	33.3	59	33.4	59.5	34.6	56.5	35.0	53	35.0	52.5	34.9	52	34.4	53	33.4
-2	28.6	84	28.6	84	28.6	84	28.6	84	29.2	84	29.3	82.5	30.7	83	31.4	81.5	29.8	81	28.9

Measured Flow = 20.1 galls./ $1\frac{1}{4}$ hrs.

TABLE 1

TEST 3

STATION	$-3\frac{1}{4}$		-3		-2		-1		0		1		2		3		$3\frac{1}{4}$	
	P_2	α	P_2	α	P_2	α	P_2	α	P_2	α	P_2	α	P_2	α	P_2	α	P_2	α
	lbs/in^2	$^\circ$	lbs/in^2	$^\circ$	lbs/in^2	$^\circ$	lbs/in^2	$^\circ$	lbs/in^2	$^\circ$	lbs/in^2	$^\circ$	lbs/in^2	$^\circ$	lbs/in^2	$^\circ$	lbs/in^2	$^\circ$
3	35.45	53	38.15	54	42.35	53	42.95	50	42.85	53	43.45	48.5	43.35	48.5	41.35	48	38.55	5
$2\frac{1}{2}$	36.65	39	40.45	36.5	44.05	39.5	44.15	38	44.15	39	44.15	38	44.05	38.5	42.55	40	40.15	41
$1\frac{1}{2}$	38.15	26	41.65	28	44.15	31	44.15	30.5	44.15	31.5	44.15	31.5	44.15	31	42.85	30	39.95	2
$\frac{1}{2}$	38.95	23	41.85	24	44.15	27	44.15	28.5	44.15	29	44.15	28	44.15	27	43.05	25	41.25	24
$-\frac{1}{2}$	39.35	23.5	41.95	24.5	44.15	26	44.15	27	44.15	27.5	44.15	27	44.15	26.5	43.05	24	41.15	23
$-1\frac{1}{2}$	38.75	17	41.45	19	43.95	23.5	43.95	20	43.85	19.5	43.95	19.5	43.85	18.5	42.45	18	40.15	1
$-2\frac{1}{2}$	36.55	5	38.75	7	43.85	10.5	43.75	9	43.25	7	43.65	8	43.45	8.5	40.35	8.5	37.35	7
-3	35.85	-2	36.95	-2	43.65	4.5	43.45	5	43.15	3	43.35	2	43.15	5	38.75	2	35.95	1

TABLE 1

TEST 3A

STATION	-3	-2 $\frac{3}{4}$	-2 $\frac{1}{2}$	-2	-1	0	1	2	3	3 $\frac{1}{2}$
	$P_3 \propto$	$P_3 \propto$	$P_3 \propto$	$P_3 \propto$	$P_3 \propto$	$P_3 \propto$	$P_3 \propto$	$P_3 \propto$	$P_3 \propto$	P_3
	lbs/in^2	lbs/in^2	lbs/in^2	lbs/in^2	lbs/in^2	lbs/in^2	lbs/in^2	lbs/in^2	lbs/in^2	lbs/in^2
2		35.4-4.5	35.6 -4.5	37.4 +4.5	37.6 +2.5	36.5 -2.5	35.5 -6		36.6 +23	36.7
1 $\frac{1}{2}$	35.7 .0	36.1 0	36.9 0	40.3 10	39.9 7.5	38.9 6	37.8 5	36.0 3.5	37.2 27.5	37.9
1	36.4 -1.5	37.3 -1.5	39.0 +7	42.1 16	42.3 15.5	41.8 15	41.1 14.5	38.0 8.5	38.0 22	39.4
$\frac{1}{2}$	37.4 4	39.1 9	41.9 19	43.0 21	43.2 23.5	43.3 24	42.9 22.5	41.3 17	41.2 19	41.7
- $\frac{1}{2}$	38.8 33.5	41.7 33	42.8 35	43.2 36	43.3 36	43.2 37	43.2 37	43.2 37	42.7 35	42.3
-1 $\frac{1}{2}$	35.9 75	38.9 64.5	41.5 58.5	41.4 59	43.3 55.5	43.4 53.5	43.4 53	43.4 52	42.6 51	41.7
-2			36.4 80	36.3 80	36.6 80	38.5 80.5	39.3 80	40.5 78.5	37.9 79	35.7

Measured Flow = 25.2 galls./1 $\frac{1}{4}$ hrs.

TABLE 1

TEST 4

STATION	$-3\frac{1}{4}$		-3		-2		-1		0		1		2		3		$3\frac{1}{4}$	
	$P_2 \propto \frac{100}{m^2}$		$P_2 \propto \frac{100}{m^2}$		$P_2 \propto \frac{100}{m^2}$		$P_2 \propto \frac{100}{m^2}$		$P_2 \propto \frac{100}{m^2}$		$P_2 \propto \frac{100}{m^2}$		$P_2 \propto \frac{100}{m^2}$		$P_2 \propto \frac{100}{m^2}$		$P_2 \propto \frac{100}{m^2}$	
3			46.52	55	51.12	53	52.12	50	51.92	55	52.32	51	52.32	52.5	50.12	50	46.62	52
$2\frac{1}{2}$	46.82	40	49.32	38.5	53.32	40	53.92	38.5	53.02	40	53.32	40.5	53.62	39	51.62	39	48.52	40
$1\frac{1}{2}$	47.02	27	51.12	33.5	54.32	30.5	54.72	34.5	53.92	34	54.02	32	53.72	31	52.42	29	50.12	28
$\frac{1}{2}$	47.62	23.5	51.12	26	54.32	21	54.32	29	54.12	29	54.12	27.5	54.02	28	52.12	25	49.62	25
$-\frac{1}{2}$	47.92	26	51.02	25	54.12	24	54.22	28.5	54.22	28	54.12	27.5	53.92	26	52.02	24.5	49.32	23.5
$-1\frac{1}{2}$	47.72	20	50.52	20	53.92	19.5	53.92	20.5	53.92	20	54.02	20	53.62	18.5	51.82	17.5	48.82	17
$-2\frac{1}{2}$	46.82	7	47.62	6.5	53.62	10	53.52	9	53.42	8.5	53.92	8.5	53.52	8	49.92	9	45.82	7
-3	43.92	0	45.52	6.5	53.52	7.5	53.62	4	53.12	3	53.22	3.5	52.92	5	47.52	+2	44.02	-1

TABLE 1

TEST #A

STATION	-3	$-2\frac{3}{4}$	$-2\frac{1}{2}$	-2	-1	0	1	2	3	3										
	$P_3 \propto$	$P_3 \propto$	$P_3 \propto$	$P_3 \propto$	$P_3 \propto$	$P_3 \propto$	$P_3 \propto$	$P_3 \propto$	$P_3 \propto$	$P_3 \propto$										
	lbs/in ²	° lbs/in ²	° lbs/in ²	° lbs/in ²	° lbs/in ²	° lbs/in ²	° lbs/in ²	° lbs/in ²	° lbs/in ²	° lbs/in ²										
2	43.37	0	43.67	0	46.17	+6	46.37	+3	44.97	0	43.37	-8	43.25	-8	45.27	+24	45.37	+		
$1\frac{1}{2}$	43.67	-8	44.17	-8.5	44.87	+0.5	49.27	10	49.27	7	47.87	5.5	46.67	4	43.87	1	45.87	26	46.87	2
1	45.07	-5	46.57	+1.5	49.17	11.5	51.97	16	52.67	17.5	52.07	17	51.37	16	47.57	9.5	47.97	18	49.37	
$\frac{1}{2}$	46.47	7	48.87	12	51.97	21	53.07	22	53.47	24.5	53.17	25	53.37	25.5	51.47	18	51.77	20	51.87	
$-\frac{1}{2}$	47.47	33.5	51.37	34	52.77	35	53.37	36	53.47	36.5	53.47	36	53.37	36.5	53.27	36	52.67	36	52.27	
$-1\frac{1}{2}$	43.47	67	46.37	67	49.47	63	49.87	62.5	53.07	59	53.57	56	53.67	55.5	53.67	55	52.27	54	50.77	
-2							44.57	84	46.97	82.5	47.37	82	48.87	80	45.47	78	43.57			

Measured Flow = 31.5 galls./16 hrs.

TEST 2 TABLE 2

STATION	-3 1/4	-3	-2	-1	0	1	2	3	3 1/4
	$\frac{P_1}{P_2}$ η	$\frac{P_1}{P_2}$ η	$\frac{P_1}{P_2}$ η	$\frac{P_1}{P_2}$ η	$\frac{P_1}{P_2}$ η	$\frac{P_1}{P_2}$ η	$\frac{P_1}{P_2}$ η	$\frac{P_1}{P_2}$ η	$\frac{P_1}{P_2}$ η
3	.986 .065	.926 .344	.837 .783	.810 .924	.820 .871	.805 .951	.818 .883	.850 .716	.902 .460
2 1/2	.905 .253	.870 .616	.796 1.0	.796 1.0	.796 1.0	.796 1.0	1.0 .818	.883 .682	
1 1/2	.837 .783	.801 .973	.796 1.0	.796 1.0	.796 1.0	.796 1.0	1.0 .805	.951 .799	
1/2	.832 .810	.815 .899	.796 1.0	.796 1.0	.796 1.0	.796 1.0	1.0 .813	.908 .799	
-1/2	.882 .560	.830 .820	.796 1.0	.796 1.0	.796 1.0	.796 1.0	1.0 .807	.940 .773	
-1 1/2	.902 .460	.862 .758	.796 1.0	.796 1.0	.796 1.0	.796 1.0	1.0 .820	.871 .667	
-2 1/2	.957 .198	.843 .505	.796 1.0	.799 .983	.796 1.0	.796 1.0	1.0 .955	.857 .344	
-3	.981 .088	.967 .246	.796 1.0	.804 .955	.804 .955	.804 .956	.807 .940	.902 .460	.183

TEST 2a TABLE 2

STATION	-3	-2 $\frac{3}{4}$	-2 $\frac{1}{2}$	-2	-1	0	1	2	3	3 $\frac{1}{4}$
2	$\frac{R}{R}$ $\frac{R}{R}$	$\frac{R}{R}$ $\frac{R}{R}$	$\frac{R}{R}$ $\frac{R}{R}$	$\frac{R}{R}$ $\frac{R}{R}$	$\frac{R}{R}$ $\frac{R}{R}$	$\frac{R}{R}$ $\frac{R}{R}$	$\frac{R}{R}$ $\frac{R}{R}$	$\frac{R}{R}$ $\frac{R}{R}$	$\frac{R}{R}$ $\frac{R}{R}$	$\frac{R}{R}$ $\frac{R}{R}$
1 $\frac{1}{2}$.986 .065	.973 .124	.973 .124	.922 .361	.922 .361	.922 .361	.922 .361	.922 .361	.922 .361	.922 .361
1	.973 .124	.963 .164	.943 .262	.868 .626	.873 .602	.895 .494	.925 .348	.986 .065	.934 .305	.913 .405
$\frac{1}{2}$.959 .189	.934 .305	.898 .478	.832 .810	.823 .810	.857 .823	.839 .774	.910 .420	.907 .435	.882 .560
$-\frac{1}{2}$.934 .305	.890 .520	.839 .774	.810 .924	.810 .924	.806 .946	.813 .909	.837 .783	.839 .774	.837 .783
$-1\frac{1}{2}$.913 .405	.849 .722	.820 .871	.810 .924	.808 .935	.808 .935	.815 .899	.818 .882	.823 .857	.829 .825
-2	.963 .169	.904 .450	.867 .732	.844 .768	.815 .899	.806 .946	.806 .946	.808 .935	.820 .871	.844 .768
-2	.986 .065	.986 .065	.986 .065	.986 .065	.966 .155	.963 .169	.919 .375	.898 .478	.946 .250	.976 .110

TEST 3 TABLE 2

STATION	-3 $\frac{1}{4}$	-3	-2	-1	0	1	2	3	3 $\frac{1}{4}$
	$\frac{P_2}{P_3}$	$\frac{P_2}{P_3}$	$\frac{P_2}{P_3}$	$\frac{P_2}{P_3}$	$\frac{P_2}{P_3}$	$\frac{P_2}{P_3}$	$\frac{P_2}{P_3}$	$\frac{P_2}{P_3}$	$\frac{P_2}{P_3}$
3	.991	.042	.921	.367	.825	.818	.882	.820	.871
2 $\frac{1}{2}$.960	.183	.869	.624	.798	.988	.796	1.0	.876
1 $\frac{1}{2}$.921	.367	.845	.743	.796	1.0	.796	1.0	.880
$\frac{1}{2}$.903	.455	.840	.767	.796	1.0	.796	1.0	.853
- $\frac{1}{2}$.893	.505	.838	.778	.796	1.0	.796	1.0	.855
-1 $\frac{1}{2}$.907	.435	.848	.727	.800	.977	.802	.966	.876
-2 $\frac{1}{2}$.962	.174	.907	.435	.802	.966	.813	.909	.941
-3	.980	.091	.954	.211	.807	.940	.815	.899	.978

TEST 3a TABLE 2

STATION	-3	$-2\frac{3}{4}$	$-2\frac{1}{2}$	-2	-1	0	1	2	3	$3\frac{1}{4}$
	$\frac{P_1}{P_3}$ η	$\frac{P_1}{P_3}$ η	$\frac{P_1}{P_3}$ η	$\frac{P_1}{P_3}$ η	$\frac{P_1}{P_3}$ η	$\frac{P_1}{P_3}$ η	$\frac{P_1}{P_3}$ η	$\frac{P_1}{P_3}$ η	$\frac{P_1}{P_3}$ η	$\frac{P_1}{P_3}$ η
2		.993 .033	.988 .055	.940 .275	.935 .300	.964 .165	.990 .045		.961 .177	.958 .193
$1\frac{1}{2}$.985 .069	.974 .120	.953 .216	.872 .606	.981 .564	.904 .450	.930 .325	.976 .110	.905 .253	.928 .335
1	.966 .155	.943 .262	.902 .460	.835 .794	.830 .820	.841 .762	.857 .682	.925 .348	.925 .348	.892 .510
$\frac{1}{2}$.940 .275	.900 .469	.839 .774	.818 .882	.814 .903	.812 .915	.820 .871	.852 .706	.855 .692	.844 .708
$-\frac{1}{2}$.906 .440	.844 .768	.822 .860	.814 .903	.812 .915	.814 .903	.814 .903	.874 .903	.874 .950	.830 .820
$-1\frac{1}{2}$.979 .098	.904 .450	.847 .732	.849 .722	.812 .915	.810 .924	.924 .924	.924 .810	.924 .826	.844 .768
-2			.993 .033	.996 .018	.961 .177	.913 .405	.895 .494	.868 .626	.928 .335	.985 .069

TEST 4 TABLE 2

STATION	-3 1/4	-3	-2	-1	0	1	2	3	3 1/4
	$\frac{R}{P_3}$ η	$\frac{R}{P_3}$ η	$\frac{R}{P_3}$ η	$\frac{R}{P_3}$ η	$\frac{R}{P_3}$ η	$\frac{R}{P_3}$ η	$\frac{R}{P_3}$ η	$\frac{R}{P_3}$ η	$\frac{R}{P_3}$ η
3	.930	.325	.846	.736	.830	.830	.820	.835	.794
2 1/2	.983	.078	.877	.584	.812	.915	.807	.940	.892
1 1/2	.920	.371	.846	.736	.796	.801	.805	.950	.864
1/2	.909	.425	.846	.736	.796	.800	.801	.970	.875
-1/2	.902	.460	.848	.727	.800	.978	.802	.966	.877
-1 1/2	.916	.390	.856	.687	.802	.966	.807	.940	.886
-2 1/2	.983	.078	.909	.425	.807	.940	.809	.930	.944
-3	.985	.069	.950	.230	.809	.930	.817	.888	.983

TEST 4a TABLE 2

STATION	-3	-2 $\frac{3}{4}$	-2 $\frac{1}{2}$	-2	-1	0	1	2	3	3 $\frac{1}{4}$
	$\frac{P_1}{P_3}$ η	$\frac{P_1}{P_3}$ η	$\frac{P_1}{P_3}$ η	$\frac{P_1}{P_3}$ η	$\frac{P_1}{P_3}$ η	$\frac{P_1}{P_3}$ η	$\frac{P_1}{P_3}$ η	$\frac{P_1}{P_3}$ η	$\frac{P_1}{P_3}$ η	$\frac{P_1}{P_3}$ η
2	.991 .183	.997 .014	.991 .001	.937 .291	.933 .310	.962 .174	.997 .014		.956 .202	.953 .216
1 $\frac{1}{2}$.991 .091	.980 .091	.964 .165	.878 .578	.878 .578	.904 .450	.927 .338	.985 .069	.943 .262	.923 .357
1	.960 .183	.929 .329	.880 .567	.833 .844	.822 .861	.831 .814	.842 .759	.910 .419	.902 .459	.876 .587
$\frac{1}{2}$.931 .320	.885 .544	.833 .804	.816 .846	.809 .930	.814 .904	.810 .924	.840 .767	.836 .789	.834 .800
- $\frac{1}{2}$.912 .411	.842 .759	.820 .871	.810 .924	.809 .930	.809 .930	.810 .924	.812 .915	.822 .861	.828 .830
-1 $\frac{1}{2}$.995 .024	.933 .310	.874 .598	.867 .632	.816 .896	.808 .935	.806 .946	.806 .946	.828 .830	.853 .720
-2					.971 .132	.921 .367	.914 .400	.885 .544	.951 .225	.993 .032

TEST 2 TABLE 3

STATION	-3 1/4	-3	-2	-1	0	1	2	3	3 1/4
	$\eta^i \text{ Sin } fda$	$\eta^i \text{ Sin } fda$	$\eta^i \text{ Sin } fda$	$\eta^i \text{ Sin } fda$	$\eta^i \text{ Sin } fda$	$\eta^i \text{ Sin } fda$	$\eta^i \text{ Sin } fda$	$\eta^i \text{ Sin } fda$	$\eta^i \text{ Sin } fda$
	$f.v. \frac{\eta^i \text{ Sin } fda}{f.v.}$	$f.v. \frac{\eta^i \text{ Sin } fda}{f.v.}$	$f.v. \frac{\eta^i \text{ Sin } fda}{f.v.}$	$f.v. \frac{\eta^i \text{ Sin } fda}{f.v.}$	$f.v. \frac{\eta^i \text{ Sin } fda}{f.v.}$	$f.v. \frac{\eta^i \text{ Sin } fda}{f.v.}$	$f.v. \frac{\eta^i \text{ Sin } fda}{f.v.}$	$f.v. \frac{\eta^i \text{ Sin } fda}{f.v.}$	$f.v. \frac{\eta^i \text{ Sin } fda}{f.v.}$
3	.255 .819 1/4	.587 .824 1/4	.886 .829 1/2	.962 .799 1/2	.934 .848 1/2	.976 .788 1/2	.941 .787 1/2	.846 .799 1/2	.679 .804 1/2
	1.050 .050 1.035 .117	1.015 .363 1.004 .383	1.007 .394 1.003 .384	1.006 .369 1.015 .167	1.015 .133				
2 1/2	.503 .676 3/8	.785 .663 3/8	.643 3/4 1	.623 3/4 1	.636 3/4 1	.629 3/4 1	.629 3/4 1	.941 .656 3/8	.826 .669 3/8
	1.040 .123 1.0205 .191	1 .482 1	.468 1	.477 1	.472 1	1.006 .230	1.075 .204		
1 1/2	.886 .470 1/2	.987 .500 1/2	.508 1	.515 1	.530 1	.530 1	.508 1	.976 .500 1/2	.894 .485 1/2
	1.015 .206 1.005 .246	1 .508 1	.508 1	.515 1	.530 1	.530 1	.508 1	1.003 .244	1.011 .214
1/2	.900 .438 1/2	.914 .438 1/2	.438 1	.454 1	.500 1	.462 1	.446 1	.954 .418 1/2	.894 .407 1/2
	1.01 .195 1.0055 .207	1 .438 1	.438 1	.454 1	.500 1	.462 1	.446 1.005	.198 1.011	.180
-1/2	.749 .407 1/2	.906 .430 1/2	1 .423 1	1 .454 1	1 .454 1	1 .458 1	1 .423 1	.970 .391 1/2	.880 .375 1/2
	1.0235 .149 1.0095 .193	1 .423 1	.423 1	.454 1	.454 1	.438 1	.423 1.003	.189 1.012	.163
-1 1/2	.679 .334 1/2	.871 .326 1/2	1 .326 1	1 .342 1	1 .342 1	1 .334 1	1 .326 1	.934 .317 1/2	.817 .276 1/2
	1.029 .110 1.013 .140	1 .326 1	.326 1	.342 1	.342 1	.334 1	.326 1.007	.147 1.018	.111
-2 1/2	.645 .122 3/8	.711 .165 3/8	1 .182 3/4 1	.992 .165 3/4 1	.156 3/4 1	.156 3/4 1	.174 3/4 1	.826 .139 3/8	.587 .130 3/8
	1.0425 .0195 1.022 .043	1 .1365 1.001 .123	1 .117 1	1 .117 1	1.002 .1275	1.015 .042	1.036 .028		
-3	.297 .052 1/4	.495 .009 1/4	1 .130 1/2 1	.978 .105 1/2 1	.978 .079 1/2 1	.970 .113 1/2 1	.679 .061 1/4	.428 .061 1/4	1.0435 .006
	1.005 .004 1.04 .001	1 .065 1.002 .051	1.002 .039 1.002 .034	1.003 .055	1.029 .010	1.039			
Σ	0.8565	1.138	2.7415	2.790	2.853	2.771	2.7265	1.227	1.039

$$\Sigma \frac{\eta^i \text{ Sin } fda}{f.v.} = 18.1425$$

TEST 2a TABLE 3

STATION	-3	-2 $\frac{3}{4}$	-2 $\frac{1}{2}$	-2	-1	0	1	2	3	3 $\frac{1}{4}$
$\eta^2 \sin x \text{ fda}$	$\eta^2 \sin x \text{ fda}$	$\eta^2 \sin x \text{ fda}$	$\eta^2 \sin x \text{ fda}$	$\eta^2 \sin x \text{ fda}$	$\eta^2 \sin x \text{ fda}$	$\eta^2 \sin x \text{ fda}$	$\eta^2 \sin x \text{ fda}$	$\eta^2 \sin x \text{ fda}$	$\eta^2 \sin x \text{ fda}$	$\eta^2 \sin x \text{ fda}$
$fV \eta^2 \sin x \frac{\text{fda}}{fV}$	$fV \eta^2 \sin x \frac{\text{fda}}{fV}$	$fV \eta^2 \sin x \frac{\text{fda}}{fV}$	$fV \eta^2 \sin x \frac{\text{fda}}{fV}$	$fV \eta^2 \sin x \frac{\text{fda}}{fV}$	$fV \eta^2 \sin x \frac{\text{fda}}{fV}$	$fV \eta^2 \sin x \frac{\text{fda}}{fV}$	$fV \eta^2 \sin x \frac{\text{fda}}{fV}$	$fV \eta^2 \sin x \frac{\text{fda}}{fV}$	$fV \eta^2 \sin x \frac{\text{fda}}{fV}$	$fV \eta^2 \sin x \frac{\text{fda}}{fV}$
2	.355 .070 $\frac{1}{8}$.352 .070 $\frac{1}{8}$.352 .070 $\frac{3}{16}$.601 $\frac{3}{8}$.601 .148 $\frac{1}{2}$.500 .148 $\frac{1}{2}$.411 .087 $\frac{1}{2}$.302 .087 $\frac{1}{2}$.146 .445 $\frac{5}{16}$.485 .346 $\frac{3}{16}$
$\frac{1}{2}$.105 .002	.1046 .003	.1046 .004	.1034 .015	.1034 .043	.104 .036	.1044 .017	.1048 .0125	.1042 .058	.104 .032
$\frac{1}{4}$.352 .035 $\frac{1}{8}$.411 .035 $\frac{1}{8}$.512 .035 $\frac{3}{16}$.791 $\frac{3}{8}$.776 .122 $\frac{1}{2}$.702 .105 $\frac{1}{2}$.590 .052 $\frac{1}{2}$.255 .046 $\frac{1}{2}$.552 .391 $\frac{5}{16}$.636 .438 $\frac{3}{16}$
1	.1046 .0015	.1044 .002	.1039 .003	.102 .0555	.1021 .046	.1027 .036	.1035 .015	.105 .012	.1037 .065	.1032 .0505
$\frac{1}{2}$.434 0 $\frac{1}{8}$.552 0 $\frac{1}{8}$.692 .165 $\frac{3}{16}$.900 $\frac{3}{8}$.925 .299 $\frac{1}{2}$.925 .284 $\frac{1}{2}$.880 .250 $\frac{1}{2}$.648 .156 $\frac{1}{2}$.660 .342 $\frac{5}{16}$.749 .423 $\frac{3}{16}$
$\frac{1}{4}$.1043 .000	.1037 .000	.1028 .021	.101 .095	.1008 .138	.1008 .131	.1012 .109	.1031 .049	.103 .070	.1023 .058
$\frac{1}{2}$.552 .061 $\frac{1}{4}$.721 .156 $\frac{1}{4}$.890 .358 $\frac{3}{8}$.962 .375 $\frac{3}{4}$.962 .407	.972 .423	.954 .399	.886 .309	.880 .334 $\frac{5}{8}$.886 .375 $\frac{3}{8}$
$\frac{1}{4}$.1037 .008	.1025 .0275	.1012 .117	.1004 .271	.1004 .390	.1003 .410	.1005 .380	.1011 .270	.1012 .182	.1011 .123
- $\frac{1}{2}$.636 .530 $\frac{1}{4}$.850 .552 $\frac{1}{4}$.934 .581 $\frac{3}{8}$.962 .595 $\frac{3}{4}$.966 .581	.966 .595	.949 .609	.960 .676	.925 .588 $\frac{5}{8}$.909 .574 $\frac{3}{8}$
- $\frac{1}{4}$.1032 .0815	.1015 .115	.1007 .202	.1004 .426	.1003 .560	.1003 .574	.1005 .574	.1006 .630	.1008 .368	.1009 .194
- $\frac{1}{2}$.411 .891 $\frac{1}{8}$.670 .895 $\frac{1}{8}$.857 .857 $\frac{3}{16}$.864 .862 $\frac{3}{8}$.969 .824 $\frac{1}{2}$.972 .799 $\frac{1}{2}$.972 .793 $\frac{1}{2}$.966 .788 $\frac{1}{2}$.934 .799 $\frac{5}{16}$.864 .829 $\frac{3}{16}$
-1	.1044 .044	.1029 .073	.1014 .136	.1013 .275	.1005 .388	.1003 .386	.1003 .383	.1003 .379	.1007 .231	.1013 .132
-2	.255 .995 $\frac{1}{8}$.255 .995 $\frac{1}{8}$.255 .995 $\frac{3}{16}$.255 .995 $\frac{3}{8}$.394 .995 $\frac{1}{2}$.411 .991 $\frac{1}{2}$.613 .993 $\frac{1}{2}$.692 .989 $\frac{1}{2}$.500 .988 $\frac{5}{16}$.332 .987 $\frac{3}{16}$
Σ	.105 .030	.105 .030	.105 .045	.105 .091	.1045 .188	.1044 .195	.1033 .295	.1028 .334	.104 .149	.1047 .059
	0.167	0.2505	0.528	1.2285	1.753	1.768	1.773	1.6865	1.103	0.6485

$$\Sigma \eta^2 \sin x \frac{\text{fda}}{fV} = 10.906$$

TEST 3 TABLE 3

STATION	-3 1/4	-3	-2	-1	0	1	2	3	3 1/4
$H^2 \text{ Sin } x \text{ fda}$	$H^2 \text{ Sin } x \text{ fda}$	$H^2 \text{ Sin } x \text{ fda}$	$H^2 \text{ Sin } x \text{ fda}$	$H^2 \text{ Sin } x \text{ fda}$	$H^2 \text{ Sin } x \text{ fda}$	$H^2 \text{ Sin } x \text{ fda}$	$H^2 \text{ Sin } x \text{ fda}$	$H^2 \text{ Sin } x \text{ fda}$	$H^2 \text{ Sin } x \text{ fda}$
$f \cdot V \frac{H^2 \text{ Sin } x \text{ fda}}{f \cdot V}$	$f \cdot V \frac{H^2 \text{ Sin } x \text{ fda}}{f \cdot V}$	$f \cdot V \frac{H^2 \text{ Sin } x \text{ fda}}{f \cdot V}$	$f \cdot V \frac{H^2 \text{ Sin } x \text{ fda}}{f \cdot V}$	$f \cdot V \frac{H^2 \text{ Sin } x \text{ fda}}{f \cdot V}$	$f \cdot V \frac{H^2 \text{ Sin } x \text{ fda}}{f \cdot V}$	$f \cdot V \frac{H^2 \text{ Sin } x \text{ fda}}{f \cdot V}$	$f \cdot V \frac{H^2 \text{ Sin } x \text{ fda}}{f \cdot V}$	$f \cdot V \frac{H^2 \text{ Sin } x \text{ fda}}{f \cdot V}$	$f \cdot V \frac{H^2 \text{ Sin } x \text{ fda}}{f \cdot V}$
3	.205 .799 1/2	.606 .869 1/2	.909 .799 1/2	.936 .799 1/2	.965 .749 1/2	.960 .749 1/2	.846 .743 1/2	.642 .777 1/2	
2 1/2	1.051 .039	1.034 .1185 3/8	1.009 .360	1.006 .358 3/4	1.007 .371	1.004 .360	1.016 .155	1.0315 .121	
1 1/2	.428 .629 3/8	.791 .595 3/8	.995 .636 3/4	.616 3/4	.629 3/4	.616 3/4	.995 .623 3/4	.917 .643 3/8	.767 .663 3/8
1/2	1.0435 .097	1.02 .173	1.004 .474	.462	.472	.462	1.004 .464	1.0085 .219	1.022 .1865
-1/2	.606 .438 1/2	.863 .470 1/2	.515	.508	.523	.523	.515	.934 .500 1/2	.753 .492 1/2
-1 1/2	1.034 .1285	1.014 .200	.515	.508	.523	.523	.515	1.007 .232	1.023 .181
-2 1/2	.675 .391 1/2	.876 .407 1/2	.454	.476	.485	.470	.454	.963 .423 1/2	.839 .415 1/2
-3	1.029 .128	1.012 .176	.454	.476	.485	.470	.454	1.006 .198	1.016 .1715
	.711 .399 1/2	.882 .415 1/2	.438	.454	.462	.454	.446	.943 .407 1/2	.833 .399 1/2
	1.026 .138	1.012 .181	.438	.454	.462	.454	.446	1.006 .191	1.016 .164
	.660 .292 1/2	.853 .326 1/2	.989 .399	.989 .362	.983 .334	.989 .334	.983 .317	.914 .309 1/2	.767 .284 1/2
	1.03 .0935	1.0165 .137	1.001 .394	1.001 .338	1.002 .328	1.001 .330	1.002 .311	1.009 .140	1.022 .1065
	.447 .087 3/8	.660 .122 3/8	.983 .182 3/4	.978 .156 3/4	.954 .139 3/4	.970 .139 3/4	.965 .108 3/4	.783 .148 3/8	.523 .130 3/8
	1.044 .013	1.03 .029	1.002 .134	1.002 .114	1.005 .099	1.003 .101	1.004 .107	1.021 .0425	1.039 .025
	.302 .055 1/4	.460 .055 1/4	.470 .113 1/2	.965 .087 1/2	.949 .052 1/2	.960 .035 1/2	.909 .087 1/2	.660 .035 1/2	.318 .055 1/4
	1.048 .0025	1.042 .004	1.003 .055	1.004 .042	1.005 .025	1.004 .017	1.0055 .021	1.03 .0055	1.008 .003
Σ	0.6395	1.0185	2.824	2.752	2.765	2.717	2.696	1.183	0.9585

$H^2 \text{ Sin } x \text{ fda}$

TEST 3a TABLE 3

STATION	-3	-2 $\frac{3}{4}$	-2 $\frac{1}{2}$	-2	-1	0	1	2	3	3 $\frac{1}{4}$
$H^{\frac{1}{2}} \sin \theta \sin \phi$	$H^{\frac{1}{2}} \sin \theta \sin \phi$	$H^{\frac{1}{2}} \sin \theta \sin \phi$	$H^{\frac{1}{2}} \sin \theta \sin \phi$	$H^{\frac{1}{2}} \sin \theta \sin \phi$	$H^{\frac{1}{2}} \sin \theta \sin \phi$	$H^{\frac{1}{2}} \sin \theta \sin \phi$	$H^{\frac{1}{2}} \sin \theta \sin \phi$	$H^{\frac{1}{2}} \sin \theta \sin \phi$	$H^{\frac{1}{2}} \sin \theta \sin \phi$	$H^{\frac{1}{2}} \sin \theta \sin \phi$
$fV \frac{H^{\frac{1}{2}} \sin \theta \sin \phi}{fV}$	$fV \frac{H^{\frac{1}{2}} \sin \theta \sin \phi}{fV}$	$fV \frac{H^{\frac{1}{2}} \sin \theta \sin \phi}{fV}$	$fV \frac{H^{\frac{1}{2}} \sin \theta \sin \phi}{fV}$	$fV \frac{H^{\frac{1}{2}} \sin \theta \sin \phi}{fV}$	$fV \frac{H^{\frac{1}{2}} \sin \theta \sin \phi}{fV}$	$fV \frac{H^{\frac{1}{2}} \sin \theta \sin \phi}{fV}$	$fV \frac{H^{\frac{1}{2}} \sin \theta \sin \phi}{fV}$	$fV \frac{H^{\frac{1}{2}} \sin \theta \sin \phi}{fV}$	$fV \frac{H^{\frac{1}{2}} \sin \theta \sin \phi}{fV}$	$fV \frac{H^{\frac{1}{2}} \sin \theta \sin \phi}{fV}$
2	.182 .078 $\frac{1}{8}$.234 .078 $\frac{3}{16}$.525 .078 $\frac{3}{8}$.567 .044 $\frac{1}{2}$.606 .044 $\frac{1}{2}$.670 .105 $\frac{1}{2}$.712 .105 $\frac{1}{2}$.750 .087 $\frac{1}{2}$.783 .061 $\frac{1}{2}$.803 .028 $\frac{3}{16}$
	1.051 .002	1.05 .003	1.038 .015	1.037 .012	1.044 .009	1.051 .011	1.051 .011	1.044 .049	1.044 .049	1.043 .028
$\frac{1}{1\frac{1}{2}}$.263 0 $\frac{1}{8}$.466 0 $\frac{3}{16}$.778 .174 $\frac{3}{8}$.751 .131 $\frac{1}{2}$.670 .105 $\frac{1}{2}$.570 .087 $\frac{1}{2}$.570 .087 $\frac{1}{2}$.532 .061 $\frac{1}{2}$.503 .462 $\frac{5}{16}$.579 .349 $\frac{3}{16}$
	1.049 .000	1.047 .000	1.021 .050	1.023 .068	1.029 .034	1.036 .024	1.047 .010	1.047 .010	1.04 .070	1.035 .042
1	.394 .026 $\frac{1}{8}$.679 .122 $\frac{3}{16}$.892 .276 $\frac{3}{8}$.906 .267 $\frac{1}{2}$.873 .259 $\frac{1}{2}$.826 .250 $\frac{1}{2}$.590 .148 $\frac{1}{2}$.590 .148 $\frac{1}{2}$.590 .395 $\frac{5}{16}$.715 .431 $\frac{3}{16}$
	1.045 .001	1.039 .002	1.011 .091	1.009 .1195	1.013 .111	1.017 .102	1.035 .042	1.035 .042	1.035 .067	1.026 .0565
$\frac{1}{2}$.525 .070 $\frac{1}{4}$.880 .326 $\frac{3}{8}$.940 .358 $\frac{3}{4}$.951 .399	.957 .407	.934 .383	.840 .501	.840 .501	.833 .326 $\frac{5}{8}$.864 .367 $\frac{3}{8}$
	1.038 .009	1.028 .026	1.006 .252	1.005 .378	1.004 .388	1.007 .355	1.016 .249	1.016 .249	1.016 .167	1.013 .117
$-\frac{1}{2}$.664 .552 $\frac{1}{4}$.844 .545 $\frac{1}{2}$.951 .588 $\frac{3}{4}$.957 .588	.951 .602	.951 .602	.951 .602	.951 .602	.922 .574 $\frac{5}{8}$.906 .566 $\frac{3}{8}$
	1.013 .089	1.007 .116	1.005 .416	1.004 .561	1.005 .570	1.005 .570	1.005 .570	1.005 .570	1.008 .329	1.009 .190
$-\frac{1}{1\frac{1}{2}}$.313 .966 $\frac{1}{4}$.856 .853 $\frac{3}{16}$.850 .862 $\frac{3}{8}$.957 .824 $\frac{1}{2}$.962 .864 $\frac{1}{2}$.962 .799	.962 .788	.962 .788	.917 .777	.864 .799 $\frac{3}{16}$
	1.048 .036	1.029 .074	1.015 .271	1.004 .392	1.004 .385	1.004 .383	1.004 .378	1.004 .378	1.008 .222	1.013 .127
-2	.182 .985 $\frac{3}{16}$.134 .985 $\frac{3}{8}$.134 .985 $\frac{3}{8}$.421 .985 $\frac{1}{2}$.636 .986 $\frac{1}{2}$.702 .985 $\frac{1}{2}$.791 .980 $\frac{1}{2}$.791 .980 $\frac{1}{2}$.579 .992 $\frac{5}{16}$.263 .976 $\frac{3}{16}$
	1.051 .032	1.052 .047	1.052 .047	1.044 .199	1.032 .304	1.027 .338	1.02 .380	1.02 .380	1.035 .172	1.049 .046
Σ	0.135	0.220	0.489	1.142	1.7095	1.801	1.783	1.629	1.076	0.6065

$$\Sigma H^{\frac{1}{2}} \sin \theta \propto \frac{f \sin \theta}{fV} = 10.591$$

TEST 4 TABLE 3

STATION	-3 1/4	-3	-2	-1	0	1	2	3	3 1/4
$\eta^2 \sin \alpha \cdot fda$	$\eta^2 \sin \alpha \cdot fda$	$\eta^2 \sin \alpha \cdot fda$	$\eta^2 \sin \alpha \cdot fda$	$\eta^2 \sin \alpha \cdot fda$	$\eta^2 \sin \alpha \cdot fda$	$\eta^2 \sin \alpha \cdot fda$	$\eta^2 \sin \alpha \cdot fda$	$\eta^2 \sin \alpha \cdot fda$	$\eta^2 \sin \alpha \cdot fda$
$f \cdot V \frac{\eta^2 \sin \alpha \cdot fda}{f \cdot V}$	$f \cdot V \frac{\eta^2 \sin \alpha \cdot fda}{f \cdot V}$	$f \cdot V \frac{\eta^2 \sin \alpha \cdot fda}{f \cdot V}$	$f \cdot V \frac{\eta^2 \sin \alpha \cdot fda}{f \cdot V}$	$f \cdot V \frac{\eta^2 \sin \alpha \cdot fda}{f \cdot V}$	$f \cdot V \frac{\eta^2 \sin \alpha \cdot fda}{f \cdot V}$	$f \cdot V \frac{\eta^2 \sin \alpha \cdot fda}{f \cdot V}$	$f \cdot V \frac{\eta^2 \sin \alpha \cdot fda}{f \cdot V}$	$f \cdot V \frac{\eta^2 \sin \alpha \cdot fda}{f \cdot V}$	$f \cdot V \frac{\eta^2 \sin \alpha \cdot fda}{f \cdot V}$
3	570.819 1/2	858.799 1/2	906.766 1/2	892.819 1/2	914.717 1/2	914.793 1/2	805.766 1/2	579.788 1/2	
	.000	1.036	.113	.337	1.045	.360	1.009	.358	.1515
2 1/2	765.623 3/8	957.643 3/4	983.623 3/4	946.643 3/4	957.649 3/4	970.629 3/4	880.629 3/8	715.643 3/8	
	1.049	.064	1.022	.181	1.005	.460	1.002	.458	1.026
1 1/2	858.552 1/2	958.508 1/2	995.508 1/2	983.559 1/2	985.530 1/2	975.505 1/2	920.485 1/2	805.477 1/2	
	1.035	.134	1.014	.233	1.001	.508	1.003	.502	1.019
1/2	858.438 1/2	958.438 1/2	983.438 1/2	989.485 1/2	989.462 1/2	985.470 1/2	906.423 1/2	771.423 1/2	
	1.035	.1265	1.014	.192	1.001	.478	1.002	.462	1.022
-1/2	853.423 1/2	989.438 1/2	995.477 1/2	995.470 1/2	989.462 1/2	983.438 1/2	900.415 1/2	765.399 1/2	
	1.029	.145	1.0165	.178	1.001	.470	1.001	.455	1.022
-1 1/2	829.342 1/2	983.354 1/2	983.350 1/2	983.342 1/2	985.342 1/2	970.317 1/2	892.301 1/2	735.292 1/2	
	1.025	.1035	1.017	.1395	1.002	.363	1.005	.336	1.025
-2 1/2	652.113 3/8	972.174 3/4	965.156 3/4	962.148 3/4	983.148 3/4	965.139 3/4	798.156 3/8	509.122 3/8	
	1.049	.012	1.035	.027	1.003	.126	1.004	.106	1.0395
-3	480.113 1/4	965.130 1/2	970.070 1/2	969.052 1/2	951.061 1/2	943.087 1/2	645.040 1/4	279.018 1/4	
	1.045	.000	1.041	.013	1.004	.0625	1.003	.034	1.005
Σ	0.585	1.0765	2.6125	2.7525	2.7705	2.721	2.660	1.140	0.910

$$\gamma \frac{\eta^2 \sin \alpha \cdot fda}{f \cdot V} = 17.228$$

TEST 40 TABLE 3

Stream	-3	-2 3/4	-2 1/2	-2	-1	0	1	2	3	3 1/2
$\eta^{1/2}$ Sine fda		$\eta^{1/2}$ Sine fda	$\eta^{1/2}$ Sine fda	$\eta^{1/2}$ Sine fda	$\eta^{1/2}$ Sine fda	$\eta^{1/2}$ Sine fda	$\eta^{1/2}$ Sine fda	$\eta^{1/2}$ Sine fda	$\eta^{1/2}$ Sine fda	$\eta^{1/2}$ Sine fda
$fV \eta^{1/2} \frac{fda}{fV}$		$fV \eta^{1/2} \frac{fda}{fV}$	$fV \eta^{1/2} \frac{fda}{fV}$	$fV \eta^{1/2} \frac{fda}{fV}$	$fV \eta^{1/2} \frac{fda}{fV}$	$fV \eta^{1/2} \frac{fda}{fV}$	$fV \eta^{1/2} \frac{fda}{fV}$	$fV \eta^{1/2} \frac{fda}{fV}$	$fV \eta^{1/2} \frac{fda}{fV}$	$fV \eta^{1/2} \frac{fda}{fV}$
2		.118 0 1/8	.202 0 3/8	.560 105 3/8	.556 .052 1/2	.417 0 1/2	.118 .139 1/2		.450 .407 5/16	.466 .366 3/16
1 1/2	.202 .139 1/8	.302 .148 1/8	.406 .089 3/16	.760 .174 3/8	.760 .122 1/2	.670 .096 1/2	.581 .070 1/2	.263 .018 1/2	.512 .438 5/16	.598 .423 3/16
1	.1051 .003	.1048 .005	.1044 .001	.1022 .0485	.1022 .045 1/2	.1029 .031	.1035 .020	.002	.1039 .068	.1034 .046
1/2	.428 .087 1/8	.574 .026 1/8	.783 .199 3/16	.896 .276 3/8	.928 .301 1/2	.902 .292 1/2	.871 .276 1/2	.667 .465 1/2	.676 .309 5/16	.767 .391 3/16
1/2	.1043 .004	.1036 .002	.1023 .0275 3/8	.101 .092	.1007 .139	.101	.1013 .118	.052	.1029 .0635	.1022 .055
1/2	.566 .122 1/4	.738 .208 1/4	.896 3/8	.946 .375 3/4	.965 .445 1	.951 .423 1	.962 .451 1	.876 .309 1	.888 .342 5/8	.895 .375 5/8
1/2	.1036 .017	.1024 .0375 1/2	.119 3/8	.106 .265	.104 .398	.1005	.1004 .114	.1012	.1011 .187	.101 .124
-1/2	.642 .552 1/4	.871 .559 1/4	.934 .574 3/8	.962 .588 3/4	.965 .595 1	.965 .588 1	.962 .595 1	.957 .588 1	.928 .588 5/8	.911 .552 5/8
-1/2	.1031 .086	.1013 .120	.1007 .199	.1004 .422	.1004 .572	.1004	.1004 .570	.1004	.1007 .340	.1009 .187
-1/2	.155 .921 1/8	.556 .921 1/8	.773 .891 3/16	.745 .887 3/8	.946 .857 1/2	.966 .829 1/2	.972 .824 1/2	.972 .819 1/2	.911 .809 5/16	.839 .839 3/16
-2	.1052 .017	.1037 .062	.1021 .126	.1019 .260	.1006 .404	.1003	.1003 .398	.1003	.1009 .229	.1016 .130
					.363 .995 1/2	.606 .991 1/2	.632 .990 1/2	.738 .915 1/2	.474 .977 5/16	.179 .977 3/16
					1.046 .173	1.034 .290	1.032 .302	1.024 .356	1.044 .139	1.051 .031
Σ	0.127	0.2265	0.4725	1.108	1.745	1.815	1.830	1.633	1.0815	0.604

$$\Sigma \eta^{1/2} \sin \alpha \frac{fda}{fV} = 10.6425$$

TEST 2 TABLE 4

STATION	-3 1/4	-3	-2	-1	0	1	2	3	3 1/4										
	$\eta \frac{1}{2} \sin \frac{fda}{fV}$	$\eta \frac{1}{2} \sin \frac{fda}{fV}$	$\eta \frac{1}{2} \sin \frac{fda}{fV}$	$\eta \frac{1}{2} \sin \frac{fda}{fV}$	$\eta \frac{1}{2} \sin \frac{fda}{fV}$	$\eta \frac{1}{2} \sin \frac{fda}{fV}$	$\eta \frac{1}{2} \sin \frac{fda}{fV}$	$\eta \frac{1}{2} \sin \frac{fda}{fV}$	$\eta \frac{1}{2} \sin \frac{fda}{fV}$										
	$\eta \frac{3}{2} \sin \frac{fda}{fV}$	$\eta \frac{3}{2} \sin \frac{fda}{fV}$	$\eta \frac{3}{2} \sin \frac{fda}{fV}$	$\eta \frac{3}{2} \sin \frac{fda}{fV}$	$\eta \frac{3}{2} \sin \frac{fda}{fV}$	$\eta \frac{3}{2} \sin \frac{fda}{fV}$	$\eta \frac{3}{2} \sin \frac{fda}{fV}$	$\eta \frac{3}{2} \sin \frac{fda}{fV}$	$\eta \frac{3}{2} \sin \frac{fda}{fV}$										
3	.065	.050	.344	.117	.783	.363	.924	.383	.871	.394	.951	.384	.583	.369	.716	.167	.460	.133	
	.003	.040			.284		.353		.363		.365		.326		.120		.061		
2 1/2	.253	.123	.616	.191		.482		.468		.477		.472		.472		.203	.682	.204	
	.031	.118			.482		.468		.477		.472		.472		.203		.139		
1 1/2	.783	.206	.973	.246		.508		.515		.530		.530		.508		.232	.799	.214	
	.161	.239			.508		.515		.530		.530		.508		.232		.171		
1/2	.810	.195	.899	.207		.438		.454		.500		.462		.446		.198	.799	.180	
	.158	.186			.438		.454		.500		.462		.446		.180		.144		
-1/2	.560	.149	.820	.193		.423		.454		.454		.438		.423		.189	.773	.163	
	.0835	.158			.423		.454		.454		.438		.423		.178		.126		
-1 1/2	.460	.110	.758	.140		.326		.342		.342		.334		.326		.147	.667	.111	
	.0505	.106			.326		.342		.342		.334		.326		.128		.074		
-2 1/2	.198	.0195	.505	.043		.1365		.983	.123		.117		.955	.1275	.682	.042	.364	.028	
	.004	.022			.1365		.121		.117		.117		.122		.029		.010		
-3	.088	.004	.245	.001		.065		.955	.051	.955	.039	.955	.034	.940	.055	.460	.010	.183	.006
	.000	.000			.065		.049		.037		.0325		.052		.005		.001		
Σ	0.491	0.869	2.6625	2.756	2.800	2.7505	2.675	1.075	0.726										

$$\Sigma \eta \frac{1}{2} \sin \alpha \frac{fda}{fV} = 16.805$$

TEST 2A TABLE 4

Stations	-3	-2 $\frac{3}{4}$	-2 $\frac{1}{2}$	-2	-1	0	1	2	3	3 $\frac{1}{4}$
η	$\eta \frac{f \sin \alpha}{f_V}$	$\eta \frac{f \sin \alpha}{f_V}$	$\eta \frac{f \sin \alpha}{f_V}$	$\eta \frac{f \sin \alpha}{f_V}$	$\eta \frac{f \sin \alpha}{f_V}$	$\eta \frac{f \sin \alpha}{f_V}$	$\eta \frac{f \sin \alpha}{f_V}$	$\eta \frac{f \sin \alpha}{f_V}$	$\eta \frac{f \sin \alpha}{f_V}$	$\eta \frac{f \sin \alpha}{f_V}$
$\eta \frac{f \sin \alpha}{f_V}$	$\eta \frac{f \sin \alpha}{f_V}$	$\eta \frac{f \sin \alpha}{f_V}$	$\eta \frac{f \sin \alpha}{f_V}$	$\eta \frac{f \sin \alpha}{f_V}$	$\eta \frac{f \sin \alpha}{f_V}$	$\eta \frac{f \sin \alpha}{f_V}$	$\eta \frac{f \sin \alpha}{f_V}$	$\eta \frac{f \sin \alpha}{f_V}$	$\eta \frac{f \sin \alpha}{f_V}$	$\eta \frac{f \sin \alpha}{f_V}$
2	.065 .002	.124 .002	.124 .004	.361 .015	.361 .043	.250 .036	.169 .017	.091 .0125	.216 .058	.235 .032
	.000	.000	.0005	.005	.016	.009	.003	.001	.013	.0075
1 $\frac{1}{2}$.124 .0015	.169 .002	.262 .003	.626 .0555	.602 .046	.494 .036	.308 .015	.065 .012	.305 .065	.405 .0505
	.000	.000	.001	.035	.028	.018	.005	.001	.020	.0205
1	.188 .000	.205 .000	.478 .021	.810 .095	.857 .138	.857 .131	.774 .109	.420 .049	.435 .070	.560 .058
	.000	.000	.010	.077	.118	.112	.084	.021	.0305	.0325
1 $\frac{1}{2}$.305 .008	.520 .0275	.776 .117	.924 .271	.924 .390	.946 .410	.909 .380	.783 .270	.774 .182	.783 .123
	.002	.014	.0905	.250	.360	.388	.345	.212	.141	.096
-1 $\frac{1}{2}$.405 .0815	.722 .115	.871 .202	.924 .426	.935 .560	.935 .574	.899 .574	.882 .630	.857 .348	.825 .194
	.033	.083	.176	.393	.524	.536	.515	.564	.299	.160
-1 $\frac{1}{2}$.169 .044	.450 .073	.732 .136	.708 .275	.899 .388	.946 .386	.946 .383	.935 .379	.871 .231	.768 .132
	.007	.033	.100	.205	.348	.365	.362	.354	.202	.099
-2	.065 .030	.065 .030	.065 .045	.065 .091	.155 .188	.169 .195	.375 .295	.478 .334	.250 .169	.110 .059
	.002	.002	.003	.006	.029	.033	.111	.160	.037	.0065
Σ	0.044	0.132	0.381	0.971	1.423	1.461	1.425	1.313	0.7425	0.422

$$\Sigma \eta \frac{f \sin \alpha}{f_V} = 8.3145$$

TEST 3 TABLE 4

STATION	-3 1/2	-3	-2	-1	0	1	2	3	3 1/2
	$\eta \left(\frac{3}{4} \sin \alpha \frac{t da}{TV} \right)$	$\eta \left(\frac{3}{4} \sin \alpha \frac{t da}{TV} \right)$	$\eta \left(\frac{3}{4} \sin \alpha \frac{t da}{TV} \right)$	$\eta \left(\frac{3}{4} \sin \alpha \frac{t da}{TV} \right)$	$\eta \left(\frac{3}{4} \sin \alpha \frac{t da}{TV} \right)$	$\eta \left(\frac{3}{4} \sin \alpha \frac{t da}{TV} \right)$	$\eta \left(\frac{3}{4} \sin \alpha \frac{t da}{TV} \right)$	$\eta \left(\frac{3}{4} \sin \alpha \frac{t da}{TV} \right)$	$\eta \left(\frac{3}{4} \sin \alpha \frac{t da}{TV} \right)$
	$\eta \left(\frac{3}{4} \sin \alpha \frac{t da}{TV} \right)$	$\eta \left(\frac{3}{4} \sin \alpha \frac{t da}{TV} \right)$	$\eta \left(\frac{3}{4} \sin \alpha \frac{t da}{TV} \right)$	$\eta \left(\frac{3}{4} \sin \alpha \frac{t da}{TV} \right)$	$\eta \left(\frac{3}{4} \sin \alpha \frac{t da}{TV} \right)$	$\eta \left(\frac{3}{4} \sin \alpha \frac{t da}{TV} \right)$	$\eta \left(\frac{3}{4} \sin \alpha \frac{t da}{TV} \right)$	$\eta \left(\frac{3}{4} \sin \alpha \frac{t da}{TV} \right)$	$\eta \left(\frac{3}{4} \sin \alpha \frac{t da}{TV} \right)$
3	.062 .039 .367 .185 .825 .360 .882 .358 .871 .371 .930 .360 .920 .358 .716 .155 .411 .121								
	.002 .0435 .297 .316 .323 .335 .330 .111 .050								
2 1/2	.183 .097 .624 .173 .988 .474 .1 .462 .1 .472 .1 .462 .988 .464 .840 .219 .587 .1865								
	.018 .108 .469 .462 .472 .462 .458 .184 .1095								
1 1/2	.367 .1285 .763 .200 .1 .515 .1 .508 .1 .523 .1 .523 .1 .515 .871 .232 .567 .181								
	.067 .149 .515 .508 .523 .523 .515 .202 .1025								
1/2	.455 .128 .767 .176 .1 .454 .1 .476 .1 .485 .1 .470 .1 .454 .888 .198 .702 .1715								
	.058 .135 .454 .476 .485 .476 .454 .176 .1205								
-1/2	.505 .138 .778 .181 .1 .438 .1 .454 .1 .462 .1 .454 .1 .446 .888 .191 .692 .164								
	.070 .141 .438 .454 .462 .454 .454 .170 .1135								
-1 1/2	.435 .0935 .727 .137 .977 .394 .977 .338 .966 .328 .977 .330 .966 .311 .835 .140 .587 .1065								
	.041 .0995 .385 .330 .317 .322 .301 .117 .0625								
-2 1/2	.174 .013 .435 .029 .966 .134 .956 .114 .809 .099 .940 .101 .930 .107 .612 .0425 .273 .025								
	.002 .013 .1295 .110 .081 .095 .0995 .026 .007								
-3	.091 .0025 .211 .004 .940 .055 .930 .042 .899 .025 .920 .017 .899 .041 .435 .0055 .101 .003								
	.000 .001 .052 .039 .0225 .016 .037 .0025 .000								
Σ	0.238 0.690 2.7395 2.695 2.6855 2.677 2.6405 0.9885 0.5655								

$$\Sigma \eta \left(\frac{3}{4} \sin \alpha \frac{t da}{TV} \right) = 15.9195$$

TEST 3a TABLE 4

STATION	-3	$-2\frac{3}{4}$	$-2\frac{1}{2}$	-2	-1	0	1	2	3	$3\frac{1}{4}$
$\eta \frac{1}{2} \sin \alpha \frac{t_{da}}{t_v}$	$\eta \frac{1}{2} \sin \alpha \frac{t_{da}}{t_v}$	$\eta \frac{1}{2} \sin \alpha \frac{t_{da}}{t_v}$	$\eta \frac{1}{2} \sin \alpha \frac{t_{da}}{t_v}$	$\eta \frac{1}{2} \sin \alpha \frac{t_{da}}{t_v}$	$\eta \frac{1}{2} \sin \alpha \frac{t_{da}}{t_v}$	$\eta \frac{1}{2} \sin \alpha \frac{t_{da}}{t_v}$	$\eta \frac{1}{2} \sin \alpha \frac{t_{da}}{t_v}$	$\eta \frac{1}{2} \sin \alpha \frac{t_{da}}{t_v}$	$\eta \frac{1}{2} \sin \alpha \frac{t_{da}}{t_v}$	$\eta \frac{1}{2} \sin \alpha \frac{t_{da}}{t_v}$
$\eta \frac{3}{2} \sin \alpha \frac{t_{da}}{t_v}$	$\eta \frac{3}{2} \sin \alpha \frac{t_{da}}{t_v}$	$\eta \frac{3}{2} \sin \alpha \frac{t_{da}}{t_v}$	$\eta \frac{3}{2} \sin \alpha \frac{t_{da}}{t_v}$	$\eta \frac{3}{2} \sin \alpha \frac{t_{da}}{t_v}$	$\eta \frac{3}{2} \sin \alpha \frac{t_{da}}{t_v}$	$\eta \frac{3}{2} \sin \alpha \frac{t_{da}}{t_v}$	$\eta \frac{3}{2} \sin \alpha \frac{t_{da}}{t_v}$	$\eta \frac{3}{2} \sin \alpha \frac{t_{da}}{t_v}$	$\eta \frac{3}{2} \sin \alpha \frac{t_{da}}{t_v}$	$\eta \frac{3}{2} \sin \alpha \frac{t_{da}}{t_v}$
2	.033 .002	.055 .003	.275 .015	.300 .012	.165 .009	.045 .011	.177 .049	.193 .028		
	.000	.000	.004	.004	.0015	.0005	.009	.005		
$1\frac{1}{2}$.069 .000	.120 .000	.216 .000	.606 .050	.564 .048	.325 .024	.110 .010	.253 .070	.335 .042	
	.000	.000	.000	.030	.027	.008	.001	.018	.014	
1	.155 .001	.262 .002	.460 .015	.794 .091	.820 .1195	.762 .111	.682 .102	.348 .042	.348 .067	.510 .0565
	.000	.0005	.007	.072	.098	.0845	.0695	.015	.023	.030
$1\frac{1}{2}$.275 .009	.469 .026	.774 .106	.882 .252	.903 .378	.915 .388	.871 .355	.706 .249	.692 .167	.748 .117
	.0025	.012	.082	.222	.342	.355	.309	.175	.116	.0875
$-1\frac{1}{2}$.440 .089	.748 .116	.860 .198	.903 .416	.915 .561	.903 .570	.903 .570	.903 .570	.850 .329	.820 .190
	.039	.0865	.170	.376	.512	.515	.515	.515	.280	.156
$-1\frac{1}{2}$.098 .036	.450 .074	.732 .135	.722 .271	.915 .392	.924 .385	.924 .383	.924 .378	.840 .222	.748 .127
	.0035	.033	.099	.195	.369	.355	.354	.349	.189	.095
-2			.033 .032	.018 .047	.177 .199	.405 .304	.494 .338	.626 .380	.335 .172	.069 .046
			.001	.001	.036	.123	.167	.238	.0575	.003
Σ	0.045	0.132	0.359	0.900	1.388	1.449	1.423	1.293	0.6925	0.3905

$$\Sigma \eta \frac{3}{2} \sin \alpha \frac{t_{da}}{t_v} = 8.072$$

TEST 4 TABLE 4

STATION	-3 1/4	-3	-2	-1	0	1	2	3	3 1/4
$\eta \frac{1}{2} \sin \frac{t \Delta}{4V}$	$\eta \frac{1}{2} \sin \frac{t \Delta}{4V}$	$\eta \frac{1}{2} \sin \frac{t \Delta}{4V}$	$\eta \frac{1}{2} \sin \frac{t \Delta}{4V}$	$\eta \frac{1}{2} \sin \frac{t \Delta}{4V}$	$\eta \frac{1}{2} \sin \frac{t \Delta}{4V}$	$\eta \frac{1}{2} \sin \frac{t \Delta}{4V}$	$\eta \frac{1}{2} \sin \frac{t \Delta}{4V}$	$\eta \frac{1}{2} \sin \frac{t \Delta}{4V}$	$\eta \frac{1}{2} \sin \frac{t \Delta}{4V}$
$\eta \frac{3}{4} \sin \frac{t \Delta}{4V}$	$\eta \frac{3}{4} \sin \frac{t \Delta}{4V}$	$\eta \frac{3}{4} \sin \frac{t \Delta}{4V}$	$\eta \frac{3}{4} \sin \frac{t \Delta}{4V}$	$\eta \frac{3}{4} \sin \frac{t \Delta}{4V}$	$\eta \frac{3}{4} \sin \frac{t \Delta}{4V}$	$\eta \frac{3}{4} \sin \frac{t \Delta}{4V}$	$\eta \frac{3}{4} \sin \frac{t \Delta}{4V}$	$\eta \frac{3}{4} \sin \frac{t \Delta}{4V}$	$\eta \frac{3}{4} \sin \frac{t \Delta}{4V}$
3	.325 .113	.736 .337	.820 .345	.794 .360	.835 .352	.835 .358	.649 .1515	.335 .110	
	.037	.248	.282	.286	.294	.298	.098	.037	
2 1/2	.078 .064	.584 .181	.915 .460	.966 .458	.894 .454	.915 .464	.940 .456	.774 .2055	.510 .168
	.005	.1055	.421	.443	.405	.424	.428	.159	.086
1 1/2	.371 .134	.736 .233	.915 .508	.988 .505	.966 .547	.970 .520	.950 .502	.846 .220	.648 .189
	.050	.171	.508	.499	.528	.505	.476	.186	.1225
1/2	.425 .1265	.736 .192	.915 .358	.988 .485	.978 .478	.978 .456	.970 .462	.820 .190	.593 .165
	.054	.141	.358	.485	.468	.446	.446	.156	.098
-1/2	.460 .145	.727 .178	.978 .434	.988 .470	.988 .466	.978 .455	.966 .432	.810 .185	.584 .150
	.067	.1295	.424	.465	.460	.445	.417	.150	.088
-1 1/2	.390 .1035	.687 .1395	.966 .320	.966 .343	.966 .335	.970 .336	.940 .309	.794 .134	.540 .105
	.040	.096	.309	.331	.324	.326	.290	.106	.057
-2 1/2	.078 .012	.425 .027	.940 .126	.930 .1125	.924 .106	.966 .109	.930 .100	.636 .046	.259 .022
	.001	.0115	.118	.1045	.098	.105	.093	.029	.006
-3	.069 .000	.230 .013	.930 .0625	.940 .034	.899 .0245	.903 .029	.888 .041	.415 .006	.078 .001
	.000	.003	.058	.032	.022	.026	.036	.0025	.000
Σ	0.217	0.6945	2.4444	2.6415	2.591	2.571	2.484	0.8865	0.4945

$$\Sigma \eta \frac{3}{4} \sin \frac{t \Delta}{4V} = 15.024$$

TEST 4a TABLE 4

STATION	-3	-2 $\frac{3}{4}$	-2 $\frac{1}{2}$	-2	-1	0	1	2	3	3 $\frac{1}{4}$				
	$\eta \frac{3}{4} \sin \alpha \frac{t da}{TV}$	$\eta \frac{3}{4} \sin \alpha \frac{t da}{TV}$	$\eta \frac{3}{4} \sin \alpha \frac{t da}{TV}$	$\eta \frac{3}{4} \sin \alpha \frac{t da}{TV}$	$\eta \frac{3}{4} \sin \alpha \frac{t da}{TV}$	$\eta \frac{3}{4} \sin \alpha \frac{t da}{TV}$	$\eta \frac{3}{4} \sin \alpha \frac{t da}{TV}$	$\eta \frac{3}{4} \sin \alpha \frac{t da}{TV}$	$\eta \frac{3}{4} \sin \alpha \frac{t da}{TV}$	$\eta \frac{3}{4} \sin \alpha \frac{t da}{TV}$				
	$\eta \frac{3}{4} \sin \alpha \frac{t da}{TV}$	$\eta \frac{3}{4} \sin \alpha \frac{t da}{TV}$	$\eta \frac{3}{4} \sin \alpha \frac{t da}{TV}$	$\eta \frac{3}{4} \sin \alpha \frac{t da}{TV}$	$\eta \frac{3}{4} \sin \alpha \frac{t da}{TV}$	$\eta \frac{3}{4} \sin \alpha \frac{t da}{TV}$	$\eta \frac{3}{4} \sin \alpha \frac{t da}{TV}$	$\eta \frac{3}{4} \sin \alpha \frac{t da}{TV}$	$\eta \frac{3}{4} \sin \alpha \frac{t da}{TV}$	$\eta \frac{3}{4} \sin \alpha \frac{t da}{TV}$				
2	.014	0	.041	0	.291	.0205	.310	.014	.008	.202	.055	.216	.031	
	.000	.000	.000	.006	.004	.000	.000	.000	.000	.011	.007	.007	.007	
1 $\frac{1}{2}$.041	.003	.091	.005	.578	.0485	.578	.045	.031	.338	.020	.069	.002	
	.000	.0005	.000	.028	.026	.014	.007	.000	.000	.018	.016	.016	.016	
1	.183	.004	.329	.002	.567	.0275	.804	.092	.861	.139	.814	.131	.759	.118
	.001	.001	.016	.074	.120	.105	.089	.022	.029	.029	.052	.419	.052	.419
1 $\frac{1}{2}$.320	.017	.544	.0375	.804	.119	.846	.265	.930	.398	.904	.401	.924	.414
2	.005	.020	.0955	.238	.370	.362	.382	.206	.147	.099	.099	.099	.099	.099
-1 $\frac{1}{2}$.411	.086	.759	.120	.871	.199	.924	.422	.930	.572	.930	.564	.924	.570
	.035	.091	.173	.389	.532	.524	.526	.510	.293	.155	.155	.155	.155	.155
-1 $\frac{1}{2}$.024	.017	.310	.062	.598	.126	.632	.260	.896	.404	.935	.398	.946	.398
	.000	.019	.075	.164	.362	.372	.376	.376	.190	.091	.091	.091	.091	.091
-2					.132	.173	.367	.290	.400	.302	.544	.356	.225	.139
					.023	.106	.121	.193	.031	.001	.001	.001	.001	.001
Σ	0.041	0.1315	0.3595	0.899	1.437	1.483	1.501	1.307	0.719	0.401	0.401	0.401	0.401	0.401

$$\Sigma \eta \frac{3}{4} \sin \alpha \frac{t da}{TV} = 8.279$$

TEST 2 TABLE 5

[illegible]

$$\sum \eta \cos \alpha \sin \alpha \frac{fda}{4V} = 14.6275$$

TEST 2a TABLE 5

Stations	-3	-2 1/2	-2	-1	0	1	2	3	3 1/2
$\eta^2 \cos \alpha \frac{fda}{fV}$	$\eta^2 \cos \alpha \frac{fda}{fV}$	$\eta^2 \cos \alpha \frac{fda}{fV}$	$\eta^2 \cos \alpha \frac{fda}{fV}$	$\eta^2 \cos \alpha \frac{fda}{fV}$	$\eta^2 \cos \alpha \frac{fda}{fV}$	$\eta^2 \cos \alpha \frac{fda}{fV}$	$\eta^2 \cos \alpha \frac{fda}{fV}$	$\eta^2 \cos \alpha \frac{fda}{fV}$	$\eta^2 \cos \alpha \frac{fda}{fV}$
$\eta \cos \alpha \sin \alpha \frac{fda}{fV}$	$\eta \cos \alpha \sin \alpha \frac{fda}{fV}$	$\eta \cos \alpha \sin \alpha \frac{fda}{fV}$	$\eta \cos \alpha \sin \alpha \frac{fda}{fV}$	$\eta \cos \alpha \sin \alpha \frac{fda}{fV}$	$\eta \cos \alpha \sin \alpha \frac{fda}{fV}$	$\eta \cos \alpha \sin \alpha \frac{fda}{fV}$	$\eta \cos \alpha \sin \alpha \frac{fda}{fV}$	$\eta \cos \alpha \sin \alpha \frac{fda}{fV}$	$\eta \cos \alpha \sin \alpha \frac{fda}{fV}$
2	.255 .418 .002 .352 .448 .003	.352 .448 .003	.448 .001 .001	.001 .001 .001	.001 .001 .001	.001 .001 .001	.001 .001 .001	.001 .001 .001	.001 .001 .001
1 1/2	.352 .448 .001 .001 .001	.448 .001 .001	.001 .001 .001	.001 .001 .001	.001 .001 .001	.001 .001 .001	.001 .001 .001	.001 .001 .001	.001 .001 .001
1	.448 .001 .001 .001 .001	.001 .001 .001	.001 .001 .001	.001 .001 .001	.001 .001 .001	.001 .001 .001	.001 .001 .001	.001 .001 .001	.001 .001 .001
1/2	.552 .418 .008 .721 .978 .0275	.978 .0275 .000	.000 .000 .000	.000 .000 .000	.000 .000 .000	.000 .000 .000	.000 .000 .000	.000 .000 .000	.000 .000 .000
-1/2	.636 .848 .0815 .850 .834 .115	.834 .115 .020	.020 .004	.004 .000	.000 .000	.000 .000	.000 .000	.000 .000	.000 .000
-1	.411 .454 .044 .670 .666 .073	.666 .073 .020	.020 .008	.008 .001	.001 .001	.001 .001	.001 .001	.001 .001	.001 .001
-2	.255 .105 .030 .255 .105 .030	.255 .105 .001	.001 .001	.001 .001	.001 .001	.001 .001	.001 .001	.001 .001	.001 .001
Σ	0.058	0.1245	0.327	0.828	1.1825	1.2025	1.076	0.465	0.3435

$$\Sigma \eta \cos \alpha \sin \alpha \frac{fda}{fV} = 6.8065$$

TEST 3 TABLE 5

[illegible]

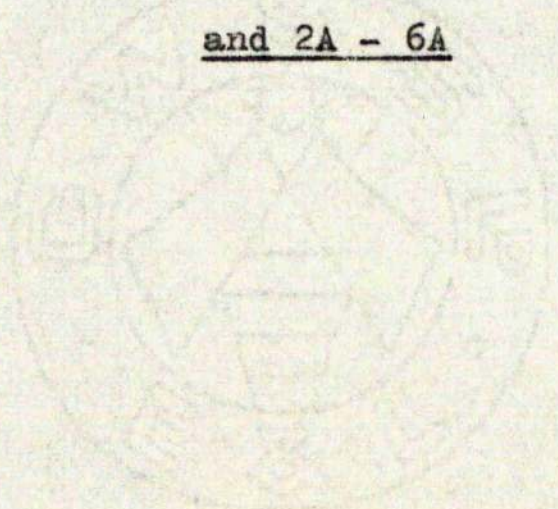
$$\sum A \cos \alpha \cdot \sin \alpha \frac{fda}{IV} = 14.081$$

TEST 4a TABLE 5

	-3	-2 1/2	-2 1/4	-2	-1	0	1	2	3	3 1/2
$\frac{1}{2}$	$\frac{1}{2}$ Cos $\frac{f}{V}$	$\frac{1}{2}$ Cos $\frac{f}{V}$	$\frac{1}{2}$ Cos $\frac{f}{V}$	$\frac{1}{2}$ Cos $\frac{f}{V}$	$\frac{1}{2}$ Cos $\frac{f}{V}$	$\frac{1}{2}$ Cos $\frac{f}{V}$	$\frac{1}{2}$ Cos $\frac{f}{V}$	$\frac{1}{2}$ Cos $\frac{f}{V}$	$\frac{1}{2}$ Cos $\frac{f}{V}$	$\frac{1}{2}$ Cos $\frac{f}{V}$
2										
1 1/2										
1										
1/2										
-1/2										
-1										
-2										
Σ	0.059	0.1295	0.3155	0.7125	1.162	1.157	1.159	0.9575	0.643	0.3825

$$\Sigma \frac{1}{2} \cos \frac{f}{V} = 6.7475$$

Series 2
Tests 2 - 6
and 2A - 6A



TEST No: - 2

MACH No. - 6

BAROMETRIC PRESS = 14.5 18/100

$P_1 = 24.3 \text{ LB/IN}^2 \text{ AB}$

$P_2 = 19.3 \text{ LB/IN}^2 \text{ AB}$

TEMP. 360°F.

STATIONS	$-3\frac{3}{4}$		$-3\frac{1}{2}$		$-3\frac{1}{4}$		-3		-2		-1		0		1		2		3		$3\frac{1}{4}$	
	P_3	α	P_3	α	P_3	α	P_3	α	P_3	α	P_3	α	P_3	α	P_3	α	P_3	α	P_3	α	P_3	α
$2\frac{3}{4}$							19.9	70	20.4	69	21.2	65	21.4	67	20.8	78	19.8	85				
$2\frac{1}{2}$													24	46	24	48	23.5	51	20.7	57	19.5	56
2	19.7	45	20.5	45	22.5	45	23.6	45	24.3	43	24.3	41	24.3	41	24.3	42	23.9	43	21.2	48	19.6	48
1	19.9	21	21.5	28	23.7	32	24.3	33	24.3	32	24.3	30	24.3	31	24.3	33.5	24.3	33	24.2	32.5	21.3	24.5
0	20	18.5	21.5	25	23	25	24.3	26	24.3	28.5	24.3	29.5	24.3	30.5	24.3	30	24.3	24	21.5	30	20.1	17
-1	20.3	22	21.5	22	23.3	23.5	24.2	24.5	24.3	25.5	24.3	25.5	24.3	26.5	24.3	25.5	24.2	24.5	21.5	25.5	20.5	25.5
-2	20	18	21	18	22.6	18.5	23.7	19	24.3	19	24.3	20	24.3	20	24.3	21	24	19	21.3	19	20.3	18
-3			20.5	10	21.4	10	23	12	24.3	11	24.3	11	24.3	12	24.3	12	24	13	20.3	7	19.8	7
-4			19.5	-5	20.1	-5	21	0	24.3	7	24.3	6	24.3	7	24.3	9	24.3	8	20.5	8	19.7	8
$-4\frac{1}{2}$					19.7	8.5	20.6	-3	24.3	4.5	24.3	4	24.3	6	24.3	6	23.7	5.5	19.7			

TEST No.: -2A

MACH. No. 6

BAROMETRIC PRESS = 14.3 LB/IN^2 $P_1 = 24.3 \text{ LB/IN}^2 \text{ Ab.}$ $P_2 = 19.3 \text{ LB/IN}^2 \text{ Ab.}$

°F

TEMP.

STATIONS	$-1\frac{3}{4}$		$-1\frac{1}{2}$		$-1\frac{1}{4}$		-1		$-\frac{1}{2}$		0		$\frac{1}{2}$		1		2		3		$3\frac{1}{2}$		4		$4\frac{1}{4}$		$4\frac{1}{2}$	
	P_3	α	P_3	α	P_3	α	P_3	α	P_3	α	P_3	α	P_3	α	P_3	α	P_3	α	P_3	α	P_3	α	P_3	α	P_3	α	P_3	α
$1\frac{1}{2}$	-	-	19.5	-	19.5	-	20.1	5	20.6	3	20.3	1	20.1	-2	19.7	-2	19.3	-	19.3	-	19.4	15	19.8	17	19.8	12		
1	-	-	19.3	-	20.2	7	21.5	10	20.9	2	21	5	20.8	3	20.4	2	19.7	-1	19.3	-	19.4	8	19.5	16	20.8	21	20.7	19
$\frac{1}{2}$	19.3	-	19.6	7	20.9	9.5	22.3	10	21.9	7	22.2	9	22.3	10	22.3	10	21.7	8	20.8	9	20.4	10	20.7	17	21.7	20	22.2	21
0	11	20.8	23.2	16.5	23.4	15	23.3	13	23.3	13	23.3	16	23.6	21	23.9	23	23.8	24	23.4	20	23.1	19	22.9	18	22.8	19	22.8	19.5
-1	21.8	23	23	18	23.6	31	23.8	31	23.9	32	23.9	31	23.7	30	23.9	34	23.8	34	23.6	33	23.5	34	23.5	33	23.3	31	23	31
-2	21.5	48	23.1	45	23.5	45	23.7	46	23.9	46	23.9	47	23.6	46	23.9	46	23.7	46	23.6	46	23.6	46	23.4	46	23	47	22.4	48
$-2\frac{1}{2}$	19.6	73	21.2	70	22.4	66	24.2	66	23.8	64	23.8	63	23.8	62	23.8	52	23.2	60	23.8	59	23.8	59	23.8	62	21.2	69	19.2	70
$-2\frac{3}{4}$	19.2	8	19.2	80	20.1	79	20.8	79	20.4	78	22.1	76	22.2	77	22.8	74.5	23.4	70.5	23.5	68	21.8	75	19.5	75	-	-	-	-

TEST No. :- 2

MACH No. :- 6

BAROMETRIC PRESS = 14.5 LB/IN²P₁ = 24.3 LB/IN² Ab.P₂ = 19.3 LB/IN² Ab.

TEMP. 380°F.

STATIONS	-3 3/4	-3 1/2	-3 1/4	-3	-2	-1	0	1	2	3	3 1/4
	$\frac{P_1}{P_2}$	$\frac{P_1}{P_2}$	$\frac{P_1}{P_2}$	$\frac{P_1}{P_2}$	$\frac{P_1}{P_2}$	$\frac{P_1}{P_2}$	$\frac{P_1}{P_2}$	$\frac{P_1}{P_2}$	$\frac{P_1}{P_2}$	$\frac{P_1}{P_2}$	$\frac{P_1}{P_2}$
2 3/4				.969	.946	.91	.901	.927	.974	.12	
2 1/2	.965	.965	.905	.873	.814	.807	.804	.955	.821	.865	.931
2	.98	.942	.857	.817	.794	.794	.794	.794	.807	.937	.91
1	.97	.897	.814	.794	.794	.794	.794	.794	.794	.992	.985
0	.965	.897	.839	.794	.794	.794	.794	.794	.794	.992	.905
-1	.951	.897	.828	.797	.794	.794	.794	.794	.794	.992	.941
-2	.965	.919	.854	.814	.794	.794	.794	.794	.804	.955	.949
-3		.942	.902	.839	.775	.794	.794	.794	.804	.955	.974
-4		.989	.96	.918	.794	.794	.794	.794	.794	.955	.98
-4 1/4			.98	.937	.794	.794	.794	.794	.814	.901	.96

Test No. :- 29.

MACH. No. 6

BAROMETRIC PRESS - 14.3

$$P = 24.3 \text{ LB} / \text{IN}^2 \text{ Ab.}$$

$P_2/P_1 = LB/IN^2 \text{ Ab.}$

1892

[illegible]

TEST No: -3

MACH No. 7

BAROMETRIC PRESS = 14.38 LB/IN²P₁ = 24.3 LB/IN² Ab.P₂ = 17.88 LB/IN² Ab. TEMP. 380°F.

STATIONS	-3 $\frac{3}{4}$	-3 $\frac{1}{2}$	-3 $\frac{1}{4}$	-3	-2	-1	0	1	2	3	3 $\frac{1}{4}$
	P ₃ α	P ₃ α	P ₃ α	P ₃ α	P ₃ α	P ₃ α	P ₃ α	P ₃ α	P ₃ α	P ₃ α	P ₃ α
2 $\frac{3}{4}$		18.18 57	19.28 57	19.68 63	20.98 64.5	21.38 60	21.98 60.5	21.38 62	19.58 62	18.78 62	17.78
2 $\frac{1}{2}$		18.38 59	20.28 59	21.38 59	22.78 55.5	23.78 51.5	23.78 50.5	23.78 51.5	22.48 56	19.68 55	17.78
2	18.78 45	18.78 45	21.88 45	23.18 45	24.3 42	24.3 40	24.3 40	24.3 41	23.98 42	21.28 44	18.58 45
1	18.58 25	20.58 29	22.78 29	23.78 31	24.3 31.5	24.3 32	24.3 30.5	24.3 33.5	24.3 33.5	21.78 33	17.68 33
0	18.88 29	20.88 29	22.78 28	23.58 30	24.3 29	24.3 32	24.3 28	24.3 29	24.3 27.5	21.78 29	20.88 29
-1	19.38 24.5	20.88 25	22.58 27	23.48 25	24.3 26	24.3 27	24.3 27	24.3 27	23.78 24	21.68 24.5	19.68 23
-2	18.68 13	20.18 18	22.08 18.5	24.29 17.5	24.3 18.5	24.3 18.5	24.3 18	24.3 19	23.88 18	20.78 18	19.08 15
-3	18.18 5	18.7 7	20.2 9	22 11	24.3 10.5	24.3 12.5	24.3 11	24.3 11	24.3 10.5	19.3 5	18 5
-4		18 -2	18.4 -3	19.5 0	24.3 4	24.3 2	24.3 2	24.3 3	23.9 2	19.1 1	17.9 1
-4 $\frac{1}{4}$		18.3 -1	18.3 -1	19.3 -1	24.3 6	24.3 2.5	24.3 4	24.3 3.5	23.4 6	18.1 6	

TEST No: 3A-

MACH. No. 7

BAROMETRIC PRESS = 14.4 LB/IN²

P₁ = 243 LB/IN² Ab.

P₂ = 1788 LB/IN² Ab.

TEMP. 380. °F

STATION	-1 3/4	-1 1/2	-1 1/4	-1	-1/2	0	1/2	1	2	3	3 1/2	4	4 1/4	4 1/2
	P ₂ α P ₃	P ₂ α P ₃	P ₂ α P ₃	P ₂ α P ₃	P ₂ α P ₃	P ₂ α P ₃	P ₂ α P ₃	P ₂ α P ₃	P ₂ α P ₃	P ₂ α P ₃	P ₂ α P ₃	P ₂ α P ₃	P ₂ α P ₃	P ₂ α P ₃
1 1/2	177	178	179	180	181	182	183	184	185	186	187	188	189	190
1	183	184	185	186	187	188	189	190	191	192	193	194	195	196
1/2	189	190	191	192	193	194	195	196	197	198	199	200	201	202
0	195	196	197	198	199	200	201	202	203	204	205	206	207	208
-1	201	202	203	204	205	206	207	208	209	210	211	212	213	214
-2	207	208	209	210	211	212	213	214	215	216	217	218	219	220
-3	213	214	215	216	217	218	219	220	221	222	223	224	225	226
-4	219	220	221	222	223	224	225	226	227	228	229	230	231	232
-5	225	226	227	228	229	230	231	232	233	234	235	236	237	238
-6	231	232	233	234	235	236	237	238	239	240	241	242	243	244
-7	237	238	239	240	241	242	243	244	245	246	247	248	249	250
-8	243	244	245	246	247	248	249	250	251	252	253	254	255	256
-9	249	250	251	252	253	254	255	256	257	258	259	260	261	262
-10	255	256	257	258	259	260	261	262	263	264	265	266	267	268

TEST No. :- 3

MACH No. 7

BAROMETRIC PRESS.

$P_1 = 24.3 \text{ LB/IN}^2 \text{ AB.}$

$P_2 = 17.88 \text{ LB/IN}^2 \text{ AB.}$

TEMP. 380°F.

STATIONS	$-3\frac{3}{4}$	$-3\frac{1}{2}$	$-3\frac{1}{4}$	-3	-2	-1	0	1	2	3	$3\frac{1}{4}$
	$\frac{P}{P_1}$	$\frac{P}{P_1}$	$\frac{P}{P_1}$	$\frac{P}{P_1}$	$\frac{P}{P_1}$	$\frac{P}{P_1}$	$\frac{P}{P_1}$	$\frac{P}{P_1}$	$\frac{P}{P_1}$	$\frac{P}{P_1}$	$\frac{P}{P_1}$
$2\frac{3}{4}$.984 .05	.926 .755	.909 .315	.853 .525	.799 .74	.814 .478	.837 .586	.918 .282	.958 .157	.959
$2\frac{1}{2}$.947 .547	.88 .42	.837 .557	.785 .792	.745 .957	.753 .925	.753 .915	.787 .786	.91	.311
2	.984 .05	.942 .2	.816 .475	.782 .845	.735 .1	.735 .1	.735 .1	.735 .1	.748 .945	.839 .58	.962 .125
1	.963 .122	.87 .457	.784 .797	.752 .928	.735 .1	.735 .1	.735 .1	.735 .1	.735 .1	.814 .578	.908 .318
0	.847 .547	.854 .52	.784 .797	.758 .902	.735 .1	.735 .1	.735 .1	.735 .1	.735 .1	.821 .65	.886 .4
-1	.923 .265	.854 .52	.792 .766	.762 .89	.735 .1	.735 .1	.735 .1	.735 .1	.735 .1	.823 .642	.908 .318
-2	.957 .142	.885 .405	.809 .697	.735 .1	.735 .1	.735 .1	.735 .1	.735 .1	.735 .1	.821 .65	.939 .212
-3	.984 .05	.955 .15	.845 .405	.612 .685	.735 .1	.735 .1	.735 .1	.735 .1	.735 .1	.926 .255	.992 .025
-4		.992 .025	.913 .086	.917 .288	.735 .1	.735 .1	.735 .1	.735 .1	.747 .95	.908 .035	.918 .005
-4 1/4			.917 .072	.925 .26	.735 .1	.735 .1	.735 .1	.735 .1	.754 .92	.908 .035	

TEST No. :- 3A.

MACH. No. 0.7

$P_1 = 24.3 \text{ LB/IN}^2 \text{ AB.}$

BAROMETRIC PRESS. = 14.4

$P_2 = 7.8 \text{ LB/IN}^2 \text{ AB.}$

TEMP. 380. °F

STATION	$-1\frac{3}{4}$	$-1\frac{1}{2}$	$-1\frac{1}{4}$	-1	$-\frac{1}{2}$	0	$\frac{1}{2}$	1	2	3	$3\frac{1}{2}$	4	$4\frac{1}{2}$	$4\frac{1}{2}$
	P_1	P_2	P_3	P_1	P_2	P_3	P_1	P_2	P_3	P_1	P_2	P_3	P_1	P_2
$1\frac{1}{2}$	S	S	S	994.017	994.017	994.017	994.017	994.017	994.017	994.017	994.017	994.017	994.017	994.017
1	994.017	994.017	994.017	994.017	994.017	994.017	994.017	994.017	994.017	994.017	994.017	994.017	994.017	994.017
$\frac{1}{2}$	994.017	994.017	994.017	994.017	994.017	994.017	994.017	994.017	994.017	994.017	994.017	994.017	994.017	994.017
0	994.017	994.017	994.017	994.017	994.017	994.017	994.017	994.017	994.017	994.017	994.017	994.017	994.017	994.017
-1	994.017	994.017	994.017	994.017	994.017	994.017	994.017	994.017	994.017	994.017	994.017	994.017	994.017	994.017
-2	994.017	994.017	994.017	994.017	994.017	994.017	994.017	994.017	994.017	994.017	994.017	994.017	994.017	994.017
$-2\frac{1}{2}$	994.017	994.017	994.017	994.017	994.017	994.017	994.017	994.017	994.017	994.017	994.017	994.017	994.017	994.017
$-2\frac{3}{4}$	994.017	994.017	994.017	994.017	994.017	994.017	994.017	994.017	994.017	994.017	994.017	994.017	994.017	994.017

TEST No: - 4

MACH No. . 8

BAROMETRIC PRESS = 14.4510/in² $P_1 = 24.3$ LB/IN² Ab. $P_2 = 16.35$ LB/IN² Ab.

TEMP. 380°F.

STATIONS	$-3\frac{3}{4}$		$-3\frac{1}{2}$		$-3\frac{1}{4}$		-3		-2		-1		0		1		2		3		$3\frac{1}{4}$		
	p_3	α	p_3	α	p_3	α	p_3	α	p_3	α	p_3	α	p_3	α	p_3	α	p_3	α	p_3	α	p_3	α	
$2\frac{3}{4}$	SS		16.78		17.48	66	18.38	66	19.88	65	21.08	62	20.98	60	19.98	61	18.58	65	17.18	65	SS		
$2\frac{1}{2}$	SS		16.88		19.08	59	20.48	59	22.58	56.5	23.98	52.5	23.98	51	23.88	52.5	22.38	59	18.88	58.5	SS		
2	SS		16.98	46	19.08	46	23.18	46	24.18	42	24.3	41.5	24.3	41.5	24.3	42.5	23.98	44	20.78	47.5	16.38		
1	SS		19.45	29	22.05	30	23.65	32	24.3	33.5	24.3	33	24.3	35	24.3	34	24.05	35	21.75	33	17.55	33.5	
0		16.45	26.5	19.75	26.5	22.65	27	23.55	28.5	24.3	30	24.3	29	24.3	27.5	24.3	30	23.95	32	21.45	30.5	19.25	27
-1	SS		20.15	25	22.25	27	23.25	27	24.3	27	24.3	28	24.3	29	24.3	27	24.15	26	21.45	26	19.45	26	
-2		17.18	19	19.38	19	21.78	23	23.28	23	24.3	21	24.3	19.5	24.3	20	24.3	20	24.08	19.5	20.58	20	18.28	22
-3	SS		17.28	12	19.28	10	21.78	12	24.3	8	24.3	10	24.3	10	24.3	10	24.3	11	19.38	11	SS		
-4	SS		16.48		17.18	3	18.38	-5	24.3	1.5	24.3	-1	23.98	-1	24.08	1	23.58	5	16.58	5			
$-4\frac{1}{4}$			16.38		16.68		18.38	-8	23.98	1.	23.98	1.5	24.3	-2	24.3	1.5	23.08	1.		SS			

TEST No: -4a

MACH. No. 8

$P_1 = 24.3 \text{ LB/IN}^2 \text{ Ab.}$

BAROMETRIC PRESS = 14.38 LB/IN^2

$P_2 = 16.35 \text{ LB/IN}^2 \text{ Ab.}$

TEMP. 380 °F

STATIONS	-1 3/4	-1 1/2	-1 1/4	-1	-1/2	0	1/2	1	2	3	3 1/2	4	4 1/4	4 1/2
	$P_3 \propto$	$P_3 \propto$	$P_3 \propto$	$P_3 \propto$	$P_3 \propto$	$P_3 \propto$	$P_3 \propto$	$P_3 \propto$	$P_3 \propto$	$P_3 \propto$	$P_3 \propto$	$P_3 \propto$	$P_3 \propto$	$P_3 \propto$
1 1/2	-	-	16.98	18.38	18.38	17.68	17.38	17.08	-	-	-	17.78	17.78	17.38
1	-	-	18.48	20.78	19.38	18.88	18.88	18.88	17.28	17.08	16.78	18.08	19.28	18.88
1/2	16.88	17.58	19.78	21.38	20.28	21.28	21.38	21.78	20.98	19.08	18.68	19.38	20.48	20.78
0	17.88	19.28	22.28	22.58	22.38	22.98	23.28	23.38	23.3	22.48	22.08	22.08	22.08	21.48
-1	19.48	22.08	22.98	23.18	23.38	23.38	23.38	23.18	22.48	22.78	22.78	22.48	22.18	21.58
-2	19.08	21.78	22.78	22.48	23.28	23.38	23.18	23.18	22.78	23.08	23.08	22.58	21.68	19.88
-2 1/2	17.48	19.58	21.18	20.18	21.68	22.28	22.38	22.78	22.88	23.08	23.48	21.38	18.18	-
-2 3/4	17.78	17.38	18.48	17.88	19.78	21.08	21.08	21.38	22.48	23.04	22.48	19.28	17.78	-

TEST No:- 4

MACH No. 0.8

BAROMETRIC PRESS -

 $P_2 = 24.3 \text{ LB/IN}^2 \text{ AB.}$ $P_2 = 16.35 \text{ LB/IN}^2 \text{ AB.}$

TEMP. - °F.

STATICS	$-3\frac{3}{4}$		$-3\frac{1}{2}$		$-3\frac{1}{4}$		-3		-2		-1		0		1		2		3		$3\frac{1}{4}$	
	P_3	P_3	P_3	P_3	P_3	P_3	P_3	P_3	P_3	P_3	P_3	P_3	P_3	P_3	P_3	P_3	P_3	P_3	P_3	P_3	P_3	P_3
$2\frac{3}{4}$	S	976	045	935	16	892	295	824	50	796	652	781	835	82	511	881	327	954	101	S	S	S
$2\frac{1}{2}$	S	97	06	858	398	797	585	726	816	684	986	684	986	685	96	734	79	866	374	S	S	S
2	S	965	072	858	398	707	882	678	983	673	1-0	673	1-0	673	1-0	684	962	788	615	S	S	S
1	S	844	45	742	765	691	946	673	1-0	673	1-0	673	1-0	673	1-0	684	962	788	615	S	S	S
0	S	827	49	721	832	695	925	673	1-0	673	1-0	673	1-0	673	1-0	684	962	788	615	S	S	S
-1	S	812	534	735	786	704	844	673	1-0	673	1-0	673	1-0	673	1-0	684	962	788	615	S	S	S
-2	S	105	501	556	727	701	905	673	1-0	673	1-0	673	1-0	673	1-0	684	962	788	615	S	S	S
-3	S	946	126	849	425	752	731	673	1-0	673	1-0	673	1-0	673	1-0	684	962	788	615	S	S	S
-4	S	992	012	953	109	89	30	673	1-0	673	1-0	673	1-0	673	1-0	684	962	788	615	S	S	S
$-4\frac{1}{4}$	S	999	0	981	035	89	30	684	982	684	982	673	1-0	673	1-0	684	962	788	615	S	S	S

Test No :- 4a

MACH. No. 8

BAROMETRIC PRESS = 14.38

$P = 243 \text{ LB} / \text{IN}^2 \text{ AB.}$

$$P_2 = 11.35 \text{ LB/IN}^2 \text{ Ab.}$$

TEMP.

STATION	-1 3/4	-1 1/2	-1 1/4	-1	-1/2	0	1/2	1	2	3	3 1/2	4	4 1/4	4 1/2
1 1/2	-	-	964	975-89	30	89	30	925	192	742	765	958	091	-
1	-	-	886	312-807	552-858	897-867	371	867	371	905	256	947	125	958
1/2	97	06	93	175-827	49	766	685	807	552	763	677	765	687	768
0	915	229	899	325	733	792	715	82	731	80	713	86	702	901
-1	832	476	74	772	702	865	707	822	7	907	7	907	706	82
-2	858	377	752	734	718	844	72	836	700	901	7	907	706	882
-2 1/2	997	155	836	465	773	662	811	54	721	832	734	79	731	80
-2 3/4	976	049	942	14	889	318	915	225	821	49	775	656	775	652

TEST No. - 5

MACH No. .9

BAROMETRIC PRESS = 14.38 LB/IN²P₁ = 30 LB/IN² AB.P₂ = 18.38 LB/IN² AB.

TEMP. -380°F.

STATIONS	-3 $\frac{3}{4}$		-3 $\frac{1}{2}$		-3 $\frac{1}{4}$		-3		-2		-1		0		1		2		3		3 $\frac{1}{4}$	
	P ₃	α	P ₃	α	P ₃	α	P ₃	α	P ₃	α	P ₃	α	P ₃	α	P ₃	α	P ₃	α	P ₃	α	P ₃	α
2 $\frac{3}{4}$	SS		18.88		21.18	60	22.18	66	24.28	67	27.18	62	27.18		24.28	67.5	21.78	67	19.78	60	SS	
2 $\frac{1}{2}$	18.78		19.38	6.1	23.08	61	35.58	66	26.98	64.5	28.88	56	29.48	61.5	27.68	61.5	25.48	64	21.68	62	18.88	1.2
2	18.88		20.78	4.8	26.58	47	21.08	47	30	44	30	42	30	42	30	43.5	29.88	47	25.88	48	20.48	4.8
1	21.08		23.68	3.1	27.58	35.5	29.28	33	29.88	34.5	30	34.5	30	34	29.48	35.5	29.38	35.5	25.98	33.5	21.88	32.5
0	20.68		24.48	2.7	27.58	27	29.28	28.5	30	30	30	31.5	30	31.5	30	31.5	30	29	26.68	30	23.38	27.5
-1	20.78	23	24.68	2.5	27.38	25	28.88	26	30	27.5	30	28	29.88	29	30	29	29.28	27	26.18	26	23.68	24
-2	20.88	19	23.88	1.9	27.48	20	29.28	19	30	19	30	19.5	30	19.5	30	21	29.88	20	25.38	21	21.98	2.1
-3	20.28	9	20.88	6	24.28	10	27.58	11	30	10	30	9.5	30	9	30	9	29.88	10	21.48	8	19.28	8
-4			19.28		19.38	-5		-1	29.88	-1.5	29.58	-2	29.38	-6.5	29.78	-3	29.28	4	19.18	-2	SS	
-4 $\frac{1}{4}$							19.18		25.78	3	25.78	-3	24.98	-5.1	25.98	-2	25.68	3	19.48			

TEST No: - 5a

MACH. No. 9

$P_1 = 30 \text{ LB/IN}^2 \text{ Ab.}$

14.38

BAROMETRIC PRESS = ~~14.38~~ LB/IN^2

$P_2 = 18.38 \text{ LB/IN}^2 \text{ Ab.}$

TEMP. 380 °F

STATIONS	-1 3/4	-1 1/2	-1 1/4	-1	-1/2	0	+1/2	1	2	3	3 1/2	4	4 1/4	4 1/2
	$P_3 \propto$	$P_3 \propto$	$P_3 \propto$	$P_3 \propto$	$P_3 \propto$	$P_3 \propto$	$P_3 \propto$	$P_3 \propto$	$P_3 \propto$	$P_3 \propto$	$P_3 \propto$	$P_3 \propto$	$P_3 \propto$	$P_3 \propto$
1 1/2	18.45 0	19.05 0	20.65 6	23.35 8	24.95 0	26.15 -1	26.65 -1	27.35 -1	28.75 -2	18.55 -2	18.55 -1	20.75 15	21.45 13	20.15 11
1	18.85 0	19.65 4	20.75 14	21.35 9	23.25 1	24.05 15	24.15 6	23.95 5	21.05 2	19.45 2	19.65 7	22.45 14	21.45 18	23.65 15
1/2	19.25 -1	20.75 9	21.05 14	21.65 10	21.15 6	21.75 11	21.55 12	21.45 12	21.65 13	22.65 9	20.65 11	25.45 15	21.75 19	21.35 18
0.	20.65 0	23.35 15	28.05 18	28.75 16	28.45 14	28.75 18	28.65 21	28.75 22	28.75 23	27.55 19	27.45 18	27.45 20	27.65 20	27.15 21
-1	21.15 25	27.15 29	28.55 32	28.85 32	28.45 33	28.15 33	28.95 34	28.65 33	28.75 34	28.85 35	28.25 35	27.45 33	27.75 33	26.15 33
-2	21.85 55	26.55 51	27.45 50	27.45 51	28.65 50	28.95 50	28.95 49	28.75 49	28.75 49	28.65 48	28.25 47	27.55 47	26.05 48	23.45 60
-2 1/4	19.25 74	20.65 76	21.15 72	22.35 72	21.45 74	21.05 73	21.05 71	21.65 69	20.25 65	20.35 66	20.15 63	25.05 66	21.05 70	18.65 73
-2 3/4	18.45 81	19.35 80	21.15 78	20.65 78	21.95 82	21.45 82	21.45 81	21.65 79	20.65 77	21.45 75	21.05 72	23.25 78	20.65 80	-

TEST No:- 5

MACH No. 0.9

BAROMETRIC PRESS = $14.38 \cdot 16 / \text{IN}^2$ $P_1 = 30 \text{ LB} / \text{IN}^2 \text{ Ab.}$ $P_2 = 18.38 \text{ LB} / \text{IN}^2 \text{ Ab.}$

TEMP. - °F.

STATIONS	-3 3/4	-3 1/2	-3 1/4	-3	-2	-1	0	1	2	3	3 1/4														
	P_3	P_3	P_3	P_3	P_3	P_3	P_3	P_3	P_3	P_3	P_3														
2 3/4	S	.972	.06	.868	.306	.83	.40	.755	.592	.845	.362	.927	.162	S	S										
2 1/2	.977	.05	.948	.12	.795	.488	.72	.685	.681	.787	.635	.43	.623	.675	.84	.72	.684	.847	.357	.973	.057				
2	.974	.055	.885	.265	.692	.756	.67	.541	.667	.83	.631	.944	.615	.995	.612	1.0	.612	.997	.709	.712	.896	.237			
1	.872	.246	.775	.541	.667	.83	.631	.944	.615	.995	.612	1.0	.612	.997	.709	.712	.896	.237	.057	.38					
0	.886	.262	.75	.605	.667	.83	.631	.944	.612	1.0	.612	1.0	.612	1.0	.612	1.0	.612	1.0	.688	.766	.786	.511			
-1	.885	.265	.745	.617	.672	.815	.636	.926	.612	1.0	.612	1.0	.612	1.0	.612	1.0	.612	1.0	.655	.704	.725	.809	.452		
-2	.88	.277	.77	.555	.668	.827	.634	.944	.612	1.0	.612	1.0	.612	1.0	.612	1.0	.612	1.0	.615	.995	.724	.674	.837	.381	
-3	.905	.216	.88	.277	.756	.59	.666	.833	.612	1.0	.612	1.0	.612	1.0	.612	1.0	.612	1.0	.615	.995	.858	.337	.952	.105	
-4	S	S	.953	.101	.946	.116	.868	.306	.615	.519	.95	.516	.125	.612	1.0	.612	1.0	.612	1.0	.615	.995	.858	.337	.952	.105
-4 1/4	S	S	S	S	S	S	.957	.660	.615	.519	.95	.516	.125	.612	1.0	.612	1.0	.612	1.0	.615	.995	.858	.337	.952	.105

TEST No: -5a-

MACH. No. 9

BAROMETRIC PRESS = 14.38 LB/IN²

P₁ = 30 LB/IN² AB

P₂ = 1838 LB/IN² AB

TEMP. 380 °F

STATIONS	-3/4	-1 1/2	-1 1/4	-1	-1/2	0	1/2	1	2	3	3 1/2	4	4 1/4	4 1/2
	P ₃	P ₃	P ₃	P ₃	P ₃	P ₃	P ₃	P ₃	P ₃	P ₃	P ₃	P ₃	P ₃	P ₃
1 1/2	995.008	964.075	894.241	787.508	837.38	848.305	881.875	903.22	98.207	991.016	991.016	885.265	848.5	836.1
1	975.05	935.141	757.590	697.742	77.552	763.572	761.576	783.518	872.276	845.116	935.141	817.431	744.62	652
1/2	954.10	885.265	705.762	664.838	702.73	673.812	667.83	677.798	686.766	804.666	804.666	736.699	736.699	744
0	889.255	786.51	654.87	639.92	645.898	639.92	636.926	639.92	639.92	639.92	677.798	644.839	659.854	673.812
-1	761.576	676.80	604.902	636.926	646.946	63.946	635.93	636.926	639.92	636.926	65.882	659.854	673.812	699.737
-2	84.372	692.756	669.825	669.825	636.926	635.93	635.93	635.93	635.93	636.926	65.882	647.83	705.721	783.519
-2 1/2	954.10	88	275.761	576.522	47.702	673.812	795.679	667.83	65.882	648.89	653.872	732.652	873.293	989.02
-2 3/4	995.008	949.11	865.313	889.255	8.475	761.576	745.617	788.694	75.677	798.679	795.824	444.974	052	5

TEST No. :- 6

MACH No. - 97

BAROMETRIC PRESS - 14.3

$P_1 = 32.5 \text{ LB/IN}^2 \text{ AB.}$

$P_2 = 18.3 \text{ LB/IN}^2 \text{ AB.}$

TEMP. - $^{\circ}\text{F.}$

STATIONS	$-3\frac{3}{4}$		$-3\frac{1}{2}$		$-3\frac{1}{4}$		-3		-2		-1		0		1		2		3		$3\frac{1}{4}$	
	P_3	α	P_3	α	P_3	α	P_3	α	P_3	α	P_3	α	P_3	α	P_3	α	P_3	α	P_3	α	P_3	α
$2\frac{3}{4}$	-	-	18.7	-	22.3	62	23.5	65	25.4	64.5	26.7	60.5	29	60	25.3	67	22.5	67	19.6	57	-	-
$2\frac{1}{2}$	-	-	19.4	60	26	53	29.1	55.5	31.5	53	32.5	47	32.5	46.5	32.1	51	30.2	57	22.5	60	-	$7\frac{1}{2}$
2	19.8	-	22.9	40.5	29.2	39	31.5	40	32.5	40	31.5	39	32.5	39	32.5	40	32.1	41	27.5	42	20.5	43
1	19.8	31	25	32	30	31	31.6	23	32.5	35	32.5	35	32.5	35	32.5	35	32.3	35	28.2	33.5	22.5	34
0	20.8	28	26.7	28	20.6	28	32	27	32.5	30.5	32.5	31	32.5	32	32.5	31	32.3	30	26.4	27.5	24.3	28.5
-1	21.8	28	26.2	26	29.2	27	30.7	28	32.3	27	32.5	27	32.5	28.5	32.3	27.5	31.5	27.5	26.8	27	22.7	27
-2	19.8	15	23.6	18	27.9	19	30.4	19.5	32.3	19	32.5	19	32.5	20	32.4	21	31.4	22	24.7	18	21	18
-3	19.35		20.7	4	25	8.5	24.6	10	32.5	8	32.5	10	32.5	8.5	32.5	10	32.2	8.5	22.8	9	19.6	7
-4			18.8	-	19.7	-9.5	22.4	-2	32.3	1	31.2	-8	29.7	-5.5	31.7	-5.5	31.6	-8	18.9	-4	-	-
$-4\frac{1}{4}$			6	5	19.3	-13	21.6	-6	32.2	1	31.4	-7	28.5	-15	31.7	-6.5	31.4	-7.5	18.9	-	-	-

TEST No.: -6a.

MACH. No. 97

$P_1 = 32.5 \text{ LB/IN}^2 \text{ Ab.}$

BAROMETRIC PRESS = 14.25 LB/IN^2

$P_2 = 18.3 \text{ LB/IN}^2 \text{ Ab.}$

TEMP. 380 °F

STATION	-1 3/4	-1 1/2	-1 1/4	-1	-1/2	0	+1/2	1	2	3	3 1/2	4	4 1/4	4 1/2
	$P_3 \propto$	$P_3 \propto$	$P_3 \propto$	$P_3 \propto$	$P_3 \propto$	$P_3 \propto$	$P_3 \propto$	$P_3 \propto$	$P_3 \propto$	$P_3 \propto$	$P_3 \propto$	$P_3 \propto$	$P_3 \propto$	$P_3 \propto$
1 1/2	1925-2	1925 5	2225 7	2595 6	2915-1	2145-1	2175-1	2095-3	1925-5	1905-6	1925 5	2215 13	2355 9	2395 7
1	1925-1	2045 8	2595 14	2905 10	2525 3	2555 4	2625 7	2495 5	2175 0	1945-1	2125 9	2535 17	2755 18	2555 12
1/2	1945-3	2135 10	2225 16	2645 13	2755 6	2915 11	2945 14	2815 12	2045 13	2125 11	2165 10	2745 17	2825 17	2725 15
0.	2095 7	2125 15	2145 20	2055 17	2045 15	2105 18	2105 20	2105 22	2095 21	2135 18	2145 18	2045 21	2152 25	2105 23
-1	2145 24	2025 29	2025 32	2055 33	2105 33	2135 33	2105 33	2075 34	2075 35	2045 34	2025 34	2175 33	2105 33	2145 33
-2	2175 56	2225 52	2225 49	2125 51	2105 50	2125 50	2105 50	2045 50	2045 50	2045 49	2045 49	2135 50	2145 53	2145 65
-2 1/2	2195 80	2035 78	2225 74	2155 74	2145 80	2145 79	2145 78	2005 76	2035 74	2075 74	2145 70	2145 75	2125 77	-
-2 3/4	-	2045 93	1935 91	1905 89	1975 86	2025 87	2105 87	2235 87	2315 86	2345 86	2425 83	2445 84	-	-

TEST No:- 6

MACH No. 97

BAROMETRIC PRESS = 14.3

 $P_1 = 32.5 \text{ LB/IN}^2 \text{ AB.}$ $P_2 = 18.3 \text{ LB/IN}^2 \text{ AB.}$

TEMP. - °F.

STATIONS	-3 3/4	-3 1/2	-3 1/4	-3	2	1	0	1	2	3	3 1/4
	P_2 P_3	P_2 P_3	P_2 P_3	P_2 P_3	P_2 P_3	P_2 P_3	P_2 P_3	P_2 P_3	P_2 P_3	P_2 P_3	P_2 P_3
2 3/4	S S	.978 .04	.82 .361	.778 .453	.72 .59	.792 .137	.631 .807	.58 .724	.375 .814	.933 .125	S S
2 1/2	S S	.942 .107	.704 .628	.629 .812	.947 .581	.564 .1	.564 .1	.98 .57	.876 .606	.813 .377	S S
2	.974 .046	.80 .405	.626 .73	.581 .947	.564 .1	.564 .1	.564 .1	.98 .57	.98 .57	.722 .892	.207
1	.923 .142	.731 .564	.61 .866	.579 .955	.564 .1	.564 .1	.564 .1	.564 .1	.991 .647	.762 .814	.375
0	.88 .235	.685 .674	.598 .897	.572 .975	.564 .1	.564 .1	.564 .1	.564 .1	.991 .647	.754 .57	
-1	.839 .32	.677 .642	.826 .82	.596 .905	.566 .991	.564 .1	.564 .1	.566 .991	.581 .185	.682 .681	.39
-2	.933 .125	.575 .46	.656 .744	.602 .887	.566 .991	.564 .1	.564 .1	.995 .565	.582 .145	.54 .872	.25
-3	.945 .101	.884 .225	.733 .557	.617 .845	.564 .1	.564 .1	.564 .1	.564 .1	.986 .814	.375 .934	.125
-4	S S	.974 .040	.93 .131	.816 .37	.566 .991	.564 .1	.564 .1	.96 .577	.58 .751	.967 .06	S S
-4 1/4	S S	S S	.948 .095	.849 .30	.568 .985	.584 .94	.642 .798	.96 .577	.582 .945	.967 .06	S S

TEST No: -60

MACH. No. 97

$P_1 = 32.5 \text{ LB/IN}^2 \text{ AB}$

BAROMETRIC PRESS = 14.25 LB/IN^2

$P_2 = 18.3 \text{ LB/IN}^2 \text{ AB}$

TEMP. 380 °F

STATIONS	$-\frac{3}{4}$	$-\frac{1}{2}$	$-\frac{1}{4}$	-1	$-\frac{1}{2}$	0	$\frac{1}{2}$	1	2	3	$3\frac{1}{2}$	4	$4\frac{1}{4}$	$4\frac{1}{2}$
	P_3	P_3	P_3	P_3	P_3	P_3	P_3	P_3	P_3	P_3	P_3	P_3	P_3	P_3
$\frac{1}{2}$.95 .09	.805 .392	.705 .225	.79 .425	.84 .311	.834 .33	.874 .245	.95 .09	.961 .068	.951 .088	.8	.405 .777	.456 .834
1	.951 .887	.895 .705	.705 .625	.83 .809	.724 .58	.716 .599	.697 .642	.735 .552	.842 .314	.922 .147	.861 .772	.722	.584 .464	.724 .716
$\frac{1}{2}$.941 .107	.858 .28	.66 .735	.838 .787	.664 .725	.628 .815	.621 .832	.634 .799	.642 .777	.754 .507	.726 .55	.661 .72	.647 .765	.66 .735
0	.874 .245	.754 .507	.617 .845	.609 .867	.6 .892	.588 .927	.588 .927	.588 .927	.591 .92	.624 .824	.621 .832	.607 .873	.611 .861	.63 .807
-1	.736 .55	.637 .791	.604 .871	.609 .867	.588 .927	.584 .94	.588 .927	.595 .907	.595 .907	.601 .89	.604 .881	.615 .85	.63 .807	.657 .742
-2	.843 .312	.67 .71	.625 .822	.637 .791	.588 .927	.585 .937	.588 .927	.593 .912	.591 .92	.599 .897	.601 .89	.624 .825	.674 .7	.78 .947
$-2\frac{1}{2}$.917 .157	.9 .191	.897 .197	.85 .796	.735 .552	.7 .636	.69 .661	.652 .755	.645 .77	.637 .791	.628 .813	.768 .5	.951 .87	-
$-2\frac{3}{4}$.992 .015	.946 .098	.96 .07	.925 .142	.904 .184	.869 .255	.819 .322	.891 .211	.78 .448	.754 .509	.922 .147	-	-

TEST:- 22

TABLE :- 3

[illegible]

Σ 19.158

TEST - 2.

TABLE - 6

1. 10. 10. 10.

	$-3\frac{3}{4}$	$-3\frac{1}{2}$	$-3\frac{1}{4}$	-3	$-2\frac{3}{4}$	$-2\frac{1}{2}$	$-2\frac{1}{4}$	-2	$-1\frac{3}{4}$	$-1\frac{1}{2}$	$-1\frac{1}{4}$	-1	0	1	2	3	4	5	6
$-3\frac{3}{4}$																			
$-3\frac{1}{2}$																			
$-3\frac{1}{4}$																			
-3																			
$-2\frac{3}{4}$																			
$-2\frac{1}{2}$																			
$-2\frac{1}{4}$																			
-2																			
$-1\frac{3}{4}$																			
$-1\frac{1}{2}$																			
$-1\frac{1}{4}$																			
-1																			
0																			
1																			
2																			
3																			
4																			
5																			
6																			
7																			
8																			
9																			
10																			
11																			
12																			
13																			
14																			
15																			
16																			
17																			
18																			
19																			
20																			
21																			
22																			
23																			
24																			
25																			
26																			
27																			
28																			
29																			
30																			
31																			
32																			
33																			
34																			
35																			
36																			
37																			
38																			
39																			
40																			
41																			
42																			
43																			
44																			
45																			
46																			
47																			
48																			
49																			
50																			
51																			
52																			
53																			
54																			
55																			
56																			
57																			
58																			
59																			
60																			
61																			
62																			
63																			
64																			
65																			
66																			
67																			
68																			
69																			
70																			
71																			
72																			
73																			
74																			
75																			
76																			
77																			
78																			
79																			
80																			
81																			
82																			
83																			
84																			
85																			
86																			
87																			
88																			
89																			
90																			
91																			
92																			
93																			
94																			
95																			
96																			
97																			
98																			
99																			
100																			

$$A = \frac{1}{2} \sin \epsilon \frac{f_{\text{obs}}}{f_{\text{ref}}}$$

$$\Sigma 15.008$$

TEST:- 2a

TABLE:-5

[illegible]
$$A = h^{\frac{1}{2}} \sin \frac{\alpha}{2}$$

Σ 7.343

TEST:- 3

TABLE :- 3

[illegible]

TEST:- 3a

TABLE :- 3

STATION	-1 3/4	-1 1/2	-1 1/4	-1	-1/2	0	1/2	1	2	3	3 1/2	4	4 1/4	4 1/2
1/2	1/25	1/25	1/25	1/25	1/25	1/25	1/25	1/25	1/25	1/25	1/25	1/25	1/25	1/25
1	1/25	1/25	1/25	1/25	1/25	1/25	1/25	1/25	1/25	1/25	1/25	1/25	1/25	1/25
1 1/2	1/25	1/25	1/25	1/25	1/25	1/25	1/25	1/25	1/25	1/25	1/25	1/25	1/25	1/25
2	1/25	1/25	1/25	1/25	1/25	1/25	1/25	1/25	1/25	1/25	1/25	1/25	1/25	1/25
2 1/2	1/25	1/25	1/25	1/25	1/25	1/25	1/25	1/25	1/25	1/25	1/25	1/25	1/25	1/25
3	1/25	1/25	1/25	1/25	1/25	1/25	1/25	1/25	1/25	1/25	1/25	1/25	1/25	1/25
3 1/2	1/25	1/25	1/25	1/25	1/25	1/25	1/25	1/25	1/25	1/25	1/25	1/25	1/25	1/25
4	1/25	1/25	1/25	1/25	1/25	1/25	1/25	1/25	1/25	1/25	1/25	1/25	1/25	1/25
4 1/4	1/25	1/25	1/25	1/25	1/25	1/25	1/25	1/25	1/25	1/25	1/25	1/25	1/25	1/25
4 1/2	1/25	1/25	1/25	1/25	1/25	1/25	1/25	1/25	1/25	1/25	1/25	1/25	1/25	1/25
Σ	1/25	1/25	1/25	1/25	1/25	1/25	1/25	1/25	1/25	1/25	1/25	1/25	1/25	1/25

TEST: - 3

TABLE :- 4

[illegible]

$$A = \eta^{\frac{1}{2}} \sin \alpha \frac{f da}{f v}$$

TEST:- 3A.

TABLE :-4

[illegible]

$$A = \frac{1}{2} \sin \alpha \int_V \frac{da}{V}$$

三

TEST-5

TABLE-5

Source	-3 3/4	-3 1/2	-3 1/4	-3	-2	-1	0	1	2	3	3 1/4
123456789101112131415161718192021222324252627282930313233343536373839404142434445464748495051525354555657585960616263646566676869707172737475767778798081828384858687888990919293949596979899100	123456789101112131415161718192021222324252627282930313233343536373839404142434445464748495051525354555657585960616263646566676869707172737475767778798081828384858687888990919293949596979899100	123456789101112131415161718192021222324252627282930313233343536373839404142434445464748495051525354555657585960616263646566676869707172737475767778798081828384858687888990919293949596979899100	123456789101112131415161718192021222324252627282930313233343536373839404142434445464748495051525354555657585960616263646566676869707172737475767778798081828384858687888990919293949596979899100	123456789101112131415161718192021222324252627282930313233343536373839404142434445464748495051525354555657585960616263646566676869707172737475767778798081828384858687888990919293949596979899100	123456789101112131415161718192021222324252627282930313233343536373839404142434445464748495051525354555657585960616263646566676869707172737475767778798081828384858687888990919293949596979899100	123456789101112131415161718192021222324252627282930313233343536373839404142434445464748495051525354555657585960616263646566676869707172737475767778798081828384858687888990919293949596979899100	123456789101112131415161718192021222324252627282930313233343536373839404142434445464748495051525354555657585960616263646566676869707172737475767778798081828384858687888990919293949596979899100	123456789101112131415161718192021222324252627282930313233343536373839404142434445464748495051525354555657585960616263646566676869707172737475767778798081828384858687888990919293949596979899100	123456789101112131415161718192021222324252627282930313233343536373839404142434445464748495051525354555657585960616263646566676869707172737475767778798081828384858687888990919293949596979899100	123456789101112131415161718192021222324252627282930313233343536373839404142434445464748495051525354555657585960616263646566676869707172737475767778798081828384858687888990919293949596979899100	
0	.057	.053	.081	.242	.425	.450	.415	.425	.410	.171	.040
-1	.024	.048	.076	.210	.394	.404	.405	.405	.372	.151	.028
-2	.007	.029	.052	.183	.300	.300	.294	.309	.294	.118	.012
-3	.001	.004	.015	.078	.179	.211	.188	.187	.179	.013	.000
-4		.000	.001	.000	.046	.022	.022	.033	.020	.000	.000
-4 1/4			.000	.001	.026	.011	.018	.015	.024	.001	
Σ	0.104	0.222	0.394	1.241	2.371	2.470	2.444	2.435	2.371	0.820	0.126

$$A = \frac{1}{2} \sin \epsilon \frac{f_{\text{obs}}}{f_{\text{ref}}}$$

TEST:- 3A
TABLE:- 5

[illegible]

$$A = \frac{1}{2} \sin \alpha \frac{fda}{fV}$$

Σ 6925

TEST:- #

TABLE :- 3

STATION	-3 3/4	-3 1/2	-3 1/4	-3	-2	-1	0	1	2	3	3 1/4
1/2	1/2	1/2	1/2	1/2	1/2	1/2	1/2	1/2	1/2	1/2	1/2
Sin d f da	Sin d f da	Sin d f da	Sin d f da	Sin d f da	Sin d f da	Sin d f da	Sin d f da	Sin d f da	Sin d f da	Sin d f da	Sin d f da
f v	f v	f v	f v	f v	f v	f v	f v	f v	f v	f v	f v
2 3/4	2 3/4	2 3/4	2 3/4	2 3/4	2 3/4	2 3/4	2 3/4	2 3/4	2 3/4	2 3/4	2 3/4
2 1/2	2 1/2	2 1/2	2 1/2	2 1/2	2 1/2	2 1/2	2 1/2	2 1/2	2 1/2	2 1/2	2 1/2
2	2	2	2	2	2	2	2	2	2	2	2
1	1	1	1	1	1	1	1	1	1	1	1
0	0	0	0	0	0	0	0	0	0	0	0
-1	-1	-1	-1	-1	-1	-1	-1	-1	-1	-1	-1
-2	-2	-2	-2	-2	-2	-2	-2	-2	-2	-2	-2
-3	-3	-3	-3	-3	-3	-3	-3	-3	-3	-3	-3
-4	-4	-4	-4	-4	-4	-4	-4	-4	-4	-4	-4
-4 1/4	-4 1/4	-4 1/4	-4 1/4	-4 1/4	-4 1/4	-4 1/4	-4 1/4	-4 1/4	-4 1/4	-4 1/4	-4 1/4
Σ	0.024	0.351	0.569	1.175	2.973	3.012	3.004	2.993	3.012	1.423	0.241

TEST:-4a

TABLE :-3

[illegible]

TEST:-4

TABLE :- 4

[illegible]

$$A = \eta^{\frac{1}{2}} \sin \alpha \frac{f da}{f v}$$

17-379

TEST :- 4A.

TABLE :- 4

THICK	-1 3/4	-1 1/2	-1 1/4	-1	-1/2	0	1/2	1	2	3	3 1/2	4	4 1/4	4 1/2
η	η	η	η	η	η	η	η	η	η	η	η	η	η	η
$\frac{f_{da}}{f_v}$	$\frac{f_{da}}{f_v}$	$\frac{f_{da}}{f_v}$	$\frac{f_{da}}{f_v}$	$\frac{f_{da}}{f_v}$	$\frac{f_{da}}{f_v}$	$\frac{f_{da}}{f_v}$	$\frac{f_{da}}{f_v}$	$\frac{f_{da}}{f_v}$	$\frac{f_{da}}{f_v}$	$\frac{f_{da}}{f_v}$	$\frac{f_{da}}{f_v}$	$\frac{f_{da}}{f_v}$	$\frac{f_{da}}{f_v}$	$\frac{f_{da}}{f_v}$
1/2														
1														
1/2														
0														
-1														
-2														
-2 1/2														
-2 3/4														
Σ														

$$A = \eta^2 \sin \alpha \frac{f_{da}}{f_v}$$

$$\Sigma 9.040$$

TEST:- 4

TABLE:- 5

[illegible]

$$A = \frac{1}{2} \sin \alpha \quad \text{fda.}$$

一

Σ 6966

TEST:- 5

TABLE :- 3

ATION	-3 3/4	-3 1/2	-3 1/4	-3	-2	-1	0	1	2	3	3 1/4
h ^{1/2} Sine f da	h ^{1/2} Sine f da	h ^{1/2} Sine f da	h ^{1/2} Sine f da	h ^{1/2} Sine f da	h ^{1/2} Sine f da	h ^{1/2} Sine f da	h ^{1/2} Sine f da	h ^{1/2} Sine f da	h ^{1/2} Sine f da	h ^{1/2} Sine f da	h ^{1/2} Sine f da
f v	f v	f v	f v	f v	f v	f v	f v	f v	f v	f v	f v
2 3/4	2 3/4	2 3/4	2 3/4	2 3/4	2 3/4	2 3/4	2 3/4	2 3/4	2 3/4	2 3/4	2 3/4
2 1/2	2 1/2	2 1/2	2 1/2	2 1/2	2 1/2	2 1/2	2 1/2	2 1/2	2 1/2	2 1/2	2 1/2
2	2	2	2	2	2	2	2	2	2	2	2
1	1	1	1	1	1	1	1	1	1	1	1
0	0	0	0	0	0	0	0	0	0	0	0
-1	-1	-1	-1	-1	-1	-1	-1	-1	-1	-1	-1
-2	-2	-2	-2	-2	-2	-2	-2	-2	-2	-2	-2
-3	-3	-3	-3	-3	-3	-3	-3	-3	-3	-3	-3
-4	-4	-4	-4	-4	-4	-4	-4	-4	-4	-4	-4
-4 1/4	-4 1/4	-4 1/4	-4 1/4	-4 1/4	-4 1/4	-4 1/4	-4 1/4	-4 1/4	-4 1/4	-4 1/4	-4 1/4
Σ	0.268	0.430	0.634	1.774	3.087	3.085	3.108	3.107	2.932	1.454	0.361

TEST:-5a

TABLE :-3

[illegible]

TEST: - 5

TABLE :- 4

[illegible]

$$A = \eta^{\frac{1}{2}} \sin \alpha \int \frac{dx}{v}$$

17.972

...

$$A = h^{\frac{1}{2}} \sin \alpha$$

TABLE--5

[illegible]

$$A = h^2 \sin \alpha \frac{f d \alpha}{2}$$

$\Sigma 7.020$

TEST:- 6

TABLE :- 3

[illegible]

Σ 20-028

28.028

TEST: - C

TABLE: - 4

STATION	-3 3/4	-3 1/2	-3 1/4	-3	-2	-1	0	1	2	3	3 1/4						
	η	η	η	η	η	η	η	η	η	η	η	η	η	η	η	η	η
	A	A	A	A	A	A	A	A	A	A	A	A	A	A	A	A	A
	$\frac{1}{2} \sin \alpha \frac{f_{do}}{f_v}$	$\frac{1}{2} \sin \alpha \frac{f_{do}}{f_v}$	$\frac{1}{2} \sin \alpha \frac{f_{do}}{f_v}$	$\frac{1}{2} \sin \alpha \frac{f_{do}}{f_v}$	$\frac{1}{2} \sin \alpha \frac{f_{do}}{f_v}$	$\frac{1}{2} \sin \alpha \frac{f_{do}}{f_v}$	$\frac{1}{2} \sin \alpha \frac{f_{do}}{f_v}$	$\frac{1}{2} \sin \alpha \frac{f_{do}}{f_v}$	$\frac{1}{2} \sin \alpha \frac{f_{do}}{f_v}$	$\frac{1}{2} \sin \alpha \frac{f_{do}}{f_v}$	$\frac{1}{2} \sin \alpha \frac{f_{do}}{f_v}$	$\frac{1}{2} \sin \alpha \frac{f_{do}}{f_v}$	$\frac{1}{2} \sin \alpha \frac{f_{do}}{f_v}$	$\frac{1}{2} \sin \alpha \frac{f_{do}}{f_v}$	$\frac{1}{2} \sin \alpha \frac{f_{do}}{f_v}$	$\frac{1}{2} \sin \alpha \frac{f_{do}}{f_v}$	$\frac{1}{2} \sin \alpha \frac{f_{do}}{f_v}$
2 3/4		04	040	361	031	453	089	59	164	792	189	807	190	58	166	375	130
		000	011		040		089		097		150		153	096		049	005
2 1/2		107	024	428	056	812	169	947	290	1	274	1	281	98	288	876	290
		003	035		137		274		274		281		282	254		046	
2	046	023	405	071	73	098	947	292	1	481	1	471	1	482	98	485	722
		001	029	071		276		481		471		482		476		186	
1	142	044	549	084	866	118	955	332	1	574	1	574	1	574	991	570	762
		006	053	102		317		574		574		574		565		222	
0	235	051	674	092	897	109	975	278	1	508	1	515	1	515	991	497	77
		012	062	098		271		508		515		530		515		494	
1	32	060	642	084	82	100	905	276	991	452	1	454	1	477	991	440	948
		019	054	082		250		448		454		477		456		425	
2	125	020	46	049	744	068	887	194	991	324	1	326	1	342	995	357	945
		003	023	051		172		321		326		342		356		343	
3	101	005	226	007	557	026	845	098	1	139	1	174	1	148	1	174	986
		001	002	015		083		139		174		148		174		144	
4			046	005	131	008	37	008	991	011	935	083	848	150	96	059	951
			000	001		003		011		078		127		057		021	
4 1/4			095	004	3	008	985	004	94	029	778	055	96	032	945	011	06
			000		002		004		027		043		031		010		000
Σ	0.042	0.226	0.466	1.551	2.857	3.043	3.146	3.023	2.781	0.893	0.124						

$$A = \eta^2 \sin \alpha \frac{f_{do}}{f_v}$$

$$\Sigma = 18.152$$

TEST :- 6A.

TABLE :- 4

[illegible]

$$\dot{A} = \dot{\eta}^2 \sin \alpha \frac{f d \alpha}{f v}$$

TEST :- 6

TABLE:- 5

	-3 3/4	-3 1/2	-3 1/4	-3	-2	-1	0	1	2	3	3 1/4
0	021	063	086	2045	438	442	450	442	430	192	056
1	014	060	094	272	470	470	470	464	213	040	
2	004	034	065	218	369	366	366	370	362	163	017
3		004	027	097	170	187	186	179	148	038	
4		001	009	025	054	083	085	049	031	008	
5											
6											
7											
8											
9											
10											
11											
12											
13											
14											
15											
16											
17											
18											
19											
20											
21											
22											
23											
24											
25											
26											
27											
28											
29											
30											
31											
32											
33											
34											
35											
36											
37											
38											
39											
40											
41											
42											
43											
44											
45											
46											
47											
48											
49											
50											
51											
52											
53											
54											
55											
56											
57											
58											
59											
60											
61											
62											
63											
64											
65											
66											
67											
68											
69											
70											
71											
72											
73											
74											
75											
76											
77											
78											
79											
80											
81											
82											
83											
84											
85											
86											
87											
88											
89											
90											
91											
92											
93											
94											
95											
96											
97											
98											
99											
100											

$$A = h^2 \sin \epsilon \frac{fda}{fda}$$

Σ. 15. 557

TABLE:- 5

[illegible]

$$A = h^2 \sin \alpha \frac{f d \alpha}{c}$$

6.916

$\Sigma = 6$ 9165

Series 3

Groups 1 and 2

TABLE OF OBSERVED READINGS OF PRESSURE AND ANGLE.

GROUP: - 1

BAROMETRIC PRESS = $\frac{P_2}{P_1} = \frac{LB/IN^2 AB}{LB/IN^2 AB}$ TEMP. °

STATIONS	$-2\frac{3}{4}$		$-2\frac{1}{2}$		$-2\frac{1}{4}$		-2		-1		0		$\frac{1}{2}$		$\frac{3}{4}$		1		$1\frac{1}{4}$		$1\frac{1}{2}$							
	P_3	α	P_3	α	P_3	α	P_3	α	P_3	α	P_3	α	P_3	α	P_3	α	P_3	α	P_3	α	P_3	α	P_3	α	P_3	α	P_3	α
18	30.7	102.3	30.3	105.4	113.4	106.4	113.4	129.4	148.4	159.4	172.4	180.4	179.4	179.4	179.4	179.4	179.4	179.4	179.4	179.4	179.4	179.4	179.4	179.4	179.4	179.4	179.4	179.4
10	12.2	92.2	105.2	113.2	123.2	134.2	148.2	157.2	165.2	173.2	180.2	180.2	180.2	180.2	180.2	180.2	180.2	180.2	180.2	180.2	180.2	180.2	180.2	180.2	180.2	180.2	180.2	180.2
5	18.9	95.2	105.2	113.2	123.2	134.2	148.2	157.2	165.2	173.2	180.2	180.2	180.2	180.2	180.2	180.2	180.2	180.2	180.2	180.2	180.2	180.2	180.2	180.2	180.2	180.2	180.2	180.2
1	21	95.2	105.2	113.2	123.2	134.2	148.2	157.2	165.2	173.2	180.2	180.2	180.2	180.2	180.2	180.2	180.2	180.2	180.2	180.2	180.2	180.2	180.2	180.2	180.2	180.2	180.2	180.2

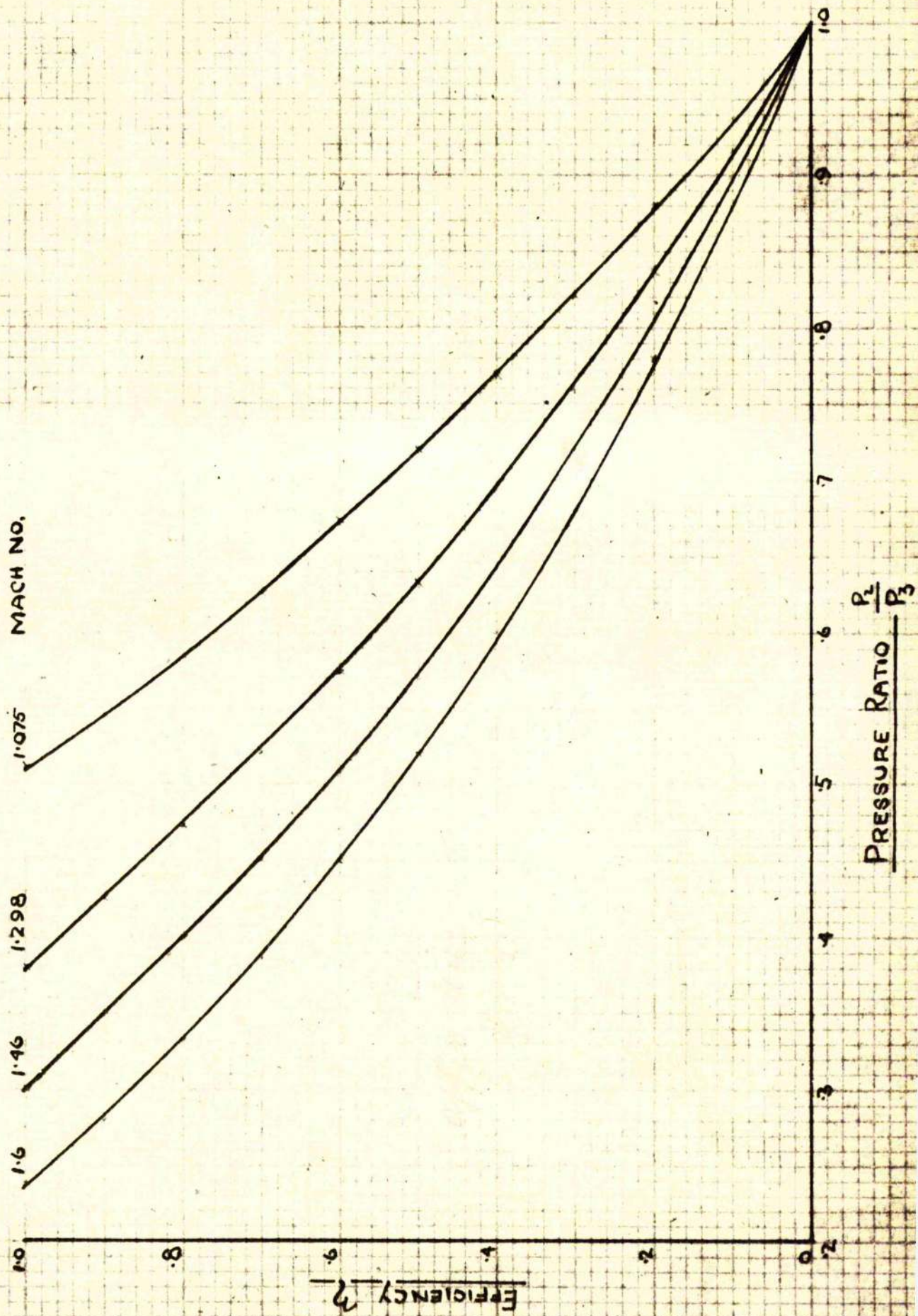
Test No. 1. Vertical Traverse slot 1' 1/4.

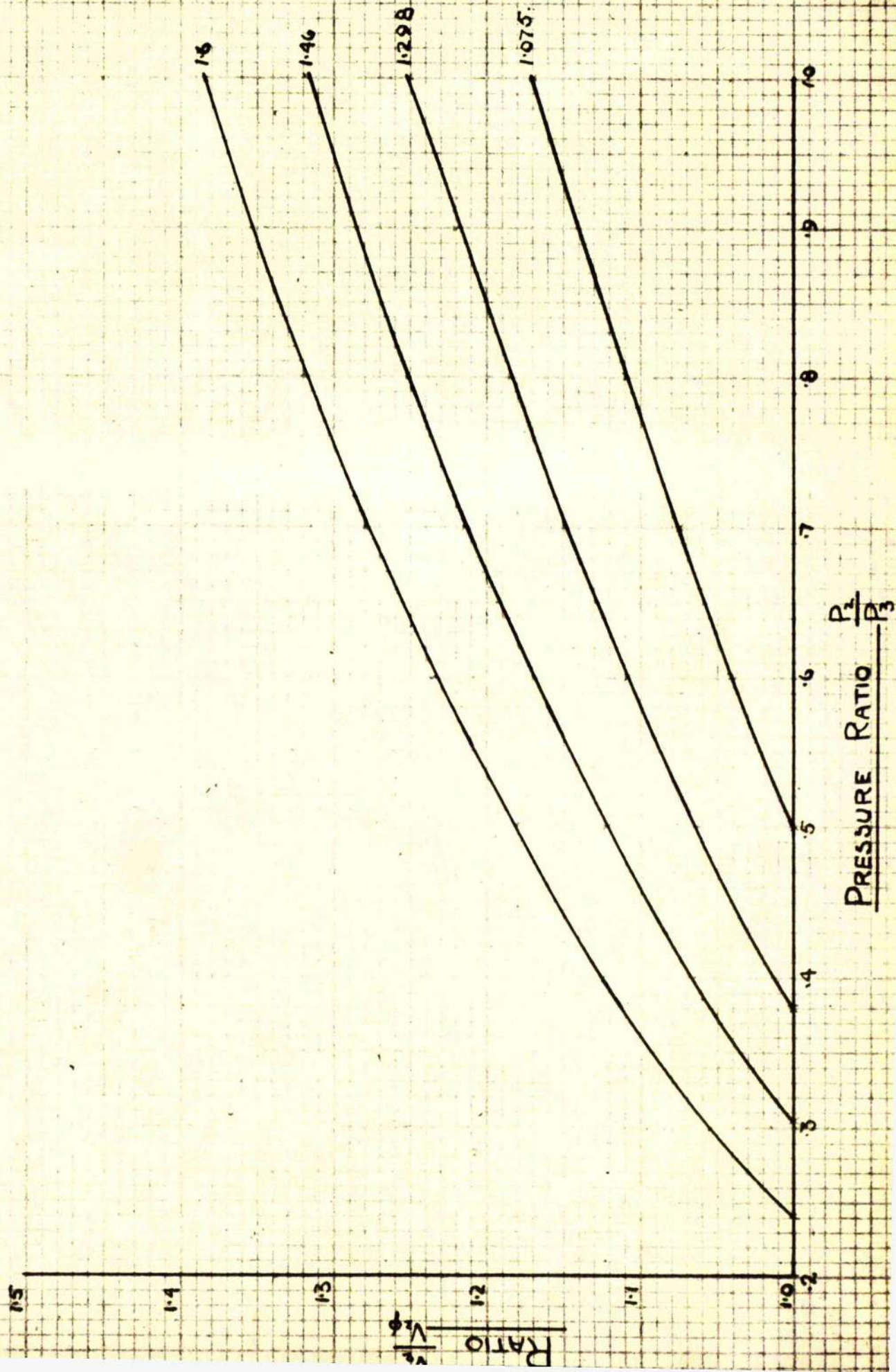
RATIO OF BACK PRESSURE AND CONVERTED ANGLE
PRESSURE READING

GROUP: - 1

BAROMETRIC PRESS =
 $P_1 =$ LB/IN² AB. $P_2 =$ LB/IN² AB. TEMP. °F

STATIONS	-2 3/4	-2 1/2	-2 1/4	-2	-1	0	1/2	3/4	1	1 1/4	1 1/2	1 3/4																																																																																																																																																																																																																																																																																																																																																																																																																																																																																																																																																																																																																																																																																																																																																																																																																																																																																																																																																																																																																																																																																																																																																																																																																																																																										
	$\frac{P_2}{P_1} \propto \frac{P_2}{P_1}$	$\frac{P_2}{P_1} \propto \frac{P_2}{P_1}$	$\frac{P_2}{P_1} \propto \frac{P_2}{P_1}$	$\frac{P_2}{P_1} \propto \frac{P_2}{P_1}$	$\frac{P_2}{P_1} \propto \frac{P_2}{P_1}$	$\frac{P_2}{P_1} \propto \frac{P_2}{P_1}$	$\frac{P_2}{P_1} \propto \frac{P_2}{P_1}$	$\frac{P_2}{P_1} \propto \frac{P_2}{P_1}$	$\frac{P_2}{P_1} \propto \frac{P_2}{P_1}$	$\frac{P_2}{P_1} \propto \frac{P_2}{P_1}$	$\frac{P_2}{P_1} \propto \frac{P_2}{P_1}$	$\frac{P_2}{P_1} \propto \frac{P_2}{P_1}$	$\frac{P_2}{P_1} \propto \frac{P_2}{P_1}$	$\frac{P_2}{P_1} \propto \frac{P_2}{P_1}$																																																																																																																																																																																																																																																																																																																																																																																																																																																																																																																																																																																																																																																																																																																																																																																																																																																																																																																																																																																																																																																																																																																																																																																																																																																																								
$P_1 = 32.5$	718	64	591	45	559	40	563	23	568	20	641	23	678	23	732	25	805	30	851	19																																																																																																																																																																																																																																																																																																																																																																																																																																																																																																																																																																																																																																																																																																																																																																																																																																																																																																																																																																																																																																																																																																																																																																																																																																																																		</





VERTICAL TRAVERSE

GROUP No 1

CALCULATION OF LOCAL EFFICIENCY & VELOCITY

	$-2\frac{3}{4}$	$-2\frac{1}{2}$	$-2\frac{1}{4}$	-2	-1	0	$\frac{1}{2}$	$\frac{3}{4}$	1	$1\frac{1}{4}$	$1\frac{1}{2}$		
1.0	2027	2385	2356	2335	2132	2000	1963	1963	1962	1970	2292		
	1600	1830	2102	2160	2075	1994	2140	2158	2139	2085	2079		
	.79	.936	.908	.934	.896	.861	.925	.921	.924	.901	.898		
1.46	2319	2385	2356	2335	2132	2000	1963	1963	1962	1970	2292		
	.691	.79	.908	.934	.896	.861	.925	.921	.924	.901	.898		
	1600	1830	2102	2160	2075	1994	2140	2158	2139	2085	2079		
	.031	.685	.752	.833	.904	.895	.891	.894	.866	.836	.806		
1.218	2120	2385	2356	2335	2132	2000	1963	1963	1962	1970	2292		
	.707	.82	.886	.945	.924	.92	.815	.768	.693	.575	.5		
	1277	1480	1591	1764	1916	1897	1888	1892	1838	1771	1710		
	1807	1975	2075	2108	2168	2260	2371	2388	2450	2539	2602		
1.075	1807	1975	2075	2108	2168	2260	2371	2388	2450	2539	2602		
	.707	.82	.886	.945	.924	.92	.815	.768	.693	.575	.5		
	1277	1480	1591	1764	1916	1897	1888	1892	1838	1771	1710		
	1807	1975	2075	2108	2168	2260	2371	2388	2450	2539	2602		
1.218	2120	2385	2356	2335	2132	2000	1963	1963	1962	1970	2292		
	.707	.82	.886	.945	.924	.92	.815	.768	.693	.575	.5		
	1277	1480	1591	1764	1916	1897	1888	1892	1838	1771	1710		
	1807	1975	2075	2108	2168	2260	2371	2388	2450	2539	2602		
1.0	2027	2385	2356	2335	2132	2000	1963	1963	1962	1970	2292		
	1600	1830	2102	2160	2075	1994	2140	2158	2139	2085	2079		
	.79	.936	.908	.934	.896	.861	.925	.921	.924	.901	.898		
	2319	2385	2356	2335	2132	2000	1963	1963	1962	1970	2292		
	.691	.79	.908	.934	.896	.861	.925	.921	.924	.901	.898		
	1600	1830	2102	2160	2075	1994	2140	2158	2139	2085	2079		
	.031	.685	.752	.833	.904	.895	.891	.894	.866	.836	.806		
	1277	1480	1591	1764	1916	1897	1888	1892	1838	1771	1710		
	1807	1975	2075	2108	2168	2260	2371	2388	2450	2539	2602		

Group 2.

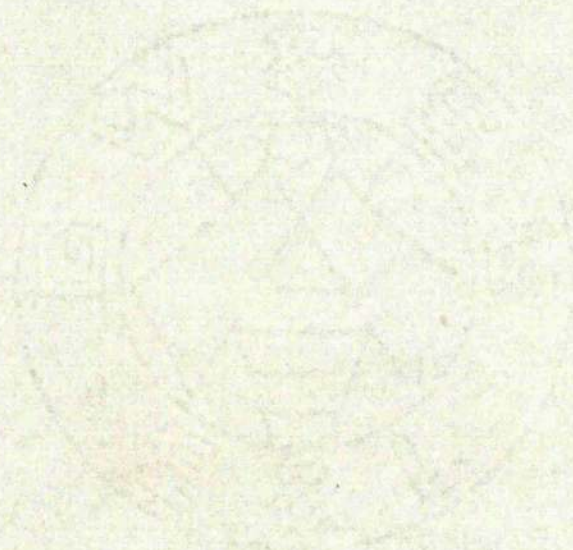


TABLE OF OBSERVED READINGS OF PRESSURE AND ANGLE

GROUP - 2

BAROMETRIC PRESS =

$P_1 =$ LB/IN² Ab.

$P_2 =$ LB/IN² Ab.

° F

TEMP.

STATIONS	-2 3/4		-2 1/2		-2 1/4		-2		-1		0		1/2		3/4		1		1 1/4		1 1/2									
	P_3	α	P_3	α	P_3	α	P_3	α	P_3	α	P_3	α	P_3	α	P_3	α	P_3	α	P_3	α	P_3	α	P_3	α	P_3	α	P_3	α	P_3	α
31-8	37.7	110	38	125	38	131	37.9	135	37.6	146	37.3	160	34.9	169	33.4	174	32.7	178	32.2	182	-	-								
28-75	36.4	109	37.7	120	37.6	126	37.9	133	37	146	37.2	160	34.4	167	32.8	172	30.9	175	29.6	180	-	-								
25-55	34.2	104	37.1	118	37.3	128	37	134	36.8	147	36.4	160	32.2	170	29.9	174	28.4	177	26.8	182	25.7	185								
22-11	33.3	103	36.4	114	37.1	126	37	133	36.2	147	36	161	32.1	170	28.8	175	26.1	178	24.2	182	22.9	186								
18-55	28	97	33.9	107	36.1	122	36.2	131	35.3	147	35.3	161	32.1	168	28.9	173	24.7	177	22.9	182	21.2	182								
16-13	27.1	98	33	107	35.7	121	36	131	35.3	147	35.3	160	30.7	169	27.9	174	24	178	20.4	182	18.8	187								
12	16.8	96	23.3	102	29.2	108	23	121	24.8	147	25	169	32.9	171	28.7	172	25.9	176	21.4	180	19.1	183								
8	12.7	97	18.8	106	23	114	28.7	126	33	145	32.8	157	32.6	167	30.9	172	29	176	25.9	180	23.3	181								
4	10.2	91	14	104	28.5	123	30.9	137	29.6	154	31.6	158	30.4	171	30.3	165	30.1	167	28.6	174	26.3	177								

BACK PRESSURE AND CONVERTED ANGLE RATIO ΔF PRESSURE READING

G-R O U P: - 2

BAROMETRIC PRESS =

$P_1 =$ LB/IN² AB

$P_2 =$ LB/IN² AB

TEMP. °F

STATIONS	$-2\frac{3}{4}$		$-2\frac{1}{2}$		$-2\frac{1}{4}$		-2		-1		0		$\frac{1}{2}$		$\frac{3}{4}$		1		$1\frac{1}{4}$		$1\frac{1}{2}$									
	$\frac{P_2}{P_3}$	α	$\frac{P_2}{P_3}$	α	$\frac{P_2}{P_3}$	α	$\frac{P_2}{P_3}$	α	$\frac{P_2}{P_3}$	α	$\frac{P_2}{P_3}$	α	$\frac{P_2}{P_3}$	α	$\frac{P_2}{P_3}$	α	$\frac{P_2}{P_3}$	α	$\frac{P_2}{P_3}$	α	$\frac{P_2}{P_3}$	α	$\frac{P_2}{P_3}$	α	$\frac{P_2}{P_3}$	α	$\frac{P_2}{P_3}$	α		
$P_1 = 4625$	886	70	882	55	882	49	884	45	888	34	894	20	937	11	966	6	98	2	99	-2	-	-	-	-	-	-	-	-	-	-
$P_1 = 432$	85	71	828	60	831	54	826	47	841	34	836	20	885	13	915	8	954	5	981	0	-	-	-	-	-	-	-	-	-	-
$P_1 = 40$	821	76	775	62	773	52	778	46	78	33	787	20	856	10	903	6	934	3	969	-2	996	-5	-	-	-	-	-	-	-	-
$P_1 = 3656$	765	77	719	66	708	54	71	47	72	33	724	19	784	10	845	5	899	2	945	-2	977	-6	-	-	-	-	-	-	-	-
$P_1 = 330$	777	83	689	73	651	58	65	49	663	33	663	19	708	12	764	7	849	3	883	-2	926	-2	-	-	-	-	-	-	-	-
$P_1 = 265$	847	84	702	78	606	72	558	59	538	33	535	21	584	9	613	7	658	4	739	0	788	-3	-	-	-	-	-	-	-	-
$P_1 = 225$	828	83	675	74	60	66	521	54	474	35	475	23	477	13	496	8	518	4	558	0	596	-1	-	-	-	-	-	-	-	-
$P_1 = 185$	748	89	552	76	431	57	407	43	42	26	401	22	413	9	444	15	415	13	43	6	454	3	-	-	-	-	-	-	-	-
$P_1 = 155$	507	87	384	67	358	78	363	41	394	21	44	17	46	18	453	22	374	19	358	11	374	6	-	-	-	-	-	-	-	-

M24

5

6

7

8

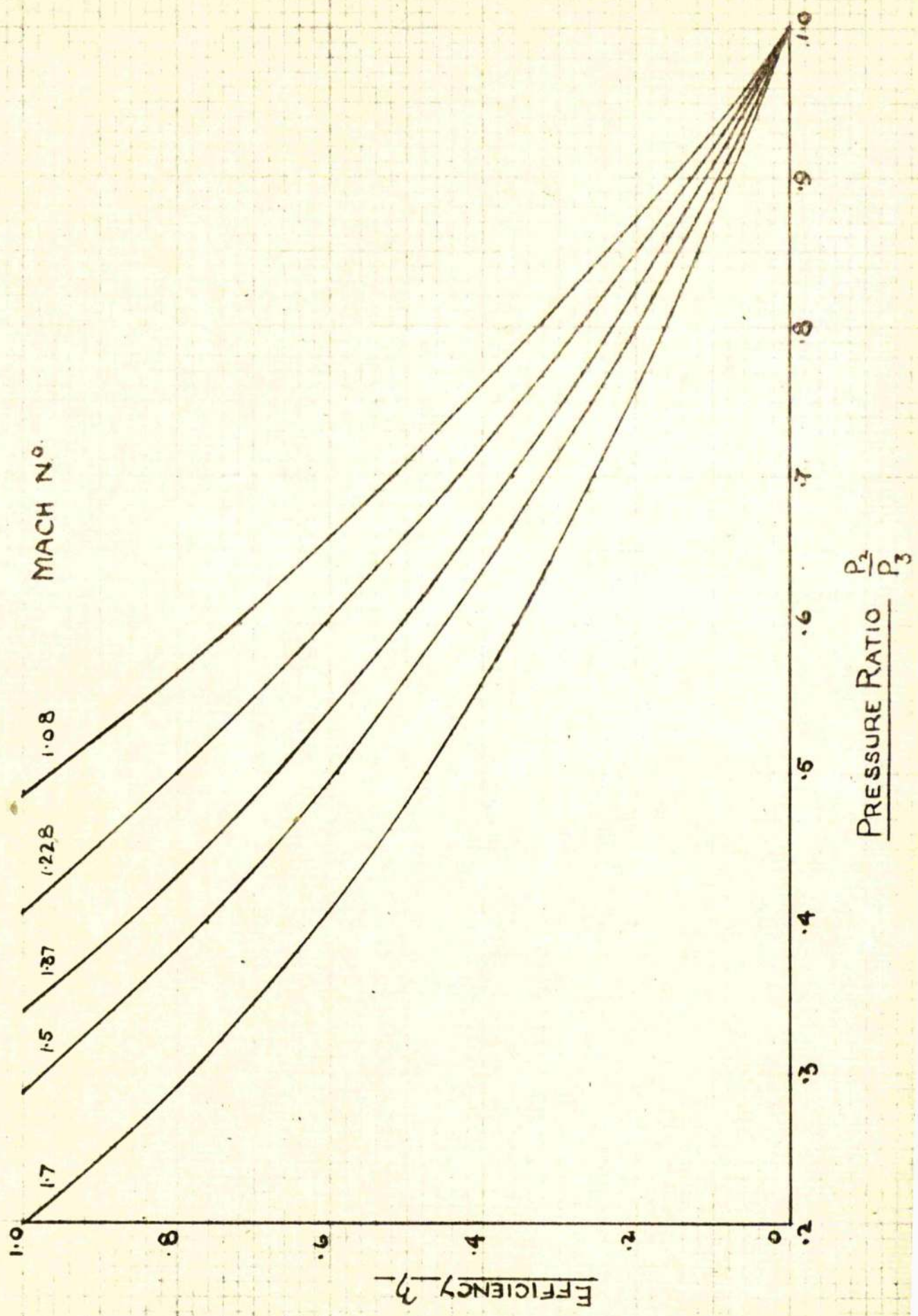
9

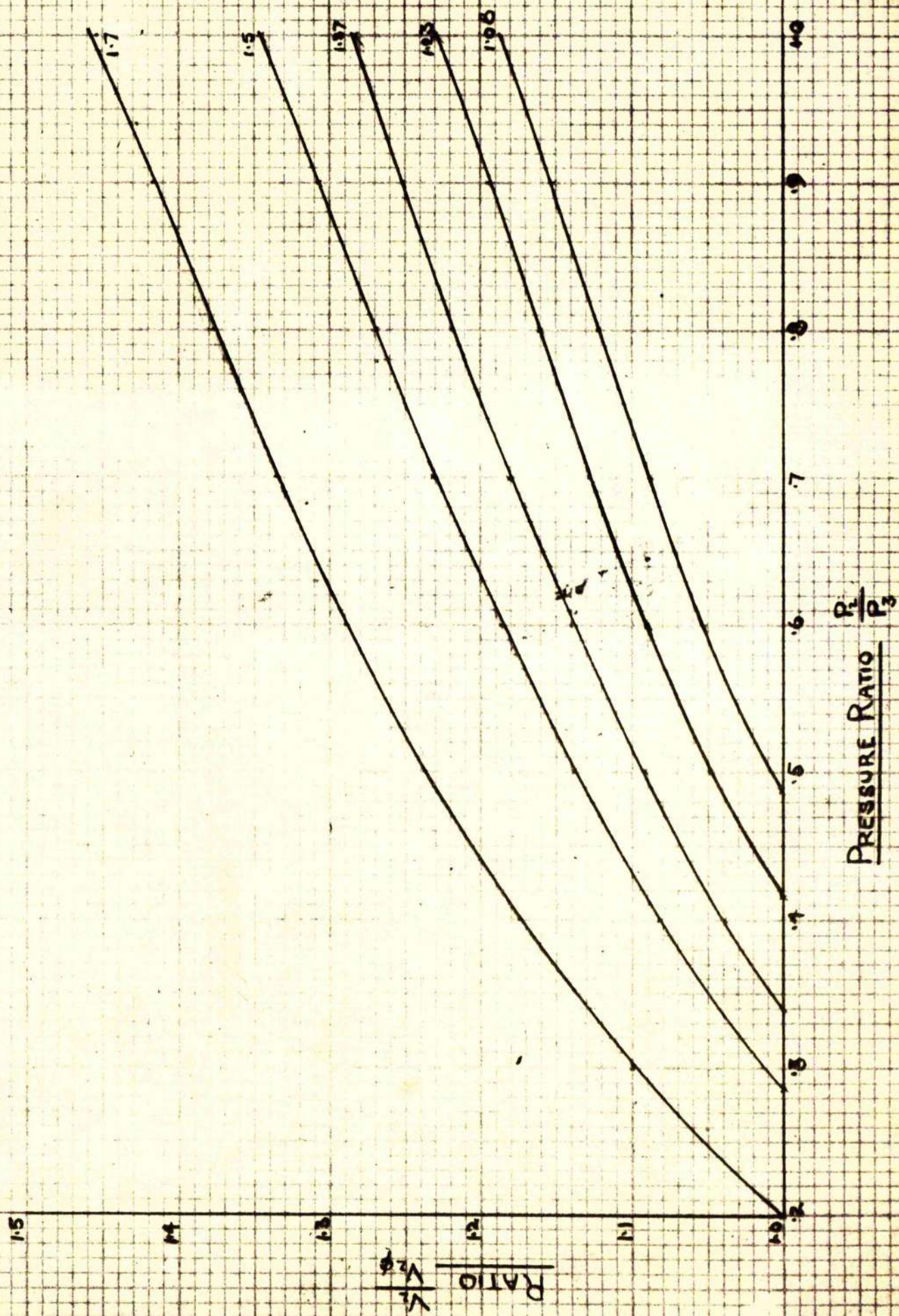
1.08

1.228

1.37

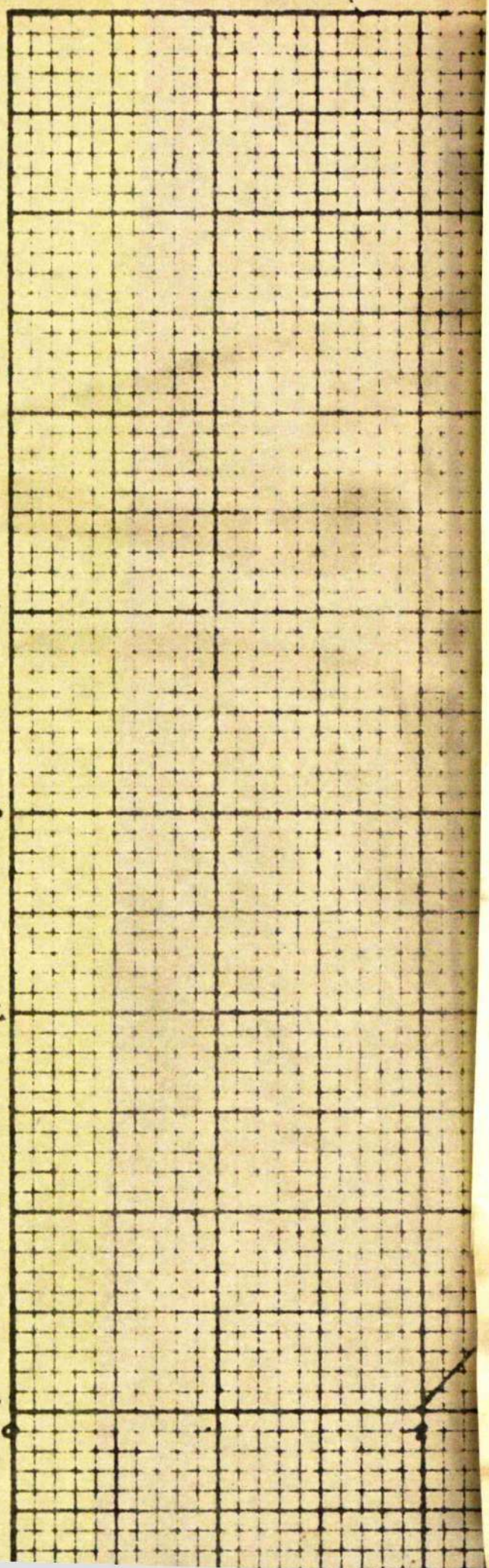
1.5



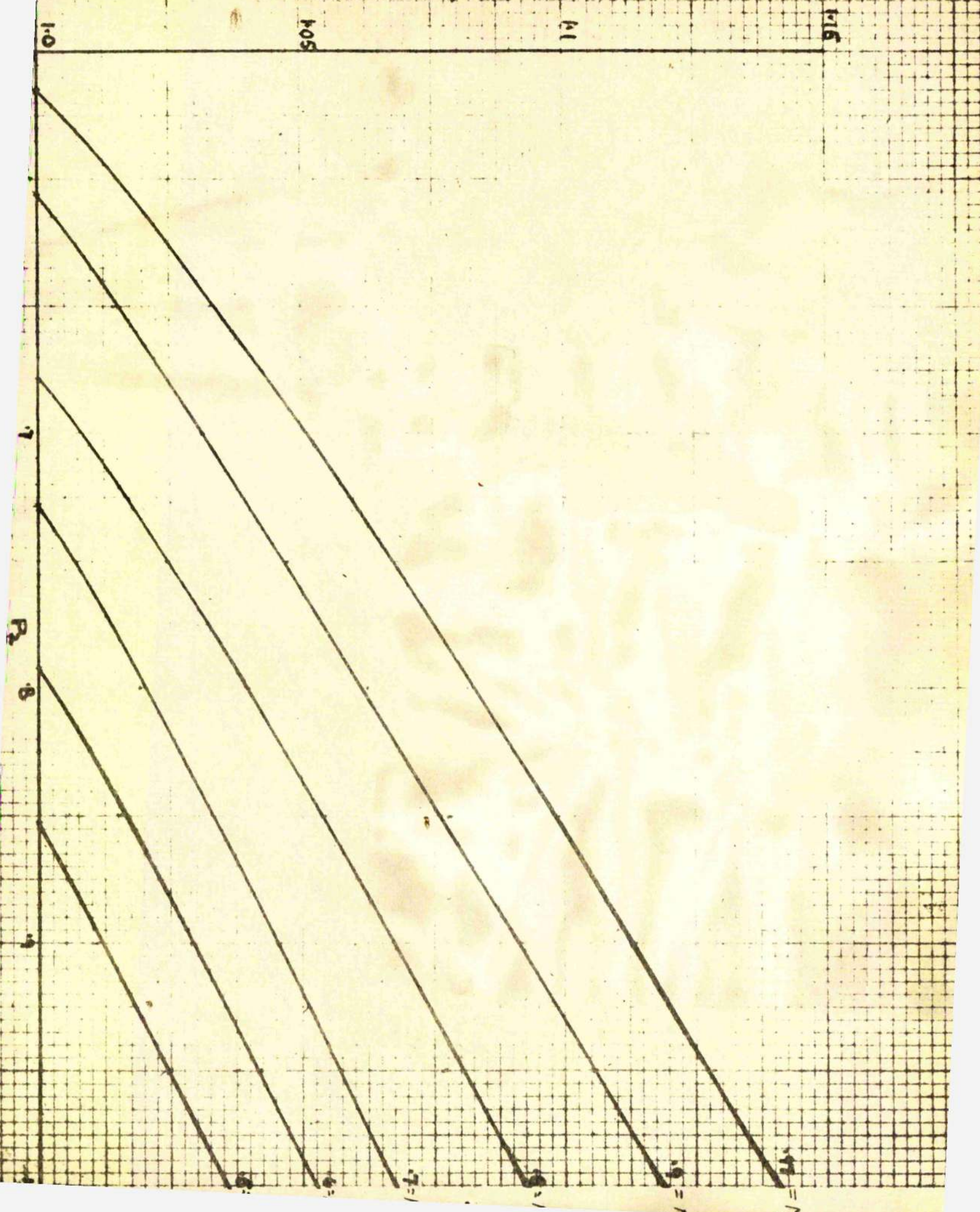


$\frac{V_2}{V_{2d}}$
RATIO

1.0
1.1
1.2
1.3
1.4
1.5



RATIO $\frac{V}{V_{2\phi}}$



READINGS OF CONVERTED PRESSURE RATIO AND LOCAL EFFICIENCY

GROUP-2

BAROMETRIC PRESSURE

$P_1 = \text{LB/IN}^2 \text{ AB}$

$P_2 = \text{LB/IN}^2 \text{ AB}$

STATIONS	$-2\frac{3}{4}$		$-2\frac{1}{2}$		$-2\frac{1}{4}$		-2		-1		0		$\frac{1}{2}$		$\frac{3}{4}$		1		$1\frac{1}{4}$		$1\frac{1}{2}$	
	$\frac{P_2}{P_3}$	η	$\frac{P_2}{P_3}$	η	$\frac{P_2}{P_3}$	η	$\frac{P_2}{P_3}$	η	$\frac{P_2}{P_3}$	η	$\frac{P_2}{P_3}$	η	$\frac{P_2}{P_3}$	η	$\frac{P_2}{P_3}$	η	$\frac{P_2}{P_3}$	η	$\frac{P_2}{P_3}$	η	$\frac{P_2}{P_3}$	η
M _{2d}																						
.5	.886	.75	.882	.781	.882	.781	.884	.761	.888	.73	.894	.7	.937	.42	.966	.215	.98	.12	.99	.052	-	-
.6	.85	.713	.828	.818	.831	.81	.826	.834	.841	.76	.836	.785	.885	.545	.915	.399	.954	.211	.981	.082	-	-
.7	.821	.651	.775	.836	.773	.85	.778	.82	.78	.815	.787	.799	.856	.515	.903	.34	.934	.221	.969	.095	.996	.011
.8	.765	.69	.719	.842	.708	.876	.71	.872	.72	.84	.724	.826	.784	.629	.845	.435	.899	.265	.945	.139	.977	.057
.9	.777	.54	.689	.768	.651	.88	.65	.881	.663	.84	.663	.84	.708	.711	.764	.57	.849	.352	.883	.27	.926	.168
1.08	.847	.25	.702	.515	.606	.714	.558	.815	.538	.865	.535	.876	.584	.75	.613	.698	.658	.606	.739	.447	.788	.352
1.228	.828	.232	.675	.47	.609	.520	.76	.471	.866	.472	.865	.474	.864	.864	.494	.805	.517	.775	.558	.69	.595	.61
1.37	.718	.29	.552	.588	.424	.82	.398	.87	.412	.845	.391	.884	.404	.86	.405	.857	.407	.856	.423	.82	.449	.766
1.5	.505	.583	.372	.82	.342	.877	.348	.868	.383	.795	.434	.709	.456	.666	.448	.678	.361	.837	.342	.879	.361	.837

TEST N°2

	$-2\frac{3}{4}$	$-2\frac{1}{2}$	$-2\frac{1}{4}$	-2	-1	0	$\frac{1}{2}$	$\frac{3}{4}$	1	$1\frac{1}{4}$	$1\frac{1}{2}$						
120	$\frac{7}{16}$	$\frac{1}{2}$	$\frac{3}{4}$	$\frac{1}{2}$	$\frac{1}{2}$	$\frac{1}{2}$	$\frac{1}{2}$	$\frac{1}{2}$	$\frac{1}{2}$	$\frac{1}{2}$	$\frac{1}{2}$						
5	800	806	804	804	804	804	804	804	804	804	804	804	804	804	804	804	804
6	1048	845	905	905	905	905	905	905	905	905	905	905	905	905	905	905	905
7	1208	806	914	914	914	914	914	914	914	914	914	914	914	914	914	914	914
8	1352	831	919	935	916	909	793	66	895	505	372	324	324	324	324	324	324
9	1520	735	876	94	916	916	844	755	594	52	790	41	41	41	41	41	41
97	1620	748	871	938	925	925	835	765	648	494	80	394	394	394	394	394	394
08	1794	5	718	903	93	936	860	835	778	669	1200	594	594	594	594	594	594
208	1978	481	777	871	93	93	93	896	881	831	1642	78	78	78	78	78	78
37	2165	539	905	933	92	94	926	925	935	706	1962	875	875	875	875	875	875
5	2315	765	936	931	872	837	815	822	914	936	2168	914	914	914	914	914	914

GROUP:- 2

TABLE :- 3

[illegible]

$$\Delta = \eta^{\frac{1}{2}} \epsilon \cdot \alpha \frac{f da}{f v}$$

